NWU ®

Synthesis and biological evaluation of 7-azaindole-based chalcones and related compounds as protein kinase inhibitors

MA Qhobosheane

iD orcid.org/0000-0003-3005-0028

Thesis submitted in fulfilment of the requirements for the degree Doctor of Philosophy in Pharmaceutical Chemistry at the

North-West University

Promoter: Prof LJ Legoabe
Co-promoter: Dr RM Beteck

Graduation: June 2021
Student number: 27836576

PREFACE

This thesis is submitted in article format in accordance with the General Academic Rules (A.13.7.3) of the North-West University.

The thesis contains one manuscript which was submitted to *Bioorganic Chemistry* (Appendix O), and two articles which were published in the following journals:

Bioorganic and Medicinal Chemistry. DOI: 10.1016/j.bmc.2020.115468

Chemical Biology & Drug Design. DOI: 10.1111/cbdd.13748

The experimental work for this thesis was conducted by Miss M.A. Qhobosheane at the North-West University, Potchefstroom campus, under supervision and assistance of all promoters.

LETTER OF PERMISSION

December 2020

To whom it may concern,

CO-AUTHORSHIP ON ORIGINAL ARTICLES

The undersigned are co-authors of original articles featured in this thesis, and hereby give permission to Ms M.A. Qhobosheane to use these articles in the thesis: **Synthesis and biological evaluation of 7-azaindole-based chalcones and related compounds as protein kinase inhibitors**, submitted for the degree *Doctor of Philosophy* in Pharmaceutical Chemistry at the North-West University.
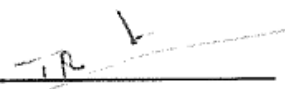
Sincerely,
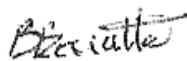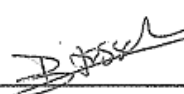

_____
Lesetja J. Legoabe

_____
Jacobus P. Petzer

_____
Stéphane Bach

_____
Blandine Baratte

_____
Richard M. Beteck

_____
Thomas Robert

_____
Sandrine Ruchaud

_____
Béatrice Josselin

ACKNOWLEDGEMENTS

"What shall I return to the LORD for all His goodness to me?"
Psalm 116:12

ABSTRACT

Protein phosphorylation is a major molecular mechanism through which proteins' functions are regulated. Protein phosphorylation occurs through protein kinases, and it consists of the transfer of a phosphate group from a donor to specific amino acid residues on proteins, usually tyrosine, serine and threonine. Processes regulated by protein phosphorylation include cell cycle progression, transcription, translocation, endocytosis, phagocytosis and apoptosis. Deregulation of protein kinase activity leads to aberrant regulation of biological processes and thus the diseases such as cancer. Because of their role in the pathogenesis of many diseases, protein kinases have emerged as attractive therapeutic targets, and they are considered the second most important drug targets after G-protein-coupled receptors. Several strategies have been developed to target protein kinases. Among others, the use of small molecules that inhibit kinase-substrate interactions, or those that bind to the adenosine triphosphate (ATP) binding site of the enzyme to inhibit catalysis are the most common.

7-Azaindole is noteworthy as an excellent scaffold for protein kinase binding; the pyridine moieties' N atom of 7-azaindole serves as a hydrogen bond acceptor, while the pyrrole moieties' NH acts a hydrogen bond donor, and together they form bidentate hydrogen bonds with the hinge region of the kinase. Chalcones on the other hand exhibit a wide range of biological properties, and they have been reported to regulate kinase activities through either direct enzyme inhibition or altering kinase expression.

The present study aimed to investigate novel 7-azaindole-based compounds as inhibitors of tumorigenic protein kinases. In this study, various substituents (benzocycloalkanones and benzaldehydes) were attached to position 3 of 7-azaindole. The compound bearing 3-coumaranone was further derivatised at position 6 of the coumaranone ring with various aryl-alkyl substituents and the resultant analogues maintained novelty. All compounds were screened against a panel of disease-relevant protein kinases (CDK2/CyclinA, CDK5/ p25, CDK9/CyclinT, Haspin, PIM1, CK1ε, GSK-3β and ABL1 and *Lm*CK1 (from the *Leishmania major* parasite)) and were considered active if they inhibited ≥ 70% of kinase activity.

A majority of active compounds synthesised in this study are potent inhibitors of Haspin kinase, and also exhibit dual inhibition for Haspin and GSK-3β. A few active compounds also demonstrated dual inhibition for Haspin and CDK9/CyclinT, as well as GSK-3β and *Lm*CK1. Haspin has only recently been classified as a protein kinase, and identification of its inhibitors may supply valuable candidates for biological studies and cancer treatment. Interestingly, this study further discovered that hybridising 7-azaindole with α-tetralone generates dual inhibitors of Haspin and CDK9/CyclinT. It is believed that dual inhibition of protein kinases could be an

effective strategy in cancer therapy because it overcomes incomplete efficacy and drug resistance, thus providing optimal effects in cancer therapy.

This study established that 3-coumaranone and α-tetralone are optimum substituents for the design of 7-azaindole-based potent Haspin inhibitors, as well as dual inhibitors of Haspin and CDK9/CyclinT. Furthermore, derivatisation of **8l** led to synthesis of novel mono- and disubstituted compounds with dual activity against Haspin and GSK-3β, as well as GSK-3β and *Lm*CK1. Compounds synthesised in this study may therefore be of value as novel anti-proliferative and leishmanicidal agents.

Keywords: Protein kinase, cancer, 7-azaindole, chalcone, Haspin, CDK9/CyclinT, GSK-3β, *Lm*CK1, dual inhibition, leishmanicidal therapy.

TABLE OF CONTENTS

LIST OF FIGURES

LIST OF ABBREVIATIONS

5-ITu	5-Iodotubercidin
Abl	Abelson
ABS	Abbot bioavailability score
Adk	Adenosine kinase
AGC	Protein kinase A, Protein kinase G, Protein kinase C
APE	Ala-Pro-Glu
aPK	Atypical protein kinases
ASK	Apoptosis signal-regulating kinase
ATP	Adenosine triphosphate
BBB	Blood-brain barrier
BAD	BCL-associated agonist of cell death
BCL	B-cell lymphoma
Bcr	Breakpoint cluster region
bFGF	Basic fibroblast growth factor
CaM	Calmodulin
CaMK	Ca^{2+}/calmodulin-dependant kinase
cAMP	Cyclic adenosine monophosphate
CDK	Cyclin-dependant kinase
CHS	Chalcone synthase
CK	Casein kinase
CLK	Cyclin-dependant kinase-like
CLL	Chronic lymphocytic leukemia
CMGC	Cyclin-dependent kinase, mitogen-activated protein kinase, glycogen synthase kinase, Cdk-like related protein kinase
CML	Chronic myeloid luekaemia
CoA	Coenzyme A
CPC	Chromosomal passenger complex
CYP	Cytochrome
DFG	Asp-Phe-Gly
DMF	N,N-dimethylformamide
DMSO-*d6*	Deuterated dimethylsulfoxide
DNA	Deoxyribonucleic acid
EGF	Epidermal growth factor
EGFR	Epidermal growth factor receptor
ePK	Eukaryotic protein kinase

ER	Endoplasmic reticulum
ERK	Extracellular signal-regulated kinase
FDA	Food and drug administration
FGF	Fibroblast growth factor
FGFR	Fibroblast growth factor receptor
FLT	Fms-like tyrosine kinase
GI	Gastrointestinal tract
GIST	Gastrointestinal stromal tumour
GSK	Glycogen synthase kinase
H3T3ph	Histone H3 at threonine-3
HIA	Human gastrointestinal absorption
HPLC	High performance liquid chromatography
Hs	*Homo sapien*
IC_{50}	50% inhibitory concentration
IL	Interleukin
IRAK	Interleukin receptor-associated kinase
Jaks	Janus kinases
Ki	Inhibition constant
LIMK	Lim domain kinases
Lm	*Leishmania major*
MAPK	Mitogen activated protein kinase
MS	Mass spectrometry
mTOR	Mammalian target of rapamycin
NF-κB	Nuclear factor kappa-light-chain-enhancer of activated B cells
NGF	Nerve growth factor
NMR	Nuclear magnetic resonance
NRTK	Non-receptor tyrosine kinase
NSCLC	Non-small-cell lung carcinoma
PAINS	Pan assay interference structures
PDDGF	Platelet derived growth factor
PDGFR	Platelet derived growth factor receptor
PI3K	Phosphatidylinositol-3-kinase
PI3KCA	Phosphatidylinositol-kinase catalytic subunit alpha
PIM	Proviral Integration site for Moloney murine leukaemia virus
PKA	Protein kinase A
PKC	Protein kinase C
PKG	Protein kinase G

PKI	Protein kinase inhibitor
PKL	Protein kinase-like
PKS	Polyketide synthase
RAF	Rapidly accelerated fibrosarcoma
RGC	Receptor guanylyl cyclase
ROCK	Rho-associated coiled-coil-containing protein kinase
RNA	Ribonucleic acid
RT	Room temperature
RTK	Receptor tyrosine kinase
Ssc	*Sus scrofa*
STE	Sterile
TGF	Transforming growth factor
TK	Tyrosine kinase
TKI	Tyrosine kinase inhibitor
TKL	Tyrosine kinase-like
TLC	Thin layer chromatography
VEGF	Vascular endothelial growth factor
VEGFR	Vascular endothelial growth factor receptor
XIAP	X-linked inhibitor of apoptosis protein

CHAPTER 1

INTRODUCTION

1.1 Background

Cancer is a major public health problem and the second leading cause of death globally (Hassanpour & Dehghani, 2017). Dysfunctional genes cause uncontrolled cell proliferation, leading to cancer (Hassanpour & Dehghani, 2017). In 2017, 9.4 million deaths occurred globally due to cancer, and this is nearly twice the number recorded in 1990 (Lin *et al.*, 2019). According to international agency for research on cancer, there is a rise in the global cancer burden, with 18.1 million new cases and 9.6 million deaths reported in 2018 (Bray *et al.*, 2018; IARC, 2018). At least one in five men and one in six women develop cancer in their lifetime, and one in eight men and one in eleven women die from the disease (IARC, 2018). Approximately 60% of cancer related deaths occurred in Africa, and this number is expected to increase to 70% by 2030 (Dent *et al.*, 2017).

According to Dent *et al.* (2017), the high prevalence of cancer in some African regions results from inaccessibility of, or limited access to cancer treatment. Other factors, including population growth, ageing, as well as changing social and economic factors are also responsible contributors to increasing cancer burden (IARC, 2018). However, in some countries, a decrease in the incidence of some cancers has been observed and this can be a result of effective prevention methods (IARC, 2018).

The abnormal activation of protein and lipid kinases arises from various types of genetic and epigenetic changes that lead to increase in specific kinase activity, its overexpression or loss of negative regulation (Gross *et al.*, 2015). Cancer cells frequently harbour somatic point mutations at structurally conserved residues or mutation hotspots that elevate kinase activity (Gross *et al.*, 2015). Point mutations are the most common mechanism of abnormal kinase activation, and they lead to an amino acid substitution in the catalytic site. This changes the general properties of the protein (Gross *et al.*, 2015). According to Bhullar *et al.* (2018), different protein kinases play overlapping and complex roles in cell transformation, cancer initiation, survival and proliferation; therefore, it is difficult to divide them with regard to their functions. However, protein kinases can be categorised based on their hallmark role(s) in cancer pathophysiology (Bhullar *et al.*, 2018). For instance, phosphatidylinositol-4,5-bisphosphate 3-kinase catalytic subunit alpha (PI3KCA) is a member of the

phosphatidylinositol 3-kinase (PI3K) family that is associated with the pathology of colorectal, ovarian, breast, endometrial and hepatocellular cancers (Bhullar *et al.*, 2018).

1.2   Protein kinases

Protein kinases are cytoplasm-based enzymes that control intracellular signaling networks by catalysing the phosphorylation of multiple protein substrates (Litalien & Beaulieu, 2011; Wilson *et al.*, 2018). Protein kinases form a large and diverse family of signaling proteins (Girault *et al.*, 2017; Wilson *et al.*, 2018). The human protein kinome encodes over 500 distinct protein kinases (Duong-Ly & Peterson, 2013; Wilson *et al.*, 2018), which constitute nearly 2% of the human genes (Taylor & Kornev, 2011; Duong-Ly & Peterson, 2013). About 478 protein kinases contain a eukaryotic protein kinase (ePK) catalytic domain (Duong-Ly & Peterson, 2013), and they can be sub-classified into nine major ePK families based on primary sequence. These families include: tyrosine kinase (TK), tyrosine kinase-like (TKL), STE (STE20, STE11, and STE7 related), casein kinase 1 (CK1), protein kinase A, protein kinase G, protein kinase C (AGC), Ca^{2+}/calmodulin-dependent kinases (CaMK), cyclin-dependent kinase, mitogen-activated protein kinase (MAPK), glycogen synthase kinase (GSK) and Cdk-like related (CMGC), receptor guanylyl cyclase (RGC) and other (Bradley *et al.*, 2017; Kanev *et al.*, 2019).

Among the ePK superfamily, 81 kinases do not fit within the nine major groups and are, therefore, classified as 'others' (Wilson *et al.*, 2018). Although the remaining kinases within the kinome have little sequence similarity to the ePK domain, they are predicted to maintain kinase activity and are thus referred to as atypical protein kinases (aPKs) (Duong-Ly & Peterson, 2013; Wilson *et al.*, 2018). Furthermore, approximately 60 kinases lack one or more amino acids required for protein phosphorylation and these are referred to as pseudokinases (Byrne *et al.*, 2017).

Catalytic domains of protein kinases contain a small β-pleated N-lobe that is connected by a short hinge fragment to an α-helical C-lobe, forming an active site with a front pocket and a back pocket (Fabbro, 2015; Ardito *et al.*, 2017). Protein kinases also contain a well-defined adenosine triphosphate (ATP) binding site and a variable substrate binding site (Tong *et al.*, 2013). ATP binds to the cleft between the N- and the C-terminal lobes of the catalytic domain where its adenine group is inserted between hydrophobic residues and makes contact with the hinge region through hydrogen bonds (Fabbro, 2015). Within the ATP binding pocket lies

a residue called the "gatekeeper" that controls access to the hydrophobic back pocket of the kinase (Fabbro, 2015).

Protein kinases play important roles in regulating cellular functions such as cell division, signal transduction, cell growth, apoptosis, motility, metabolism, as well as repairing of damaged deoxyribonucleic acid (DNA) (Ardito *et al.*, 2017; Liu *et al.,* 2017; Sakkiah *et al.*, 2017). Hyperactivity or overexpression of protein kinases have been implicated in a broad range of diseases, including neurodegenerative disorders, inflammatory diseases, cardiovascular diseases, metabolic diseases (diabetes, Gaucher's disease, maple syrup urine disease and phenylketonuria) and cancer (Lawson *et al.*, 2016; Bhullar *et al.*, 2018; Zhao & Bourne, 2018).

Protein kinase inhibitors have played a crucial role in treatment of cancer and other diseases (Gross *et al.*, 2015), and they are of great benefit over conventional chemotherapy especially when they are more selective and less cytotoxic to non-cancerous cells (Ghione *et al.*, 2020). Imatinib is the first approved protein kinase inhibitor used in cancer therapy. It blocks the kinase activity of the aberrant protein breakpoint cluster region-Abelson (Bcr-Abl) (Ghione *et al.*, 2020). Imatinib is approved for the treatment of chronic myeloid leukaemia (CML), as well as gastrointestinal stromal tumours (GIST) possessing c-Kit mutations, and dermatofibrosarcoma protuberans (Ghione *et al.*, 2020).

Because cancer arises from the malfunctioning of multiple cellular processes, the idea of targeting tumours at multiple sites is theoretically attractive (Branca, 2005). Sorafenib is a multi-kinase inhibitor which prevents cancer cell proliferation by inhibiting rapidly accelerated fibrosarcoma (RAF), MAPK, extracellular signal-regulated kinase (ERK) pathway, and on the other hand hinders angiogenesis by inhibiting vascular endothelial growth factor receptor (VEGFR)-2 and platelet derived growth factor receptor (PDGFR) alpha (Branca, 2005). Sorafenib also inhibits other kinases including fms -like tyrosine kinase 3 (FLT-3) and c-KIT (Branca, 2005). However, multi-kinase inhibitors are non-specific, thus could have more side-effects (Branca, 2005). According to Levitzki and Klein (2019), the current approach to cancer treatment is to combine targeted agents with one another or with cytotoxic drugs. Combination regimens such as erlotinib plus bevacizumab have been reported as a promising approach to improving the outcomes attained with epidermal growth factor receptor (EGFR)-tyrosine kinase inhibitor monotherapy in patients with EGFR+ mutations (Batson *et al.*, 2017).
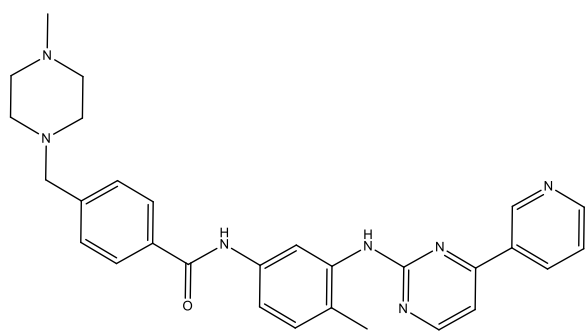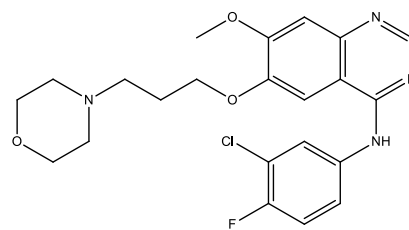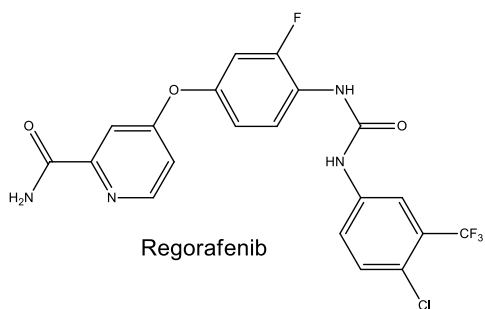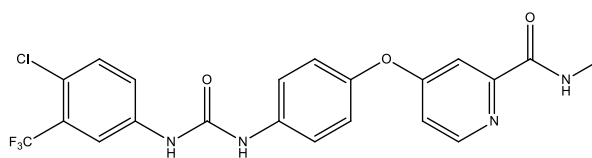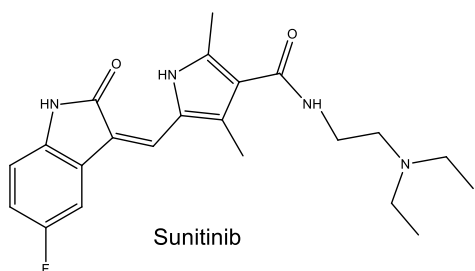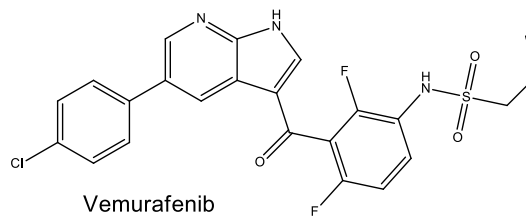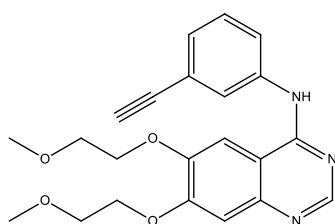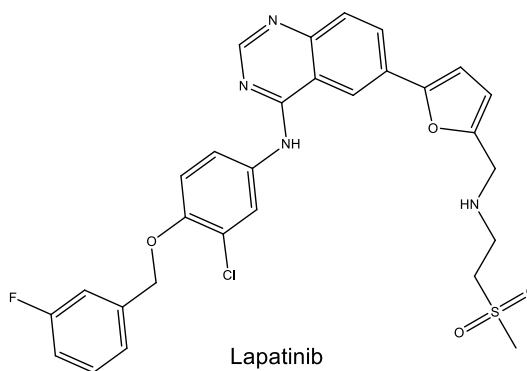
Figure 1.1: Chemical structures of some protein kinase inhibitors approved as anticancer drugs.

1.3   Justification of the study

Reversible protein phosphorylation which is mediated by kinases regulates almost all aspects of cellular activities (Cohen, 2001) and many diseases are a consequence of deregulation of protein kinase activity (Cicenas *et al.*, 2018). Dysfunctional genes cause uncontrolled cell proliferation, leading to cancer, as well as several manifestations of cardiovascular disease such as ischaemia, hypertrophy, atherogenesis and angiogenesis (Force *et al.*, 2004). In addition, numerous naturally occurring toxins and pathogens alter the phosphorylation state of proteins (Cohen, 2001). Protein kinases are the second most targeted group of proteins, following the G-protein coupled receptors (Bhullar *et al.*, 2018), and they represent a vast resource of drug targets for therapeutic intervention in human diseases, particularly oncology (Eyers, 2013).

Multi-kinase inhibitors are more effective than mono-kinase inhibitors in cancer chemotherapy (Petrelli & Giordano, 2008), and they are a new perspective and an innovative approach to cancer treatment. In this study, the activity of some novel 7-azaindole derivatives will be evaluated on a panel of disease relevant protein kinases that include various cyclin-dependant kinases (CDKs): *Hs*CDK2/CyclinA, *Hs*CDK5/p25, *Hs*CDK9/CyclinT, human Proto-oncogene serine/threonine-protein kinase PIM1, *Hs*Haspin, *Lm*CK1 (from the intracellular parasite *Leishmania major*), porcine casein kinase 1 δ/ε (*Ssc*CK1δ/ε) and porcine GSK-3 (*Ssc*GSK3α/β). This study will also determine the selectivity and binding patterns of the newly synthesised compounds.

1.4   Hypothesis of the study

7-Azaindole is known as an excellent hinge-binding element (Tong *et al.*, 2013; Irie & Sawa, 2018), and its derivatives have been reported to exhibit interesting activities against several protein kinases (Tsou *et al.*, 2010; Nakano *et al.*, 2012; Tong *et al.*, 2013). Structural modification of 7-azaindoles has led to the discovery of potent multi-kinase inhibitors. The nature and position of substituents attached to the 7-azaindole core greatly impacts on the inhibition profile of 7-azaindole derivatives (Daydé-Cazals *et al.*, 2016).

Daydé-Cazals *et al.* (2016) synthesised a series of 7-azaindole derivatives to improve the activity of a dual ABL/SRC Type I inhibitor (**1**, Figure 1.2) by attaching substituents to position C4 of the 2-methylphenyl ring *via* an amide linker. Attaching a 4-pyridinyl substituent bearing a trifluoromethyl group adjacent to the nitrogen atom as seen in compound **2** led to loss of activity (Daydé-Cazals *et al.*, 2016). Contrary to this, derivatives bearing a 3-pyridine

substituent (**3** and **4**) inhibited five kinases. Adding bulkier substituents as seen in **5** and **6** led to a significant improvement in activity (Daydé-Cazals *et al.*, 2016). Compounds **5** and **6** exhibited excellent inhibitory activity against a panel of six protein kinases including B-Raf, EGFR, fibroblast growth factor receptor (FGFR)-2, PDGFRA, SRC and VEGFR2 (Daydé-Cazals *et al.*, 2016). In accordance with these reports, we envisage that a similar trend might be observed by attaching different polar and non-polar substituents to 7-azaindole ─ this might potentiate multiple kinase inhibition.

Nitrogen atoms within the 7-azaindole backbone anchor the inhibitors into the protein binding pocket by forming bidentate hydrogen bonds at the ATP binding site of the hinge region. We predict that leaving N-1 and N-7 of our inhibitors unsubstituted will increase their binding affinity to the target proteins' binding sites.
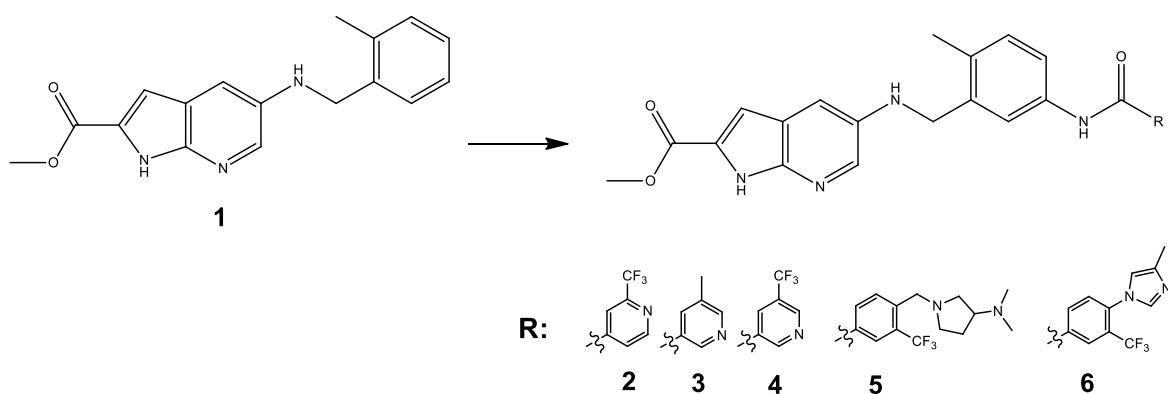
Figure 1.2: **Chemical structures of some reported multi-kinase inhibitors (Daydé-Cazals *et al.*, 2016).**

1.5 Aim of the study

The aim of this study is to investigate novel 7-azaindole-based compounds as inhibitors of selected tumorigenic protein kinases.

The primary objectives of this study are:

- Synthesis of novel mono- and disubstituted 7-azaindole derivatives.
- *In vitro* evaluation of protein kinase inhibitory properties of the synthesised compounds.
- Evaluation of the selectivity of synthesised compounds by determination of the IC_{50}.

- Determination of structure-activity relationships of target compounds as inhibitors of selected protein kinases.
- Molecular modelling to identify essential interactions between hit compound(s) and the target proteins.

REFERENCES

Ardito, F., Giuliani, M., Perrone, D., Troiano, G. & Lo Muzio, L. 2017. The crucial role of protein phosphorylation in cell signaling and its use as targeted therapy. *International journal of molecular medicine*, 40(2):271-280.

Batson, S., Mitchell, S.A., Windisch, R., Damonte, E., Munk, V.C. & Reguart, N. 2017. Tyrosine kinase inhibitor combination therapy in first-line treatment of non-small-cell lung cancer: systematic review and network meta-analysis. *OncoTargets and therapy*, 10:2473.

Bhullar, K.S., Lagaron, N.O., McGowan, E.M., Parmar, I., Jha, A., Hubbard, B.P. & Rupasinghe, H.P.V. 2018. Kinase-targeted cancer therapies: progress, challenges and future directions. *Molecular cancer*, 17(1):48.

Bradley, D., Vieitez, C., Rajeeve, V., Cutillas, P.R. & Beltrao, P. 2017. Global analysis of specificity determinants in eukaryotic protein kinases. *BioRxiv*:195115.

Branca, M.A. 2005. Multi-kinase inhibitors create buzz at ASCO. *Nature biotechnology*, 23(6):639

Bray, F., Ferlay, J., Soerjomataram, I., Siegel, R.L., Torre, L.A. & Jemal, A. 2018. Global cancer statistics 2018: GLOBOCAN estimates of incidence and mortality worldwide for 36 cancers in 185 countries. *CA: a cancer journal for clinicians*, 68(6):394-424.

Byrne, D.P., Foulkes, D.M. & Eyers, P.A. 2017. Pseudokinases: update on their functions and evaluation as new drug targets. *Future medicinal chemistry*, 9(2):245-265.

Cicenas, J., Zalyte, E., Bairoch, A. & Gaudet, P. 2018. Kinases and cancer. *Cancers*, 10(3):63.

Cohen, P. 2001. The role of protein phosphorylation in human health and disease. The Sir Hans Krebs medal lecture. *European journal of biochemistry*, 268(19):5001-5010.

Daydé-Cazals, B., Fauvel, B., Singer, M., Feneyrolles, C., Bestgen, B., Gassiot, F., Spenlinhauer, A., Warnault, P., Van Hijfte, N., Borjini, N., Chevé, G. & Yasri, A. 2016. Rational Design, Synthesis, and Biological Evaluation of 7-Azaindole Derivatives as Potent Focused Multi-Targeted Kinase Inhibitors. *Journal of medicinal chemistry*, 59(8):3886-3905.

Dent, J., Manner, C.K., Milner, D., Mutebi, M., Ng'ang'a, A., Olopade, O.I., Rebbeck, T.R. & Stefan, C.D. 2017. Africa's emerging cancer crisis: A call to action. In Health, B.V.F.G. (Ed.). Duong-Ly, K.C. & Peterson, J.R. 2013. The human kinome and kinase inhibition as a therapeutic strategy. *Current protocols in pharmacology*, 2:1-21.

Eyers, P.A. 2013. Getting to grips with drug resistance in the human protein kinase superfamily. *European pharmaceutical review*, 18(1):49-54.

Fabbro, D. 2015. 25 years of small molecular weight kinase inhibitors: potentials and limitations. *Molecular pharmacology*, 87(5):766-775.

Force, T., Kuida, K., Namchuk, M., Parang, K. & Kyriakis, J.M. 2004. Inhibitors of protein kinase signaling pathways: emerging therapies for cardiovascular disease. *Circulation*, 109(10):1196-1205.

Ghione, S., Mabrouk, N., Paul, C., Bettaieb, A. & Plenchette, S. 2020. Protein kinase inhibitor-based cancer therapies: considering the potential of nitric oxide (NO) to improve cancer treatment. *Biochemical pharmacology,* 176:113855.

Girault, J.A., Greengard, P. & Nairn, A.C. 2017. Chapter 29 - regulation of striatal signaling by protein phosphatases. *(In* Steiner, H. & Tseng K.Y., *eds.* Handbook of behavioral neuroscience. Elsevier. p. 583-607).

Gross, S., Rahal, R., Stransky, N., Lengauer, C. & Hoeflich, K.P. 2015. Targeting cancer with kinase inhibitors. *The journal of clinical investigation*, 125(5):1780-1789.

Hassanpour, S.H. & Dehghani, M. 2017. Review of cancer from perspective of molecular. *Journal of cancer research and practice*, 4(4):127-129.

IARC (International Agency for Cancer Research). 2018. *Latest global cancer data: Cancer burden rises to 18.1 million new cases and 9.6 million cancer deaths in 2018* [Press release]. 12 September. (Accessed 22 May 2020).

Irie, T. & Sawa, M. 2018. 7-azaindole: a versatile scaffold for developing kinase inhibitors (Patent: WO 2012175168A1).

Kanev, G.K., de Graaf, C., de Esch, I.J., Leurs, R., Würdinger, T., Westerman, B.A. & Kooistra, A.J. 2019. The landscape of atypical and eukaryotic protein kinases. *Trends in pharmacological sciences*, 40(11):818-832.

Lawson, M., Rodrigo, J., Baratte, B., Robert, T., Delehouzé, C., Lozach, O., Ruchaud, S., Bach, S., Brion, J.-D. & Alami, M. 2016. Synthesis, biological evaluation and molecular modeling studies of imidazo [1, 2-a] pyridines derivatives as protein kinase inhibitors. *European journal of medicinal chemistry*, 123:105-114.

Levitzki, A. & Klein, S. 2019. My journey from tyrosine phosphorylation inhibitors to targeted immune therapy as strategies to combat cancer. *Proceedings of the national academy of sciences*, 116(24):11579-11586.

Lin, L., Yan, L., Liu, Y., Yuan, F., Li, H. & Ni, J. 2019. Incidence and death in 29 cancer groups in 2017 and trend analysis from 1990 to 2017 from the Global Burden of Disease Study. *Journal of hematology & oncology*, 12(1):96.

Litalien, C. & Beaulieu, P. 2011. Molecular mechanisms of drug actions: From receptors to effectors A$_2$. *(In* Zimmerman, J.J., *ed.* Pediatric critical care. Saint Louis: Mosby. p. 1553-1568).

Liu, M., Zhao, G., Cao, S., Zhang, Y., Li, X. & Lin, X. 2017. Development of certain protein kinase inhibitors with the components from traditional Chinese medicine. *Frontiers in pharmacology*, 7:523.

Nakano, H., Saito, N., Parker, L., Tada, Y., Abe, M., Tsuganezawa, K., Yokoyama, S., Tanaka, A., Kojima, H., Okabe, T. & Nagano, T. 2012. Rational evolution of a novel type of potent and selective proviral integration site in Moloney murine leukemia virus kinase 1 (PIM1) inhibitor from a screening-hit compound. *Journal of medicinal chemistry*, 55(11):5151-5164.

Petrelli, A. & Giordano, S. 2008. From single- to multi-target drugs in cancer therapy: when aspecificity becomes an advantage. *Current medicinal chemistry*, 15(5):422-432.

Sakkiah, S., Ping Cao, G., P Gupta, S. & Woo Lee, K. 2017. Overview of the structure and function of protein kinases. *Current enzyme inhibition*, 13(2):81-88.

Taylor, S.S. & Kornev, A.P. 2011. Protein kinases: evolution of dynamic regulatory proteins. *Trends in biochemical sciences*, 36(2):65-77.

Tong, Y., Stewart, K.D., Florjancic, A.S., Harlan, J.E., Merta, P.J., Przytulinska, M., Soni, N., Swinger, K.K., Zhu, H. & Johnson, E.F. 2013. Azaindole-based inhibitors of Cdc7 kinase: impact of the Pre-DFG residue, Val 195. *ACS medicinal chemistry letters*, 4(2):211-215.

Tsou, H.R., MacEwan, G., Birnberg, G., Grosu, G., Bursavich, M.G., Bard, J., Brooijmans, N., Toral-Barza, L., Hollander, I., Mansour, T.S., Ayral-Kaloustian, S. & Yu, K. 2010. Discovery and optimization of 2-(4-substituted-pyrrolo[2,3-b]pyridin-3-yl)methylene-4-hydroxybenzofuran-3(2H)-ones as potent and selective ATP-competitive inhibitors of the mammalian target of rapamycin (mTOR). *Bioorganic & medicinal chemistry letters*, 20(7):2321-2325.

Wilson, L.J., Linley, A., Hammond, D.E., Hood, F.E., Coulson, J.M., MacEwan, D.J., Ross, S.J., Slupsky, J.R., Smith, P.D. & Eyers, P.A. 2018. New perspectives, opportunities, and challenges in exploring the human protein kinome. *Cancer research*, 78(1):15-29.

Zhao, Z. & Bourne, P.E. 2018. Progress with covalent small-molecule kinase inhibitors. *Drug discovery today*, 23 (3):727-735.

CHAPTER 2
LITERATURE REVIEW

2.1   Cancer

Cancer is a heterogeneous group of related diseases that are caused by multiple changes in gene expression (Ruddon, 2007). It is characterised by uncontrolled growth, division and spread of cells that often invade and destroy adjacent tissues (Avendaño & Menéndez, 2015). Cancer may also metastasize to other regions of the body, leading to stage IV cancer; 90% of cancer deaths is attributed to this stage (Avendaño & Menéndez, 2015). Cancer remains one of the most difficult diseases to treat (Ruddon, 2007; Avendaño & Menéndez, 2015) and continues to be the leading cause of death worldwide, surpassing cardiovascular diseases (El-Azab & ElTahir, 2012).

Tumorigenesis (Carcinogenesis) is a multistep process in which normal cells acquire malignant properties including small-scale changes such as point mutations in DNA sequences, larger-scale chromosomal abnormalities such as translocation, deletions and amplifications (Avendaño & Menéndez, 2015), evasion of apoptosis and immunosurveillence (Cao, 2017), as well as abnormal DNA methylation or acetylation of histones ─ which lead to abnormal chromatin structure and dysfunctional epigenetics (Avendaño & Menéndez, 2015; Cao, 2017). These processes are distinctive and complementary, and they have been generalised as hallmarks of cancer (Hanahan & Weinberg, 2011; Cao, 2017). About 2000 to 3000 proteins are involved in these processes (Avendaño & Menéndez, 2015). According to Cao (2017), changes in gene sequences or expression levels of over 3000 genes (including classical oncogenes and tumour suppressor genes) have been implicated in carcinogenesis.

Chemotherapy, surgery and radiotherapy are deemed successful interventions in cancer treatment (Arruebo *et al.*, 2011; Avendaño & Menéndez, 2015). Most chemotherapeutics act on both healthy and cancerous cells, this none selectivity inevitably causes severe side-effects (Pucci *et al.*, 2019). A lot of efforts have been made towards finding new and efficient chemotherapies with reduced side-effects. According to Pucci *et al.* (2019), nanomedicine offers a versatile approach of delivering conventional chemotherapeutics directly on to cancer cells, thereby avoiding side-effects that arise from killing healthy cells. Natural antioxidants and many phytochemicals have recently been introduced as anti-cancer adjuvants because of their antiproliferative and pro-apoptotic properties (Arsova-Sarafinovska & Aleksandar, 2013; Pucci *et al.*, 2019). Gene therapy is another promising strategy deployed in cancer treatment; it is currently under evaluation in a variety of clinical trials worldwide (Cross &

Burmester, 2006; Pucci *et al.*, 2019). Thermal ablation of tumours and magnetic hyperthermia provide new opportunities to localised treatment (Cabuy, 2012; Chang *et al.*, 2018), and they may be a potential substitute for more invasive practices such as surgery (Cabuy, 2012; Pucci *et al.*, 2019).

Targeted therapy is another branch of cancer therapy that aims at targeting a specific site such as tumour vasculature or intracellular organelles, leaving the surrounding tissues unaffected (Pucci *et al.*, 2019). Mutations in protein kinases are often implicated in many cancers (Dixit & Verkhivker, 2014), as a result, protein kinases have undoubtedly proven to be a promising class of drug targets for the development of new cancer therapies (Sawyers, 2004). The clinical success of imatinib motivated further development of new small molecule inhibitors that target kinases in cancer (Baker & Reddy, 2010).

2.2   Protein kinases

Protein kinases are enzymes that catalyse the phosphorylation of multiple protein substrates (Wilson *et al.*, 2018), by transferring the γ-phosphate of ATP to these protein substrates, thus altering their functions (Zhou *et al.*, 2012). The human kinome (figure 2.1) encodes more than 500 protein kinases, which phosphorylate approximately 70% of all human proteins (Sugiyama *et al.*, 2019). At least 497 kinases are classified as ePKs, and they are all structurally related (Dissmeyer & Schnittger, 2011), while 58 kinases are referred to as aPKs due to their lack of sequence similarity to ePKs (Kanev *et al.*, 2019). The ePKs are further classified into nine major groups based on their sequence similarity. These groups are; TKs, TKLs, STE, CK1, CaMK, AGC, CMGC, RGC and pther (Kanev *et al.*, 2019).

Interestingly, the first aPK structures revealed that several of these kinases have a prototypical ePK fold despite their lack of sequence similarity to ePKs (Kanev *et al.*, 2019). Of the 58 reported aPKs, 26 are classified as protein kinase-like (PKL) because they have the same structural fold as ePKs (Kanev *et al.*, 2019). The prototypical kinase fold of both ePKs and aPKs can be easily recognised by the two main lobes; the N-lobe and the C-lobe, which are connected by a linker of three to five residues (Kanev *et al.*, 2019). According to Roskoski (2007), protein kinases are divided into enzymes that catalyse the phosphorylation of serine/threonine or tyrosine, and dual-specificity protein kinases that phosphorylate serine/threonine and tyrosine.
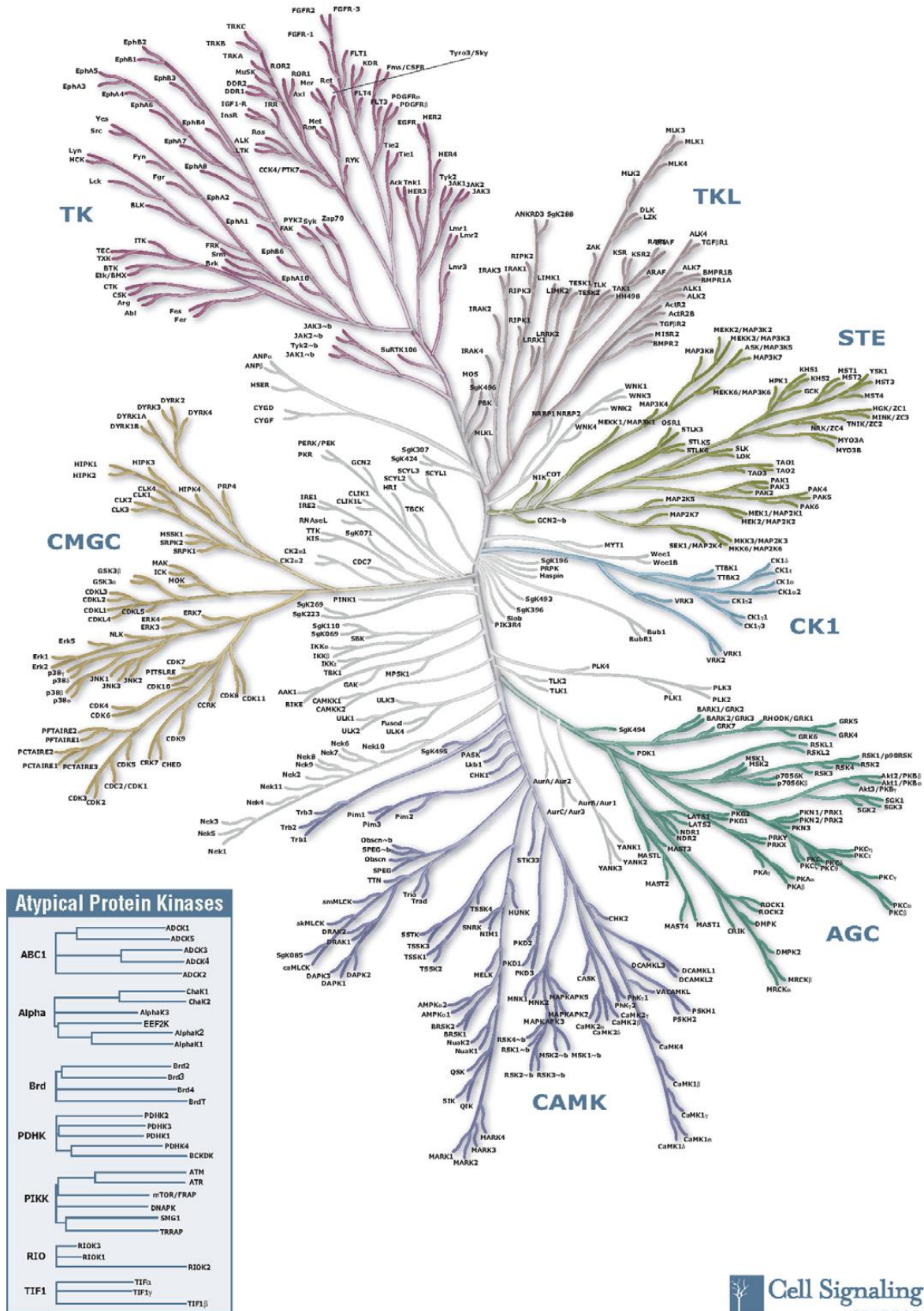
The Human Protein Kinases

Figure 2.1: The human protein kinome tree (Lacal, 2006)

2.2.1 Eukaryotic protein kinases

The eukaryotic protein kinase family is one of the largest superfamilies of homologous proteins which are related by virtue of their catalytic domains (Hanks & Hunter, 1995). This family comprises multitudes of structurally diverse kinases of known sequences (Hanks & Hunter, 1995). According to Hanks and Hunter (1995), ePKs also possess some common structural features, in spite of their structural and functional diversity. The catalytic domains of ePKs are composed of approximately 250-300 amino acid residues (Hanks & Hunter, 1995). Within the catalytic domain are found 12 conserved subdomains that fold into a common catalytic core (Figure 2.2). The structural core of ePKs comprises two lobes: a small β-pleated N-lobe and a larger α-helical C-lobe that converge to form a deep cleft within which the adenine ring of ATP is bound (Taylor *et al.*, 2012; Meharena *et al.*, 2013). In this conformation, the γ-phosphate group is positioned at the outer edge of the cleft where phosphorylation takes place (Taylor *et al.*, 2012).

The N-lobe is predominantly constructed of a five-stranded antiparallel β-sheet which is coupled to a single conserved αC-helix (Taylor & Kornev, 2011; Taylor *et al.*, 2012; Meharena *et al.*, 2013). The first two β-strands (β1 and β2) contain a highly conserved sequence motif called the glycine-rich loop or the phosphate-binding loop (P-loop) (Taylor & Kornev, 2011; Fabbro *et al.*, 2015). This loop is the most flexible part of the N-lobe; it folds over the nucleotide to anchor and position ATP for phosphorylation (Taylor & Kornev, 2011; Taylor *et al.*, 2012), but it makes no contact with the purine moiety of ATP (Taylor & Kornev, 2011). Towards the N-terminal of the hinge region is a residue known as the gatekeeper, which lies within the ATP pocket and regulates access to the hydrophobic back-pocket of the kinase (Fabbro *et al.*, 2015).

The C-terminal of the C-helix continues into the hinge region, while the N-terminal interacts with the activation loop (A-loop) (Fabbro *et al.*, 2015). The A-loop comprises of approximately 20-30 residues, and it occurs in either open or closed conformations. When the A-loop assumes a closed conformation, the protein substrate site is blocked and the kinase is inactive (Huse & Kuriyan, 2002; Fabbro *et al.*, 2015). Contrary to the N-lobe, the C-lobe is extremely stable and it comprises of mainly α-helices (Taylor *et al.*, 2012). The helical subdomain which forms the core of the kinase also serves as a tethering surface for protein substrates (Taylor & Kornev, 2011). A four stranded β-sheet lies on the helical core and forms the bottom surface of the active site cleft (Taylor *et al.*, 2012). This β-sheet contains much of the catalytic machinery that is associated with phosphorylation of proteins (Taylor & Kornev, 2011).
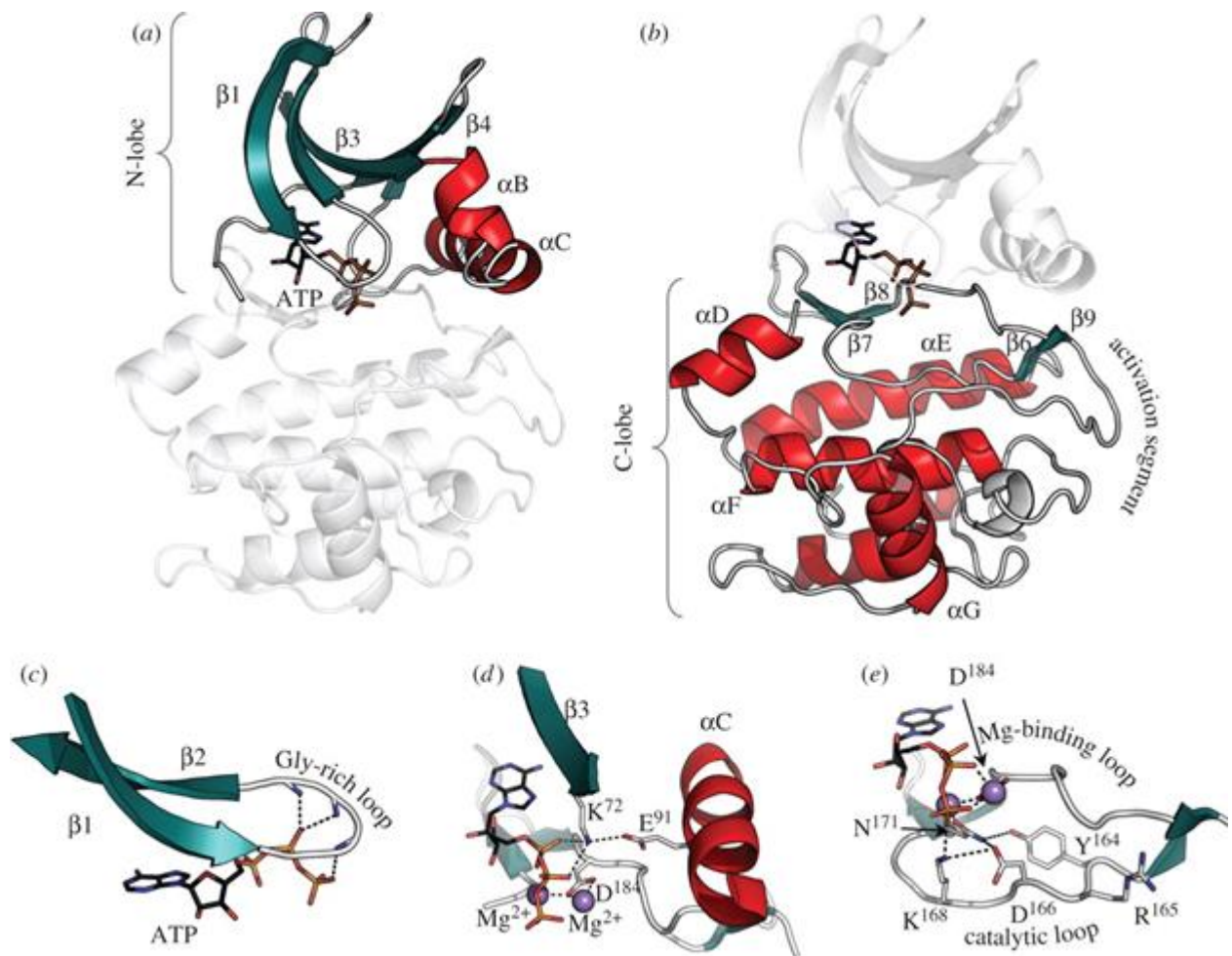
Figure 2.2: Conserved core of the eukaryotic protein kinases. The bottom panels (c–e) highlight functional motifs in the N-lobe (a) and the C-lobe (b) using PKA as a prototype for the ePK family. Helices are shown in red; b-strands in teal (Taylor *et al.*, 2012).

2.2.1.1   TK group

The conventional protein tyrosine kinase (TK) group is a broad multigene family. TK includes a large number of enzymes with closely related kinase domains that selectively phosphorylate tyrosine residues (Hanks & Hunter, 1995; Robinson *et al.,* 2000). TKs are found predominantly in metazoans, wherein they regulate processes such as cell growth, differentiation, adhesion, motility and cell death (Robinson *et al.,* 2000). These kinases are classified into transmembrane receptor TKs (RTKs) and non-receptor TKs (NRTKs) (Hubbard & Till, 2000).

The RTK family includes insulin receptors and receptors for many other growth factors such as platelet-derived growth factor (PDGF), fibroblast growth factor (FGF), vascular endothelial growth factor (VEGF), epidermal growth factor (EGF) and nerve growth factor (NGF) (Hubbard & Till, 2000). On the other hand, the NRTK family includes Src, Janus kinases (Jaks) and Abl (Hubbard & Till, 2000). According to Hubbard and Till (2000), NRTKs are triggered by other cell surface receptors such as G-protein coupled receptors. In humans, TKs have been shown to play important roles in development of many diseases such as diabetes and cancer (Robinson *et al.*, 2000). Tyrosine kinase genes have also been associated with a wide variety of congenital syndromes including down syndrome, cystic fibrosis and cerebral palsy (Robinson *et al.*, 2000).

2.2.1.2 AGC kinase group

This kinase group is represented by three kinase families, namely; protein kinase A (PKA) also referred to as cAMP-dependent protein kinase, protein kinase G (PKG) (also known as cGMP-dependent protein kinase), and protein kinase C (PKC) (Arencibia *et al.*, 2013). To date, fourteen AGC kinase domain structures have been identified, and they all show the prototypical bilobal kinase fold that contains a small N-lobe and a large C-lobe which sandwich one molecule of ATP (Pearce *et al.*, 2010). The AGC group of kinases are basic amino acid-directed enzymes that make up 12% of the human kinome (Arencibia *et al.*, 2013), and they phosphorylate serine/threonine residues which lie near arginine and lysine (Hanks & Hunter, 1995). The AGC family encompasses 60 members which share a conserved catalytic domain (Pearce *et al.*, 2010), with amino acid sequence identities frequently between 35% and 45% (Arencibia *et al.*, 2013). AGC kinases are reported to be involved in numerous cellular functions, and their dysregulation contributes to the pathogenesis of many human diseases including cancer, diabetes (Pearce *et al.*, 2010), obesity, inflammation, neurological disorders as well as viral infections (Rakshambikai *et al.*, 2015).

2.2.1.3 CaMK kinase group

CaMK represents a diverse group of protein kinases which are involved in calcium signalling (Duong-Ly & Peterson, 2013). They are activated by the binding of Ca^{2+}/calmodulin to a small domain located near the C-terminal of the catalytic domain (Hanks & Hunter, 1995). However, some kinases in this group are activated independently of phosphorylation or require additional phosphorylation to complete their activation (Sakkiah *et al.*, 2017). Binding of Ca^{2+} markedly changes the conformation of calmodulin (CaM) and increases its affinity for a wide-range of CaM-binding kinases; Ca^{2+}/calmodulin-dependent protein kinase kinase (CaMKK), CaMKI, CaMKII and CaMKIV (Brzozowski & Skelding, 2019). CaMK has two globular domains

which are connected by a linker to form an autoinhibitory cleft and a CaM-binding domain (Sakkiah *et al.*, 2017). Furthermore, CaMK is found in the cytosol and the nucleus, and it responds to Ca^{2+} changes in these organelles (Sakkiah *et al.*, 2017). According to Brzozowski and Skelding (2019), CaM kinases control a broad range of cellular processes which include regulating dendritic spine morphology, hematopoietic stem cell maintenance, cell proliferation, apoptosis, glucose uptake, adipogenesis and normal immune cell function.

2.2.1.4 CMGC kinase group

The CMGC group is a diverse group of kinases (Duong-Ly & Peterson, 2013) whose members exhibit a single domain (Rakshambikai *et al.*, 2015). This group has a total of 62 members, which can be further classified into eight subfamilies including cyclin-dependent kinases (CDKs), MAPKs, GSKs and CDK-like kinases (CLKs) among others (Keskitalo, 2017; Sakkiah *et al.*, 2017). The CDKs and MAPKs are the largest families within the CMGC group, with 21 and 14 members, respectively (Keskitalo, 2017). According to Keskitalo (2017), kinase families within the CMGC group are highly conserved and exhibit a specific CMGC-insert segment which is absent in other protein kinases. This insert is located in the C-lobe and it binds to co-proteins that participate in kinase function (Kannan & Neuwald, 2004; Oruganty & Kannan, 2012; Keskitalo, 2017). CMGC kinases are regulated predominantly through tyrosine phosphorylation in the activation loop, or through the substrate pre-phosphorylation (Oruganty & Kannan, 2012; Keskitalo, 2017). CMGC kinases regulate a variety of cell functions including control of the cell (CDKs), cell fate decisions (MAPKs), regulation of multiple signalling pathways (GSKs) and ribonucleic acid (RNA) splicing (CLKs) (Keskitalo, 2017; Sakkiah *et al.*, 2017).

2.2.1.5 RGC kinase group

The receptor guanylyl cyclase (RGC) group is the smallest family of kinases (Duong-Ly & Peterson, 2013). This family is characterised by a set of four structural motifs, namely; an extracellular ligand binding domain, a transmembrane domain, an intracellular protein kinase-like domain and an intracellular catalytic domain (Aparicio & Applebury, 1996). According to Manning *et al.* (2002), members of the RGC group are similar in sequence to tyrosine kinases and they have a catalytically inactive domain (Manning, 2005). Aparicio and Applebury (1996) reported that the kinase activity of RGC kinases is dependent on Mg^{2+}. Furthermore, the kinase activity of this group is unaffected by Ca^{2+}, cyclic nucleotides and phorbols, but it is inhibited by high concentrations of staurosporine (Aparicio & Applebury, 1996).

2.2.1.6 CK1 group

Casein kinases (CK) are serine/threonine kinases which exist in two isoforms, CK1 and CK2 due to the high conservation in their catalytic domains (Schittek & Sinnberg, 2014). Seven CK1 isoforms (α, β, γ1, γ2, γ3, δ and ε) have been identified in vertebrates, and they differ in length and sequence of the N-terminal (9-76 amino acids) and C-terminal (24-200 amino acids) non-catalytic domain (Schittek & Sinnberg, 2014). According to Schittek and Sinnberg (2014), the C-terminal domain plays an important role in the regulation of kinase activity. CK1 isoforms are highly conserved. For example, CK1δ and CK1ε have 98% sequence identity in their kinase domain, and they are 53% identical in their C-terminal regulatory domain (Schittek & Sinnberg, 2014). CK1 family members are involved in multiple cellular processes which include regulation of membrane trafficking, cytokinesis, vesicular transport, signal transduction pathway and circadian rhythm (Schittek & Sinnberg, 2014). Moreover, CK1 kinases regulate major signalling pathways which are involved in tumour progression (Schittek & Sinnberg, 2014).

2.2.1.7 STE group

The sterile (STE) serine/threonine kinases can be divided in to three classes based on the test proteins. These classes include: STE7 (MAP2K), STE11 (MAP3K) and STE20 (MAP4K) (Duong-Ly & Peterson, 2013). According to Duong-Ly and Peterson (2013), members of the STE family include the p21-activated kinases (Paks) which are important in regulating a variety of signalling pathways that are involved in normal cell survival and function. Paks elicit their biological effects by interacting with proteins or kinase substrates involved in regulatory pathways that contribute to cell transformation and tumour cell invasion (Kumar *et al.*, 2006). Pak1 is crucial for cell transformation that is induced by various oncogenes, and its overexpression occurs in several types of tumours (Kumar *et al.*, 2006; Duong-Ly & Peterson, 2013).

2.2.1.8 TKL group

Tyrosine kinase-like (TKL) kinases are serine/threonine protein kinases which resemble tyrosine kinases on an amino acid sequence level (Duong-Ly & Peterson, 2013). In addition, TKL is the most diverse group of protein kinases, containing both receptor and non-receptor kinases (Duong-Ly & Peterson, 2013). Members of the TKL group include interleukin 1 (IL-1) receptor-associated kinase (IRAK), RAF kinases, Lim domain kinases (LIMK) and the transforming growth factor beta (TGFβ) receptor (Duong-Ly & Peterson, 2013).

2.2.1.9 Haspin

Haploid germ cell-specific nuclear kinase (Haspin) proteins are highly divergent members of the eukaryotic protein kinase family (Amoussou *et al.*, 2018). They lack the ATP/Mg^{2+} binding motif Asp-Phe-Gly (DFG), and the Ala-Pro-Glu (APE) motif which is usually found at the C-terminal of the activation segment of ePKs. Haspin share only weak sequence homology with ePKs (Eswaran *et al.*, 2009). According to Feizbakhsh *et al.* (2017), human Haspin is a 798 amino acid serine/threonine kinase whose catalytic domain possesses special structural features that are absent in other members of the ePK family. The crystal structure of Haspin (figure 2.3) revealed that the N-terminal lobe is completely buried by an additional layer created by an N-terminal extension and two insertions (Amoussou *et al.*, 2018). In addition, there is reorganisation of the activation segment, which leads to the creation of an unusual substrate-binding site (Amoussou *et al.*, 2018). Other structural features include an additional insertion between β7 and β8 loop that contains two β-strands (Amoussou *et al.*, 2018). Haspin specifically phosphorylates Histone H3 at threonine-3 (H3T3ph) in mitotic cells (Qhobosheane *et al.*, 2020a), and this essentially occurs at the inner centromere regions (Eswaran *et al.*, 2009).
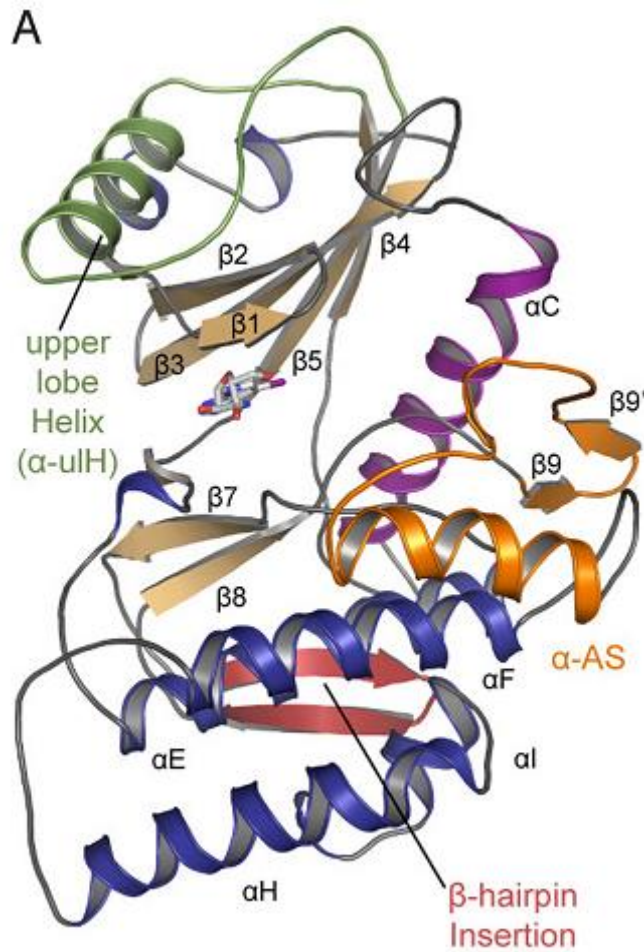
Figure 2.3: Overall structure of Haspin (Eswaran *et al.*, 2009)

2.2.2 Protein kinases in diseases

Protein phosphorylation is a mechanism by which various cellular processes are regulated, and it occurs predominantly at serine residues, while phosphorylation of threonine and tyrosine residues is considerably rare (St-Denis & Gingras, 2012). Reversible phosphorylation is crucial for coordination of cellular functions such as protein synthesis, cell division, metabolism, signal transduction, cell growth, development, aging, survival and apoptosis (Shchemelinin *et al.*, 2006; Ardito *et al.*, 2017). Aberrant protein phosphorylation leads to many diseases including cancer, diabetes, inflammatory disease and neurodegeneration (Cohen, 2005; St-Denis & Gingras, 2012). According to Wilson *et al.* (2018), more than 450 kinases have been implicated in development and progression of diseases. Of these, at least 448 kinases have been linked to various genetic and signalling hallmarks of cancer, while 230 kinases likely play a role in the development of other diseases (Wilson *et al.*, 2018). It is interesting to note that many tumour suppressor genes and dominant oncogenes identified to

date are protein kinases (Devanand, 2017). For example, c-Src, c-Abl, MAPK, PI3K, protein kinase B (also known as Akt) and EGFR are often activated in cancer cells, and they contribute to tumorigenesis (Devanand, 2017). Thus, protein kinases have become one of the most important drug targets in oncology.

2.2.3 Protein kinase inhibitors

Protein kinase inhibitors are chemically diverse, low-molecular weight, hydrophobic heterocycles (Shchemelinin *et al.*, 2006), which can be categorised according to their mechanisms of action as reversible (noncovalent) and irreversible (covalent) inhibitors (Fabbro, 2015; Bhullar *et al.*, 2018). Noncovalent inhibitors are predominantly non-selective, and they bind either competitively or non-competitively to the ATP binding site of the kinase domain (Duong-Ly & Peterson, 2013). With a few exceptions like the rapalogs (e.g. everolimus and temsirolimus) and trametinib (figure 2.4), most small molecular weight kinase inhibitors are directed towards the ATP-binding site (Fabbro, 2015). Because the ATP binding site is an evolutionarily well conserved region in nearly all kinases, these ATP mimics often cross-react with many other different kinases, resulting in compounds with promiscuous activity profiles, e.g. dasatinib and sunitinib (figure 2.4) (Arslan *et al.*, 2006; Fabbro, 2015).

Everolimus

Temsirolimus

Trametinib

Sunitinib
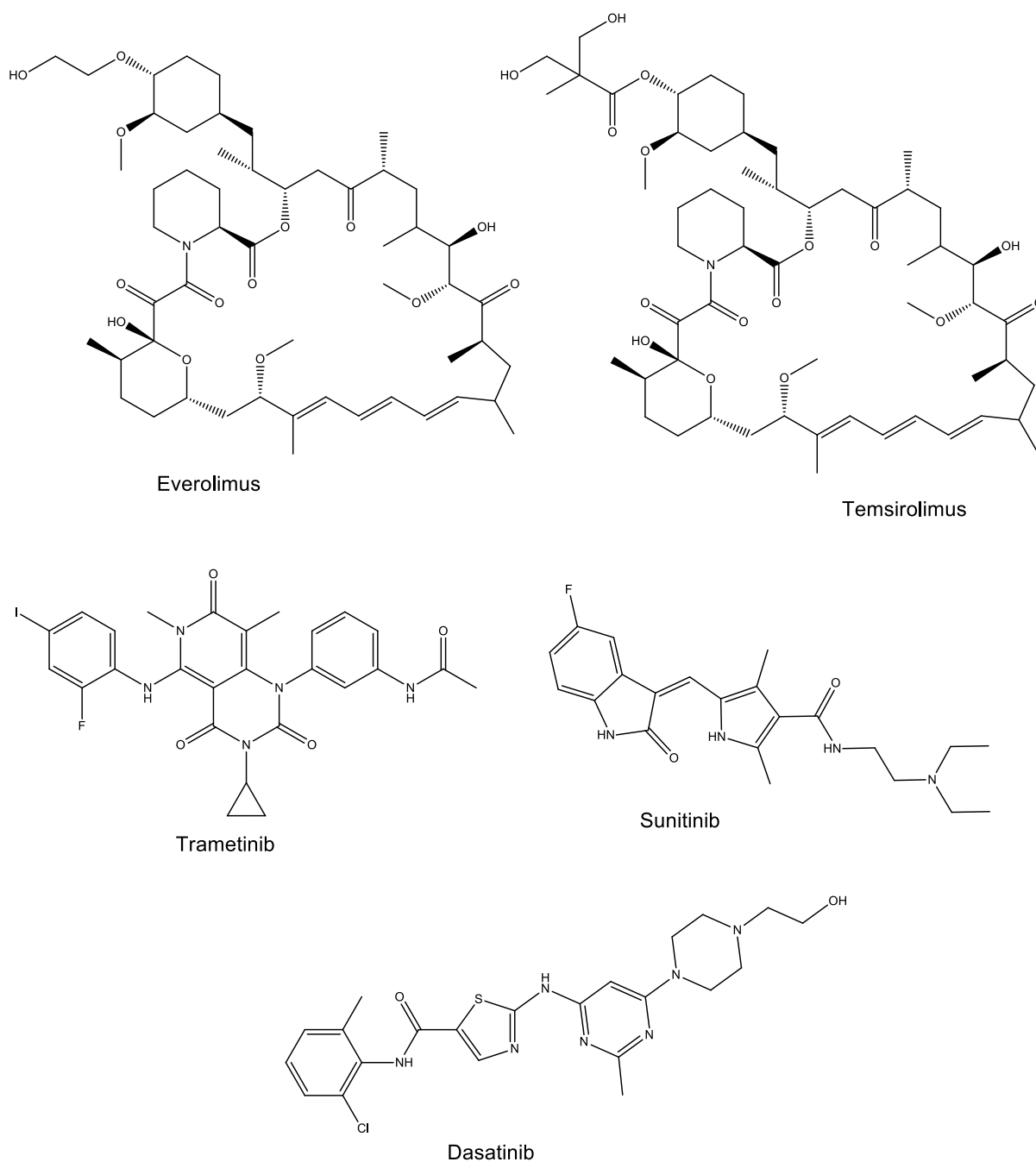
Dasatinib

Figure 2.4: Structures of everolimus, temsirolimus, trametinib, dasatinib and sunitinib.

2.2.3.1 ATP-competitive protein kinase inhibitors

ATP-competitive protein kinase inhibitors are kinase inhibitors which bind to the ATP-binding site of the enzyme, thus inhibiting its ability to drive catalysis (Devanand, 2017). The potencies of these inhibitors vary with ATP concentration (Duong-Ly & Peterson, 2013). ATP-competitive inhibitors are further classified as type I and type II inhibitors (Duong-Ly & Peterson, 2013). Type I inhibitors bind to the hinge region and target an active conformation of the kinase, which

is also known as the DFG-in conformation (Duong-Ly & Peterson, 2013; Fabbro, 2015). Type I inhibitors usually contain a heterocyclic system that occupies the purine binding site. The heterocyclic system serves as a core for side chains that occupy adjacent regions within the ATP binding site (Bhullar *et al.*, 2018). For example, erlotinib and gefitinib (figure 2.5) possess a quinazoline (core) moiety that mimics the adenine base of ATP and aniline rings (side chains) that bind to the back pocket of EGFR (Duong-Ly & Peterson, 2013). On the other hand, type II inhibitors target the inactive conformation (DFG-out) of kinases, maintaining contact to the hinge region and displaying similar behaviour to type I inhibitors (Duong-Ly & Peterson, 2013; Fabbro, 2015; Bhullar *et al.*, 2018). Type II inhibitors bind to an additional hydrophobic pocket adjacent to the ATP binding site (Fabbro, 2015), which is exposed by the conformational change of the DFG N-terminal loop from the active to the inactive conformation (Bhullar *et al.*, 2018). Imatinib (figure 2.5) is a type II inhibitor that targets Bcr-Abl kinase (Duong-Ly & Peterson, 2013). This compound possesses a 2-phenylaminopyrimidine ring which occupies the adenine pocket of the ATP binding site, consequently changing the orientation of the activation loop DFG motif (Duong-Ly & Peterson, 2013). Furthermore, the opening to the back hydrophobic pocket widens, allowing the pyrimidine ring of imatinib to bind to this region (Duong-Ly & Peterson, 2013).
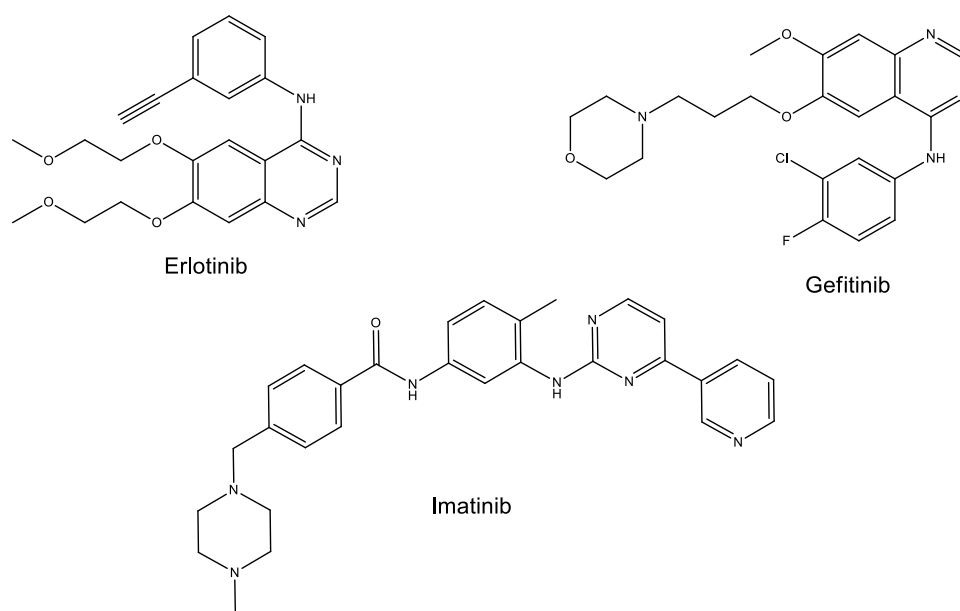

Figure 2.5: Structures of erlotinib, gefitinib and imatinib.

2.2.3.2 Non-ATP-competitive inhibitors

These are inhibitors whose potencies are not affected by ATP concentration because they bind outside the catalytic domain and regulate kinase activity in an allosteric manner (Duong-

Ly & Peterson, 2013; Bhullar *et al.*, 2018). Thus, non-ATP competitive inhibitors are known as allosteric inhibitors or type III inhibitors. Contrary to the ATP-competitive inhibitors, type III inhibitors are highly selective because they exploit binding sites and physiological mechanisms that are unique to a particular kinase (Duong-Ly & Peterson, 2013; Fabbro, 2015; Bhullar *et al.*, 2018). According to Bhullar *et al.* (2018), CI-1040 (figure 2.6) is one of the earliest highly specific allosteric inhibitors of MAPK/ ERK 1 (MEK1)/MEK2 pathway. Moreover, IPA-3 (figure 2.6) is a type III inhibitor of Pak1, which was identified by its ability to inhibit Pak1 in the presence of high concentrations of ATP (Duong-Ly & Peterson, 2013).
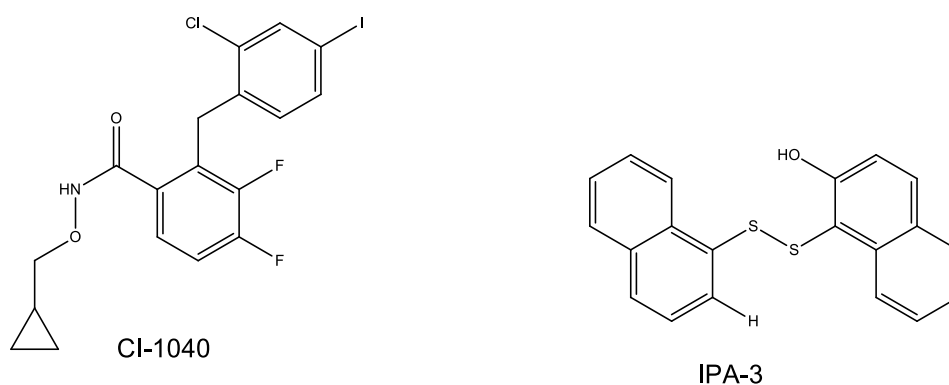
Figure 2.6: Structures of CI-1040 and IPA-3.

2.2.3.3 Substrate-directed inhibitors

These inhibitors are also known as type IV inhibitors, and they interact reversibly with the binding site outside the ATP binding pocket (Bhullar *et al.*, 2018). Type IV inhibitors are non-ATP competitive, as a result, they are highly selective against targeted kinases (Bhullar *et al.*, 2018). For example, ON012380 (figure 2.7) is a type IV inhibitor, which is selective against Bcr-Abl (Bhullar *et al.*, 2018).

Figure 2.7: Structure of ON012380.

2.2.3.4 Covalent inhibitors

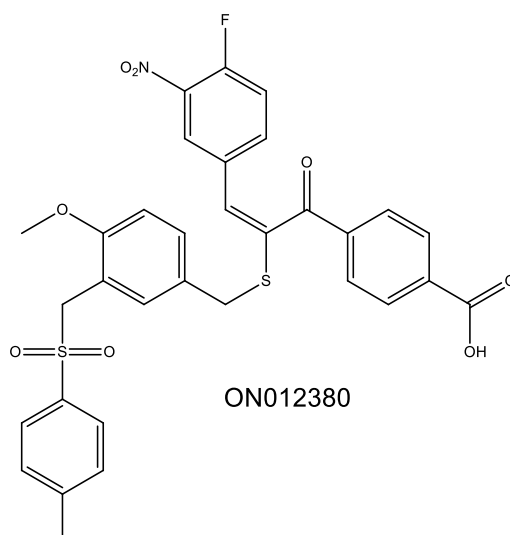These are irreversible inhibitors which form covalent bonds with the active site of kinases and target the catalytic nucleophilic cysteine within the kinase active site (Bhullar *et al.*, 2018). These inhibitors are also known as type V inhibitors, and they target specific kinases by forming a rapidly, reversible collision complex, which is followed by an irreversible enzyme-inhibitor complex (Bhullar *et al.*, 2018). The irreversible kinase inhibitors of EGFR (CL387785 and naretinib) (figure 2.8) were designed to target the cysteine residue located at the lip of the ATP binding pocket (Chahrour *et al.*, 2012).
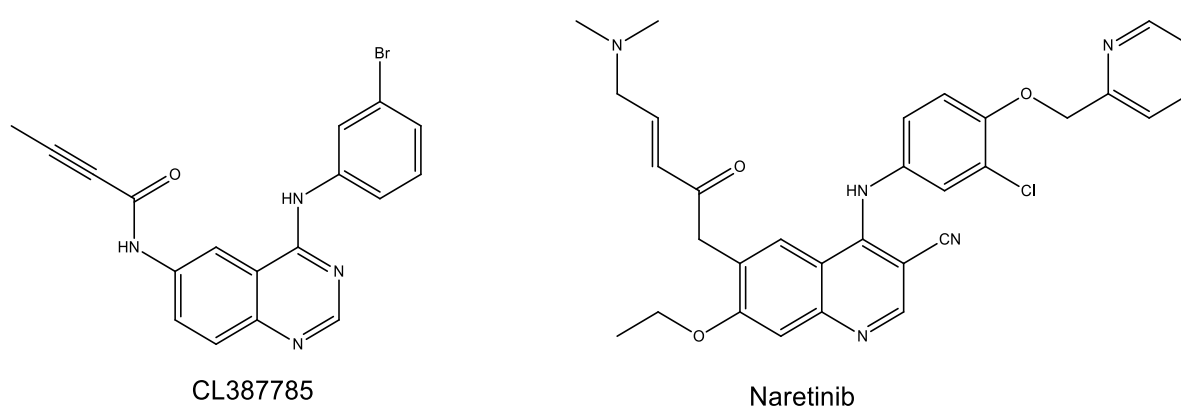

CL387785

Naretinib

Figure 2.8: Structures of CL387785 and naretinib.

2.2.4 Protein kinase inhibitors as anticancer drugs

Protein kinase inhibitors are potent anticancer drugs which target kinases that possess the oncogenic transformational capacity and mutations that primarily drive tumorigenesis. Their usage has tremendously improved the clinical management of cancer (Bhullar *et al.*, 2018). As of January 2020, approximately 52 small molecule kinase inhibitors were approved for clinical use (Roskoski, 2020). Of these, 28 drugs target RTKs, eleven target NRTKs, eleven target protein-serine/threonine protein kinases, while two are directed against dual specificity protein kinases (Roskoski, 2020). In addition, the majority of approved kinase inhibitors are used to treat malignancies including leukaemias and lymphomas, and a few of them are used for non-oncological indications such as ulcerative colitis, Crohn's disease, glaucoma, rheumatoid arthritis and organ rejection (Roskoski, 2020; Qhobosheane *et al.*, 2020a).

Bhullar *et al.* (2018) indicated that protein kinase inhibitors are classified according to the activation state of the protein kinase target, as well as the nature of the DFG-Asp, the C-helix, and the regulatory spine. Furthermore, most of these inhibitors form hydrophobic bonds with catalytic spine residues, interact with the RS3 R-spine residue inside the C-helix, and also interact with the gatekeeper residue (Bhullar *et al.*, 2018). According to Kannaiyan and Mahadevan (2018), the effectiveness of protein kinase inhibitors depends on the degree of addiction to the target kinase, as well as the pharmacodynamics and pharmacokinetic properties of the inhibitor.

2.2.4.1 CDK inhibitors

CDKs are serine/threonine protein kinases which are only activated in the presence of a regulatory partner (cyclins), and they are primarily involved in cell cycle regulation (Dai & Grant, 2003). Research has established that deregulation of CDK function is a fundamental characteristic of neoplastic cells (Dai & Grant, 2003; Balakrishnan *et al.*, 2016). For this reason, CDK inhibitors have gained extensive interest in cancer research (Dai & Grant, 2003). It has been theorised that CDK inhibitors halt the uncontrolled, cellular proliferation seen in cancer by blocking CDK (Balakrishnan *et al.*, 2016). CDK inhibitors are molecules that particularly inhibit the activities of CDK during cell cycle progression (Cheng & Scadden, 2009). They exist in two major classes; the inhibitor of cyclin-dependent kinase 4 (INK4) family, which specifically bind to and inhibit monomeric cyclin-D associated kinases (CDK4 and CDK6), and the Cip/Kip family, which inhibit most CDKs (Dai & Grant, 2003; Yang, 2012).

Flavopiridol (alvocidib) (figure 2.9) is a semisynthetic flavonoid, and a synthetic derivative of rohitukine ─ an alkaloid isolated from the bark of *Dysoxylum binectaferum*. Flavopiridol

possesses anti-inflammatory, immuno-modulatory and anticancer properties (Peyressatre *et al.*, 2015). Flavopiridol is the first CDK inhibitor tested in human clinical trials (Balakrishnan *et al.*, 2016), and it has demonstrated great potency against a wide range of CDKs (Dai & Grant, 2003; Peyressatre *et al.*, 2015). According to Chen *et al.* (2005), flavopiridol inhibits CDKs by competing with ATP. Flavopiridol has been shown to inhibit the activities of CDK1, CDK2, CDK4, CDK6 and CDK7 with inhibitory concentration at 50% (IC_{50}) values in the range of 20 to 300 nM; CDK1/CyclinB (IC_{50} = 30 – 40 nM), CDK2/CyclinA and CDK2/CyclinE (IC_{50} = 100 nM), CDK4/CyclinD (IC_{50} = 20 – 40 nM), CDK6/CyclinD (IC_{50} = 60 nM) and CDK7/CyclinH (IC_{50} = 110 – 300 nM) (Dai & Grant, 2003; Chen *et al.*, 2005). Furthermore, flavopiridol interferes with transcription of certain cell cycle and survival related genes such as c-myc by inhibiting CDK9, and this justifies its anticancer potency (Peyressatre *et al.*, 2015). Flavopiridol also acts against chronic lymphotic leukemia (CLL) cells *in vitro,* and in the treatment of advanced stage disease by mediating endoplasmic reticulum (ER) stress and downstream MAP3K5/apoptosis signal-regulating kinase 1 (ASK1), ultimately leading to cell death (Chen *et al.*, 2005; Mahoney *et al.*, 2013).
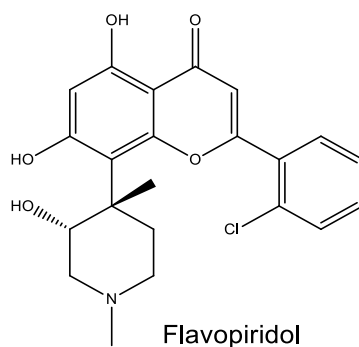

Figure 2.9: Structure of flavopiridol.

2.2.4.2 Haspin inhibitors

Haspin is associated with the phosphorylation of histone 3 during mitosis. Its overexpression or deletion results in defective mitosis (Amoussou *et al.*, 2018). Haspin inhibitors are considered to be efficient antimitotic agents (Huertas *et al.*, 2012), and considering that H3T3ph is the only substrate for Haspin, inhibition of Haspin might have fewer side-effects compared to other anticancer drugs (Amoussou *et al.*, 2018). A number of small molecule Haspin inhibitors has been discovered *via* high throughput screening, among which CHR-6494 (figure 2.10) demonstrated antiproliferative properties against a number of cell lines including cervical, colon and breast cancer cells (Han *et al.*, 2017). Previous studies have indicated that CHR-6949 blocked H3T3ph (IC_{50}= 2 nM), resulting in an irregular mitotic spindle, a defective

chromosomal alignment and centrosomes (Amoussou *et al.*, 2018). CHR-6949 has also been demonstrated to block basic FGF-induced vessel sprouting and suppressed tumour cell growth in a HCT-116 xenografted mouse model (Amoussou *et al.*, 2018).

5-Iodotubercidin (5-ITu) (figure 2.10) is another potent inhibitor (IC_{50} = 5-9 nM), which targets the ATP binding site of Haspin (De Antoni *et al.*, 2012). It causes dose-dependent displacement of chromosomal passenger complex (CPC) subunits (Amoussou *et al.*, 2018). Initially, 5-ITu was characterised as an adenosine kinase (Adk) inhibitor, for which it acts as both a substrate (i.e. it accepts the phosphoryl group from the nucleotide triphosphate) and an inhibitor (i.e. it competes with adenosine, which is the primary physiological substrate of Adk) (Kestav *et al.*, 2017; Amoussou *et al.*, 2018).
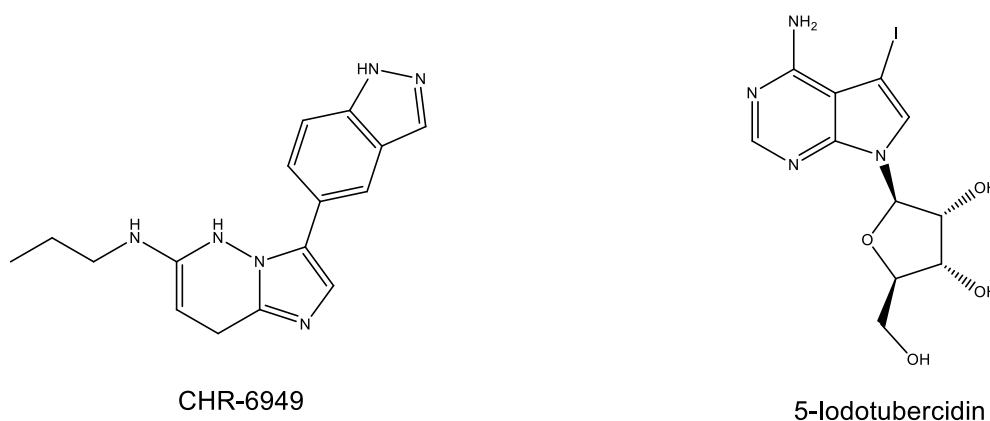

CHR-6949   5-Iodotubercidin

Figure 2.10: Structures of CHR-6949 and 5-iodotubercidin.

2.2.4.3 PIM inhibitors

Proviral integration site for moloney murine leukaemia virus (PIM) kinase is a serine/threonine kinase that exists in three isoforms; PIM-1, PIM-2 and PIM-3 (Tursynbay *et al.*, 2016; Asati *et al.*, 2019). These isoforms are widely distributed, and they are implicated in various cellular functions such as cell proliferation, cell differentiation, cell survival and apoptosis (Tursynbay *et al.*, 2016; Asati *et al.*, 2019). PIM plays an important role in development and progression of several cancers including myeloma, leukaemia, prostate and breast cancers (Tursynbay *et al.*, 2016). As a result, several medicinally privileged heterocyclic scaffolds such as benzofuran, indole, triazole, thiazolidine, oxazolidine, quinolone and pyrrole have been synthesised and evaluated as PIM inhibitors (Asati *et al.*, 2019).

According to Luszczak *et al.* (2020), monotherapeutic approaches (employing ATP-competitive inhibitors) are currently used in PIM kinase-based cancer treatment. AZD1208

(figure 2.11) is a highly potent, selective ATP-competitive pan-PIM kinase inhibitor that effectively inhibits all three isoforms at nanomolar potencies (Keeton *et al.*, 2014; Luszczak *et al.*, 2020). It inhibits cell growth and induces apoptosis in MOLM-16 cells (Keeton *et al.*, 2014), inhibits motility, changes cellular morphology and sensitises radiation (Luszczak *et al.*, 2020). TP-3654 (SGI-9481) (figure 2.11) is another potent small molecule pan-PIM inhibitor which targets PIM1, PIM2 and PIM3 with Ki (inhibition constant) values of 5 nM, 239 nM and 42 nM, respectively (Luszczak *et al.*, 2020). Luszczak *et al.* (2020) reported that TP-3654 also reduced phosphorylation of BCL2 associated agonist of cell death (BAD) protein expression, displayed no treatment toxicity and reduced tumour volume.
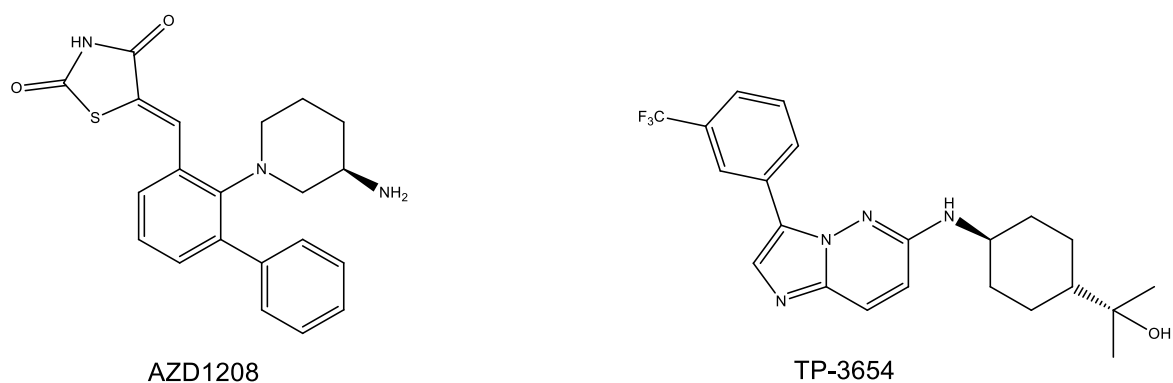

AZD1208   TP-3654

Figure 2.11: Structures of AZD1208 and TP-3654

2.2.4.4 CK1 inhibitors

Protein kinases of the CK1 family regulate various physiological processes including Wnt signalling, actin cytoskeleton, DNA damage response and circadian rhythms (Bibian *et al.*, 2013; Liu *et al.*, 2019). Dysregulated expression, mutation and aberrant activity of CK1 are consequences of human pathologies including neurodegenerative disorders, sleep disorders and cancer (Bibian *et al.*, 2013; Liu *et al.*, 2019). According to Bibian *et al.* (2013), CK1 is highly expressed in some cancers, and it controls tumour cell growth, apoptosis, metabolism and proliferation. PF-670462 (figure 2.12) is a potent CK1δ/ε inhibitor which hinders the Wnt signalling, but only moderately inhibits cell proliferation (Cheong *et al.*, 2011). PF-670462 also inhibits microenvironmental interactions (i.e. chemotaxis, invasion and communication with stromal cells) in primary CLL cells (Janovska *et al.*, 2018).
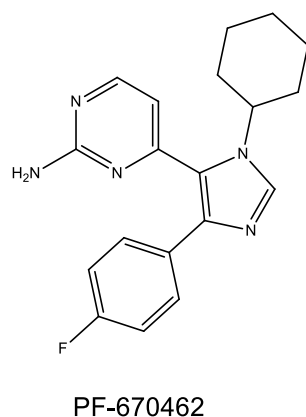
PF-670462

Figure 2.12: Structure of PF-670462.

2.2.4.5 GSK3 inhibitors

GSK-3 is a serine/threonine protein kinase which is also known as a "multitasking kinase" due to its versatile role in various signalling pathways (Saraswati *et al.*, 2018). According to Tejeda-Muñoz and Robles-Flores (2015), GSK-3 regulates a wide range of signalling pathways including the Wnt signalling. Dysregulation of GSK-3 causes numerous human diseases including diabetes, obesity, inflammation, Alzheimer's disease and cancer. As a result, it is perceived as an attractive target in multiple disorders (Tejeda-Muñoz & Robles-Flores, 2015). In cancer, GSK-3β is well known for its ability to regulate post transcriptional activity of nuclear factor kappa-light-chain-enhancer of activated B cells (NF-κB), which is involved in tumour chemoresistance, neovascularisation, invasion of metastasis (Kuroki *et al.*, 2019). In addition, GSK-3β has been shown to regulate NF-κB-mediated cancer cell survival, and its inhibition decreases the survival of cancer cells through suppression of NF-κB-mediated Mcl-2 and X-linked inhibitor of apoptosis protein (XIAP) expression in leukaemia, pancreatic and renal cancer cells (Kuroki *et al.*, 2019). Kuroki *et al.* (2019) investigated the antitumor effects of a small molecule GSK-3β inhibitor (9-ING-41) (figure 2.13) and established that it causes cell cycle arrest, autophagy and apoptosis in bladder cancer.
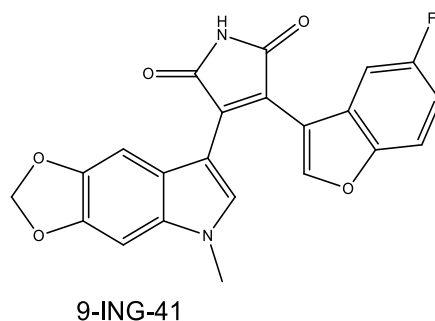
9-ING-41

Figure 2.13: Structure of 9-ING-41

2.2.4.6   TK inhibitors

TK is one of the major signalling enzymes involved in cell signal transduction; it regulates cell growth, differentiation and death (Jiao *et al.*, 2018). According to Jiao *et al.* (2018), abnormal expression of tyrosine kinase leads to uncontrolled cell proliferation, and is associated with tumour invasion, metastasis and tumour angiogenesis. TK inhibitors (TKIs) compete with ATP for the catalytic domain of some oncogenic tyrosine kinases (Arora & Scholar, 2005), thereby hindering cancer cell proliferation (Jiao *et al.*, 2018). TKIs are classified according to targets on which they act, namely Bcr-Abl TKIs (e.g. imatinib, dasatinib and nilotinib), EGFR TKIs (e.g. gefitinib and erlotinib) and VEGFR TKIs (e.g. sunitib and sorafenib). TKIs may also be classified according to their generations (Ho *et al.*, 2019). Four generations of TKIs exist, which differ by the period during which they were discovered, and also by their mechanisms of action. First generation TKIs (e.g. imatinib and gefitinib) are reversible ATP-competitive single target inhibitors, while second generation (e.g. afatinib (figure 2.14) and dasatinib) and newer generation TKIs like osimertinib (figure 2.14) are primarily irreversible and multi-targeted (Ho *et al.*, 2019).

Imatinib was the first TKI developed and introduced into clinical oncology (Hartmann *et al.*, 2009; Ho *et al.*, 2019). In 2001, imatinib was approved for the treatment of chronic myeloid leukaemia (CML) (Pray, 2008; Ho *et al.*, 2019). It has also proven to be effective in steroid refractory chronic graft-versus-host because of its anti- PDGFR action (Iqbal & Iqbal, 2014). According to Marcucci *et al.* (2003), imatinib binds to the ATP binding site of Bcr-Abl and stabilises the inactive non-ATP-binding form of Bcr-Abl. This prevents tyrosine autophosphorylation. This process consequently leads to "switching off" the downstream signalling pathways that promote leukemogenesis (Marcucci *et al.*, 2003; Iqbal & Iqbal, 2014).
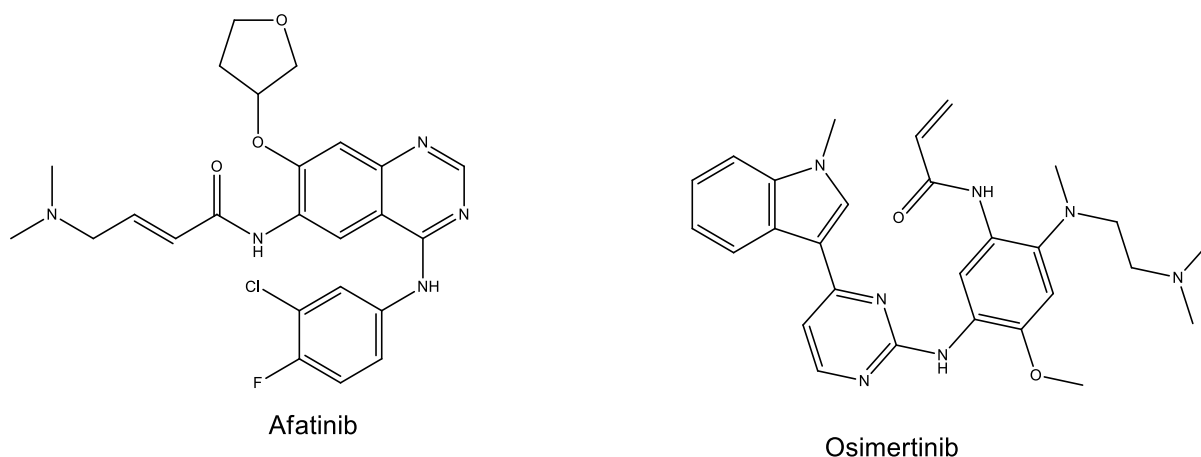
Figure 2.14: Structures of afatinib and osimertinib

2.2.5 Kinase resistance in cancer

Cancers are caused by alteration of various molecular pathways, and they can develop diverse mechanisms of resistance to therapy with single agents (Humphrey *et al.*, 2011). Selective anticancer drugs should specifically eliminate tumours and reduce adverse effects in healthy cells. However, the effectiveness of single target agents is short-lived due to development of resistance (Stankovic *et al.*, 2018). Bhullar *et al.* (2018) have reported two types of anticancer drug resistance; *de novo* resistance and acquired resistance. *De novo* resistance is the inability of an agent to produce any detectable response after initial treatment, while acquired resistance is the ability of a tumour to advance in the presence of treatment to which it initially responded (Bhullar *et al.*, 2018). Most of the kinase resistant cases are acquired, and they are caused by mutations of the kinase gatekeeper residue (Bhullar *et al.*, 2018). According to Bhullar *et al.* (2018), changes in the gatekeeper residue hinder the activity of kinase inhibitors because this residue allows the inhibitor to access the "gated" hydrophobic regions of the binding pocket.

2.2.6 Strategies to overcoming protein kinase resistance in cancer treatment

2.2.6.1 Multiple kinase inhibition

Inhibiting multiple targets with a single drug is known as polypharmacology, and it is an effective strategy to overcoming drug resistance (Stankovic *et al.*, 2018; Qhobosheane *et al.*, 2020a). Multi-target agents offer an opportunity to effectively halt tumour progression, while avoiding mechanisms of resistance that are commonly activated by the tumour (Daydé-Cazals *et al.*, 2016). Moreover, multi-targeted kinase inhibitors can be used to treat a wide range of

cancers and they are effective as combination therapy, but lack the disadvantages associated with combination therapy such as drug-drug interactions and multiple side-effects (Daydé-Cazals *et al.*, 2016). According to Daydé-Cazals *et al.* (2016), most TKIs are multikinase inhibitors that simultaneously target several kinases, consequently affecting multiple cellular processes deregulated in cancers. Imatinib is a multikinase inhibitor which targets Bcr-Abl, as well as PDGFR and mast/stem cell growth receptor (c-KIT) (Stankovic *et al.*, 2018). Furthermore, ZD6474 is a competitive inhibitor of ATP binding site of VEGFR-2. It also inhibits EGFR-1 at nanomolar concentrations (De Jonge & Verweij, 2006).
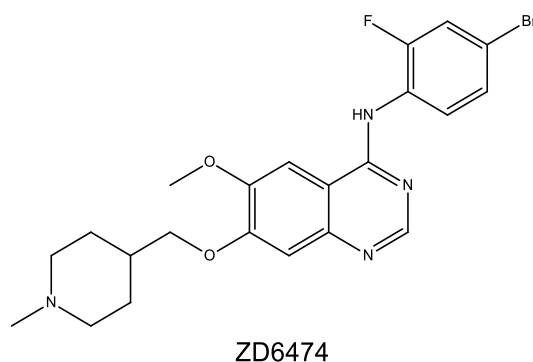

ZD6474

Figure 2.15: Structure of ZD6474.

2.2.6.2 Combination therapy

Combination therapy is another treatment strategy in cancer therapy (Lu *et al.*, 2013). Its therapeutic benefits have been proven to exceed those of monotherapies (Humphrey *et al.*, 2011). An ideal combination therapy must possess clinically proven active single agents which have no overlapping toxicities and no cross-resistance (Zhang *et al.*, 2016). These single agents must have different mechanisms of action and target different cell cycles (Zhang *et al.*, 2016). Many new combination therapies are currently undergoing early phase clinical studies; for example, the combination of a first generation EGFR TKI (gefitinib) with osimetinib is currently in phase III clinical trials (Pottier *et al.*, 2020). By far, the combination of gefitinib and carboplatin/pemetrexed is the recommended first line treatment for non-small-cell lung carcinoma (NSCLC) (Pottier *et al.*, 2020). Furthermore, nanomedicine of synergistic drug combinations has also shown promising superior therapeutic effects to current combination therapy used in clinical practice (Zhang *et al.*, 2016). According to Zhang *et al.* (2016), two drugs combination can be delivered using several ways, i.e. one drug can be delivered by a

nanocarrier, and the other as a free form, or both drugs can be co-encapsulated into the same nanocarrier (Zhang *et al.*, 2016).

2.3   7-Azaindoles

2.3.1   General background

Azaindoles are the most biologically active pyrrolopyridine derivatives. They possess anticancer properties and other therapeutic effects (El-Gamal & Anbar, 2017). The 7-azaindoles (1H-Pyrrolo[2,3-b]pyridine) are the most widely studied analogues of the indole ring system (Saify *et al.*, 2014), and they are present in only a few naturally occurring products such as alkaloids from the variolin family (Popowycz *et al.*, 2007). 7-Azaindole (figure 2.16) contains one nitrogen atom in the 5-membered pyrrole ring and one nitrogen atom in the pyridine ring (Mérour & Joseph, 2001), and it is considered a bioisostere of the purine moiety (Popowycz *et al.*, 2007). According to Popowycz *et al.* (2007), the pyridine N-atom of 7-azaindole is a hydrogen bond acceptor while the pyrrole NH is a hydrogen bond donor. At room temperature, 7-azaindole tautomerises as a result of proton transfer reactions (Mérour & Joseph, 2001).
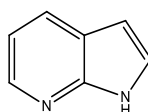

Figure 2.16: General structure of 7-azaindole

7-Azaindole is considered a privileged scaffold because of its ability to reversibly bind to the hinge region of various protein kinases (Sudhamani *et al.*, 2016; Qhobosheane *et al.*, 2020b). It has attracted tremendous attention because of its broad spectrum of biological activities, which include antimicrobial activity against Gram-negative and Gram-positive bacteria (Saify *et al.,* 2015), analgesic and hypotensive properties (Mushtaq *et al.*, 2008), anti-angiogenic, antifungal, antiviral, antimalarial, antiproliferative, antimycobacterial and anticancer properties (Sudhamani *et al.*, 2016). A study carried out by Yang *et al.* (2017) revealed four derivatives of 7-azaindole (**1-4**, figure 2.17) as potent inhibitors of PI3K. These derivatives exhibited subnanomolar activity, and displayed potent antiproliferative activities against a panel of human tumour cells. Moreover, the 7-azaindole scaffold has been used to synthesise inhibitors of various protein kinases, antihistamines, dopamine antagonists and antagonists of the corticotropin and gonadotropin releasing hormone (Schirok, 2006).
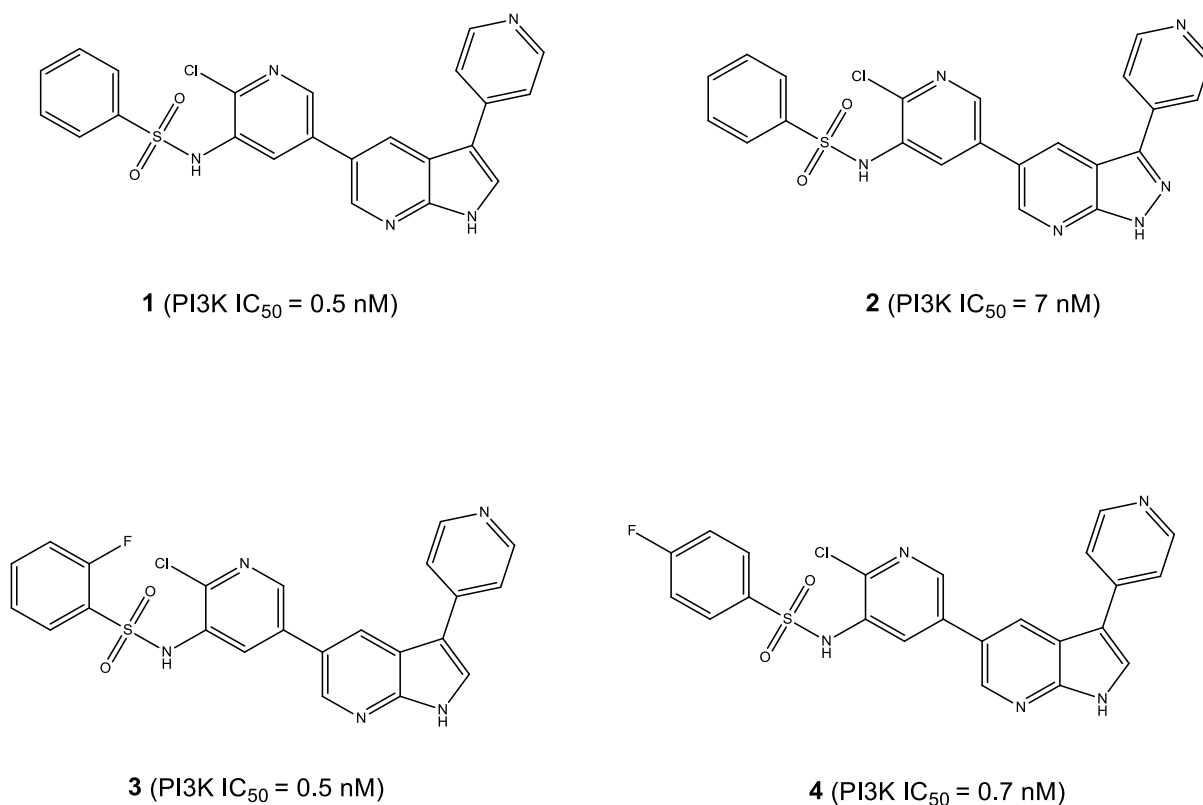
1 (PI3K IC$_{50}$ = 0.5 nM)

2 (PI3K IC$_{50}$ = 7 nM)

3 (PI3K IC$_{50}$ = 0.5 nM)

4 (PI3K IC$_{50}$ = 0.7 nM)

Figure 2.17: 7-Azaindole based PI3K kinase inhibitors (Yang *et al.*, 2017)

2.3.2 Synthetic methods

The 7-azaindole scaffold can be synthesised by employing the conventional synthetic strategies (Fischer, Madelung, or Reissert reaction) used to prepare the indole core, however, these methods result in poor yields (Popowycz *et al.*, 2007). Several methods of synthesis have been used to prepare the 7-azaindoles (figure 2.18) (Mérour & Joseph, 2001). The most general method involves annulation of a pyrrole into the preformed pyridine ring (Mérour & Joseph, 2001). The Pd-catalysed coupling of 2-amino-3-halogenopyridines has been used to attach the C3-C3a bond (**A**), accompanied by intramolecular cyclisation to form the five-membered ring (**B**), which is accomplished by the use of strong bases (e.g. KH, KOtBu or CstBu) (Rodriguez *et al.*, 2000; Schirok, 2006), iodine, copper iodide or palladium catalysts (Schirok, 2006). In addition, 7-azaindoles may be synthesised using Pd-catalysed annulation of 2-amino-3-iodopyridines with allele acetate (**C**) (Schirok, 2006). Carbolithiation of vinyl pyridines also affords 7-azaindoles (**D**) (Schirok, 2006). According to Schirok (2006), other synthetic methods include cyclisation of (2-aminopyridin-3-yl)methylphosphonates (**E**), the intramolecular Hedegus-Mori-Heck reaction of enamines or enaminones (**F**), as well as the Hemetsberger-Knittel reaction (**G**) and a Sommelet-Hauser type rearrangement of azasulfonium salts (**H**) (Schirok, 2006).
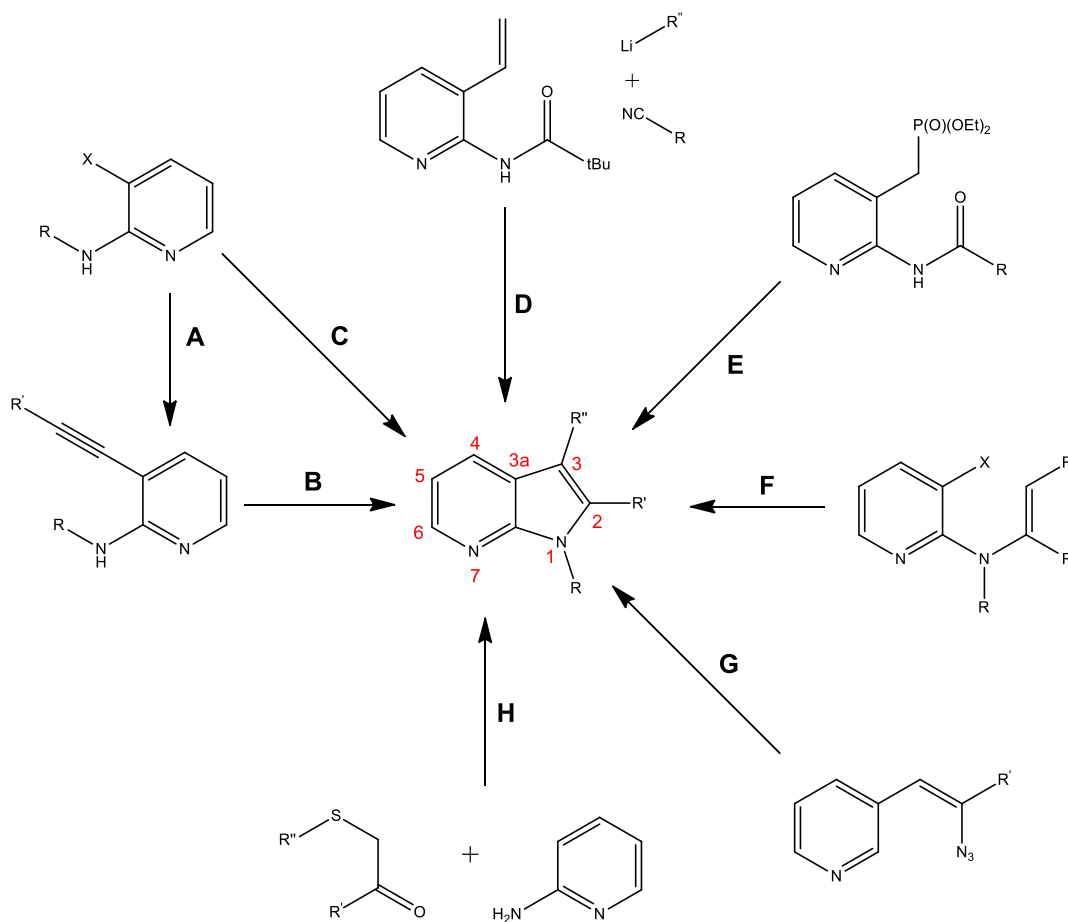
35

Figure 2.18: Routes of synthesis of the 7-azaindole skeleton reported by Schirok (2006).

2.4 Chalcones

2.4.1 General background

Chalcones are naturally occurring compounds which are considered precursors of flavonoids and isoflavonoids. They are abundant in a variety of edible plants (Patil *et al.*, 2009; Zhou & Xing, 2015; Zhuang *et al.*, 2017). Chalcones, also known as chalconoids, have two aromatic rings (ring A and ring B) linked by a three-carbon α,β-unsaturated carbonyl system (Patil *et al.*, 2009; Zhuang *et al.*, 2017; Amakali *et al.*, 2018). According to Zhuang *et al.* (2017), chalcones exist as *cis* and *trans* isomers (figure 2.19), in which the *trans* isomer is the most thermodynamically stable. Natural and synthetic chalcones are well documented due to their wide range of biological activities, which include anti-inflammatory, antidiabetic, anticancer (Zhuang *et al.*, 2017), antimicrobial, antiviral, cytotoxic and antioxidative properties (Tekale *et al.*, 2020). To date, chalcone derivatives have been used to treat cardiovascular diseases, viral diseases and stomach cancer (Tekale *et al.*, 2020).
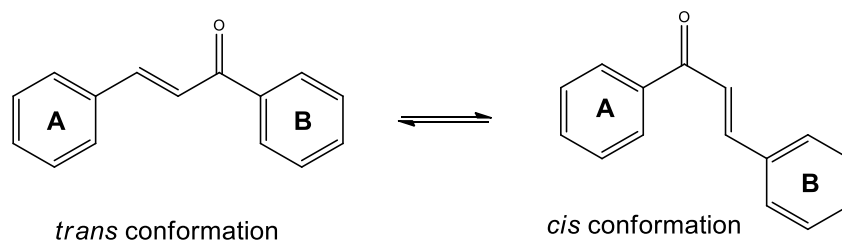
trans conformation   cis conformation

Figure 2.19: General structure of a chalcone

Chalcones have demonstrated promising therapeutic activity against several types of cancer, and they have also displayed activity as inhibitors of TK-EGFR (Sangpheak *et al.*, 2019). Alswah *et al.* (2018) evaluated a series of novel triazoloquinoxaline-chalcone hybrids, which demonstrated dual EGFR-TKI and tubulin polymerisation inhibition activities. The most potent of these inhibitors (**5** and **6**, figure 2.20) exhibited IC_{50} values of 0.083 μM and 0.039 μM, respectively against EGFR (Alswah *et al.*, 2018).

5 (EGFR IC_{50} = 0.083 μM)   **6** (EGFR IC_{50} = 0.039 μM)
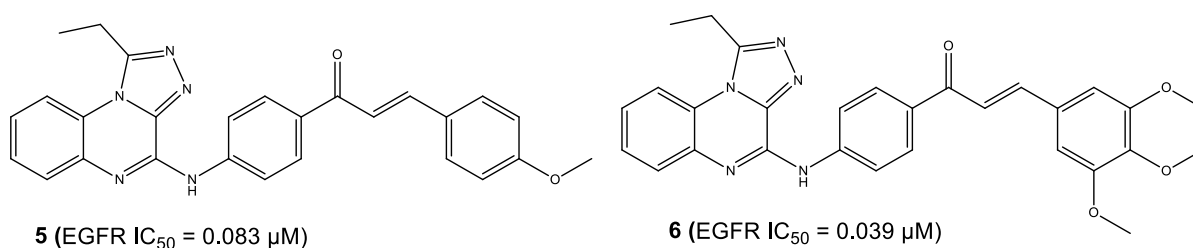
Figure 2.20: Novel triazoloquinoxaline-chalcone hybrids reported by Alswah *et al.* (2018).

2.4.2 Synthetic methods

Chalcones can be synthesised by plants through different cyclisation methods which use coumaroyl-Coenzyme A (CoA) and malonyl-CoA (Bode & Müller, 2003). Several synthetic techniques have been reported for the synthesis of chalcones, and Aldol condensation and Claisen-Schmidt condensation are the most commonly used (Syed *et al.*, 2013). Other synthetic methods include Suzuki reaction, Witting reaction, Friedel-Crafts acylation with cinnamoyl chloride and Photo-Fries rearrangement of phenyl cinnamates (Syed *et al.*, 2013).

2.4.2.1 Biosynthesis

Chalcone synthase (CHS) is the first type III polyketide synthase (PKS) which is abundantly found in higher plants (Zhuang *et al.*, 2017). CHS exists as a homodimer which has a

conserved active site that is constituted by Cys164, Phe215, His303 and Asn303 (Zhuang *et al.*, 2017). The initial step in the biosynthesis of chalcones is the transfer of a coumaroyl moiety from one 4-coumaroyl-CoA to Cys164, and this is followed by formation of an intermediate from three malonyl-CoA thioesters, via a polyketide reaction (figure 2.21) (Zhuang *et al.*, 2017). According to Zhuang *et al.* (2017), a regiospecific Claisen-type cyclisation occurs after the generation of a thioester-linked tetraketide, and it forms a new ring system to generate naringenin chalcone. Naringenin chalcone is then converted into 6'-deoxynaringenin (isoliquiritigenin/ 6'-deoxychalcone) in the presence of chalcone reductase (Zhuang *et al.*, 2017).
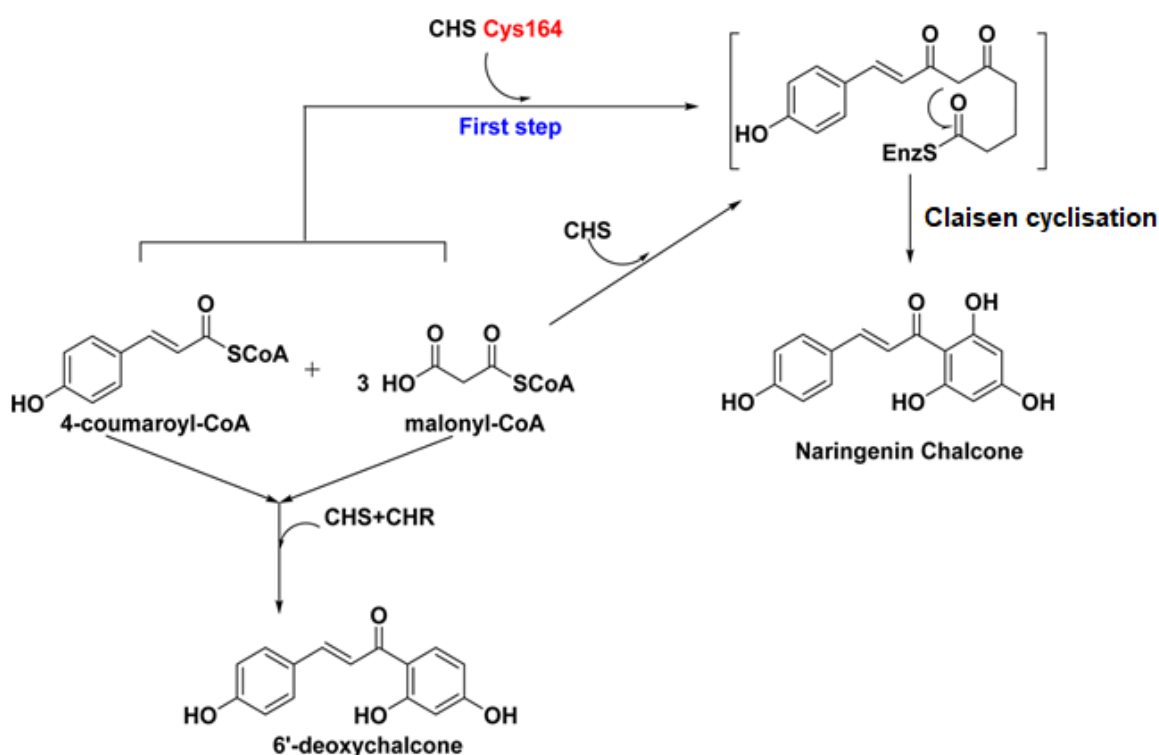
Figure 2.21: Biosynthesis of chalcones depicted by Zhuang *et al.* (2017).

2.4.2.2 Chemical synthesis

The most common method of synthesising chalcone is the Claisen-Schmidt condensation (figure 2.22), which involves aldol condensation of various acetophenones with a variety of aryl and/or heteroaryl aldehydes, followed by dehydration (Patil *et al.*, 2009; Padarthi *et al.*, 2013). Syed *et al.* (2013) states that the condensation leads to formation of an α,β-unsaturated

ketone. This classical Claisen-Schmidt condensation is carried out in the presence of a basic or an acidic catalyst (Patil *et al.*, 2009; Ahmad *et al.*, 2016; Zhuang *et al.*, 2017).
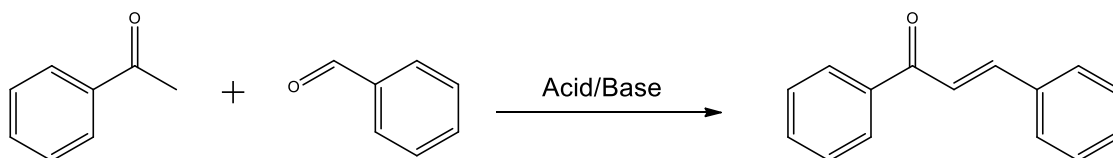

Figure 2.22: Claisen-Schmit condensation of chalcones.

2.5   Summary

Cancer is the uncontrolled growth of abnormal cells, which is caused by various factors. It is the second leading cause of death worldwide. Aberrant phosphorylation of protein kinases plays a key role in the pathology of some cancers, as a result, protein kinases are deemed promising targets in the discovery of anticancer drugs. Chalcones and 7-azaindoles possess a multitude of biological activities, among which are protein kinase inhibition, antiproliferative and anticancer properties. Chalcone derivatives of 7-azaindole have been reported to possess excellent binding affinities for B-Raf kinases (Giles *et al.*, 2019). The present study aims to investigate the biological activities of 7-azaindole-based chalcones against a panel of cancer-related protein kinases.

References

Ahmad, M.R., Sastry, V.G., Bano, N. & Anwar, S. 2016. Synthesis of novel chalcone derivatives by conventional and microwave irradiation methods and their pharmacological activities. *Arabian journal of chemistry*, 9:S931-S935.

Alswah, M., Bayoumi, A.H., Elgamal, K., Elmorsy, A., Ihmaid, S. & Ahmed, H.E. 2018. Design, synthesis and cytotoxic evaluation of novel chalcone derivatives bearing triazolo [4, 3-a]-quinoxaline moieties as potent anticancer agents with dual EGFR kinase and tubulin polymerization inhibitory effects. *Molecules*, 23(1):48.

Amakali, K.T., Legoabe, L.J., Petzer, A. & Petzer, J.P. 2018. Synthesis and in vitro evaluation of 2-heteroarylidene-1-tetralone derivatives as monoamine oxidase inhibitors. *Drug research*, 68(12):687-695.

Amoussou, N.G., Bigot, A., Roussakis, C. & Robert, J. M.H. 2018. Haspin: a promising target for the design of inhibitors as potent anticancer drugs. *Drug discovery today*, 23(2):409-415.

Aparicio, J.G. & Applebury, M.L. 1996. The photoreceptor guanylate cyclase is an autophosphorylating protein kinase. *Journal of biological chemistry*, 271(43):27083-27089.

Ardito, F., Giuliani, M., Perrone, D., Troiano, G. & Lo Muzio, L. 2017. The crucial role of protein phosphorylation in cell signaling and its use as targeted therapy. *International journal of molecular medicine*, 40(2):271-280.

Arencibia, J.M., Pastor-Flores, D., Bauer, A.F., Schulze, J.O. & Biondi, R.M. 2013. AGC protein kinases: from structural mechanism of regulation to allosteric drug development for the treatment of human diseases. *Biochimica et biophysica acta (bba)-proteins and proteomics*, 1834(7):1302-1321.

Arora, A. & Scholar, E.M. 2005. Role of tyrosine kinase inhibitors in cancer therapy. *Journal of pharmacology and experimental therapeutics*, 315(3):971-979.

Arruebo, M., Vilaboa, N., Sáez-Gutierrez, B., Lambea, J., Tres, A., Valladares, M. & González-Fernández, Á. 2011. Assessment of the evolution of cancer treatment therapies. *Cancers*, 3(3):3279-3330.

Arslan, M.A., Kutuk, O. & Basaga, H. 2006. Protein kinases as drug targets in cancer. *Current cancer drug targets*, 6(7):623-634.

Arsova-Sarafinovska, Z. & Aleksandar, D. 2013. Natural antioxidants in cancer prevention. *Macedonian pharmaceutical bulletin*, 59:3-14.

Asati, V., Mahapatra, D.K. & Bharti, S.K. 2019. PIM kinase inhibitors: structural and pharmacological perspectives. *European journal of medicinal chemistry*, 172:95-108.

Avendaño, C. & Menéndez, J.C. 2015. Chapter 1 - General aspects of cancer chemotherapy. *(In* Avendaño, C. & Menéndez J.C., *eds.* Medicinal chemistry of anticancer drugs (second edition). Boston: Elsevier. p. 1-22).

Baker, S.J. & Reddy, E.P. 2010. Targeted inhibition of kinases in cancer therapy. *Mount Sinai journal of medicine: A journal of translational and personalized medicine*, 77(6):573-586.

Balakrishnan, A., Vyas, A., Deshpande, K. & Vyas, D. 2016. Pharmacological cyclin dependent kinase inhibitors: Implications for colorectal cancer. *World journal of gastroenterology*, 22(7):2159.

Bhullar, K.S., Lagaron, N.O., McGowan, E.M., Parmar, I., Jha, A., Hubbard, B.P. & Rupasinghe, H.P.V. 2018. Kinase-targeted cancer therapies: progress, challenges and future directions. *Molecular cancer*, 17(1):48.

Bibian, M., Rahaim, R.J., Choi, J.Y., Noguchi, Y., Schürer, S., Chen, W., Nakanishi, S., Licht, K., Rosenberg, L.H. & Li, L. 2013. Development of highly selective casein kinase 1δ/1ε (CK1δ/ε) inhibitors with potent antiproliferative properties. *Bioorganic & medicinal chemistry letters*, 23(15):4374-4380.

Bode, H.B. & Müller, R. 2003. Possibility of bacterial recruitment of plant genes associated with the biosynthesis of secondary metabolites. *Plant physiology*, 132(3):1153-1161.

Brzozowski, J.S. & Skelding, K.A. 2019. The multi-functional calcium/calmodulin stimulated protein kinase (CaMK) family: Emerging targets for anti-cancer therapeutic intervention. *Pharmaceuticals*, 12(1):8.

Cabuy, E. 2012. Thermal ablation in cancer treatment. *Reliable cancer therapies*, 2:1-68.

Cao, Y. 2017. Tumorigenesis as a process of gradual loss of original cell identity and gain of properties of neural precursor/progenitor cells. *Cell & bioscience*, 7(1):61.

Chahrour, O., Cairns, D. & Omran, Z. 2012. Small molecule kinase inhibitors as anti-cancer therapeutics. *Mini reviews in medicinal chemistry*, 12(5):399-411.

Chang, D., Lim, M., Goos, J.A.C.M., Qiao, R., Ng, Y.Y., Mansfeld, F.M., Jackson, M., Davis, T.P. & Kavallaris, M. 2018. Biologically targeted magnetic hyperthermia: Potential and limitations. *Frontiers in pharmacology*, 9(831).

Chen, R., Keating, M.J., Gandhi, V. & Plunkett, W. 2005. Transcription inhibition by flavopiridol: mechanism of chronic lymphocytic leukemia cell death. *Blood*, 106(7):2513-2519.

Cheng, T. & Scadden, D.T. 2009. Chapter 9 - cell cycle regulators in adult stem cells. *(In* Lanza, R., Gearhart J., Hogan B., Melton D., Pedersen R., Thomas E.D., Thomson J. & Wilmut I., *eds.* Essentials of stem cell biology (Second Edition). San Diego: Academic Press. p. 81-87).

Cheong, J., Hung, N., Wang, H., Tan, P., Voorhoeve, P., Lee, S. & Virshup, D. 2011. IC261 induces cell cycle arrest and apoptosis of human cancer cells via CK1δ/ε and Wnt/β-catenin independent inhibition of mitotic spindle formation. *Oncogene*, 30(22):2558-2569.

Cohen, P. 2005. Protein kinase inhibitors for the treatment of disease: the promise and the problems. *(In* Pinna, L.A. & Cohen P.T.W., *eds.* Inhibitors of protein kinases and protein phosphates. Springer. p. 1-7).

Cross, D. & Burmester, J.K. 2006. Gene therapy for cancer treatment: past, present and future. *Clinical medicine & research*, 4(3):218-227.

Dai, Y. & Grant, S. 2003. Cyclin-dependent kinase inhibitors. *Current opinion in pharmacology*, 3(4):362-370.

Daydé-Cazals, B., Fauvel, B., Singer, M., Feneyrolles, C., Bestgen, B., Gassiot, F., Spenlinhauer, A., Warnault, P., Van Hijfte, N., Borjini, N., Chevé, G. & Yasri, A. 2016. Rational design, synthesis, and biological evaluation of 7-azaindole derivatives as potent focused multi-targeted kinase inhibitors. *Journal of medicinal chemistry*, 59(8):3886-3905.

De Antoni, A., Maffini, S., Knapp, S., Musacchio, A. & Santaguida, S. 2012. A small-molecule inhibitor of Haspin alters the kinetochore functions of Aurora B. *Journal of cell biology*, 199(2):269-284.

De Jonge, M. & Verweij, J. 2006. Multiple targeted tyrosine kinase inhibition in the clinic: all for one or one for all? *European journal of cancer*, 42(10):1351-1356.

Devanand, V. 2017. Drugging protein kinases in cancer: From small molecules to nanoparticles. *MedCrave online journal of proteomics & bioinformatics*, 5(5):00173.

Dissmeyer, N. & Schnittger, A. 2011. The age of protein kinases. *(In* Dissmeyer, N. & Schnittger A., *eds*. Plant kinases. New Jersey: Springer. p. 7-52).

Dixit, A. & Verkhivker, G.M. 2014. Structure-functional prediction and analysis of cancer mutation effects in protein kinases. *Computational and mathematical methods in medicine*, 2014.

Duong-Ly, K.C. & Peterson, J.R. 2013. The human kinome and kinase inhibition as a therapeutic strategy. *Current protocols in pharmacology*, 2:1-21.

El-Azab, A.S. & ElTahir, K.E.H. 2012. Design and synthesis of novel 7-aminoquinazoline derivatives: Antitumor and anticonvulsant activities. *Bioorganic & medicinal chemistry letters*, 22(5):1879-1885.

El-Gamal, M.I. & Anbar, H.S. 2017. Recent advances of pyrrolopyridines derivatives: a patent and literature review. *Expert opinion on therapeutic patents*, 27(5):591-606.

Eswaran, J., Patnaik, D., Filippakopoulos, P., Wang, F., Stein, R.L., Murray, J.W., Higgins, J.M. & Knapp, S. 2009. Structure and functional characterization of the atypical human kinase haspin. *Proceedings of the National Academy of Sciences*, 106(48):20198-20203.

Fabbro, D. 2015. 25 years of small molecular weight kinase inhibitors: potentials and limitations. *Molecular pharmacology*, 87(5):766-775.

Fabbro, D., Cowan-Jacob, S.W. & Moebitz, H. 2015. Ten things you should know about protein kinases: IUPHAR Review 14. *British journal of pharmacology*, 172(11):2675-2700.

Feizbakhsh, O., Place, M., Fant, X., Buron, F., Routier, S. & Ruchaud, S. 2017. The mitotic protein kinase Haspin and its inhibitors. *(In* Prigent, C., *ed.* Protein phosphorylation. Croatia: InTech. p. 31-47).

Giles, D., Saiprabha, V. & Yeshna, G. 2019. Design of chalcones of 7-azaindole as raf-B inhibitors. *Journal of advanced chemical sciences*, 4(4):606-608.

Han, L., Wang, P., Sun, Y., Liu, S. & Dai, J. 2017. Anti-melanoma activities of haspin inhibitor CHR-6494 deployed as a single agent or in a synergistic combination with MEK inhibitor. *Journal of cancer*, 8(15):2933.

Hanahan, D. & Weinberg, R.A. 2011. Hallmarks of cancer: the next generation. *Cell*, 144(5):646-674.

Hanks, S.K. & Hunter, T. 1995. Protein kinases 6. The eukaryotic protein kinase superfamily: kinase (catalytic) domain structure and classification. *The FASEB journal*, 9(8):576-596.

Hartmann, J.T., Haap, M., Kopp, H.-G. & Lipp, H.-P. 2009. Tyrosine kinase inhibitors-a review on pharmacology, metabolism and side effects. *Current drug metabolism*, 10(5):470-481.

Ho, V.W.T., Tan, H.Y., Wang, N. & Feng, Y. 2019. Cancer management by tyrosine kinase inhibitors: Efficacy, limitation, and future strategies. *(In* Ren, H., *ed.* Tyrosine kinases as druggable targets in cancer. China: IntechOpen. p. 1-32).

Hubbard, S.R. & Till, J.H. 2000. Protein tyrosine kinase structure and function. *Annual review of biochemistry*, 69(1):373-398.

Huertas, D., Soler, M., Moreto, J., Villanueva, A., Martinez, A., Vidal, A., Charlton, M., Moffat, D., Patel, S. & McDermott, J. 2012. Antitumor activity of a small-molecule inhibitor of the histone kinase Haspin. *Oncogene*, 31(11):1408.

Humphrey, R.W., Brockway-Lunardi, L.M., Bonk, D.T., Dohoney, K.M., Doroshow, J.H., Meech, S.J., Ratain, M.J., Topalian, S.L. & Pardoll, D.M. 2011. Opportunities and challenges in the development of experimental drug combinations for cancer. *Journal of the national cancer institute*, 103(16):1222-1226.

Huse, M. & Kuriyan, J. 2002. The conformational plasticity of protein kinases. *Cell*, 109(3):275-282.

Iqbal, N. & Iqbal, N. 2014. Imatinib: a breakthrough of targeted therapy in cancer. *Chemotherapy research and practice*, 2014.

Janovska, P., Verner, J., Kohoutek, J., Bryjova, L., Gregorova, M., Dzimkova, M., Skabrahova, H., Radaszkiewicz, T., Ovesna, P. & Vondalova Blanarova, O. 2018. Casein kinase 1 is a therapeutic target in chronic lymphocytic leukemia. *Blood, the journal of the American Society of Hematology*, 131(11):1206-1218.

Jiao, Q., Bi, L., Ren, Y., Song, S., Wang, Q. & Wang, Y.-s. 2018. Advances in studies of tyrosine kinase inhibitors and their acquired resistance. *Molecular cancer*, 17(1):1-12.

Kanev, G.K., de Graaf, C., de Esch, I.J., Leurs, R., Würdinger, T., Westerman, B.A. & Kooistra, A.J. 2019. The landscape of atypical and eukaryotic protein kinases. *Trends in pharmacological sciences*, 40(11):818-832.

Kannaiyan, R. & Mahadevan, D. 2018. A comprehensive review of protein kinase inhibitors for cancer therapy. *Expert review of anticancer therapy*, 18(12):1249-1270.

Kannan, N. & Neuwald, A.F. 2004. Evolutionary constraints associated with functional specificity of the CMGC protein kinases MAPK, CDK, GSK, SRPK, DYRK, and CK2α. *Protein science*, 13(8):2059-2077.

Keeton, E.K., McEachern, K., Dillman, K.S., Palakurthi, S., Cao, Y., Grondine, M.R., Kaur, S., Wang, S., Chen, Y. & Wu, A. 2014. AZD1208, a potent and selective pan-Pim kinase inhibitor, demonstrates efficacy in preclinical models of acute myeloid leukemia. *Blood*, 123(6):905-913.

Keskitalo, S. 2017. CMGC kinases and cancer. Helsinki: University of Helsinki. (PhD-Thesis).

Kestav, K., Uri, A. & Lavogina, D. 2017. Structure, roles and inhibitors of a mitotic protein kinase haspin. *Current medicinal chemistry*, 24(21):2276-2293.

Kumar, R., Gururaj, A.E. & Barnes, C.J. 2006. p21-activated kinases in cancer. *Nature reviews cancer*, 6(6):459-471.

Kuroki, H., Anraku, T., Kazama, A., Bilim, V., Tasaki, M., Schmitt, D., Mazar, A.P., Giles, F.J., Ugolkov, A. & Tomita, Y. 2019. 9-ING-41, a small molecule inhibitor of GSK-3beta, potentiates the effects of anticancer therapeutics in bladder cancer. *Scientific reports*, 9(1):1-9.

Lacal, J.C. 2006. Changing the course of oncogenesis: The development of tyrosine kinase inhibitors. *European journal of cancer supplements*, 4(7):14-20.

Liu, C., Witt, L., Ianes, C., Bischof, J., Bammert, M.-T., Baier, J., Kirschner, S., Henne-Bruns, D., Xu, P. & Kornmann, M. 2019. Newly developed CK1-specific inhibitors show specifically stronger effects on CK1 mutants and colon cancer cell lines. *International journal of molecular sciences*, 20(24):6184.

Lu, D., Lu, T. & Cao, S. 2013. Drug combinations in cancer treatment. *Clinical experimental pharmacology*, 3(4):134.

Luszczak, S., Kumar, C., Sathyadevan, V.K., Simpson, B.S., Gately, K.A., Whitaker, H.C. & Heavey, S. 2020. PIM kinase inhibition: co-targeted therapeutic approaches in prostate cancer. *Signal transduction and targeted therapy*, 5(1):1-10.

Mahoney, E., Byrd, J.C. & Johnson, A.J. 2013. Autophagy and ER stress play an essential role in the mechanism of action and drug resistance of the cyclin-dependent kinase inhibitor flavopiridol. *Autophagy*, 9(3):434-435.

Manning, G. 2005. Genomic overview of protein kinases. In Iva, G. (Ed.). *WormBook* (pp. 1): C. *elegans* biology.

Manning, G., Whyte, D.B., Martinez, R., Hunter, T. & Sudarsanam, S. 2002. The protein kinase complement of the human genome. *Science*, 298(5600):1912-1934.

Marcucci, G., Perrotti, D. & Caligiuri, M.A. 2003. Understanding the molecular basis of imatinib mesylate therapy in chronic myelogenous leukemia and the related mechanisms of resistance. *Clinical cancer research*, 9(4):1248-1252.

Meharena, H.S., Chang, P., Keshwani, M.M., Oruganty, K., Nene, A.K., Kannan, N., Taylor, S.S. & Kornev, A.P. 2013. Deciphering the structural basis of eukaryotic protein kinase regulation. *PLoS biology*, 11(10).

Mérour, J.-Y. & Joseph, B. 2001. Synthesis and reactivity of 7-azaindoles (1H-Pyrrolo (2, 3-b) pyridine). *Current organic chemistry*, 5(5):471-506.

Mushtaq, N., Saify, Z., Noor, F., Takween, S., Akhtar, S., Arif, M. & Khan, K.M. 2008. Synthesis and pharmacological activities of 7-azaindole derivatives. *Pakistan journal of pharmaceutical sciences*, 21(1):36-39.

Oruganty, K. & Kannan, N. 2012. Design principles underpinning the regulatory diversity of protein kinases. *Philosophical transactions of the Royal Society B: biological sciences*, 367(1602):2529-2539.

Padarthi, P.K., Sridhar, S., Jagatheesh, K. & Elangovan, N. 2013. Synthesis and biological activity of imidazole derived chalcones and it's pyrimidines. *International journal of research in ayurveda and pharmacy* 4(3):355-362.

Patil, C.B., Mahajan. S. K. & Suvarna. AK. 2009. Chalcone: A versatile molecule. *Journal of pharmaceutical sciences and research*, 1(3):11-22.

Pearce, L.R., Komander, D. & Alessi, D.R. 2010. The nuts and bolts of AGC protein kinases. *Nature reviews molecular cell biology*, 11(1):9-22.

Peyressatre, M., Prével, C., Pellerano, M. & Morris, M.C. 2015. Targeting cyclin-dependent kinases in human cancers: from small molecules to peptide inhibitors. *Cancers*, 7(1):179-237.

Popowycz, F., Routier, S., Joseph, B. & Mérour, J.-Y. 2007. Synthesis and reactivity of 7-azaindole (1H-pyrrolo [2, 3-b] pyridine). *Tetrahedron*, 5(63):1031-1064.

Pottier, C., Fresnais, M., Gilon, M., Jérusalem, G., Longuespée, R. & Sounni, N.E. 2020. Tyrosine kinase inhibitors in cancer: Breakthrough and challenges of targeted therapy. *Cancers*, 12(3):731.

Pray, L. 2008. Gleevec: the breakthrough in cancer. *Nature education*, 1(1):37.

Pucci, C., Martinelli, C. & Ciofani, G. 2019. Innovative approaches for cancer treatment: current perspectives and new challenges. *Ecancermedicalscience*, 13.

Qhobosheane, M.A., Legoabe, L.J., Josselin, B., Bach, S., Ruchaud, S., Petzer, J.P. & Beteck, R.M. 2020a. Synthesis and evaluation of 7-azaindole derivatives bearing benzocycloalkanone motifs as protein kinase inhibitors. *Bioorganic & medicinal chemistry*, 28(11):115468.

Qhobosheane, M.A., Legoabe, L.J., Josselin, B., Bach, S., Ruchaud, S. & Beteck, R.M. 2020b. Synthesis and evaluation of C3 substituted chalcone-based derivatives of 7-azaindole as protein kinase inhibitors. *Chemical biology & drug design*.

Rakshambikai, R., Manoharan, M., Gnanavel, M. & Srinivasan, N. 2015. Typical and atypical domain combinations in human protein kinases: functions, disease causing mutations and conservation in other primates. *Royal Society of Chemistry Advances*, 5(32):25132-25148.

Robinson, D.R., Wu, Y.-M. & Lin, S.-F. 2000. The protein tyrosine kinase family of the human genome. *Oncogene*, 19(49):5548-5557.

Rodriguez, A.L., Koradin, C., Dohle, W. & Knochel, P. 2000. Versatile indole synthesis by a 5-endo-dig cyclization mediated by potassium or cesium bases. *Angewandte chemie international edition*, 39(14):2488-2490.

Roskoski, R. 2007. Enzyme Structure and Function. *(In* Enna, S.J. & Bylund D.B., *eds.* xPharm: The Comprehensive Pharmacology Reference. New York: Elsevier. p. 1-7).

Roskoski, R. 2020. Properties of FDA-approved small molecule protein kinase inhibitors: A 2020 update. *Pharmacological research*, 152:104609.

Ruddon, R.W. 2007. Cancer biology: Oxford University Press.

Saify, Z.S., Sultana, N., Khan, A. & Haider, S. 2015. (1H-Pyrrolo [2, 3-b] pyridine) 7-Azaindole derivatives and their antiurease, phosphodiesterase and ß-glucuronidase activity. *International journal of biochemistry research & review*, 8(1):1-2.

Saify, Z.S., Sultana, N., Mushtaq, N. & Hasan, N.Z.U. 2014. (1H-Pyrrolo [2, 3-B] Pyridine) 7-Azaindole as cholinesterase/glycation inhibitors. *International journal of biochemistry research & review*, 4(6):624.

Sakkiah, S., Ping Cao, G., P Gupta, S. & Woo Lee, K. 2017. Overview of the structure and function of protein kinases. *Current enzyme inhibition*, 13(2):81-88.

Sangpheak, K., Tabtimmai, L., Seetaha, S., Rungnim, C., Chavasiri, W., Wolschann, P., Choowongkomon, K. & Rungrotmongkol, T. 2019. Biological evaluation and molecular dynamics simulation of chalcone derivatives as epidermal growth factor-tyrosine kinase inhibitors. *Molecules*, 24(6):1092.

Saraswati, A.P., Ali Hussaini, S.M., Krishna, N.H., Babu, B.N. & Kamal, A. 2018. Glycogen synthase kinase-3 and its inhibitors: potential target for various therapeutic conditions. *European journal of medicinal chemistry*, 144:843-858.

Sawyers, C. 2004. Targeted cancer therapy. *Nature*, 432(7015):294-297.

Schirok, H. 2006. Microwave-assisted flexible synthesis of 7-azaindoles. *The Journal of organic chemistry*, 71(15):5538-5545.

Schittek, B. & Sinnberg, T. 2014. Biological functions of casein kinase 1 isoforms and putative roles in tumorigenesis. *Molecular cancer*, 13(1):231.

Shchemelinin, I., Sefc, L. & Necas, E. 2006. Protein kinases, their function and implication in cancer and other diseases. *Folia biologica*, 52(3):81.

St-Denis, N. & Gingras, A.-C. 2012. Mass spectrometric tools for systematic analysis of protein phosphorylation. *Progress in molecular biology and translational science*, 106:3-32.

Stankovic, T., Dinic, J., Podolski-Renic, A., Musso, L., Buric, S., Dallavalle, S. & Pesic, M. 2018. Dual inhibitors as a new challenge for cancer multidrug resistance treatment. *Current medicinal chemistry*, 25:1-30.

Sudhamani, H., Basha, S.T., Reddy, S.M.C., Sreedhar, B., Adam, S. & Raju, C.N. 2016. Synthesis and evaluation of biological activities of new sulfonamide and carbamate derivatives of 1H-pyrrolo [2, 3-b] pyridine (7-azaindole). *Research on chemical intermediates*, 42(10):7471-7486.

Sugiyama, N., Imamura, H. & Ishihama, Y. 2019. Large-scale discovery of substrates of the human kinome. *Scientific reports*, 9(1):1-12.

Syed, N.A.B., Jasamai, M., Jantan, I. & Ahmad, W. 2013. Review of methods and various catalysts used for chalcone synthesis. *Mini-reviews in organic chemistry*, 10(1):73-83.

Taylor, S.S., Keshwani, M.M., Steichen, J.M. & Kornev, A.P. 2012. Evolution of the eukaryotic protein kinases as dynamic molecular switches. *Philosophical transactions of the Royal Society B: Biological sciences*, 367(1602):2517-2528.

Taylor, S.S. & Kornev, A.P. 2011. Protein kinases: evolution of dynamic regulatory proteins. *Trends in biochemical sciences*, 36(2):65-77.

Tejeda-Muñoz, N. & Robles-Flores, M. 2015. Glycogen synthase kinase 3 in Wnt signaling pathway and cancer. *International union biochemistry molecular bioology life*, 67(12):914-922.

Tekale, S., Mashele, S., Pooe, O., Thore, S., Kendrekar, P. & Pawar, R. 2020. Biological role of chalcones in medicinal chemistry. *(In* Claborn, D., Bhattacharya S. & Roy S., *eds.* Vector-borne diseases-recent developments in epidemiology and control. IntechOpen.

Tursynbay, Y., Zhang, J., Li, Z., Tokay, T., Zhumadilov, Z., Wu, D. & Xie, Y. 2016. Pim-1 kinase as cancer drug target: an update. *Biomedical reports*, 4(2):140-146.

Wilson, L.J., Linley, A., Hammond, D.E., Hood, F.E., Coulson, J.M., MacEwan, D.J., Ross, S.J., Slupsky, J.R., Smith, P.D. & Eyers, P.A. 2018. New perspectives, opportunities, and challenges in exploring the human protein kinome. *Cancer research*, 78(1):15-29.

Yang, C., Zhang, X., Wang, Y., Yang, Y., Liu, X., Deng, M., Jia, Y., Ling, Y., Meng, L.-h. & Zhou, Y. 2017. Discovery of a novel series of 7-azaindole scaffold derivatives as PI3K inhibitors with potent activity. *ACS medicinal chemistry letters*, 8(8):875-880.

Yang, V.W. 2012. Chapter 15 - The Cell Cycle. *(In* Johnson, L.R., Ghishan F.K., Kaunitz J.D., Merchant J.L., Said H.M. & Wood J.D., *eds.* Physiology of the gastrointestinal tract (Fifth Edition). Boston: Academic Press. p. 451-471).

Zhang, R.X., Wong, H.L., Xue, H.Y., Eoh, J.Y. & Wu, X.Y. 2016. Nanomedicine of synergistic drug combinations for cancer therapy–Strategies and perspectives. *Journal of controlled release*, 240:489-503.

Zhou, B. & Xing, C. 2015. Diverse molecular targets for chalcones with varied bioactivities. *Medicinal chemistry*, 5(8):388.

Zhou, X., Herbst-Robinson, K.J. & Zhang, J. 2012. Chapter sixteen - Visualizing Dynamic Activities of Signaling Enzymes Using Genetically Encodable Fret-Based Biosensors: From Designs to Applications. *(In* Conn, P.M., *ed.* Methods in Enzymology. Academic Press. p. 317-340).

Zhuang, C., Zhang, W., Sheng, C., Zhang, W., Xing, C. & Miao, Z. 2017. Chalcone: a privileged structure in medicinal chemistry. *Chemical reviews*, 117(12):7762-7810.

CHAPTER 3

PUBLISHED ARTICLE 1

Synthesis and evaluation of 7-azaindole derivatives bearing benzocycloalkanone motifs as protein kinase inhibitors

Malikotsi A. Qhobosheane[a], Lesetja J. Legoabe[a,*], Béatrice Josselin[b,c], Stéphane Bach[b,c], Sandrine Ruchaud[b], Jacobus P. Petzer[a,d], Richard M. Beteck[a]

[a] Centre of Excellence for Pharmaceutical Sciences, North-West University, Private Bag X6001, Potchefstroom 2520, South Africa
[b] Sorbonne Université, CNRS, UMR 8227, Integrative Biology of Marine Models Laboratory (LBI2M), Station Biologique de Roscoff, 29680 Roscoff, France
[c] Sorbonne Université, CNRS, FR 2424, Plateforme de criblage KISSf (Kinase Inhibitor Specialized Screening facility), Station Biologique de Roscoff, 29680 Roscoff, France
[d] Pharmaceutical Chemistry, School of Pharmacy, North-West University, Private Bag X6001, Potchefstroom 2520, South Africa

ABSTRACT

Protein kinases are important drug targets, especially in the area of oncology. This paper reports the synthesis and biological evaluation of new 7-azaindole derivatives bearing benzocycloalkanone motifs as potential protein kinase inhibitors. Four compounds **8g**, **8h**, **8i**, and **8l** were discovered to inhibit cyclin-dependent kinase 9 (CDK9/CyclinT) and/or Haspin kinase in the micromolar to nanomolar range. **8l** was identified as the most potent Haspin inhibitor (IC_{50} = 14 nM), while **8g** and **8h** acted as dual inhibitors of CDK9/CyclinT and Haspin. These novel compounds constitute a promising starting point for the discovery of dual protein kinase inhibitors that have potential to be developed as anticancer agents, since both CDK9/CyclinT and Haspin are considered to be drug targets in oncology.

1. Introduction

Protein kinases are one of the most crucial target classes for treating human disorders. These enzymes catalyse the phosphorylation of proteins[1] by transferring a γ-phosphate group from a donor (usually ATP) to tyrosine, serine and threonine residues.[2,3] It was discovered that the human genome encodes for 518 protein kinases. This so-called "kinome" includes 478 typical and 40 atypical enzymes that are involved in various biological processes within the cell,[3,4] including cell fate and regulation of metabolism.[5] Protein kinase domains contain a small β-pleated N-lobe which is connected to a large α-helical C-lobe by a short hinge fragment.[6] ATP binds to the cleft between the N- and the C-terminal lobes of the kinase domain where the adenine group of ATP is sandwiched between hydrophobic residues and makes contact with the hinge region via hydrogen bonds.[6] Within the ATP pocket lies a residue called the "gatekeeper", which controls access to the hydrophobic "back pocket" of the kinase.[6]

The dysregulation of kinase signaling pathway plays a major role in disease pathophysiology, and this has been demonstrated in a wide variety of diseases including cancer, neurodegenerative disorders, cardiovascular disorders, inflammatory disorders and metabolic diseases.[2,4,7] Protein kinases thus represent attractive drug targets for development of novel drugs.[8,9] As reported in literature[10] 20–33% of drug discovery efforts worldwide are directed at the protein kinase superfamily. As a result of this intensive screening program, 48 small molecule protein kinase inhibitors have been approved by US food and drug administration (FDA) to date, most of which are for oncological indications.[10] The majority of approved kinase inhibitors are used in the treatment of malignancies (36 against solid tumors including lymphomas and seven against non-solid tumors, e.g. leukemias),[10] and a few of them are used to treat non oncological disorders including rheumatoid arthritis, idiopathic pulmonary fibrosis, cerebral vasospasm, glaucoma, Crohn's disease, ulcerative colitis and organ rejection.[6,10] In addition, at least 175 kinase inhibitors are reported to be in clinical trials worldwide.[10]

Targeting two or more protein kinases with a single inhibitor, coined as polypharmacology, represents an effective strategy to cancer treatment.[11] According to literature,[12] selective drugs against cancer cells should eradicate tumours more specifically, reducing side effects in normal cells. However, inhibition of a single target often shows transient efficacy due to the development of resistance. Dual targeting agents are better at overcoming incomplete efficacy and drug resistance, therefore they provide optimal effects in cancer treatment.[12]

Protein kinase inhibitors have successfully been discovered in

---

1 (PIM1 IC$_{50}$ = 410 nM)

2 (PIM1 IC$_{50}$ = 3 nM)

3 (mTOR IC$_{50}$ = 0.46 nM)

4 (mTOR IC$_{50}$ = 0.94 nM)
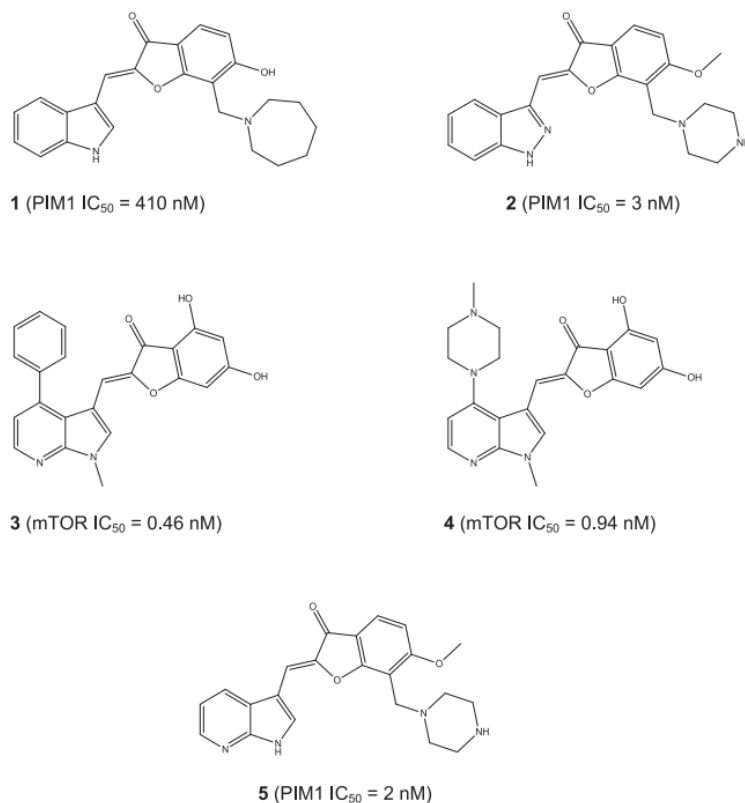
5 (PIM1 IC$_{50}$ = 2 nM)

Fig. 1. 7-azaindole derivatives bearing benzocycloalkanone motifs reported in previous studies.[15,18]

previous studies, however, the design of selective small-molecule kinase inhibitors proves challenging due of the high conservation of amino acids in the ATP-binding site of the majority of protein kinases.[7,13] High resolution structural studies may reveal unique kinase active site features, which can be exploited to develop target specific inhibitors.[14] This has proved to be an effective strategy in developing selective protein kinase inhibitors in previous studies.[15] For instance,[15] structural information of the proviral integration site for Moloney murine leukemia virus-1 (PIM1) complexed with **1** led to the discovery of a selective PIM1 inhibitor, **2** (Fig. 1). Replacing the homopiperidine ring of **1**, which extends into the specificity area of PIM1 but forms no significant binding interactions, with a piperazine ring (**2**) improves selectivity by formation of additional hydrogen bonds with Asp-128 and Glu-171, while retaining key interactions.[15] As a result, the piperazine ring is reported to be a critical substituent for selectivity and potency in this regard.[15]

The 7-azaindole scaffold is well known as a privileged fragment for kinase inhibition, and it has been confirmed as an excellent hinge-binding element in many protein kinase inhibitors.[16,17] More than 90 human kinases have shown sensitivity to 7-azaindole based inhibitors including compounds that have been developed to target Janus kinase 3 (JAK3), aurora kinases (STK), and rho-associated, coiled-coil-containing protein kinase 1 (ROCK1).[16]

7-Azaindole derivatives bearing benzocycloalkanone motifs have been developed in recent studies and have demonstrated good potencies for protein kinase inhibition. A previous study[18] reported 7-azaindole-benzofuranone hybrids as potent and selective inhibitors of the mammalian target of rapamycin (mTOR). Several inhibitors were synthesised, and the majority selectively inhibited mTOR with nanomolar potencies.[18] The most potent inhibitor (**3**) exhibited an IC$_{50}$ value of 0.46 nM for mTOR. Furthermore, a 4-piperazinyl bearing compound (**4**) was cocrystallised with phosphoinositide 3-kinase gamma (PI3Kγ), which was used as a substitute in crystallographic studies, owing to its high similarity to mTOR at the ATP binding sites.[18] The predicted binding mode revealed that the 7-N forms a hydrogen bond to Val-2240 in the hinge region of the ATP binding site of the protein.[18] The 4-hydroxy group of the benzofuranone ring of **4** forms a hydrogen bond to Lys-2187. Moreover, the 6-hydroxy group forms a hydrogen bond to Asp-2195 and the backbone NH of Phe-2358.[18] Additionally, a series of substituted benzofuranone derivatives bearing azaindole moieties was synthesised.[15] The analogue bearing 7-azaindole (**5**) was among the most potent protein kinase inhibitors reported in this study. Although it was non-selective, **5** inhibited PIM1, death-associated protein kinase 1 (DAPK1), glycogen synthase kinase 3β (GSK3β), protein kinase C α (PKCα), polycystic kidney disease 2 (PKD2) and ROCK1 with nanomolar potencies.[15]

In the present study, we synthesised thirteen 7-azaindole derivatives bearing various benzocycloalkanone motifs at position C3. Among others, α-tetralone and 1-indanone were considered. The benzocycloalkanones were further substituted with polar and non-polar

2

Table 1
Synthesis of 7-azaindole derivatives bearing benzocycloalkanone motifs (**8a-l**).

8a-l: R = OH, OCH$_3$

X = O, CH$_2$, (CH$_2$)$_2$, CH$_2$O, CH$_2$S,
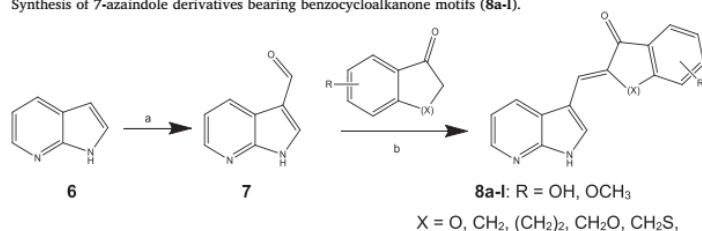
Compound	X	R	Yield (%)[a]
7	–	–	38
8a	(CH$_2$)$_2$	6-OCH$_3$	74
8b	CH$_2$	5- OCH$_3$	73
8c	(CH$_2$)$_2$	6,7-di OCH$_3$	90
8d	(CH$_2$)$_2$	7-OCH$_3$	86
8e	CH$_2$O	–	45
8f	CH$_2$S	–	48
8g	(CH$_2$)$_2$	–	72
8h	(CH$_2$)$_2$	6-OH	61
8i	CH$_2$	5,6-di OCH$_3$	62
8j	CH$_2$	5,6-methylenedioxy	95
8k	CH$_2$	–	95
8l	O	6-OH	97

[a] Isolated yields. Reaction conditions: (a) AcOH, H$_2$O, hexamethylenetetramine, 120 °C, 1 h; (b) HCl/MeOH, 100 °C, 6 h.

functional groups to provide a wide range of compounds with varying activities.

2. Results and discussion

2.1. Chemistry

The target compounds were prepared following the synthetic route outlined in Table 1. As key intermediate, **7** was synthesised from **6** in a yield of 38%, employing the Duff reaction as described in the experimental section.[19,20] Formation of **7** was confirmed by ^{13}C NMR analysis; the signal at 185.8 is representative of a carbonyl carbon, and confirms successful formylation of **6**. The test compounds (**8a-l**) were subsequently synthesised by introducing a variety of commercial benzocycloalkanones to **7** via an acid catalysed aldol condensation.[21]

2.2. Biological results

In an effort to discover new protein kinase inhibitors, we synthesised 12 novel compounds and screened them against a small panel of disease-relevant protein kinases including various cyclin-dependent kinases (CDKs): *Hs*CDK2/CyclinA, *Hs*CDK5/p25, *Hs*CDK9/CyclinT, *Hs*Haspin, human Proto-oncogene serine/threonine-protein kinase PIM1, porcine casein kinase 1 δ/ε (*Ssc*CK1δ/ε), *Lm*CK1 (from the intracellular parasite *Leishmania major*) and porcine Glycogen-Synthase Kinase 3 (*Ssc*GSK3α/β). All compounds were initially tested at concentrations of 1 μM (Table 2) and 10 μM (Table 2a in supplementary data). Compounds that inhibited more than 70% of the kinase activity at 1 μM inhibitor concentration were considered active and were further tested over a wide range of concentrations. From the data obtained, sigmoidal plots of kinase activity versus inhibitor concentration were constructed. As example, the curve obtained for compound **8l** is reported in Fig. 2. The IC$_{50}$ values of the active compounds were determined from these plots, and the results are reported in Table 3.

Four compounds showed promising activity for Haspin and CDK9/CyclinT (**8g, 8h, 8i** and **8l**), with IC$_{50}$ values in the micromolar to nanomolar range.

Haspin is a serine/threonine kinase overexpressed in cancer cells,[24] that specifically phosphorylates histone H3 at threonine 3 during mitosis.[22,23] As a result, inhibition of Haspin activity is considered as a promising strategy for cancer treatment.[24]

Moreover, CDK9/CyclinT is the catalytic subunit of positive transcription elongation factor b (p-TEFb) that has the ability to phosphorylate the C-terminal domain subunit of RNA polymerase II, and reach RNA transcription elongation.[25] In recent years, CDK9/CyclinT has emerged as a druggable target for the development of cancer therapeutics.[26] Inhibition of CDK9/CyclinT associated with blocking RNA synthesis can lead to a reduction in levels of short-lived pro-survival proteins and the induction of apoptosis, which provides an effective way to control tumour growth.[27]

The 7-azaindole derivatives showed varied degrees of activity depending on the nature of the substituents attached. While most compounds in this series were inactive against all tested kinases, compounds **8i, 8g, 8h** and **8l** showed promising activity as inhibitors of Haspin and/or CDK9/CyclinT. **8l** was discovered as the most potent Haspin inhibitor (IC$_{50}$ = 14 nM), and it displayed high selectivity. Moreover, the structurally similar analogue **8i** also selectively inhibited Haspin, with lower enzymatic potency (IC$_{50}$ = 3305 nM) owing to the steric bulk of the 5,6-dimethoxy substituent on the indanone ring. The high potency of compounds **8h** (IC$_{50}$ = 77 nM) and **8l** could be ascribed to the 6-hydroxy substituent attached to α-tetralone and 3-coumaranone rings of **8h** and **8l** respectively, which may likely form hydrogen bonds with the binding site amino acids, as seen in Figs. 3 and 4.

Furthermore, the bulkier α-tetralone analogues **8g** and **8h** are noteworthy as dual inhibitors of CDK9/CyclinT and Haspin, contrary to the corresponding 1-indanone and 3-coumaranone derivatives (**8i** and **8l**), and they possess varying specificities for both kinases. The analogue bearing α-tetralone with a 6-hydroxy substituent (**8h**) was more potent for Haspin than its unsubstituted counterpart (**8g**, IC$_{50}$ = 1321 nM). Replacing the coumaranone ring of **8l** with α-tetralone, as exemplified by **8g** and **8h** created analogues with improved CDK9/CyclinT potency (IC$_{50}$ = 424 nM and 495 nM, respectively). The additional CH$_2$ present in tetralones could be actively involved in the orientation of the inhibitors in the binding pocket of

Table 2

Percentage of kinase inhibition by compounds **7** and **8a-l**. The table displays the remaining activities detected after treatment with 1 μM of the tested compounds. 100% of residual activity is measured in the absence of inhibitor. The ATP concentration used in the kinase assays was 10 μmol/L (values are given as means, n = 2). Kinases are from human origin (*Homo sapiens*) unless specified: Ssc, *Sus scrofa*; Lm, *Leishmania major*.

Compound	% residual activity measured at 1 μM of the test compounds							
	CDK2/Cyclin A	CDK5/p25	CDK9/CyclinT	HASPIN	PIM1	*Ssc*_CK1δ/ε	*Ssc*_GSK3α/β	*Lm*_CK1
7	≥100	≥100	59	93	≥100	61	91	61
8a	84	86	56	75	≥100	83	81	57
8b	≥100	≥100	53	35	99	84	36	79
8c	≥100	≥100	70	84	≥100	86	92	83
8d	≥100	≥100	87	≥100	94	92	≥100	76
8e	≥100	77	56	81	97	80	66	96
8f	≥100	77	56	81	97	80	66	96
8g	70	85	11	33	98	76	42	84
8h	94	89	16	16	72	66	37	64
8i	≥100	≥100	59	21	≥100	68	49	90
8j	≥100	89	59	36	90	77	42	71
8k	82	98	49	36	91	79	45	89
8l	69	87	46	12	73	64	35	70
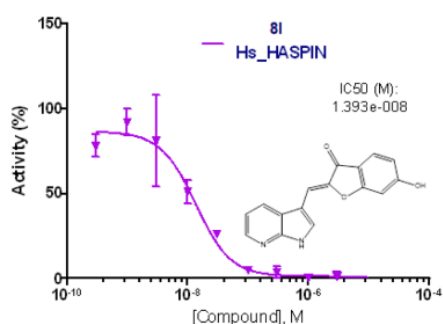
Fig. 2. Sigmoidal dose response curve of kinase activity versus the inhibitor concentration for the inhibition of Haspin by **8l** (IC$_{50}$ = 14 nM). The ATP concentration used in the kinase assays was 10 μmol/L. Values are means, n = 2.

CDK9/CyclinT. Interestingly, **8g** and **8h** displayed similar CDK9/CyclinT potency, which suggests that the 6-hydroxy substituent of **8h** plays no significant role in CDK9/CyclinT activity.

The above observations suggest that α-tetralone may be the most optimal substituent for dual inhibition of CDK9/CyclinT and Haspin among the compounds of this study. Furthermore, conjugating coumaranone and 7-azaindole is a suitable strategy for developing potent and selective Haspin inhibitors. It may therefore be concluded that substitution of the 7-azaindole moiety with appropriate benzocycloalkanone rings is necessary for CDK9/CyclinT and Haspin inhibition.

2.3. Molecular modelling

To gain insight into potential binding modes and interactions of the newly synthesized 7-azaindole derivatives, the most potent Haspin inhibitor, compound **8l**, was docked into the active sites of Haspin and CDK9/CyclinT, respectively. For this purpose, the Discovery Studio 3.1 modelling software (Accelrys) was used, and molecular docking was carried out according to a modification of a previously reported protocol with the CDOCKER application of the Discovery Studio.[28] The structures of Haspin co-crystallised with 5-iodotubercidin (PDB entry: 6G34)[29] and CDK9/CyclinT co-crystallised with CAN508 (PDB entry: 3TN8)[30] were used (Fig. 5). These models were selected based on the high resolution of the crystallographic structures. The pKa values and protonation states of the models were calculated, followed by energy

Table 3

Dose-dependent effect of 7-azaindole derivatives (**8g-l**) on the inhibition activity of human CDK9/CyclinT and Haspin protein kinases.

Compound	Structure	IC$_{50}$[a]	
		*Hs*_CDK9/CyclinT	*Hs*_HASPIN
8g		424	1321
8h		495	77
8i		NA[c]	3305
8l		NA[c]	14

[b]ATP concentration used in the kinase assays was 10 μmol/L.

[a] IC$_{50}$ values are reported in nM. Values are given as means, n = 2.

[c] No activity observed at a maximal tested concentration of 10 μM.

minimization, removal of crystal waters and co-crystallised ligands. The structures of the ligands were constructed in Discovery Studio, and after docking with CDOCKER, the docking orientations were refined using in situ ligand minimization. For each ligand, the highest ranked orientation was selected among the ten solutions generated.

The accuracy of the docking procedure was evaluated by redocking the co-crystallised ligands, 5-iodotubercidin and CAN508, into the active sites of Haspin and CDK9/CyclinT, respectively. The root mean square deviation (RMSD) of the docked orientation from the position of the co-crystallised ligand was subsequently calculated. The best ranked
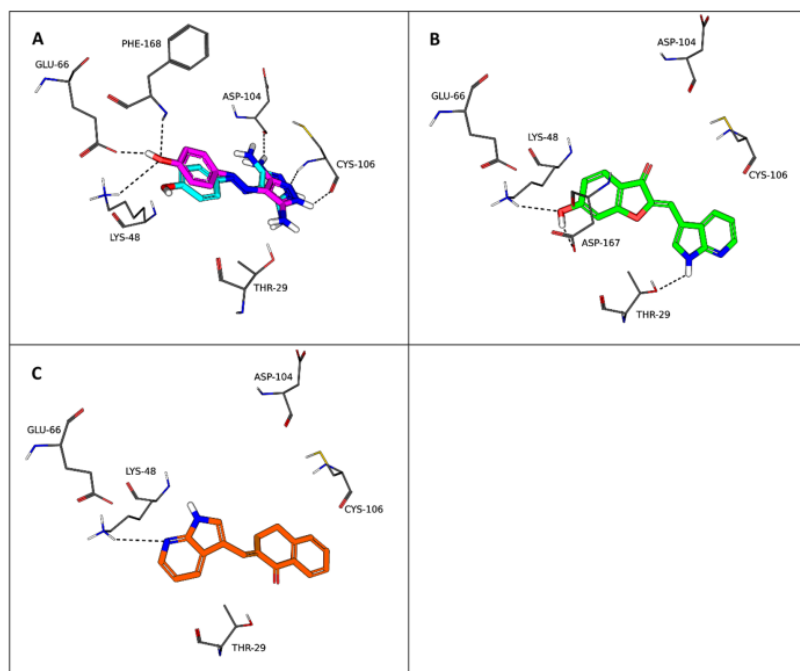
4

51
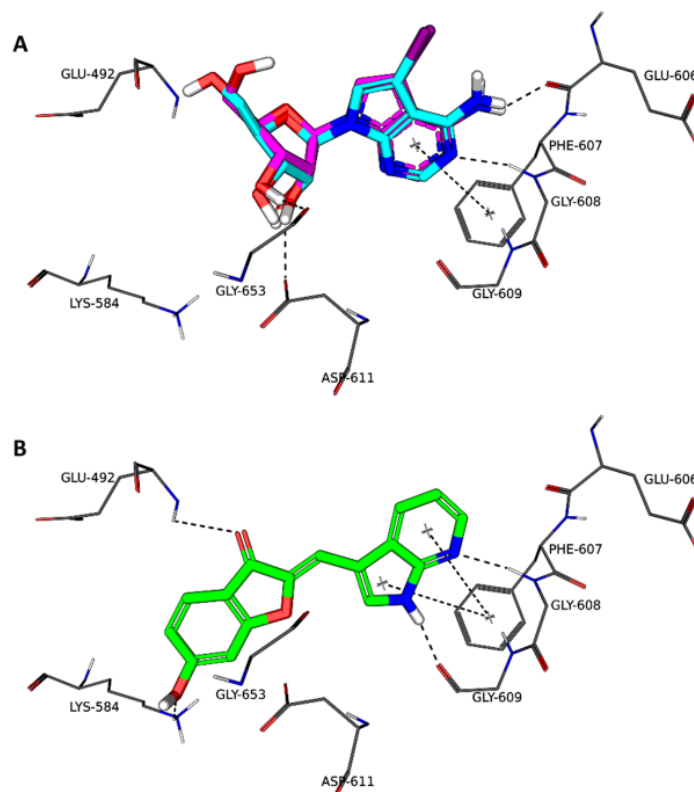
Fig. 3. The docked binding orientations of 5-iodotubercidin (cyan) compared to the orientation of the co-crystallized ligand (magenta) in the X-ray crystal structure of Haspin (A), as well as selected interactions formed by **8l** (green) in the Haspin active site (B). (Cut-off values for hydrogen bonding, 3.4 Å; π-π stacking, 6 Å). (For interpretation of the references to colour in this figure legend, the reader is referred to the web version of this article.)
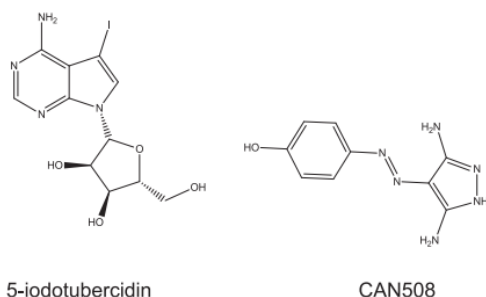
orientations of 5-iodotubercidin and CAN508 exhibited RMSD values of 0.656 Å and 1.07 Å, respectively, from the position of the co-crystallized ligand (Figs. 3 and 4). RMSD values < 1.5 Å are considered to be successful, and this protocol was thus deemed appropriate for docking experiments with Haspin and CDK9/CyclinT.[31] For the docking of **8l** into the active site of Haspin (Fig. 3), the highest ranked solution shows that the 7-azaindole moiety of **8l** binds in the similar position as the pyrrolo[2,3-*d*]pyrimidine cycle of 5-iodotubercidin. Hydrogen bonding occurs between the benzofuranone moiety and Glu-492 and Lys-584, and between the 7-azaindole moiety and Gly-608 and Gly-609. For 5-iodotubercidin, hydrogen bonding occurs between the ribofuranosyl and Asp-611 and Gly-653, and between the pyrrolo[2,3-*d*]pyrimidine cycle and Glu-606 and Gly-608. π-π stacking with Phe-607 is likely an important stabilizing interaction and occurs for both ligands. Based on the similarity between the binding modes and interactions of **8l** and 5-iodotubercidin it may be proposed that active Haspin inhibitors should contain an aromatic nitrogen-containing heterocycle (for hydrogen bonding and π stacking) as well as an oxygen rich side chain that can undergo hydrogen bond interactions towards the entrance of the active site.

For the docking of **8l** into the active site of CDK9/CyclinT (Fig. 4), the highest ranked solution shows that the benzofuranone moiety of **8l** binds in the same position as the 4-hydroxyphenyl of CAN508 where hydrogen bonding occurs with Lys-48 and the side chain of Asp-167. In

this region CAN508 is also stabilized by hydrogen bonding to Lys-48 as well as Glu-66 and the backbone nitrogen of Phe-168.[30] The 7-azaindole moiety of **8l** binds in a region distinct from the pyrazole of CAN508 and is hydrogen bonded to Thr-29. Interestingly, **8g**, the most potent CDK9/CyclinT inhibitor, exhibits a reversed binding orientation to **8l**, which suggests that the hydrogen bonding by the hydroxyl group of **8l** plays an important role in determining the orientation of binding in the active site. Although the molecular basis for the higher CDK9/CyclinT inhibition by **8g** versus **8l** is not apparent, the difference between the binding of **8l** in Haspin compared to CDK9/CyclinT might arise as a result of stronger interaction network between **8l** and Haspin, than that between **8l** and CDK9/CyclinT.

3. Conclusion

The current study evaluated the 7-azaindole derivatives bearing benzocycloalkanone moieties as potential protein kinase inhibitors. The most potent inhibitor among the evaluated compounds (**8l**) inhibited human Haspin with an IC$_{50}$ of 14 nM. We have identified two compounds (**8g** and **8h**) as dual inhibitors of Haspin and CDK9/CyclinT, with IC$_{50}$ values in the micromolar range. None of the tested compounds showed any activity against the other six protein kinases. Because of their ability to inhibit both Haspin and CDK9/CyclinT with high potencies, it may be concluded that 7-azaindole derivatives

Fig. 4. The docked binding orientations of CAN508 (cyan) compared to the orientation of the co-crystallized ligand (magenta) in the X-ray crystal structure of CDK9/CyclinT (A), as well as selected interactions formed by **8l** (green) and **8g** (orange) in the CDK9/CyclinT active site (B and C, respectively). (Cut-off value for hydrogen bonding, 3.4 Å). (For interpretation of the references to colour in this figure legend, the reader is referred to the web version of this article.)

Fig. 5. Structures of 5-iodotubercidin and CAN508.

synthesised in this study are good leads for the future development of Haspin and CDK9/CyclinT inhibitors, and potential anticancer drugs.

4. Experimental section

4.1. Chemicals and instrumentation

Unless otherwise noted, all starting materials and reagents were obtained from Sigma-Aldrich or AK Scientific and were used without further purification. Proton (^{1}H) and carbon (^{13}C) nuclear magnetic resonance (NMR) spectra were recorded on a Bruker Avance III 600 spectrometer at frequencies of 600 MHz and 151 MHz, respectively, with DMSO-d_6 serving as NMR solvent. All chemical shifts are reported in parts per million (δ) and were referenced to the residual solvent signal (DMSO-d_6: 2.50 and 39.52 ppm for ^{1}H and ^{13}C, respectively). Spin multiplicities are given as s (singlet), d (doublet), dd (doublet of doublets), t (triplet) and m (multiplet). High resolution mass spectra (HRMS) were recorded on a Bruker micrOTOF-Q II mass spectrometer in atmospheric-pressure chemical ionisation (APCI) mode.

Chemical purities were determined by HPLC (Agilent 1200 system) with a Venusil XBP C18 column (4.60 × 150 mm, 5 μm) and a mobile phase of 30% acetonitrile and 70% MilliQ water at a flow rate of 1 ml/min. At the start of each injection, a solvent gradient program was initiated by linearly increasing the percentage acetonitrile to 85% over a period of 5 min. Each run lasted 15 min, 20 μl of the test compounds in acetonitrile (1 mM) was injected into the HPLC system and the eluent was monitored at wavelengths of 210 and 254 nm. The melting points (mp) were determined with a Buchi B-545 melting point apparatus and are uncorrected. Thin layer chromatography (TLC) was carried out using silica gel 60 F254 pre-coated aluminium sheets (0.25 mm, Merck), while column chromatography was carried out with silica gel 60 (Fluka, particle size 0.063–0.200 mm). Full-length kinases were used unless specified.

Peptide substrates were obtained from Proteogenix (Schiltigheim, France).

4.2. Synthesis of 1H-pyrrolo[2,3-b]pyridine-3-carbaldehyde (7)

To a solution of 7-azaindole (10.0 g, 85 mmol) in water/acetic acid (2:1 v/v) (100 ml/50 ml) was added hexamethylenetetramine (HMTA) (23.7 g, 169 mmol) and the reaction was refluxed at 100–120 °C for 1 h. The work up was done by cooling the reaction mixture on an ice-bath,

6

53

c

and the resulting precipitate was collected by filtration and dried.[19,20]
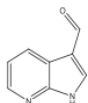
Yield: 38%; white solid; mp 199–212 °C (reported mp 194–196 °C[32]). ^{1}H NMR (600 MHz, DMSO) δ 12.71 (s, 1H), 9.93 (s, 1H), 8.48 (s, 1H), 8.43–8.35 (m, 2H), 7.28 (dd, J = 7.8, 4.7 Hz, 1H). ^{13}C NMR (151 MHz, DMSO) δ 185.9, 149.9, 145.3, 139.2, 129.7, 118.9, 117.1, 116.9. APCI-HRMS m/z: calcld for $C_8H_7N_2O$ (MH[+]), 147.0553, found 147.0550. Purity (HPLC): 98.4%.

4.3. General procedure for the synthesis of 7-azaindole analogues

To a solution of (**7**) 1-(1*H*-pyrrolo[2,3-*b*]pyridine-3-carbaldehyde (0.300 g, 2.053 mmol) in 32% aqueous HCl/methanol (1.5:1 v/v) (4.5 ml/3 ml) was added a selected bicyclic scaffold (tetralone, indanone, 3-coumaranone, 4-chromanone and thiochroman-4-one) (2.053 mmol) and the reaction was refluxed for at least 6 h at 60–80 °C. The progress of the reaction was monitored by silica gel TLC with ethyl acetate as mobile phase. When the reaction reached completion, the target products were isolated by precipitation with ice-cold water, after which they were purified by recrystallisation with ethanol.

4.4. (E)-2-((1H-pyrrolo[2,3-b]pyridin-3-yl)methylene)-6-methoxy-3,4-dihydronaphthalen-1(2H)-one (8a)
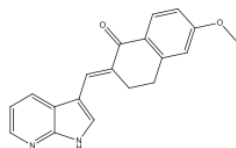
Yield: 74%; yellow needles; mp 251–252 °C (ethanol). ^{1}H NMR (600 MHz, DMSO) δ 12.95 (s, 1H), 8.51 (d, J = 7.5 Hz, 1H), 8.44 (s, 1H), 8.04 (s, 1H), 7.94 (s, 2H), 7.39 (s, 1H), 6.92 (s, 2H), 3.85 (s, 3H), 3.12 (s, 2H), 2.97 (s, 2H). ^{13}C NMR (151 MHz, DMSO) δ 185.2, 163.5, 146.2, 144.8, 140.6, 132.7, 131.4, 130.2, 129.5, 127.1, 126.1, 122.5, 116.9, 114.0, 112.8, 111.3, 55.9, 28.3, 27.9. APCI-HRMS m/z: calcld for $C_{19}H_{17}N_2O_2$ (MH[+]), 305.1285, found 305.1278. Purity (HPLC): 96.8%.

### 4.5. (E)-2-((1H-pyrrolo[2,3-b]pyridin-3-yl)methylene)-5-methoxy-2,3-dihydro-1H-inden-1-one (8b)
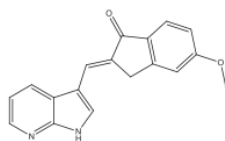
Yield: 73%; yellow powder; mp 281–282 °C (ethanol). ^{1}H NMR (600 MHz, DMSO) δ 12.82 (s, 1H), 8.54 (s, 1H), 8.40 (s, 1H), 8.07 (s, 1H), 7.78 (s, 1H), 7.70 (s, 1H), 7.52 – 6.76 (m, 3H), 3.93 (m, 5H). ^{13}C NMR (151 MHz, DMSO) δ 191.6, 165.1, 146.9, 142.5, 131.4, 129.7, 129.6, 125.6, 122.9, 121.2, 117.2, 115.5, 113.9, 111.4, 110.6, 104.2, 56.2, 33.1. APCI-HRMS m/z: calcld for $C_{18}H_{15}N_2O_2$ (MH[+]), 291.1128, found 291.1119. Purity (HPLC): 97.7%

### 4.6. (E)-2-((1H-pyrrolo[2,3-b]pyridin-3-yl)methylene)-6,7-dimethoxy-3,4-dihydronaphthalen-1(2H)-one (8c)
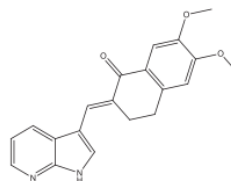
Yield: 90%; yellow powder; mp 292 °C (ethanol). ^{1}H NMR (600 MHz, DMSO) δ 12.88 (s, 1H), 8.48 (d, J = 7.6 Hz, 1H), 8.43 (d, J = 4.7 Hz, 1H), 8.03 (s, 1H), 7.92 (s, 1H), 7.45 (s, 1H), 7.41 – 7.31 (m, 1H), 6.95 (s, 1H), 3.87 (s, 3H), 3.81 (s, 3H), 3.12 (s, 2H), 2.93 (s, 2H). ^{13}C NMR (151 MHz, DMSO) δ 185.1, 153.7, 148.3, 145.2, 140.9, 138.5, 132.5, 131.1, 129.4, 126.5, 125.9, 122.3, 116.9, 111.2, 111.1, 109.5, 56.3, 55.9, 28.2, 27.7. APCI-HRMS m/z: calcld for $C_{20}H_{19}N_2O_3$ (MH[+]), 335.1390, found 335.1391. Purity (HPLC): 92.4%

4.7. (E)-2-((1H-pyrrolo[2,3-b]pyridin-3-yl)methylene)-7-methoxy-3,4-dihydronaphthalen-1(2H)-one (8d)
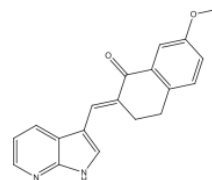
Yield: 86%; yellow powder; mp 263–264 °C (ethanol).
^{1}H NMR (600 MHz, DMSO) δ 12.64 (s, 1H), 8.38 (d, J = 4.6 Hz, 1H), 8.34 (d, J = 7.8 Hz, 1H), 8.03 (s, 1H), 8.00 (s, 1H), 7.44 (d, J = 2.5 Hz, 1H), 7.37–7.22 (m, 2H), 7.15 (dd, J = 8.2, 2.7 Hz, 1H), 3.82 (s, 3H), 3.12 (t, J = 5.7 Hz, 2H), 2.92 (t, J = 6.2 Hz, 2H). ^{13}C NMR (151 MHz, DMSO) δ 186.2, 158.6, 147.4, 142.9, 135.9, 134.7, 131.4, 130.2, 129.34, 129.04, 127.7, 121.1, 120.7, 117.1, 110.80, 110.69, 55.7, 28.1, 27.1. APCI-HRMS m/z: calcld for $C_{19}H_{17}N_2O_2$ (MH[+]), 305.1285, found 305.1268. Purity (HPLC): 96.3%

4.8. (E/Z)-3-((1H-pyrrolo[2,3-b]pyridin-3-yl)methylene)chroman-4-one (8e)
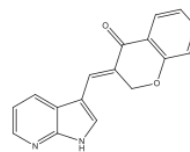
Yield: 45%; yellow needles; mp 231–233 °C (ethanol). ^{1}H NMR (600 MHz, DMSO) δ 12.67 (s, 1H), 8.57 – 8.21 (m, 2H), 8.02 (s, 1H), 7.98 – 7.81 (m, 2H), 7.58 (t, J = 7.7 Hz, 1H), 7.27 (dd, J = 7.5, 4.7 Hz, 1H), 7.20–6.96 (m, 2H), 5.50 (s, 2H). ^{13}C NMR (151 MHz, DMSO) δ 180.7, 160.9, 148.6, 144.2, 136.1, 130.5, 128.1, 127.53, 127.47, 126.2, 122.17, 122.10, 120.4, 118.2, 117.5, 109.6, 68.9. APCI-HRMS m/z: calcld for $C_{17}H_{13}N_2O_2$ (MH[+]), 277.0972, found 277.0962. Purity (HPLC): 96.5%.

7

54

4.9. (E)-3-((1H-pyrrolo[2,3-b]pyridin-3-yl)methylene)thiochroman-4-one (8f)
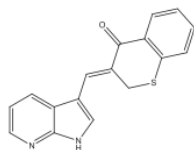
Yield: 48%; yellow plates; mp 238 °C (ethanol). ^{1}H NMR (600 MHz, DMSO) δ 12.89 (s, 1H), 8.41 (d, J = 6.1 Hz, 2H), 8.21 (s, 1H), 8.05 (d, J = 7.0 Hz, 1H), 7.92 (s, 1H), 7.58 – 7.45 (m, 1H), 7.41 (d, J = 7.3 Hz, 1H), 7.38–7.24 (m, 2H), 4.38 (s, 2H). ^{13}C NMR (151 MHz, DMSO) δ 184.8, 146.5, 142.3, 140.8, 133.5, 132.7, 130.11, 130.07, 129.9, 128.60, 128.43, 128.28, 126.3, 121.5, 117.3, 110.2, 29.8. APCI-HRMS m/z: calcld for C$_{17}$H$_{13}$N$_2$OS (MH$^+$), 293.0743, found 293.0734. Purity (HPLC): 96.3%.

4.10. (E)-2-((1H-pyrrolo[2,3-b]pyridin-3-yl)methylene)-3,4-dihydronaphthalen-1(2H)-one (8g)
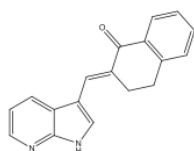
Yield: 72%; yellow needles; mp 257 °C (ethanol). ^{1}H NMR (600 MHz, DMSO) δ 13.06 (s, 1H), 8.56 (d, J = 7.6 Hz, 1H), 8.45 (d, J = 4.5 Hz, 1H), 8.07 (s, 1H), 8.04–7.87 (m, 2H), 7.56 (t, J = 7.1 Hz, 1H), 7.49–7.26 (m, 3H), 3.14 (s, 2H), 2.99 (s, 2H). ^{13}C NMR (151 MHz, DMSO) δ 186.4, 144.5, 143.6, 140.3, 133.70, 133.61, 132.6, 131.8, 129.9, 128.9, 127.66, 127.37, 126.8, 122.7, 117.0, 111.3, 27.93, 27.87. APCI-HRMS m/z: calcld for C$_{18}$H$_{15}$N$_2$O (MH$^+$), 275.1179, found 275.1168. Purity (HPLC): 97.3%.

4.11. (E)-2-((1H-pyrrolo[2,3-b]pyridin-3-yl)methylene)-6-hydroxy-3,4-dihydronaphthalen-1(2H)-one (8h)
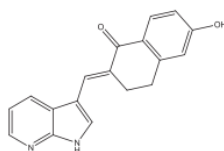
Yield: 61%; light orange powder; mp 268–270 °C (ethanol). ^{1}H NMR (600 MHz, DMSO) δ 12.99 (s, 1H), 8.54 (d, J = 7.5 Hz, 1H), 8.45 (s, 1H), 7.96 (d, J = 74.1 Hz, 2H), 7.85 (d, J = 8.4 Hz, 1H), 7.56 – 7.30 (m, 1H), 6.80 (d, J = 8.2 Hz, 1H), 6.72 (s, 1H), 3.17 (s, 1H), 3.10 (s, 2H), 2.89 (s, 2H). ^{13}C NMR (151 MHz, DMSO) δ 185.0, 162.6, 146.2, 144.2, 140.0, 133.2, 131.9, 130.5, 129.5, 125.8, 125.5, 122.8, 116.9, 115.1, 114.4, 111.4, 28.3, 27.9. APCI-HRMS m/z: calcld for C$_{18}$H$_{15}$N$_2$O$_2$ (MH$^+$), 291.1128, found 291.1122. Purity (HPLC): 96.4%.

4.12. (E)-2-((1H-pyrrolo[2,3-b]pyridin-3-yl)methylene)-5,6-dimethoxy-2,3-dihydro-1H-inden-1-one (8i)
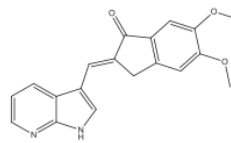
Yield: 62%; yellow powder; mp 282 °C (ethanol). ^{1}H NMR (600 MHz, DMSO) δ 12.80 (s, 1H), 8.55 (d, J = 7.7 Hz, 1H), 8.40 (d, J = 4.4 Hz, 1H), 8.04 (s, 1H), 7.75 (s, 1H), 7.33 (dd, J = 7.6, 4.9 Hz, 1H), 7.20 (d, J = 8.9 Hz, 2H), 3.91 (m, 6H), 3.84 (s, 2H). ^{13}C NMR (151 MHz, DMSO) δ 191.9, 155.4, 149.7, 144.5, 142.3, 132.8, 131.3, 129.83, 129.81, 129.45, 122.4, 121.3, 117.2, 111.4, 108.5, 105.0, 56.41, 56.12, 32.7. APCI-HRMS m/z: calcld for C$_{19}$H$_{17}$N$_2$O$_3$ (MH$^+$), 321.1234, found 321.1236. Purity (HPLC): 97.7%.

4.13. (E)-2-((1H-pyrrolo[2,3-b]pyridin-3-yl)methylene)-6-amino-3,4-dihydronaphthalen-1(2H)-one (8j)
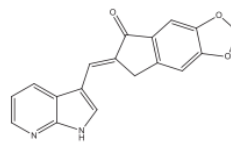
Yield: 95%; yellow powder; mp 301 °C (ethanol). ^{1}H NMR (600 MHz, DMSO) δ 12.82 (s, 1H), 8.53 (d, J = 7.4 Hz, 1H), 8.40 (s, 1H), 8.04 (s, 1H), 7.74 (s, 1H), 7.53–7.21 (m, 1H), 7.15 (d, J = 5.3 Hz, 2H), 6.18 (s, 2H), 3.90 (s, 2H). ^{13}C NMR (151 MHz, DMSO) δ 191.3, 173.2, 153.9, 148.4, 146.9, 142.4, 133.2, 132.5, 129.77, 129.63, 122.7, 117.25, 117.21, 111.3, 106.3, 102.80, 102.3, 32.9. APCI-HRMS m/z: calcld for C$_{18}$H$_{13}$N$_2$O$_3$ (MH$^+$), 305.0921, found 305.0904. Purity (HPLC): 95.5%.

4.14. (E)-2-((1H-pyrrolo[2,3-b]pyridin-3-yl)methylene)-2,3-dihydro-1H-inden-1-one (8k)
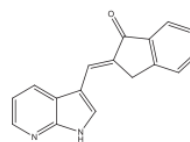
Yield: 95%; light orange powder; mp 283 °C (ethanol). ^{1}H NMR (600 MHz, DMSO) δ 13.01 (s, 1H), 8.61 (s, 1H), 8.42 (s, 1H), 8.14 (s, 1H), 7.88 (s, 1H), 7.77 (d, J = 5.5 Hz, 1H), 7.68–7.57 (m, 2H), 7.47 (s, 1H), 7.37 (s, 1H), 4.04 (s, 2H). ^{13}C NMR (151 MHz, DMSO) δ 191.6, 165.1, 152.6, 142.3, 132.5, 131.9, 129.71, 129.66, 125.67, 125.61, 122.8, 117.2, 115.5, 111.4, 110.6, 56.2, 33.1. APCI-HRMS m/z: calcld for C$_{17}$H$_{13}$N$_2$O (MH$^+$), 261.1022, found 261.1012. Purity (HPLC): 96.9%.

8

4.15. (Z)-2-((1H-pyrrolo[2,3-b]pyridin-3-yl)methylene)-6-hydroxybenzofuran-3(2H)-one (8l)
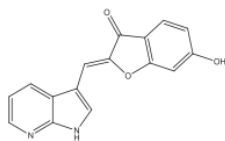
Yield: 97%; light orange powder; mp 361 °C (ethanol). ^{1}H NMR (600 MHz, DMSO) δ 12.97 (s, 1H), 11.24 (s, 1H), 8.78 (d, J = 7.7 Hz, 1H), 8.43 (d, J = 4.1 Hz, 1H), 8.31 (s, 1H), 7.60 (d, J = 8.3 Hz, 1H), 7.52–7.30 (m, 1H), 7.20 (s, 1H), 6.91 (s, 1H), 6.75 (d, J = 8.3 Hz, 1H). ^{13}C NMR (151 MHz, DMSO) δ 180.9, 167.5, 166.6, 146.3, 145.9, 141.4, 132.6, 131.8, 126.0, 120.9, 117.3, 114.1, 113.3, 108.4, 104.2, 99.2. APCI-HRMS m/z: calcld for $C_{16}H_{11}N_2O_3$ (MH$^+$), 279.0764, found 279.0755. Purity (HPLC): 99.0%.

4.16. Kinase inhibition assay

Kinase enzymatic activities were assayed in 384-well plates using the ADP-GloTM assay kit (Promega, Madison, WI) according to the recommendations of the manufacturer. This assay is a luminescent ADP detection assay that provides a homogeneous and high-throughput screening method to measure kinase activity by quantifying the amount of ADP produced during a kinase reaction. Briefly, the reactions were carried out in a final volume of 6 µl for 30 min at 30 °C in appropriate kinase buffer, with either protein or peptide as substrate in the presence of 10 µM ATP. After that, 6 µl of ADP-GloTM Kinase Reagent was added to stop the kinase reaction. After an incubation time of 50 min at room temperature (RT), 12 µl of Kinase Detection Reagent was added for one hour at RT. The transmitted signal was measured using the Envision (PerkinElmer, Waltham, MA) microplate luminometer and expressed in Relative Light Unit (RLU). In order to determine the half maximal inhibitory concentration (IC$_{50}$), the assays were performed in duplicate in the absence or presence of increasing doses of the tested compounds. Kinase activities are expressed in % of maximal activity, i.e. measured in the absence of inhibitor.

4.16.1. Buffer

(A) 10 mM MgCl$_2$, 1 mM EGTA, 1 mM DTT, 25 mM Tris-HCl pH 7.5, 50 µg/ml heparin

4.16.2. Kinases

*Hs*CDK2/CyclinA (cyclin-dependent kinase-2, human, kindly provided by Dr. A. Echalier-Glazer, Leicester, UK) was assayed in buffer A with 0.8 µg/µl of histone H1 as substrate;

*Hs*CDK5/p25 (human, recombinant, expressed in bacteria) was assayed in buffer A with 0.8 µg/µl of histone H1 as substrate;

*Hs*CDK9/CyclinT (human, recombinant, expressed by baculovirus in Sf9 insect cells) was assayed in buffer A with 0.27 µg/µl of the following peptide: YSPTSPSYSPTSPSYSPTSPSKKKK, as substrate;

*Hs*Haspin-k$_d$ (human, kinase domain, amino acids 470 to 798, recombinant, expressed in bacteria) was assayed in buffer A with 0.007 µg/µl of Histone H3 (1–21) peptide (ARTKQTARKSTGGKAPRK-QLA) as substrate;

*Hs*Pim-1 (human proto-oncogene, recombinant, expressed in bacteria) was assayed in buffer A with 0.8 µg/µl of histone H1 (Sigma #H5505) as substrate;

*Lm*CK1 (from *Leishmania major*, recombinant, expressed in bacteria) was assayed in buffer A with 0.028 µg/µl of the following peptide: RRKHAAIGSpAYSITA as CK1-specific substrate;

*Ssc*CK1δ/ε (casein kinase 1δ/ε, porcine brain, native, affinity purified) was assayed in buffer A with 0.022 µg/µl of the following peptide: RRKHAAIGSpAYSITA ("Sp" stands for phosphorylated serine) as CK1-specific substrate;

*Ssc*GSK-3α/β (glycogen synthase kinase-3, porcine brain, native, affinity purified) isoforms were assayed in buffer A with 0.010 µg/µl of GS-1 peptide, a GSK-3-selective substrate (YRRAAVPPSPSLSRHSSP-HQSpEDEEE).

4.17. Molecular docking

Modelling calculations were carried out with Discovery Studio 3.1. All applications in Discovery Studio were set to their default values, and X-ray crystal structures were obtained from the Protein Data Bank. The pKa values and protonation states of the protein models were firstly calculated and hydrogen atoms were added to the amino acid residues at pH 7.4. A fixed atom constraint was applied to the protein backbone, and the models were energy minimized using the Smart Minimizer algorithm (maximum steps, 50000) with the implicit generalized Born solvation model with molecular volume. The co-crystallized ligands, waters and the backbone constraints were removed and the binding sites were identified. The structures of the test ligands were drawn in Discovery Studio and submitted to the Prepare Ligands protocol. Atom potential types and partial charges were assigned with the Momany and Rone CHARMm forcefield, and docking of the ligands was carried out with the CDOCKER algorithm. For this purpose, ten random ligand conformations were generated, the heating target temperature was set to 700 K and full potential mode was employed. The docking solutions were finally refined using in situ ligand minimization with the Smart Minimizer algorithm. Illustrations were prepared with PyMOL.[33]

Declaration of Competing Interest

The authors declare that they have no known competing financial interests or personal relationships that could have appeared to influence the work reported in this paper.

Appendix A. Supplementary material

Supplementary data to this article can be found online at https://doi.org/10.1016/j.bmc.2020.115468.

References

1. Litalien C, Beaulieu P. Molecular mechanisms of drug actions: From receptors to effectors A$_2$. In: Zimmerman JJ, ed. *Pediatric critical care*. Saint Louis: Mosby; 2011:1553–1568.
2. Bhullar KS, Lagaron NO, McGowan EM, et al. Kinase-targeted cancer therapies: progress, challenges and future directions. *Mol Cancer*. 2018;17:48.
3. Manning G, Whyte DB, Martinez R, et al. The protein kinase complement of the human genome. *Science*. 2002;298:1912–1934.

4. Lawson M, Rodrigo J, Baratte B, et al. Synthesis, biological evaluation and molecular modeling studies of imidazo [1, 2-a] pyridines derivatives as protein kinase inhibitors. *Eur J Med Chem.* 2016;123:105–114.
5. Cheng HC, Qi RZ, Paudel H, Zhu HJ. Regulation and function of protein kinases and phosphatases. *Enzyme Res.* 2011;2011:794089.
6. Fabbro D. 25 years of small molecular weight kinase inhibitors: potentials and limitations. *Mol Pharmacol.* 2015;87:766–775.
7. Zhao Z, Bourne PE. Progress with covalent small-molecule kinase inhibitors. *Drug Discov Today.* 2018;23:727–735.
8. Doerig C, Billker O, Haystead T, et al. Protein kinases of malaria parasites: an update. *Trends Parasitol.* 2008;24:570–577.
9. Srinivasan N, Krupa A. A genomic perspective on protein kinases in *Plasmodium falciparum*. *Proteins: Struct, Funct, Bioinf.* 2005;58:180–189.
10. Roskoski R. Properties of FDA-approved small molecule protein kinase inhibitors. *Pharmacol Res.* 2019;144:19–50.
11. Wang W, Qin JJ, Voruganti S, et al. Discovery and characterization of dual inhibitors of MDM2 and nfat1 for pancreatic cancer therapy. *Cancer Res.* 2018;78:5656–5667.
12. Stankovic T, Dinic J, Podolski-Renic A, et al. Dual inhibitors as a new challenge for cancer multidrug resistance treatment. *Curr Med Chem.* 2018;25:1–30.
13. Arslan MA, Kutuk O, Basaga H. Protein kinases as drug targets in cancer. *Curr Cancer Drug Tar.* 2006;6:623–634.
14. Müller S, Chaikuad A, Gray NS, Knapp S. The ins and outs of selective kinase inhibitor development. *Nat Chem Biol.* 2015;11:818.
15. Nakano H, Saito N, Parker L, et al. Rational evolution of a novel type of potent and selective proviral integration site in Moloney murine leukemia virus kinase 1 (PIM1) inhibitor from a screening-hit compound. *J Med Chem.* 2012;55:5151–5164.
16. Irie T, Sawa M. 7-azaindole: a versatile scaffold for developing kinase inhibitors (Patent: WO 2012175168A1). 2018.
17. Tong Y, Stewart KD, Florjancic AS, et al. Azaindole-based inhibitors of Cdc7 kinase: impact of the Pre-DFG residue, Val 195. *ACS Med Chem Lett.* 2013;4:211–215.
18. Tsou HR, MacEwan G, Birnberg G, et al. Discovery and optimization of 2-(4-substituted-pyrrolo[2,3-b]pyridin-3-yl)methylene-4-hydroxybenzofuran-3(2H)-ones as potent and selective ATP-competitive inhibitors of the mammalian target of rapamycin (mTOR). *Bioorg Med Chem Lett.* 2010;20:2321–2325.
19. Jia H, Dai G, Weng J, et al. Discovery of (S)-1-(1-(Imidazo[1,2-a]pyridin-6-yl)ethyl)-6-(1-methyl-1H-pyrazol-4-yl)-1H-[1,2, 3]triazolo[4,5-b]pyrazine (volitinib) as a highly potent and selective mesenchymal-epithelial transition factor (c-Met) inhibitor in clinical development for treatment of cancer. *J Med Chem.*
20. 2014;57:7577–7589.
20. Narva S, Chitti S, Bala BR, et al. Synthesis and biological evaluation of pyrrolo[2,3-b] pyridine analogues as antiproliferative agents and their interaction with calf thymus DNA. *Eur J Med Chem.* 2016;114:220–231.
21. Janse van Rensburg HD, Legoabe LJ, Terre'Blanche G, Van der Walt MM. Methoxy substituted 2-benzylidene-1-indanone derivatives as A1 and/or A2A AR antagonists for the potential treatment of neurological conditions. *Medchemcomm.* 2019;10:300–309.
22. Amoussou NG, Bigot A, Roussakis C, Robert JMH. Haspin: a promising target for the design of inhibitors as potent anticancer drugs. *Drug Discov Today.* 2018;23:409–415.
23. Huertas D, Soler M, Moreto J, et al. Antitumor activity of a small-molecule inhibitor of the histone kinase Haspin. *Oncogene.* 2012;31:1408.
24. Kim JE, Lee SY, Jang M, et al. Coumestrol epigenetically suppresses cancer cell proliferation: Coumestrol is a natural haspin kinase inhibitor. *Int J Mol.* 2017;18:2228.
25. Morales F, Giordano A. Overview of CDK9 as a target in cancer research. *Cell Cycle.* 2016;15:519–527.
26. Sonawane YA, Taylor MA, Napoleon JV, et al. Cyclin dependent Kinase 9 inhibitors for cancer therapy: miniperspective. *J Med Chem.* 2016;59:8667–8684.
27. Li Y, Guo Q, Zhang C, et al. Discovery of a highly potent, selective and novel CDK9 inhibitor as an anticancer drug candidate. *Bioorg Med Chem Lett.* 2017;27:3231–3237.
28. Mostert S, Petzer A, Petzer JP. Indanones as high-potency reversible inhibitors of monoamine oxidase. *ChemMedChem.* 2015;10:862–873.
29. Heroven C, Georgi V, Ganotra GK, et al. Halogen–aromatic π interactions modulate inhibitor residence times. *Angew Chem Int Ed.* 2018;57:7220–7224.
30. Baumli S, Hole AJ, Noble MEM, Endicott JA. The CDK9 C-helix exhibits conformational plasticity that may explain the selectivity of CAN508. *ACS Chem Biol.* 2012;7:811–816.
31. Hevener KE, Zhao W, Ball DM, et al. Validation of molecular docking programs for virtual screening against dihydropteroate synthase. *J Chem Inf Model.* 2009;49:444–460.
32. Bahekar RH, Jain MR, Jadav PA, et al. Synthesis and antidiabetic activity of 2, 5-disubstituted-3-imidazol-2-yl-pyrrolo [2, 3-b] pyridines and thieno [2, 3-b] pyridines. *Bioorg Med Chem.* 2007;15:6782–6795.
33. DeLano WL. *Pymol: An open-source molecular graphics tool.* San Carlos, USA: DeLano Scientific; 2002.

10

57

CHAPTER 4

PUBLISHED ARTICLE 2

C&B WILEY

Synthesis and evaluation of C3 substituted chalcone-based derivatives of 7-azaindole as protein kinase inhibitors

Malikotsi A. Qhobosheane[1] | Lesetja J. Legoabe[1] |
Béatrice Josselin[2,3] | Stéphane Bach[2,3] | Sandrine Ruchaud[2] | Richard M. Beteck[1]

[1]Centre of Excellence for Pharmaceutical Sciences, North-West University, Potchefstroom, South Africa

[2]Sorbonne Université, CNRS, UMR 8227, Integrative Biology of Marine Models Laboratory (LBI2M), Station Biologique de Roscoff, Roscoff Cedex, France

[3]Sorbonne Université, CNRS, FR2424, Plateforme de criblage KISSf (Kinase Inhibitor Specialized Screening facility), Station Biologique de Roscoff, Roscoff, France

Correspondence
Lesetja J. Legoabe, Centre of Excellence for Pharmaceutical Sciences, North-West University, Private Bag X6001, Potchefstroom 2520, South Africa.
Email: lesetja.legoabe@nwu.ac.za

Funding information
National Research Foundation of South Africa, Grant/Award Number: 96135

Abstract

Chalcones are a group of naturally occurring or synthetic compounds which possess a wide range of biological activities. In this paper, a series of twenty-three 7-azaindole-chalcone hybrids (**5a–w**) were synthesized and evaluated as potential protein kinase inhibitors. Analyses of structure–activity relationships revealed that some of these compounds exhibit significant activity against Haspin kinase, with compounds **5f** and **5q** exhibiting IC_{50} values of 0.47 and 0.41 μM, respectively. Furthermore, **5f** also inhibits cyclin-dependent kinase 9 (CDK9/CyclinT) in a micromolar potency ($IC_{50} = 2.26$ μM). This novel dual-target inhibitor is a promising lead for the development of chemopreventive/chemotherapeutic agents.

KEYWORDS

7-azaindole, CDK9/CyclinT, chalcone, dual inhibitor, Haspin, protein kinase, structure–activity relationships

1 | INTRODUCTION

The protein kinase family is one of the superfamilies of enzymes comprising of more than 500 proteins which are known to be highly evolutionary conserved across numerous eukaryotic species (Saxena et al., 2017). These proteins regulate various cellular events, including cell survival, growth, differentiation and migration (London, 2013). They regulate these events by catalysing the transfer of phosphate(s) to serine, threonine and tyrosine residues of their substrate proteins (Drewry et al., 2017). According to Tong et al. (2013), the protein kinase structure is made of a structurally well-defined ATP binding site and a structurally variable substrate binding site. The ATP binding site comprises of approximately 25 residues, some of which are nearly fully conserved for all kinases. However, some residues, particularly the "gatekeeper," exhibit higher variation.

Abnormal phosphorylation, hyperactivity or overexpression of protein kinases is implicated in a variety of human diseases, including cancer, diabetes and rheumatoid arthritis (Roskoski, 2019; Zhao & Bourne, 2018). As a result, this enzyme family has become one of the most important drug targets. Recent studies reported that approximately 20%–30% of drug discovery efforts worldwide are directed towards the protein kinase superfamily (Roskoski, 2019). Zhang, Yang, and Gray (2009) reported that small molecule inhibitors of protein function are the most common and effective agents for molecularly targeted therapy aimed at treating human diseases and malignancies.

The concept "one drug multiple targets," coined as polypharmacology, is emerging as the next paradigm of drug discovery (Reddy & Zhang, 2013). According to Stankovic et al. (2018), inhibition of a single kinase often shows transient efficacy due to the development of resistance. To slow

the onset of resistance, it has been suggested that multiple kinase inhibitors could be used as a therapeutic strategy for the treatment of human malignancies (Bhullar et al., 2018). Dual targeting agents are better at overcoming transient activity and drug resistance; they therefore provide optimal effects in cancer treatment (Stankovic et al., 2018). For example, a newly discovered drug candidate, fadraciclib (CYC065; Figure 1), which is currently in phase I clinical trials, has been found to potently inhibit CDK2 and CDK9, and it has shown promising activity against a variety of cancers including laryngeal tumours (Do et al., 2018).

Several small molecule protein kinase inhibitors have been approved for clinical use or are currently in clinical trials (Griffith, Brown, McCluskey, & Ashman, 2006). According to Roskoski (2019), the US Food and Drug Administration (FDA) has to date approved 48 small molecule protein kinase inhibitors for malignancies such as breast and lung cancer. Among these, 25 drugs target receptor protein tyrosine kinases, and 10 target non-receptor protein tyrosine kinases, while 13 target serine/threonine protein kinases (Roskoski, 2019).

The breakthrough in the discovery of imatinib (Figure 1) as the first small molecule kinase inhibitor approved for cancer treatment motivated scientists to design newer protein kinase inhibitors with improved activity (Bhullar et al., 2018; Gao et al., 2013; Roskoski, 2019). Despite this fact, target promiscuity has largely limited the rational design strategies of these inhibitors (Gao et al., 2013). Due to the high degree of conservation in the ATP binding pocket of a majority of protein kinases, specific inhibition remains a challenge (Hanson et al., 2019). Furthermore, development of drug resistance due to the emergence of kinase target mutations has also proved to be a great challenge (Arslan, Kutuk, & Basaga, 2006; Gross, Rahal, Stransky, Lengauer, & Hoeflich, 2015). Mutations in the essential gatekeeper of several receptor tyrosine kinases have previously been studied, and they were reportedly overcome by small molecule inhibitors which do not require the gatekeeper for binding (Arslan et al., 2006). These findings suggest that there is a need for the discovery of more novel and highly selective protein kinase inhibitors (Zhao & Bourne, 2018).

Chalcones have attracted considerable attention because of their promising therapeutic effects. Natural and synthetic chalcones have demonstrated a broad spectrum of therapeutic effects including antibacterial, antifungal, antiviral, anti-inflammatory, antioxidant, and most importantly, anticancer activities (Sangpheak et al., 2019). According to Mphahlele, Maluleka, Parbhoo, and Malindisa (2018), chalcone-based compounds have several mechanisms of action, among which are induction of apoptosis, DNA and mitochondrial damage, inhibition of angiogenesis and kinase inhibition. Mphahlele et al., (2018) synthesized a series of benzofuran-chalcone hybrids and evaluated their activity against several targets, including the epidermal growth factor receptor tyrosine kinase (EGFR-TK). The tested compounds inhibited EGFR-TK with sub-micromolar IC_{50} values, and the most potent compound (**1**) exhibited an IC_{50} value of 0.09 ± 0.03 μM (Mphahlele et al., 2018).

The 7-azaindole scaffold has attracted a great deal of interest for the synthesis of a variety of therapeutic agents due to its pivotal role in lead identification and optimization (Mushtaq et al., 2008). Different acylated azaindoles have been reported for analgesic and anti-inflammatory activities (Mushtaq et al., 2008). According to Mushtaq et al. (2008), azaindole analogues have been found to possess blood pressure lowering activities and also act as effective coronary vasodilator, cardiovascular and hypotensive agents. Azaindole derivatives have also been found to be useful in treating disorders such as autoimmune disorders (Farina, Constantin, Laudanna, & Misiano, 2008), cancer (Heinrich, Wucherer-Plietker & Buchstaller, 2015) and Alzheimer's disease (Sreenivasachary et al., 2017).

Because of its outstanding ability to bind to the hinge region of multiple protein kinases, 7-azaindole has been acknowledged as a privileged fragment against kinases, and therefore, it has been incorporated into many kinase inhibitors (Irie & Sawa, 2018). In an attempt to study their pharmacokinetic properties and potentially improve their pharmacological activity, Giles, Saiprabha, and Yeshna (2019) designed a series of 7-azaindole-chalcones and studied their docking interactions with B-Raf kinase. It was interesting to discover that substituting positions -3 and -4 of 7-azaindole with

Fadraciclib (CYC065)
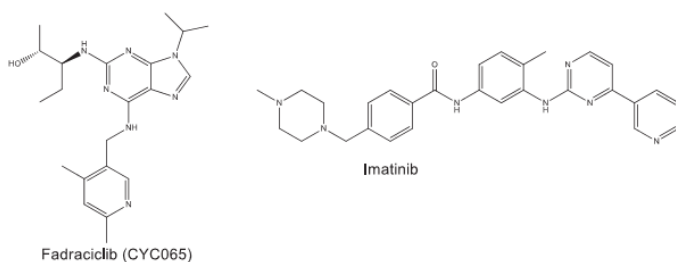
Imatinib

FIGURE 1 Structures of fadraciclib (CYC065) and imatinib

hydroxyl and methyl groups (**2**), respectively, increased the inhibitor binding affinity for B-Raf (Giles et al., 2019). This study suggested that conjugating 7-azaindole and chalcone has potential to increase the inhibitor-kinase binding affinity, and this may be a useful starting point for the development of protein kinase inhibitors (Figure 2). To this effect, in the present study, we synthesized numerous compounds containing the 7-azaindole-chalcone core. The 7-azaindole scaffold was acetylated at position C3 (**4**), after which it was treated with different substituted and unsubstituted aromatic aldehydes to yield a variety of chalcone derivatives (**5a–w**) as shown in Scheme 1.

1-(1H-pyrrolo[2,3-b]pyridin-3-yl)ethanone (**4**) was prepared in a yield of 77% and used as key intermediate. The intermediate was prepared by Friedel-Crafts acylation following a method previously described by Zhang et al. (2002), and it was used in the next step without further purification. The target compounds (**5a–w**) were synthesized in poor to excellent yields (10%–92%) using an acid catalysed aldol condensation method shown in Scheme 1 (Amakali, Legoabe, Petzer, & Petzer, 2018; Nel, Petzer, Petzer, & Legoabe, 2016). Confirmation of synthesis of the target compounds was done by NMR spectroscopic analysis. The absence of a singlet resonating around 2.6 ppm on the proton NMR spectrum of compounds **5a–w** confirmed the successful formation of target compounds. This peak is assigned to the $-CH_3$ of the acetyl unit, which is characteristic of compound **4**.

We screened a library of 23 synthetic 7-azaindole-chalcones against a panel of eight disease-related protein kinases composed of cyclin-dependent kinases (CDKs): *Hs*CDK2/CyclinA, *Hs*CDK5/p25, *Hs*CDK9/CyclinT; *Hs*Haspin, human Proto-oncogene serine/threonine–protein kinase PIM1, porcine casein kinase 1 δ/ε (*Ssc*CK1δ/ε), *Lm*CK1 (from the intracellular parasite *Leishmania major*) and porcine glycogen synthase kinase 3 (*Ssc*GSK3α/β). These compounds were tested at initial concentrations of 1 μM (Table 1) and 10 μM (Table 2a Appendix S1). Compounds that showed <30% residual kinase activity at 1 μM inhibitor concentration, for either CDK9/CyclinT or Haspin, were considered active and were further tested over a wide range of concentrations on both kinases. Sigmoidal curves of kinase activity versus inhibitor concentration were constructed, and from them, IC_{50} values were determined. Figure 3 shows the dose–response curve of compound **5q**, the most potent Haspin inhibitor. The IC_{50} values are summarized in Table 2.

While most of the compounds screened did not inhibit the kinases studied here, **5f** and **5q** showed interesting activities against Haspin and/or CDK9/CyclinT. Compound **5q**, bearing a phenolic substituent, displayed a high degree of selectivity, and it is noteworthy as the most potent Haspin inhibitor (IC_{50} = 0.410 μM). Interestingly, the corresponding unsubstituted compound, **5a**, showed no activity against Haspin. With the exception of **5q**, introducing electron-donating group to the *para* position of the styrene ring led to complete loss of activity against all the tested kinases, as exemplified by **5g**, **5h**, **5j** and **5k**. A similar trend was observed in their electron-withdrawing counterparts; no activity was reported for compounds bearing nitro, halogen or carboxyl groups. For example, compounds **5g**, **5e**, **5i**, **5l**, **5m**, **5n**, **5o**, **5p**, **5v** and **5w** were inactive against all tested protein kinases. Docking study shows that **5q** makes interactions with Hs_HASPIN through the NH of the 7-azaindole ring

FIGURE 2　Chalcone-based protein kinase inhibitors reported in the previous studies (Giles et al., 2019; Mphahlele et al., 2018)

1 (EGFR-TK IC_{50} = 0.09 ± 0.03 μM)　　　　**2**
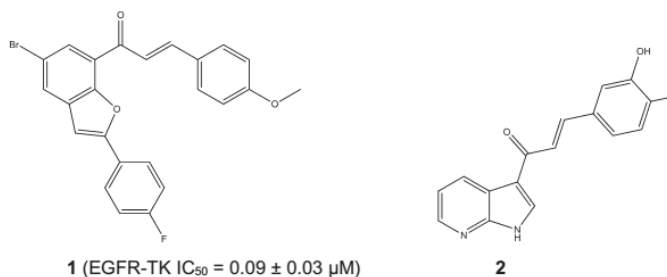
SCHEME 1　Synthesis of 7-azaindole derivatives[a]. [a]Reagents and conditions: (a) AlCl₃, DCM, AcCl, rt, 2 hr; (b) HCl/MeOH, 100°C, 24 hr

[a]Reagents and conditions: (a) AlCl₃, DCM, AcCl, rt, 2h; (b) HCl/MeOH, 100 °C, 24h
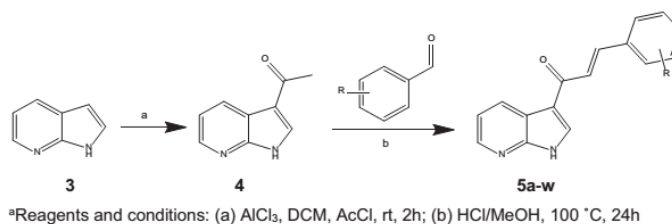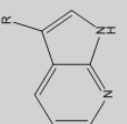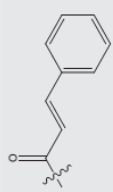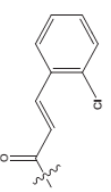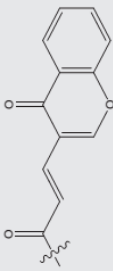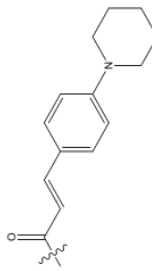
TABLE 1 Percentage of kinase inhibition of **4** and **5a–w**

Compound	R	Residual kinase activity in the presence of 1 μM of tested compound							
		CDK2/Cyclin A	CDK5/p25	CDK9/CyclinT	HASPIN	PIM1	Ssc_CK1δ/ε	Ssc_GSK3α/β	Lm_CK1
4		≥100	≥100	66	63	≥100	79	87	67
5a		≥100	94	47	34	≥100	74	65	61
5b		76	86	80	66	≥100	85	94	99
5c		93	75	90	79	50	67	63	94
5d		≥100	≥100	58	≥100	≥100	69	88	80
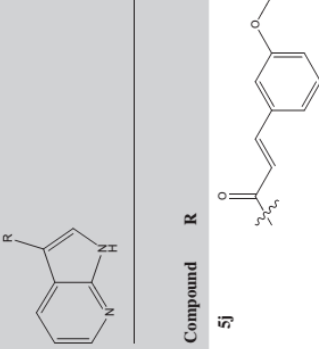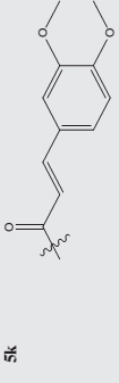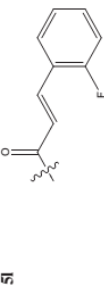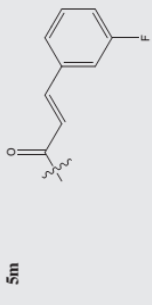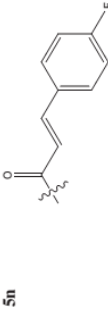
TABLE 1 (Continued)

Compound	R	Residual kinase activity in the presence of 1 μM of tested compound							
		CDK2/Cyclin A	CDK5/p25	CDK9/CyclinT	HASPIN	PIM1	Ssc_CK1δ/ε	Ssc_GSK3α/β	Lm_CK1
5e		85	78	51	88	81	72	91	66
5f		≥100	≥100	30	42	80	68	70	68
5g		91	92	63	56	90	72	91	55
5h		99	96	55	74	≥100	70	88	62
5i		≥100	≥100	56	69	≥100	76	86	76
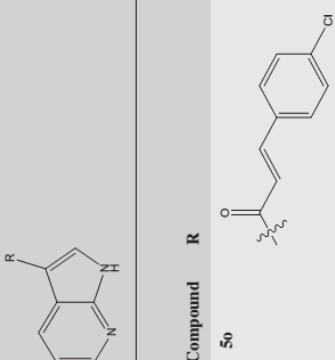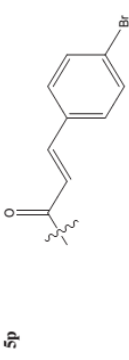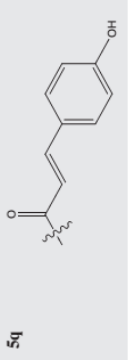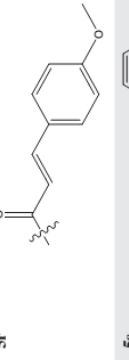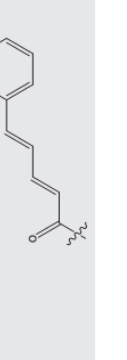
(Continues)

TABLE 1 (Continued)

Compound	R	Residual kinase activity in the presence of 1 μM of tested compound							
		CDK2/Cyclin A	CDK5/p25	CDK9/CyclinT	HASPIN	PIM1	Ssc_CK1δ/ε	Ssc_GSK3α/β	Lm_CK1
5j		≥100	98	56	57	≥100	69	81	86
5k		≥100	≥100	74	69	94	81	72	77
5l		≥100	96	79	63	91	80	83	82
5m		68	96	73	81	95	89	98	78
5n		87	83	58	72	≥100	81	78	75
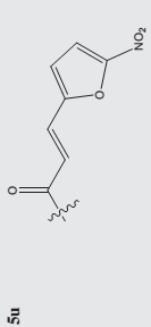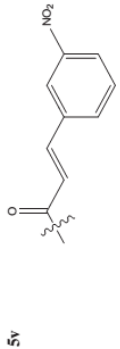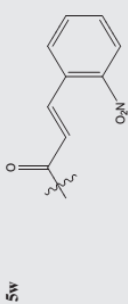
(Continues)

TABLE 1 (Continued)

Compound	R	Residual kinase activity in the presence of 1 µM of tested compound							
		CDK2/Cyclin A	CDK5/p25	CDK9/CyclinT	HASPIN	PIM1	Ssc_CK1δ/ε	Ssc_GSK3α/β	Lm_CK1
5o		84	94	52	53	93	63	92	47
5p		≥100	94	58	72	99	68	63	70
5q		≥100	≥100	45	23	90	76	84	63
5r		≥100	84	65	48	≥100	91	89	78
5s		82	94	55	54	80	60	97	60
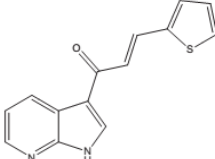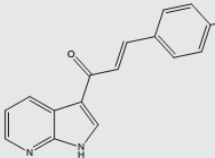
64

TABLE 1 (Continued)

Compound	R	Residual kinase activity in the presence of 1 μM of tested compound							
		CDK2/Cyclin A	CDK5/p25	CDK9/CyclinT	HASPIN	PIM1	Ssc_CK1δ/ε	Ssc_GSK3α/β	Lm_CK1
5t		96	≥100	61	49	85	≥100	84	87
5u		86	≥100	62	42	76	90	84	68
5v		≥100	95	94	63	96	≥100	≥100	98
5w		91	88	90	95	≥100	89	87	75

Note: The table displays the residual activities detected after treatment with 1 μM of the tested compounds expressed in percentage. 100% of residual activity is measured in the absence of inhibitor. ATP concentration used in the kinase assays was 10 μmol/L (values are means, $n = 2$). Kinases are from human origin (*Homo sapiens*) unless specified: Ssc, *Sus scrofa*; Lm, *Leishmania major*.

TABLE 2 Structures and IC$_{50}$ (µM) of compound **5f** and **5q** against human CDK9/CyclinT and Haspin protein kinases

Compound	Structure	IC$_{50}$[a]	
		*Hs*_CDK9/CyclinT	*Hs*_HASPIN
5f		2.260	0.470
5q		NP[b]	0.410

[a]IC$_{50}$ values are reported in µM. Kinase activities were measured using 10 µM ATP. Values are means, $n = 2$.

[b]Not performed because of low activity at 1 µM (see Table 1).
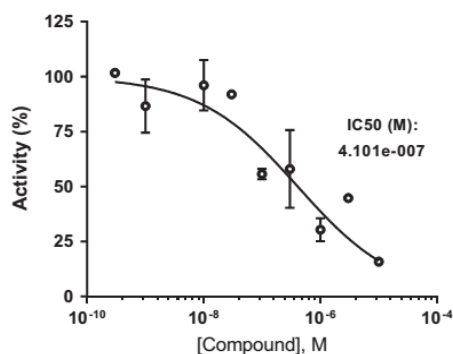
FIGURE 3 Haspin kinase activity versus increasing concentration of compound 5q. Recombinant Haspin kinase was assayed in the presence of 10 µM ATP and increasing concentrations of 5q compound. Kinase activities are expressed in % of maximal activity, that is, measured in the absence of inhibitor (mean $\pm$ *SD* = 2)

and Glu-165 and through the oxygen of the ketone moiety and H$_3$O$^+$ molecule in the enzyme. Replacing the OH group in **5q** with H, F, CH$_3$, OCH$_3$ groups generates analogues wherein the interactions seen with **5q** become weaker or lost completely. This observation suggests the OH as optimal substituent at this position.

Larger groups in the 4-position of the phenyl ring such as piperidinyl (compound **5d**) resulted in a loss of activity, suggesting that bulky non-polar substituents may be undesirable. Furthermore, increasing the length of the linker between the 7-azaindole and the phenyl ring (**5s**) was accompanied by loss of activity.

Most interestingly, replacing styrene as present in compound **5a** with 2-vinylthiophene to give compound **5f** yielded a potent dual inhibitor for Haspin (IC$_{50}$ = 0.470 µM) and CDK9/CyclinT (IC$_{50}$ = 2.260 µM). It is notable that **5f** and **5q** exhibit similar potencies for Haspin (IC$_{50}$ = 0.470 and 0.410 µM, respectively) even though they contain different substituents. Also of note is the fact that replacing the thiophene ring of **5f** with an α-substituted nitrofuran (**5u**) led to decreased activity. These data led to an interesting observation that unsubstituted 5-membered heterocycles may be optimum substituents for the development of 7-azaindole derivatives as dual inhibitors of CDK9/CyclinT and Haspin. However, meaningful structure activity relationships (SARs) could not be derived since most of the evaluated compounds did not inhibit the target kinases. It may therefore be concluded that compounds in this series constitute a promising starting point for the discovery on dual kinase inhibitors.

The binding interactions of **5f** and **5q** with the crystal structure of Hs_HASPIN (PDB code: 6G34), as well as the binding interactions of **5f** with the crystal structure of Hs_CDK9/CyclinT (PDB code: 3TN8), were studied using Glide ligand docking as implemented in Maestro in the Schrödinger package. Enzyme crystal structures were obtained from protein data bank (PDB). The protein–ligand interactions of **5f** and **5q** with Hs_HASPIN show the presence of intermolecular hydrogen bonding between the NH of the 7-azaindole ring and Glu-165 (see entry A and B, Table 3). **5q** also interacted with Hs_HASPIN through hydrogen bonding between the oxygen of the ketone moiety and H$_3$O$^+$ molecule in the enzyme. Both **5f** and **5q** seem to be making the same essential interactions with Hs_HASPIN, and this is also evident in their equipotent activity against the enzyme. The docking scores of

TABLE 3 Binding interactions of **5q** and **5f** against CDK9/CyclinT and Haspin protein kinases

Entry	Enzyme PDB code	Binding affinity	Protein–ligand interaction	Docking pose
A: **5q**	6G34	−6.9792		
B: **5f**	6G34	−8.5801		

(Continues)

TABLE 3 (Continued)

Entry	Enzyme PDB code	Binding affinity	Protein–ligand interaction	Docking pose
C: 5f	3TN8	−7.8810		

5f and **5q** against Hs_HASPIN are −8.5801 and −6.9792, respectively. **5f** interacted with Hs_CDK9/CyclinT through distance interactions above 2 Å (see entry C, Table 3). The docking scores of **5f** against Hs_CDK9/CyclinT are −7.8810.

2 | CONCLUSION

In summary, we investigated a series of chalcone-based 7-azaindole derivatives as potential protein kinase inhibitors. Although most compounds were inactive, two compounds (**5f** and **5q**) were identified as potent inhibitors of CDK9/CyclinT and Haspin kinase. **5f** inhibited both CDK9/CyclinT and Haspin in high-micromolar potencies. SAR analysis suggests that the presence of an unsubstituted 2-thienyl group on the 7-azaindole framework may be necessary for designing multiple protein kinase inhibitors. This study demonstrates that 7-azaindole-chalcone-based compounds are good chemical scaffolds for the design of protein kinase inhibitors and have potential to be developed as anticancer drugs.

CONFLICT OF INTEREST
Stéphane Bach is a founder and member of the scientific advisory board of SeaBeLife Biotech (Roscoff, France). This company is developing novel therapies for treating liver and kidney acute disorders. The authors have no conflict of interest to declare.

DATA AVAILABILITY STATEMENT
Detailed characterization data together with ^{1}H, ^{13}C and HRMS spectra for target compounds **5a–w** are available in the Appendix S1. Samples of compounds can be obtained from corresponding authors upon request.

ORCID
Malikotsi A. Qhobosheane 🔵 https://orcid.org/0000-0003-3005-0028
Lesetja J. Legoabe 🔵 https://orcid.org/0000-0003-2440-4993
Richard M. Beteck 🔵 https://orcid.org/0000-0002-6282-043X

REFERENCES
Amakali, K. T., Legoabe, L. J., Petzer, A., & Petzer, J. P. (2018). Synthesis and in vitro evaluation of 2-heteroarylidene-1-tetralone derivatives as monoamine oxidase inhibitors. *Drug Research*, *68*(12), 687–695. https://doi.org/10.1055/a-0620-8309

Arslan, M. A., Kutuk, O., & Basaga, H. (2006). Protein kinases as drug targets in cancer. *Current Cancer Drug Targets*, *6*(7), 623–634.

Bhullar, K. S., Lagaron, N. O., McGowan, E. M., Parmar, I., Jha, A., Hubbard, B. P., & Rupasinghe, H. P. V. (2018). Kinase-targeted cancer therapies: Progress, challenges and future directions. *Molecular Cancer*, *17*(1), 48. https://doi.org/10.1186/s12943-018-0804-2

Do, K. T., Chau, N., Wolanski, A., Beardslee, B., Hassinger, F., Bhushan, K., … Zheleva, D. I. (2018). Abstract CT037: Phase I safety, pharmacokinetic and pharmacodynamic study of CYC065, a cyclin dependent kinase inhibitor, in patients with advanced cancers (NCT02552953). *American Association for Cancer Research*. *78*(13), https://doi.org/10.1158/1538-7445.AM2018-CT037

Drewry, D. H., Wells, C. I., Andrews, D. M., Angell, R., Al-Ali, H., Axtman, A. D., … Willson, T. M. (2017). Progress towards a public chemogenomic set for protein kinases and a call for contributions. *PLoS One*, *12*(8), 1–20. https://doi.org/10.1371/journal.pone.0181585

Farina, C., Constantin, G., Laudanna, C., & Misiano, P. (2008). Indole and azaindole derivatives for the treatment of inflammatory and autoimmune diseases. *Google Patents*.

Gao, Y., Davies, S. P., Augustin, M., Woodward, A., Patel, U. A., Kovelman, R., & Harvey, K. J. (2013). A broad activity screen in support of a chemogenomic map for kinase signalling research and drug discovery. *Biochemical Journal*, *451*(2), 313–328. https://doi.org/10.1042/BJ20121418

Giles, D., Saiprabha, V., & Yeshna, G. (2019). Design of chalcones of 7-azaindole as raf-B inhibitors. *Journal of Advanced Chemical Sciences*, *4*(4), 606–608. https://doi.org/10.30799/jacs.183.18040404

Griffith, R., Brown, M., McCluskey, A., & Ashman, L. (2006). Small molecule inhibitors of protein kinases in cancer-how to overcome resistance. *Mini Reviews in Medicinal Chemistry*, *6*(10), 1101–1110.

Gross, S., Rahal, R., Stransky, N., Lengauer, C., & Hoeflich, K. P. (2015). Targeting cancer with kinase inhibitors. *The Journal of Clinical Investigation*, *125*(5), 1780–1789. https://doi.org/10.1172/JCI76094

Hanson, S. M., Georghiou, G., Thakur, M. K., Miller, W. T., Rest, J. S., Chodera, J. D., & Seeliger, M. A. (2019). What makes a kinase promiscuous for inhibitors? *Cell Chemical Biology*, *26*, 1–10.

Heinrich, T., Wucherer-Plietker, M., & Buchstaller, H.-P. (2015). 7-Azaindole derivatives suitable for treatment of cancers. *Google Patents*.

Irie, T., & Sawa, M. (2018). 7-Azaindole: a versatile scaffold for developing kinase inhibitors. *Chemical and Pharmaceutical Bulletin*, *66*(1), 29–36. https://doi.org/10.1248/cpb.c17-00380

London, C. A. (2013). Kinase dysfunction and kinase inhibitors. *Veterinary Dermatology*, *24*(1), 181.e140.

Mphahlele, M., Maluleka, M., Parbhoo, N., & Malindisa, S. (2018). Synthesis, evaluation for cytotoxicity and molecular docking studies of benzo [c] furan-chalcones for potential to inhibit tubulin polymerization and/or EGFR-tyrosine kinase phosphorylation. *International Journal of Molecular Sciences*, *19*(9), 2552. https://doi.org/10.3390/ijms19092552

Mushtaq, N., Saify, Z., Noor, F., Takween, S., Akhtar, S., Arif, M., & Khan, K. M. (2008). Synthesis and pharmacological activities of 7-azaindole derivatives. *Pakistan Journal of Pharmaceutical Sciences*, *21*(1), 36–39.

Nel, M. S., Petzer, A., Petzer, J. P., & Legoabe, L. J. (2016). 2-Heteroarylidene-1-indanone derivatives as inhibitors of monoamine oxidase. *Bioorganic Chemistry*, *69*, 20–28. https://doi.org/10.1016/j.bioorg.2016.09.004

Reddy, A. S., & Zhang, S. (2013). Polypharmacology: Drug discovery for the future. *Expert Review of Clinical Pharmacology*, *6*(1), 41–47. https://doi.org/10.1586/ecp.12.74

Roskoski, R. (2019). Properties of FDA-approved small molecule protein kinase inhibitors. *Pharmacological Research*, *144*, 19–50. https://doi.org/10.1016/j.phrs.2019.03.006

Sangpheak, K., Tabtimmai, L., Seetaha, S., Rungnim, C., Chavasiri, W., Wolschann, P., … Rungrotmongkol, T. (2019). Biological evaluation and molecular dynamics simulation of chalcone derivatives as epidermal growth factor-tyrosine kinase inhibitors. *Molecules*, *24*(6), 1092. https://doi.org/10.3390/molecules24061092

Saxena, A., Scaini, G., Bavaresco, D. V., Leite, C., Valvassoria, S. S., Carvalho, A. F., & Quevedo, J. (2017). Role of protein kinase C in bipolar disorder: A review of the current literature. *Molecular Neuropsychiatry*, *3*(2), 108–124. https://doi.org/10.1159/000480349

Sreenivasachary, N., Kroth, H., Benderitter, P., Hamel, A., Varisco, Y., Hickman, D. T., … Muhs, A. (2017). Discovery and characterization of novel indole and 7-azaindole derivatives as inhibitors of beta-amyloid-42 aggregation for the treatment of Alzheimer's disease. *Bioorganic and Medicinal Chemistry Letters*, *27*(6), 1405–1411.

Stankovic, T., Dinic, J., Podolski-Renic, A., Musso, L., Buric, S., Dallavalle, S., & Pesic, M. (2018). Dual inhibitors as a new challenge for cancer multidrug resistance treatment. *Current Medicinal Chemistry*, *25*, 1–30.

Tong, Y., Stewart, K. D., Florjancic, A. S., Harlan, J. E., Merta, P. J., Przytulinska, M., … Penning, T. D. (2013). Azaindole-based inhibitors of Cdc7 kinase: Impact of the Pre-DFG residue, Val 195. *ACS Medicinal Chemistry Letters*, *4*(2), 211–215. https://doi.org/10.1021/ml300348c

Zhang, J., Yang, P. L., & Gray, N. S. (2009). Targeting cancer with small molecule kinase inhibitors. *Nature Reviews Cancer*, *9*(1), 28–39. https://doi.org/10.1038/nrc2559

Zhang, Z., Yang, Z., Wong, H., Zhu, J., Meanwell, N. A., Kadow, J. F., & Wang, T. (2002). An effective procedure for the acylation of azaindoles at C-3. *The Journal of Organic Chemistry*, *67*(17), 6226–6227. https://doi.org/10.1021/jo020135i

Zhao, Z., & Bourne, P. E. (2018). Progress with covalent small-molecule kinase inhibitors. *Drug Discovery Today*, *23*(3), 727–735. https://doi.org/10.1016/j.drudis.2018.01.035

SUPPORTING INFORMATION

Additional supporting information may be found online in the Supporting Information section.

CHAPTER 5

EXPLORATION OF 7-AZAIDOLE-COUMARANONE HYBRIDS AND THEIR ANALOGUES AS PROTEIN KINASE INHIBITORS

Malikotsi A Qhobosheane[1], Richard M. Beteck[1], Blandine Baratte[2,3], Thomas Robert[2,3], Sandrine Ruchaud[2], Stéphane Bach[1,2,3], Lesetja J. Legoabe[1]*

[1] *Centre of Excellence for Pharmaceutical Sciences, North-West University, Private Bag X6001, Potchefstroom 2520, South Africa*

[2] *Sorbonne Université, CNRS, UMR8227, Integrative Biology of Marine Models Laboratory (LBI2M), Station Biologique de Roscoff, 29680 Roscoff, France*

[3] *Sorbonne Université, CNRS, FR2424, Plateforme de criblage KISSf (Kinase Inhibitor Specialized Screening facility), Station Biologique de Roscoff, 29680 Roscoff Cedex, France*

Abstract

7-Azaindole has been labelled a privileged scaffold for the design of new potent inhibitors of protein kinases. In this paper, we determined the inhibition profiles of novel mono- and disubstituted derivatives of 7-azaindole-coumaranone hybrids on various disease-related protein kinases. Eight hit compounds were characterised, among which **7h** was the most potent Haspin inhibitor (IC_{50} = 0.15 µM). An interesting observation was that all active monosubstituted compounds displayed dual inhibition for Haspin and GSK-3β, while disubstituted derivatives inhibited GSK-3β and *Lm*CK1 from *Leishmania major* parasite. Analyses of structure activity relationships (SARs) also revealed that mono-substitution with *para*-fluorobenzyloxy ring produced an equipotent inhibition of Haspin and GSK-3β. Haspin and GSK-3β are relevant targets for developing new anticancer agents while *Lm*CK1 is an innovative target for leishmanicidal drugs. Novel compounds reported in this paper constitute promising starting points for the development of new anticancer and leishmanicidal drugs.

Keywords: 7-azaindole, coumaranone, protein kinase, Haspin, GSK-3β, *Lm*CK1, polypharmacology, anticancer drugs, leishmanicidal drugs.

Graphical abstract

7h
IC_{50}: Haspin: 0.15 µM
IC_{50}: GSK-3β: 0.54 µM
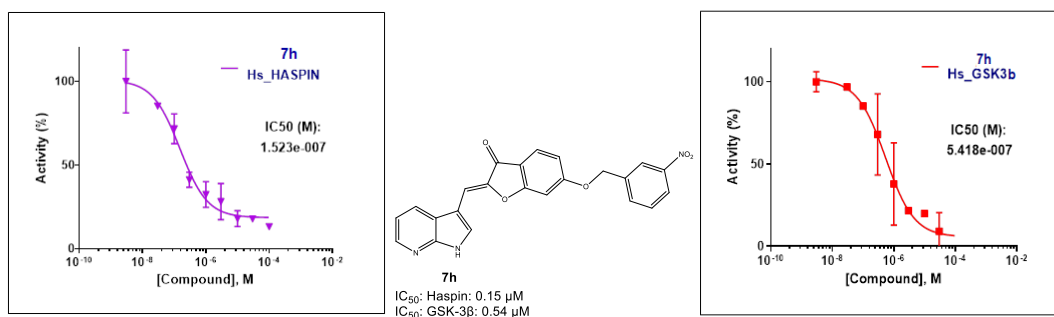
1. Introduction

Protein phosphorylation was originally discovered as a regulatory mechanism for the control of glycogen metabolism. It was subsequently identified as a major regulatory mechanism of protein kinase function [1, 2]. Protein phosphorylation is one of the main processes by which cells regulate their structural and enzymatic proteins. It is catalysed by protein kinases [3]. Protein kinases are a ubiquitous group of enzymes that transfer a phosphate group from adenosine triphosphate (ATP) to multiple protein substrates, consequently altering their functions [4-6]. Reversible phosphorylation regulates primarily all physiological functions [3], while aberrant phosphorylation is associated with various diseases [1] such as cancer, inflammatory disease, diabetes and neurodegenerative diseases including Alzheimer's disease [7]. Because of their role in the development of many diseases, protein kinases have become one of the most important drug targets in the past two decades [8].

Protein kinase inhibitors are a well-established class of clinically useful drugs which have played a significant role in the treatment of diseases and malignancies [9, 10]. Small molecule kinase inhibitors are the most common and effective agents for treatment of human malignancies [11, 12], however, inhibitor selectivity remains a confounding challenge, primarily due to the high structural similarity in the ATP binding site of many protein kinases [13, 14]. The majority of currently available small molecule kinase inhibitors exhibit some degree of promiscuity, causing undesired "off-target" effects [13]. With an increase in structure-based knowledge of protein kinases, unique kinase active site features have been revealed, and they can be exploited to develop target-specific inhibitors [11, 12]. There are currently 63 available small molecule kinase inhibitors approved for clinical use, the majority of which are for oncological indications (for example, 41 inhibitors are active against solid tumours including lymphomas, while eight are active against non-solid tumours, e.g. leukaemias) [15].

Single kinase inhibitors are susceptible to various mechanisms of resistance in cancer treatment [16]. Combination regimens and multiple kinase inhibitors overcome incomplete efficacy and drug resistance associated with single kinase inhibitors [5, 12, 14, 16, 17], thus they are considered as an ideal approach to cancer therapy [12]. This strategy, also called poly-pharmacological approach, already met success in drug development as, from 2015 to 2017, 21% of the new molecular entities (NMEs) approved by the US food and drug administration (FDA) were multi-target drugs [18].

Various protein kinase inhibitors have been developed to competitively bind the ATP binding sites of many kinases [19]. 7-Azaindole is well-known for its ability to form bidentate hydrogen bonds with the hinge region of protein kinases [19, 20], as a result, it has been identified as a

privileged scaffold for kinase inhibition [12, 19]. A previous survey revealed that over 90 protein kinases are sensitive to 7-azaindole-based compounds, and this suggests that 7-azaindole is a useful starting point for the development of various protein kinase inhibitors [19]. A B-Raf kinase inhibitor vemurafenib (**fig. 1**) was the first FDA-approved 7-azaindole-based protein kinase inhibitor [19]. Notably, several 7-azaindole-based protein kinase inhibitors are currently undergoing clinical evaluation, and most of them have been developed to target kinases such as colony stimulating factor receptor 1, rho-associated, coiled-coil-containing protein kinase 1 (ROCK1), aurora kinases and Janus kinase 3 (JAK3) [19].
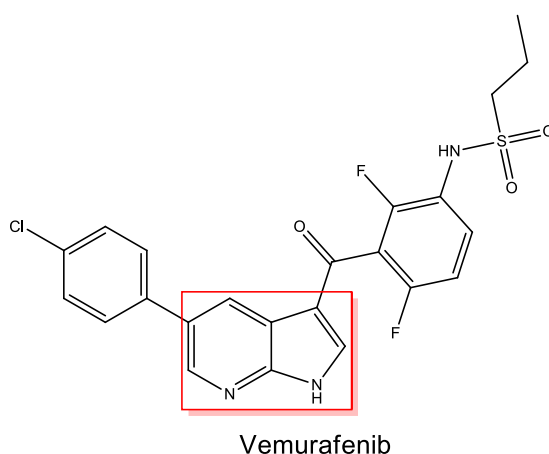
Vemurafenib

Fig. 1: Chemical structure of vemurafenib.

Some 7-azaindole-coumaranone hybrids (scaffold depicted in **fig. 2**) have previously shown very promising kinase inhibitory activities. In our previous paper, we reported four 7-azaindole-benzocycloalkanones which displayed moderate to high enzymatic potencies against cyclin dependant kinase 9 (CDK9)/CyclinT and Haspin kinases [12]. Compound **1** (see **fig. 3**), which bears a coumaranone moiety, was noteworthy as the most potent and selective inhibitor (Haspin IC$_{50}$ = 14 nM) [12]. Similar studies reported 7-azaindole-coumaranone derivatives as potent inhibitors of mTOR, PI3K and PIM1 [21, 22]. For instance, Nakano and co-workers [21] reported a series of 7-azaindole derivatives bearing a coumaranone moiety at position 3, in which they discovered that attaching hydroxyl groups to positions 4 and 6 of the coumaranone ring (**2**) improves inhibitor selectivity against mammalian target of rapamycin (mTOR) 137-fold over phosphatidylinositol-3-kinase (PI3K). Furthermore, Tsou and colleagues [22] also synthesised a series of azaindole-based coumaranone derivatives and the derivative bearing 7-azaindole (**3**) was noted as the most potent proviral integration site for moloney murine leukaemia virus (PIM)-1 inhibitor (IC$_{50}$ = 0.41 nM). Inspired by these promising activities, this paper investigates how derivatisation of **1** affects its biological activity.
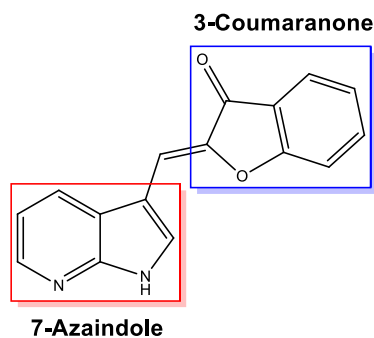
Fig. 2: Scaffold of 7-azaindole-3-coumaranone hybrid, highlighting the 7-azaindole and 3 coumaranone moieties.

1 (Haspin IC$_{50}$ = 14 nM)   **2** (mTOR IC$_{50}$ = 0.46 nM)   **3** (PIM1 IC$_{50}$ = 0.41 nM)
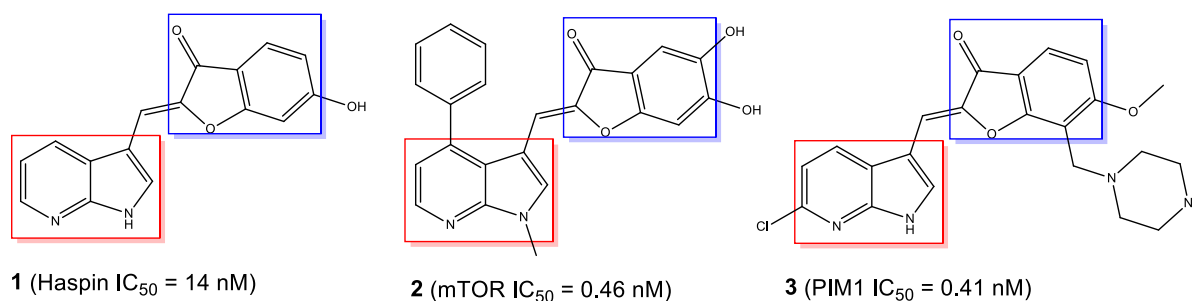
Fig. 3: Structures of 7-azaindole-coumaranone hybrids with known protein kinase inhibitory activity [12, 21, 22].

2.   Results and discussion

2.1.   *Chemistry*
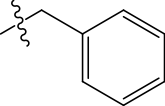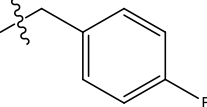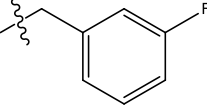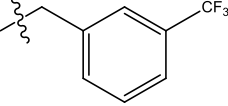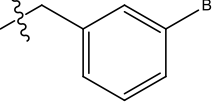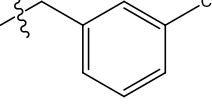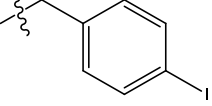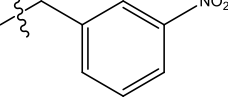
The monosubstituted derivatives of 7-azaindole-coumaranone hybrids (**7a-k**) were synthesised in poor to good yields (9-70%) using a two-step procedure illustrated in **scheme 1**. Commercially available 6-hydroxy-3-coumaranone (**4**) and appropriate substituted aryl-alkyl bromides were suspended in acetonitrile in the presence of K$_3$CO$_2$ [23], employing the Williamson Ether synthesis reaction to produce the key intermediates (**5**). These intermediates were further reacted with 7-azaindole-3-carboxaldehyde (**6**) to yield the target compounds (**7a-k**). With the exception of **7d**, the target compounds were purified by recrystallisation from ethyl acetate. Compound **7d** was purified by recrystallisation from methanol. The disubstituted derivatives (**9a-b**) (**scheme 2**) were synthesised by suspending a previously synthesised compound **1** with appropriately substituted aryl-alkyl bromides (**8**) in N,N-Dimethylformamide (DMF) in the presence of K$_2$CO$_3$ [23]. Compounds **9a** and **9b** were produced in moderate yields (48-60%), and they were recrystallised from acetonitrile and methanol respectively.
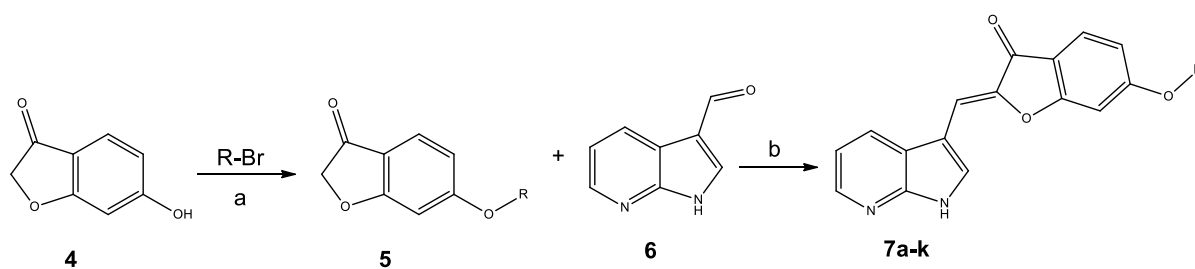
Scheme 1: Synthesis of monosubstituted derivatives of 7-azaindole-coumaranone (**7a-k**). Reaction conditions: (a) AcN, K_2CO_3, 80 °C, 4 h; (b) HCl/MeOH, 100 °C, 24 h.

Table 1

Percentage yields obtained from **7a-k**

Compound	R	Yield
7a		40
7b		47
7c		55
7d		9
7e		40
7f		32
7g		69
7h		26

7i		27
7j		54
7k		70

9a (60%): R = H

9b (48%): R = 3-CF$_3$
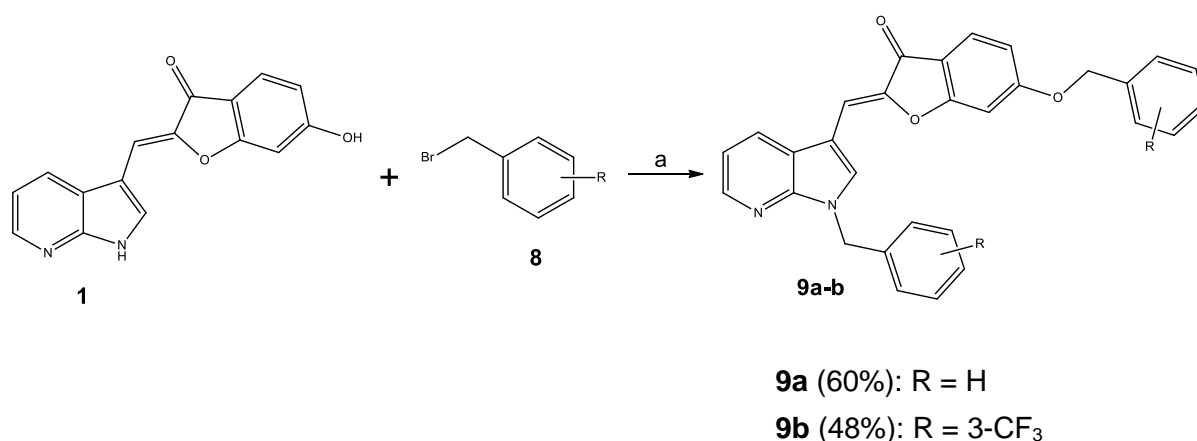
Scheme 2: Synthesis of disubstituted 7-azaindole-coumaranone derivatives (**9a-b**). Reaction conditions: (a) DMF, K$_2$CO$_3$, rt, 24 h.

2.2. *Biological evaluation*

Compounds **7a-k** and **9a-b** were evaluated against a panel of eight human protein kinases (CDK2/CyclinA, CDK5/ p25, CDK9/CyclinT, Haspin, PIM1, CK1ε, GSK-3β and ABL1) and *Lm*CK1 (from the *Leishmania major* parasite) using a method reported by Zeinyeh and co-workers [24], and the results are expressed as % of residual kinase activities at 1 µM and 10 µM compound concentrations (**table 1**). The IC$_{50}$ values were determined only for compounds that inhibited ≥ 70% of kinase activity at both inhibitor concentrations and they are reported in **table 2**. It is noteworthy that most of the tested compounds generally exhibited good activity towards human kinases (Haspin and GSK-3β) and *Lm*CK1. *Leishmaniasis* is a parasitic disease caused by flagellate protozoan *Leishmania* spp, and it is one of the most prevalent tropical diseases, with high morbidity and mortality rates in the tropics and subtropics [25, 26]. Protein kinases have been identified as essential drug targets for the development of antikinetoplastid agents, among which are antileishmanial drugs [27].

Of the thirteen tested compounds, eight hits were established (**7a, 7b, 7c, 7h, 7i, 7j, 9a** and **9b**). From the results, it is evident that all active monosubstituted derivatives of 7-azaindole-coumaranone hybrids (**7a, 7b, 7c, 7h, 7i** and **7j**) are potent dual inhibitors of Haspin and GSK-3β , with varying selectivity for both kinases. On the other hand, the disubstituted derivatives (**9a** and **9b**) are dual-inhibitors of GSK-3β and *Lm*CK1, possessing IC_{50} values in the micromolar range. With the exception of **9a** and **9b**, all compounds possess a benzyloxy moiety attached to position C6 of the coumaranone ring. Compounds **9a** and **9b** bear an additional benzyl moiety at position N1 of the 7-azaindole ring.

Compound **7h**, which bears a 3-nitrobenzyloxy substituent is notable as the most potent Haspin inhibitor (IC_{50} = 0.15 µM). This promising activity may be attributed to the possible formation of hydrogen bonds between the nitro group of the inhibitor and the binding side amino acids. This compound also showed high potency against GSK-3β (IC_{50} = 0.54 µM), however, it is 3-fold more selective for Haspin. The comparison of IC_{50} values for **7b** and **7c** showed that shifting the position of the *para*-fluoro substituent in **7b** to the *meta*-position as seen in **7c** led to decrease in activity for Haspin, while it improved inhibitor activity towards GSK-3β . Another interesting observation was that **7b** is equipotent to Haspin and GSK-3β , with IC_{50} values of 0.86 µM and 0.87 µM respectively. This observation may lead to an assumption that the *para*-fluorobenzyloxy substituent is optimal for the synthesis of equipotent dual inhibitors of Haspin and GSK-3β . Attaching an unsubstituted benzyloxy ring to position C6 of 3-coumaranone (**7a**) had no significant change in activity, in fact, **7a** is among the most potent dual kinase inhibitors (Haspin IC_{50} = 0.94 µM, GSK-3β = 0.71 µM).

Furthermore, replacing the *para*-fluoro substituent of **7b** with a 4-ethoxy substituent (**7j**) significantly improved inhibition of both kinases; IC_{50} = 0.46 µM and 0.75 µM for Haspin and GSK-3β respectively. Regarding solely the inhibition of GSK-3β , derivatives bearing *meta*-substituents on the benzyloxy ring were preferred to *para*-substituted derivatives as exemplified by **7c** and **7h** (IC_{50} = 0.45 µM and 0.54 µM respectively). Interestingly, *para*-substituted derivatives (**7b** and **7j**) displayed superior Haspin activity, contrary to *meta*-substituted derivatives, with the exception of **7h**. This difference in activities may arise from the orientation of inhibitors within the kinase binding pockets, as well as their interactions with the binding site amino acids.

It is worth noting that joining the coumaranone ring and the aryl-alkyl substituent with a longer linker, as seen in **7i** greatly reduced the activity of the inhibitor towards Haspin (IC_{50} = 6.03 µM), relative to derivatives bearing shorter linkers. Moreover, using a longer linker showed no

significant change on the inhibitor activity towards GSK-3β. On the other hand, the disubstituted derivatives **9a** and **9b** inhibited GSK-3β and *Lm*CK1. Disubstitution of the 7-azaindole-coumaranone hybrids led to complete loss of activity for Haspin, as well as significant decrease in activity for GSK-3β. Although speculative, this loss of activity may be attributed to the increased steric bulk of the inhibitors, which in turn increases steric hindrance. It is also believed that attaching a substituent to N1 of 7-azaindole hindered the formation of bidentate hydrogen bonds, leading to decrease and loss of activity for GSK-3β and Haspin respectively.

It is interesting to note that **9b**, which bears a 3-trifluoromethyl substituent at the benzyl and benzyloxy rings is more potent for GSK-3β than its unsubstituted counterpart **9a**. Previous studies have reported that some polyfluorinated compounds possess beneficial pharmacological properties. For instance, a potent CDK inhibitor roniciclib and an antiparasitic agent primaquine possess a trifluoromethyl moiety [28]. This superior activity of **9b** towards GSK-3β may thus be attributable to the fact that it bears a trifluoromethyl group. Conversely, **9a** is more potent for *Lm*CK1 (IC_{50} = 5.17 μM) than **9a** (IC_{50} = 13.04 μM). Although meaningful SARs could not be derived because of limited data (i.e. only two disubstituted compounds were synthesised in this series), this interesting observation may be used to supplement the existing knowledge on the discovery of protein kinase inhibitors for the treatment of leishmaniasis.

Table 2

Residual kinase activity in the presence of 1 and 10 µM of tested compounds (**7a-k** and **9a-b**). Kinases are from human origin (*Homo sapiens*) unless specified: *Lm*, *Leishmania major*.

Cpd	% residual activity measured at 1 µM and 10 µM of analytes								
	*Hs*_CDK2/Cyclin A	*Hs*_CDK5/p25	*Hs*_CDK9/Cyclin T	*Hs*_HASPIN	*Hs*_PIM1	*Hs*_CK1ε	*Hs*_GSK-3β	*Lm*_CK1	*Hs*_ABL1
7a	73 (69)	≥100 (95)	97 (56)	25 (3)	77 (17)	88 (28)	79 (3)	87 (-1)	66 (38)
7b	≥100 (51)	≥100 (≥100)	96 (68)	24 (3)	≥100 (39)	77 (26)	76 (4)	58 (45)	62 (37)
7c	89 (84)	≥100 (≥100)	99 (69)	34 (6)	66 (63)	93 (28)	68 (6)	66 (68)	75 (38)
7d	≥100 (≥100)	≥100 (≥100)	90 (≥100)	65 (24)	≥100 (94)	58 (37)	72 (14)	81 (14)	65 (47)
7e	75 (80)	≥100 (90)	≥100 (88)	67 (18)	57 (36)	75 (46)	76 (15)	60 (38)	48 (40)
7f	≥100 (91)	≥100 (83)	≥100 (≥100)	53 (20)	≥100 (45)	70 (51)	78 (20)	46 (58)	43 (42)
7g	57 (61)	≥100 (95)	≥100 (98)	52 (12)	≥100 (60)	75 (48)	55 (19)	59 (67)	58 (49)
7h	≥100 (77)	≥100 (≥100)	≥100 (≥100)	29 (16)	≥100 (69)	81 (57)	81 (22)	134 (74)	59 (39)
7i	49 (≥100)	≥100 (≥100)	95 (79)	48 (20)	54 (53)	93 (51)	61 (7)	≥100 (31)	60 (44)
7j	49 (46)	≥100 (≥100)	≥100 (53)	25 (10)	37 (24)	79 (45)	65 (3)	77 (49)	47 (38)
7k	56 (50)	≥100 (≥100)	≥100 (≥100)	49 (16)	63 (44)	77 (53)	75 (21)	71 (40)	44 (19)
9a	66 (≥100)	≥100 (≥100)	96 (83)	75 (43)	≥100 (≥100)	81 (51)	88 (25)	90 (11)	48 (41)
9b	≥100 (85)	≥100 (≥100)	≥100 (≥100)	49 (61)	≥100 (≥100)	77 (51)	72 (16)	28 (21)	40 (41)

Values represent the percentage residual kinase activity at 10 µM and 1 µM inhibitor concentrations. ATP concentration used in the kinase assays was 10 µmol/L (values are means, n=2). ≥100 indicates that the compound cannot inhibit the enzymatic activity at the tested concentration.

Table 3: IC_{50} values for the inhibition of human Haspin and GSK-3β and parasitic *Lm*CK1 by selected monosubstituted and disubstituted derivatives of 7-azaindole-coumaranone hybrids. IC_{50} values (in µM) were determined from dose-response curves by using Prism-GraphPad (GraphPad software, San Diego, CA, USA).

Cpd	IC_{50} (µM)		
	*Hs*_Haspin	*Hs*GSK-3β	*Lm*CK1
7a	0.94	0.71	NP[a]
7b	0.86	0.87	NP[a]
7c	1.79	0.45	NP[a]
7h	0.15	0.54	NP[a]
7i	6.03	0.96	NP[a]
7j	0.46	0.75	NP[a]
9a	NP[a]	1.50	5.17
9b	NP[a]	1.14	13.04

[a.]Not performed

2.3 *In silico* evaluation

The physicochemical, pharmacokinetic, drug-like properties as well as medicinal chemistry friendliness of compounds **7a-c, 7h-j** and **9a-b** were evaluated using SwissADME, and the results are illustrated in **table 4-6**, respectively. In this discussion, more focus will be placed on **7h** because it is the most potent inhibitor. **Fig. 4** demonstrates the bioavailability radar of **7h**, which enables a first glance at a molecule's drug likeness [29]. The pink area constitutes the optimal range for each physicochemical parameter; lipophilicity (XLOGP3: -0.7 - 5.0), size (MW: 150 - 500), polarity (TPSA: 20 - 130), solubility (logS < 6), saturation (fraction CSp^3 > 0.25) and flexibility (no. of rotatable bonds < 9) [29]. Although **7h** meets most of these physicochemical parameters; XLOGP3 = 4.28, MW = 413.38 g/mol, TPSA = 110.03 Å^2, logS = -5.27 and no. of rotatable bonds = 5, it is considered not orally bioavailable because it does not meet the saturation fraction (CSp^3 = 0.04).
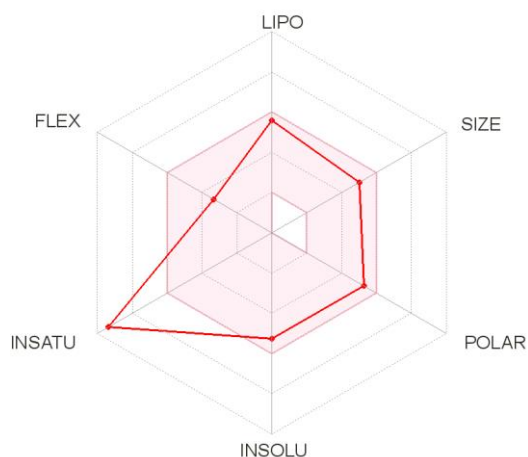
Fig. 4: Bioavailability radar of **7h**. The pink area shows the optimal range for lipophilicity (LIPO), size (SIZE), polarity (POLAR), solubility (INSOLU), saturation (INSATU) and flexibility (FLEX).

Evaluation of passive human gastrointestinal absorption (HIA) and brain penetration (BBB) were done using the BOILED-Egg model, in which the position of **7h** was visualised in the WLOGP-*versus*-TPSA referential (**fig. 5**). This prediction indicates that **7h** has a high probability of passive gastrointestinal (GI) absorption, but it does not permeate the BBB. The inability of **7h** to permeate the BBB may be due to the presence of a hydrophilic nitro-group within its structure. Compound **7h** is also devoid of P-gp substrate properties. Previous studies have reported that P-gp plays a major role in the control of the transcellular flux of molecules, therefore, molecules that are non-P-gp substrates are likely to penetrate the BBB [30].
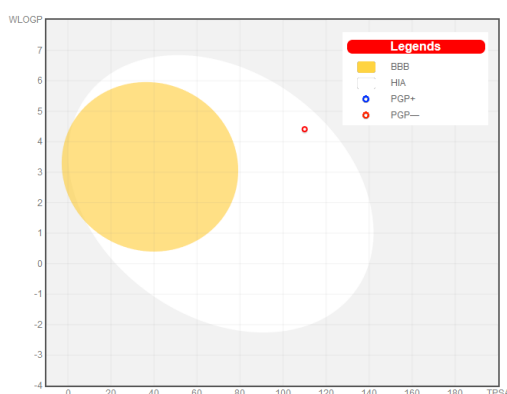
Fig. 5: The BOILED-Egg model of **7h**. The white region represents the probability of passive absorption by the GIT, while the yellow region (yolk) represents the probability of brain penetration. The red dot in the white region indicates that **7h** is non- P-gp substrate (PGP−).

Cytochrome P450 (CYP) is a family of isoenzymes that are responsible for biotransformation of several drugs [31]. Inhibition of the cytochrome P450 metabolism system may cause several drug-drug interactions, which can result in drug toxicities and adverse reactions [31]. Compound **7h** is predicted to be an inhibitor of four major CYP isoforms (CYP1A2, CYP2C19, CYP2C9 and CYP3A4). It is crucial for drug discovery to predict the extent to which a molecule will cause significant drug-drug interactions by inhibiting CYPs, and to determine which isoforms are affected [29]. The likelihood of **7h** to become an oral drug with respect to bioavailability (drug-likeness) was evaluated using rule-based filters from Lipinski, Ghose, Veber, Egan and Muegge, and none of these were violated [29].

Table 4: Physicochemical properties of compounds **7a-c**, **7h-j** and **9a-b**

	Physicochemical properties						Lipophilicity	Water solubility
	Molecular formula	Molecular weight (g/mol)	Fraction Csp3	No. of rotatable bonds	Molar refractivity	TPSA (Å^2)	XLOGP3	Consensus logS
7a	$C_{23}H_{18}N_2O_3$	370.40	0.13	4	106.32	64.21	3.84	-4.69
7b	$C_{23}H_{17}FN_2O_3$	388.39	0.13	4	106.28	64.21	4.28	-4.85
7c	$C_{23}H_{15}FN_2O_3$	386.38	0.04	4	106.41	64.21	4.55	-5.37
7h	$C_{23}H_{17}N_3O_5$	413.38	0.04	5	115.27	110.03	4.28	-5.27
7i	$C_{25}H_{20}N_2O_3$	396.44	0.12	6	116.06	64.21	5.27	-5.74
7j	$C_{25}H_{20}N_2O_4$	412.44	0.12	6	117.75	73.44	4.79	-5.52
9a	$C_{30}H_{22}N_2O_3$	458.51	0.07	6	135.84	53.35	6.00	-6.64
9b	$C_{32}H_{20}F_6N_2O_3$	594.50	0.12	8	145.84	53.35	7.77	-8.36

The Abbot bioavailability score (ABS) (a parameter which seeks to predict a compound's probability to have at least 10% oral bioavailability in rat or measureable Caco-2 permeability) of **7h** is 0.55, and this indicates that **7h** obeys the rule of 5 [32]. In terms of medicinal chemistry, two complementary pattern recognition methods that allow for identification of potentially problematic fragments were used; PAINS and Brenk violations [29]. Pan assay interference structures (PAINS) are molecules that contain structures that show significant response in assays, regardless of the protein target and readout method, and they yield false positive biological results [29]. On the other hand, Brenk violations are 105 fragments identified by

Brenk and co-workers, that may be metabolically unstable, chemically reactive or bear properties responsible for poor pharmacokinetics [29, 33].

Table 5: Pharmacokinetic properties of compounds **7a-c**, **7h-j** and **9a-b**

	GI absorption	BBB permeation	Pgp substrate	CYP1A2 inhibitor	CYP2C19 inhibitor	CYP2C9 inhibitor	CYP2D6 inhibitor	CYP3A4 inhibitor
7a	High	Yes	No	Yes	Yes	Yes	No	Yes
7b	High	Yes	No	Yes	Yes	Yes	No	Yes
7c	High	Yes	No	Yes	Yes	Yes	No	Yes
7h	High	No	No	Yes	Yes	Yes	No	Yes
7i	High	Yes	Yes	Yes	Yes	Yes	No	Yes
7j	High	No	Yes	Yes	Yes	Yes	No	Yes
9a	High	No	No	Yes	Yes	Yes	No	Yes
9b	Low	No	No	No	No	Yes	Yes	Yes

Compound **7h** contains no PAINS liable groups, and it has three Brenk violations because it possesses one Michael acceptor, a nitro group and an oxygen-nitrogen single bond. It is crucial to demonstrate that compounds lack reactivity interference before any further development to avoid wastage of resources [33]. Compound **7h** is also predicted to be devoid of lead-like properties because it falls outside the optimum range of physicochemical properties that qualify it as a lead-like compound. For a compound to satisfy the criteria of lead-likeness, it must have affinity > 0.1 μM, MW < 350 and ClogP < 3 [34]. Compound **7h** violates some of these parameters; MW > 350 and XLOGP3 >3, therefore it cannot be optimised. Based on all predicted physicochemical properties, a conclusion may be drawn that **7h** is a good candidate to be developed as a drug.

Table 6: Drug-likeness and medicinal chemistry friendliness of compounds **7a-c**, **7h-j** and **9a-b**

	Drug likeness						Medicinal chemistry		
Number of violations							**Number of violations**		
	Lipinski[a]	Ghose[b]	Veber[c]	Egan[d]	Muegge[e]	Bioavailability score[f]	PAINS[g]	Brenk[h]	Lead-likeness[i]
7a	0	0	0	0	0	0.55	0	1	2
7b	0	0	0	0	0	0.55	0	1	2
7c	0	0	0	0	0	0.55	0	1	2

7h	0	0	0	0	0	0.55	0	3	2
7i	0	0	0	0	1	0.55	0	1	2
7j	0	0	0	0	0	0.55	0	1	2
9a	0	2	0	1	1	0.55	0	1	2
9b	2	3	0	1	1	0.17	0	1	3

[a] Lipinski: MW < 500, MLOGP < 4.15, N or O < 10, NH or OH < 5

[b] Ghose: 160 < MW < 480, −04 < WLOGP < 5.6, 40 < MR < 130, 20 < atoms < 70

[c] Veber: Num. rotatable bonds < 10, TPSA < 140

[d] Egan: WLOGP < 5.88, TPSA < 131.6

[e] Muegge: 200 < MW < 600, −2 < XLOGP < 5, TPSA < 150, num. rings < 7, num. carbon > 4, num. heteroatoms > 1, num. rotatable bonds < 15,
num. H-bond acceptors < 10, num. H-bond donors < 5

[f] The probability that a compound will have > 10% bioavailability in rat or measurable Caco-2 permeability

[g] PAINS: pan assay interference structures

[h] Brenk: structural alert

[i] Lead-likeness: 250 < MW < 350, XLOGP3 < 3

3. Conclusion

This paper evaluated a series of novel mono- and disubstituted coumaranone-based 7-azaindole derivatives as protein kinase inhibitors. All active monosubstituted compounds are dual inhibitors of human Haspin and GSK-3β . As dual inhibition of protein kinases was shown to be an effective strategy for developing new potent drug candidates, the results described here qualified these hits as promising scaffolds for the design of new anticancer drugs. Furthermore, disubstituted derivatives were noted as potent inhibitors of *Lm*CK1 in addition to GSK-3β , and they represent essential starting points for the development of leishmanicidal drugs. In conclusion, these novel coumaranone-based 7-azaindole derivatives underlined the interest in these structures for the discovery of new human therapeutics against cancer and intracellular parasites.

Experimental section
Chemicals and instrumentation

All starting materials and reagents were procured from AK Scientific or Sigma-Aldrich and used without further purification, unless otherwise noted. Proton (^{1}H) and carbon (^{13}C) NMR spectra were recorded on a Bruker Avance III 600 spectrometer at frequencies of 600 MHz and 151 MHz, respectively, in deuterated dimethylsulfoxide (DMSO-d6). Chemical shifts are reported in parts per million (δ), in reference to the residual solvent signal (DMSO-d6: 2.50 ppm and 39.52 ppm for ^{1}H and ^{13}C, respectively). Spin multiplicities are indicated as follows; s (singlet), d (doublet), dd (doublet of doublets), t (triplet) and m (multiplet). High resolution mass spectra (HRMS) were recorded on a Bruker micrOTOF-Q II mass spectrometer in atmospheric-pressure chemical ionisation (APCI) mode.

Chemical purities were determined by high performance liquid chromatography (HPLC) (Agilent 1200 system) with a Venusil XBP C18 column (4.60 × 150 mm, 5 µm) and a mobile phase of 70% ultrapure water and 30% acetonitrile at a flow rate of 1 mL/min. The melting points (mp) were determined by a Buchi B-545 melting point apparatus and are uncorrected. Thin layer chromatography (TLC) was carried out using silica gel 60 F254 pre-coated aluminium sheets (0.25 mm, Merck). Full-length kinases were used unless specified. Peptide substrates were obtained from Proteogenix (Schiltigheim, France).

General procedure for the synthesis of monosubstituted products (7a-k)

An appropriately substituted aryl-alkyl bromide (2.00 mmol) was added to commercially available 6-hydroxy-3-coumaranone (0.3 g, 2.00 mmol) in acetonitrile containing K_2CO_3 and the reaction was heated under reflux for at least 4 hours [35]. Upon completion, the solvent was evaporated *in vacuo*, and the resultant residue was allowed to stand for 2 hours, after which it solidified. The solid residue was washed with water for 10 minutes and then filtered and dried. A selected intermediate (0.3 g, 1.18 mmol) was added to a mixture of 7-azaindole-3-carboxaldehyde (1.18 mmol) in 32% aqueous HCl/methanol (1.5:1 v/v) and the mixture was stirred at reflux for 24 hours [12]. The reaction progress was monitored by silica gel TLC with petroleum ether: EtOAc (1: 3) as mobile phase. The work-up was done by precipitating the products with ice-cold water, after which they were purified by recrystallisation from ethyl acetate.

**(2*E*)-6-(benzyloxy)-2-(1*H*-pyrrolo[2,3-*b*]pyridin-3-ylmethylidene)-1-benzofuran-3(2*H*)-one (7a)**
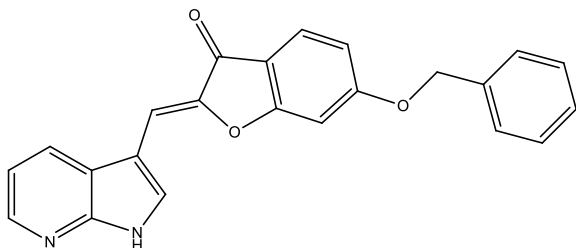
Yield: 40%; (EtoAC); mp 263-266 °C. ^{1}H NMR (600 MHz, DMSO) δ 12.46 (s, 1H), 8.48 (dd, *J* = 7.9, 1.3 Hz, 1H), 8.24 (dd, *J* = 4.6, 1.5 Hz, 1H), 8.17 (d, *J* = 2.5 Hz, 1H), 7.58 (d, *J* = 8.5 Hz, 1H), 7.40 (d, *J* = 7.2 Hz, 2H), 7.33 (t, *J* = 7.5 Hz, 2H), 7.27 (t, *J* = 7.3 Hz, 1H), 7.21 (d, *J* = 2.1 Hz, 1H), 7.14 (dd, *J* = 8.0, 4.5 Hz, 2H), 6.81 (dd, *J* = 8.5, 2.1 Hz, 1H), 5.19 (s, 2H). ^{13}C NMR (151 MHz, DMSO) δ 181.2, 167.5, 166.4, 149.6, 145.9, 144.8, 136.8, 132.8, 129.3, 129.1, 128.97, 128.74, 125.8, 119.4, 117.8, 115.9, 113.5, 108.0, 106.4, 98.7, 71.0. APCI-HRMS m/z: calcld for $C_{23}H_{17}N_2O_3$ (MH$^+$),369.1234, found 369.1218. Purity (HPLC): 82.7%.

(2*E*)-6-[(4-fluorobenzyl)oxy]-2-(1*H*-pyrrolo[2,3-*b*]pyridin-3-ylmethylidene)-1-benzofuran-3(2*H*)-one (7b)
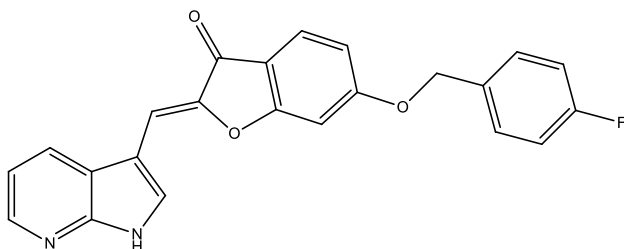
Yield: 47%; (EtoAC); mp 51 °C. ^{1}H NMR (600 MHz, DMSO) δ 12.92 (s, 1H), 8.75 (d, *J* = 7.9 Hz, 1H), 8.43 (d, *J* = 4.9 Hz, 1H), 8.32 (s, 1H), 7.69 (d, *J* = 8.5 Hz, 1H), 7.58 (dd, *J* = 8.2, 5.7 Hz, 2H), 7.39 (dd, *J* = 7.8, 4.9 Hz, 1H), 7.33 – 7.24 (m, 4H), 6.94 – 6.89 (m, 1H), 5.28 (s, 2H). ^{13}C NMR (151 MHz, DMSO) δ 181.3, 167.6, 166.4, 163.5, 161.9, 147.1, 146.3, 133.19, 133.01 (d, *J* = 3.0 Hz), 131.49, 131.09 (d, *J* = 8.4 Hz), 125.9, 120.7, 117.8, 116.1 (d, *J* = 21.4 Hz), 115.8, 113.6, 108.5, 105.6, 98.7, 70.3. APCI-HRMS m/z: calcld for $C_{23}H_{16}FN_2O_3$ (MH$^+$), 387.1139, found 387.1118. Purity (HPLC): 97.4%.

(2*E*)-6-[(3-fluorobenzyl)oxy]-2-(1*H*-pyrrolo[2,3-*b*]pyridin-3-ylmethylidene)-1-benzofuran-3(2*H*)-one (7c)
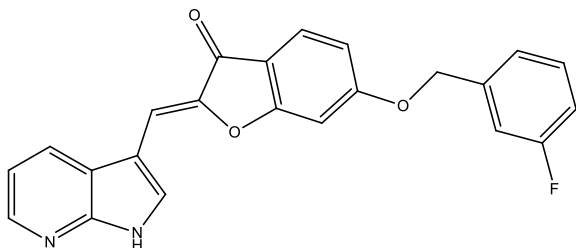
Yield: 55%; (EtoAC); mp 255-258 °C. ^{1}H NMR (600 MHz, DMSO) δ 12.92 (s, 1H), 8.75 (d, *J* = 7.9 Hz, 1H), 8.43 (d, *J* = 4.8 Hz, 1H), 8.32 (s, 1H), 7.70 (d, *J* = 8.5 Hz, 1H), 7.55 – 7.46 (m, 1H), 7.41 – 7.33 (m, 3H), 7.30 (d, *J* = 1.9 Hz, 1H), 7.27 – 7.19 (m, 2H), 6.94 (dd, *J* = 8.5, 2.0 Hz, 1H), 5.32 (s, 2H). ^{13}C NMR (151 MHz, DMSO) δ 181.6, 167.8, 166.5, 164.1, 162.4, 147.4, 146.6, 142.9, 139.9 (d, *J* = 7.5 Hz), 133.4, 131.7 (d, *J* = 8.2 Hz), 126.2, 124.8 (d, *J* = 2.6 Hz), 121.0, 118.1, 116.20, 116.02 (d, *J* = 20.9 Hz), 115.5 (d, *J* = 21.9 Hz), 113.8, 108.8, 106.0, 99.1, 70.4. APCI-HRMS m/z: calcld for $C_{23}H_{16}FN_2O_3$ (MH[+]), 387.1139, found 387.1118. Purity (HPLC): 97.4%.

(2*E*)-2-(1*H*-pyrrolo[2,3-*b*]pyridin-3-ylmethylidene)-6-{[3-(trifluoromethyl)benzyl]oxy}-1-benzofuran-3(2*H*)-one (7d)
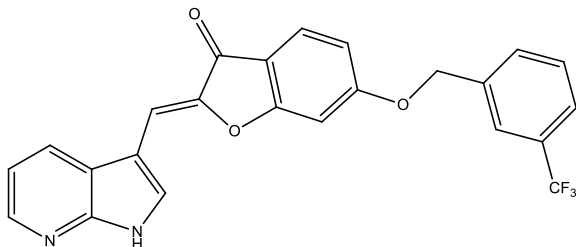
Yield: 9%; (EtoAC); mp 189-192 °C. ^{1}H NMR (600 MHz, DMSO) δ 12.62 (s, 1H), 8.66 – 8.61 (m, 1H), 8.39 (dd, *J* = 4.6, 1.3 Hz, 1H), 8.32 (d, *J* = 2.5 Hz, 1H), 7.93 (s, 1H), 7.87 (d, *J* = 7.6 Hz, 1H), 7.79 (d, *J* = 7.8 Hz, 1H), 7.74 (t, *J* = 8.1 Hz, 2H), 7.39 (d, *J* = 2.0 Hz, 1H), 7.32 – 7.26 (m, 2H), 7.00 (dd, *J* = 8.5, 2.1 Hz, 1H), 5.45 (s, 2H). ^{13}C NMR (151 MHz, DMSO) δ 181.2, 167.4, 166.1, 149.7, 145.9, 144.9, 138.3, 132.9, 132.7, 130.47, 130.14, 129.93, 129.18, 125.86 (d, *J* = 19.5 Hz), 125.64, 125.09, 119.3, 117.7, 116.1, 113.4, 108.0, 106.5, 98.8, 70.0. APCI-HRMS m/z: calcld for $C_{24}H_{16}F_3N_2O_3$ (MH[+]), 437.11076, found 437.1088. Purity (HPLC): 100%.

(2*E*)-6-[(3-bromobenzyl)oxy]-2-(1*H*-pyrrolo[2,3-*b*]pyridin-3-ylmethylidene)-1-benzofuran-3(2*H*)-one (7e)
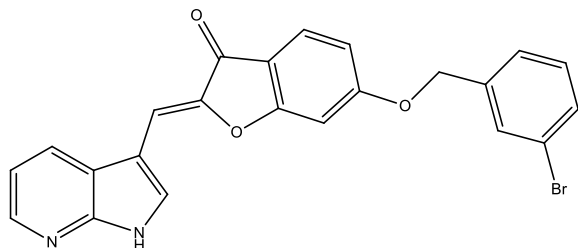
Yield: 40%; (EtoAC); mp 238-243 °C. ^{1}H NMR (600 MHz, DMSO) δ 12.89 (s, 1H), 8.75 (d, *J* = 7.9 Hz, 1H), 8.43 (dd, *J* = 4.8, 1.3 Hz, 1H), 8.33 (s, 1H), 7.78 – 7.70 (m, 2H), 7.61 (d, *J* = 8.0 Hz, 1H), 7.55 (d, *J* = 7.8 Hz, 1H), 7.43 (t, *J* = 7.8 Hz, 1H), 7.39 – 7.33 (m, 2H), 7.30 (s, 1H), 6.97 (dd, *J* = 8.5, 2.1 Hz, 1H), 5.34 (s, 2H). ^{13}C NMR (151 MHz, DMSO) δ 180.9, 167.2, 165.9, 147.4, 145.9, 142.8, 139.3, 132.8, 131.49, 131.26, 130.94, 130.62, 127.3, 125.6, 122.2, 120.1, 117.4, 115.7, 113.2, 108.1, 105.6, 98.6, 69.7. APCI-HRMS m/z: calcld for $C_{23}H_{16}BrN_2O_3$ (MH[+]), 447.0339, found 447.0304. Purity (HPLC): 98.0%.

(2*E*)-6-[(3-chlorobenzyl)oxy]-2-(1*H*-pyrrolo[2,3-*b*]pyridin-3-ylmethylidene)-1-benzofuran-3(2*H*)-one (7f)
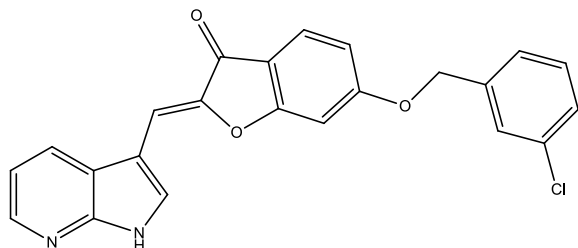
Yield: 32%; (EtoAC); mp 242-248 °C. ^{1}H NMR (600 MHz, DMSO) δ 12.85 (s, 1H), 8.73 (d, *J* = 7.9 Hz, 1H), 8.45 – 8.40 (m, 1H), 8.33 (s, 1H), 7.73 (d, *J* = 8.5 Hz, 1H), 7.61 (s, 1H), 7.52 – 7.38 (m, 3H), 7.38 – 7.32 (m, 2H), 7.29 (s, 1H), 6.97 (dd, *J* = 8.5, 2.0 Hz, 1H), 5.34 (s, 2H). ^{13}C NMR (151 MHz, DMSO) δ 181.3, 167.4, 166.2, 147.8, 146.1, 143.2, 139.3, 133.93, 133.07, 131.2, 130.7, 128.85, 128.27, 127.1, 125.9, 120.3, 117.7, 115.9, 113.5, 108.3, 105.9, 98.8, 70.0. APCI-HRMS m/z: calcld for $C_{23}H_{16}ClN_2O_3$ (MH[+]), 403.0844, found 403.0823. Purity (HPLC): 98.8%.

(2*E*)-6-[(4-iodobenzyl)oxy]-2-(1*H*-pyrrolo[2,3-*b*]pyridin-3-ylmethylidene)-1-benzofuran-3(2*H*)-one (7g)
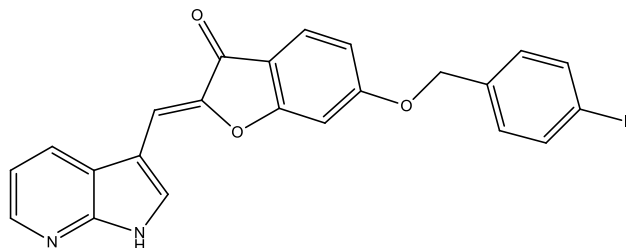
Yield: 69%; (EtoAC); mp 248-258 °C. ^{1}H NMR (600 MHz, DMSO) δ 12.99 (s, 1H), 8.79 (dd, *J* = 7.9, 1.2 Hz, 1H), 8.45 (dd, *J* = 4.9, 1.4 Hz, 1H), 8.34 (s, 1H), 7.86 – 7.79 (m, 2H), 7.72 (d, *J* = 8.5 Hz, 1H), 7.37 (ddd, *J* = 14.1, 6.9, 3.5 Hz, 4H), 7.30 (s, 1H), 6.94 (dd, *J* = 8.5, 2.1 Hz, 1H), 5.30 (s, 2H). ^{13}C NMR (151 MHz, DMSO) δ 181.2, 167.5, 166.3, 147.1, 146.2, 142.6, 138.1, 136.6, 133.1, 131.4, 130.8, 125.9, 120.7, 117.7, 115.9, 113.5, 108.5, 105.6, 98.8, 95.1, 70.3. APCI-HRMS m/z: calcld for $C_{23}H_{16}IN_2O_3$ (MH$^+$), 495.0200, found 495.0176. Purity (HPLC): 96.3%.

(2*E*)-6-[(3-nitrobenzyl)oxy]-2-(1*H*-pyrrolo[2,3-*b*]pyridin-3-ylmethylidene)-1-benzofuran-3(2*H*)-one (7h)
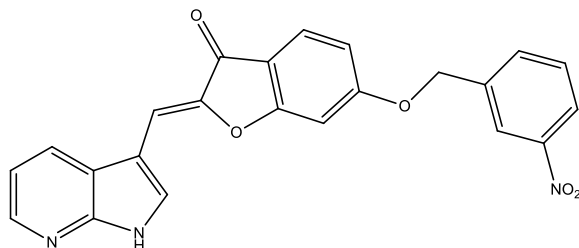
Yield: 26%; (EtoAC); mp 254-257 °C. ^{1}H NMR (600 MHz, DMSO) δ 12.90 (s, 1H), 8.74 (d, *J* = 7.8 Hz, 1H), 8.43 (d, *J* = 4.2 Hz, 1H), 8.39 (s, 1H), 8.32 (s, 1H), 8.25 (d, *J* = 7.9 Hz, 1H), 7.99 (d, *J* = 7.4 Hz, 1H), 7.95 – 7.67 (m, 2H), 7.61 – 7.31 (m, 2H), 7.27 (s, 1H), 7.08 – 6.92 (m, 1H), 5.47 (s, 2H). ^{13}C NMR (151 MHz, DMSO) δ 181.3, 167.4, 166.0, 148.6, 147.4, 146.1, 142.9, 139.1, 134.9, 133.1, 131.0, 130.9, 126.0, 123.7, 122.9, 120.4, 117.7, 116.0, 113.4, 108.4, 105.8, 98.8, 69.6. APCI-HRMS m/z: calcld for $C_{23}H_{16}FN_3O_5$ (MH$^+$), 414.1084, found 414.1052. Purity (HPLC): 96.9%.

(2*E*)-6-(3-phenylpropoxy)-2-(1*H*-pyrrolo[2,3-*b*]pyridin-3-ylmethylidene)-1-benzofuran-3(2*H*)-one (7i)
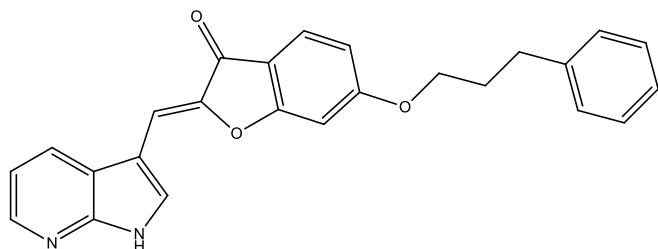
Yield: 27%; (EtoAC); mp 223-225 °C. ^{1}H NMR (600 MHz, DMSO) δ 12.93 (s, 1H), 8.77 (dd, *J* = 7.9, 1.2 Hz, 1H), 8.44 (dd, *J* = 4.9, 1.3 Hz, 1H), 8.34 (s, 1H), 7.70 (d, *J* = 8.5 Hz, 1H), 7.41 – 7.27 (m, 6H), 7.24 (dd, *J* = 11.2, 4.6 Hz, 2H), 6.88 (dd, *J* = 8.5, 2.1 Hz, 1H), 4.19 (t, *J* = 6.4 Hz, 2H), 2.85 – 2.77 (m, 2H), 2.17 – 2.07 (m, 2H). ^{13}C NMR (151 MHz, DMSO) δ 181.0, 167.4, 166.5, 147.2, 145.9, 142.6, 141.6, 132.7, 130.8, 128.8, 126.3, 125.5, 120.2, 117.4, 115.30, 113.1, 108.2, 105.3, 98.0, 68.3, 40.5, 31.8, 30.5. APCI-HRMS m/z: calcld for $C_{25}H_{21}N_2O_3$ (MH$^+$), 397.1547, found 397.1522. Purity (HPLC): 100.0%.

(2*Z*)-6-[(4-ethoxyphenyl)methoxy]-2-[(1*H*-pyrrolo[2,3-*b*]pyridin-3-yl)methylidene]-1-benzofuran-3(2*H*)-one (7j)
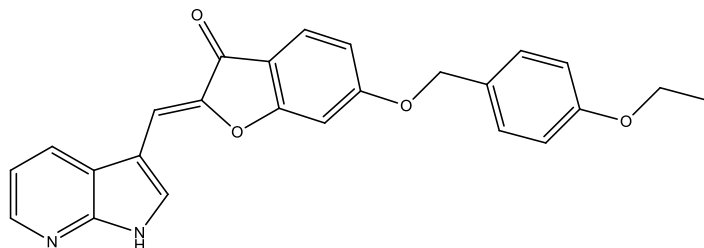
Yield: 54%; (EtoAC); mp 51 °C. ^{1}H NMR (600 MHz, DMSO) δ 13.43 (s, 1H), 9.28 (d, *J* = 7.9 Hz, 1H), 8.96 (d, *J* = 4.8 Hz, 1H), 8.86 (s, 1H), 8.23 (d, *J* = 8.5 Hz, 1H), 7.92 – 7.79 (m, 5H), 7.59 – 7.49 (m, 3H), 7.44 (dd, *J* = 8.5, 1.9 Hz, 1H), 5.10 – 5.03 (m, 2H), 4.97 – 4.89 (m, 2H), 3.06 (s, 3H). ^{13}C NMR (151 MHz, DMSO) δ 181.09, 167.40, 166.28, 158.70, 147.36, 145.97, 142.78, 132.88, 130.83, 130.09, 125.68, 121.40, 120.23, 117.51, 115.57, 115.03, 113.24, 108.25, 105.57, 98.23, 68.04, 66.39, 60.28. APCI-HRMS m/z: calcld for $C_{25}H_{21}N_2O_4$ (MH$^+$), 413.1496, found 399.1313. Purity (HPLC): 79.9%.

4-({[(2*E*)-3-oxo-2-(1*H*-pyrrolo[2,3-*b*]pyridin-3-ylmethylidene)-2,3-dihydro-1-benzofuran-6-yl]oxy}methyl)benzonitrile (7k)
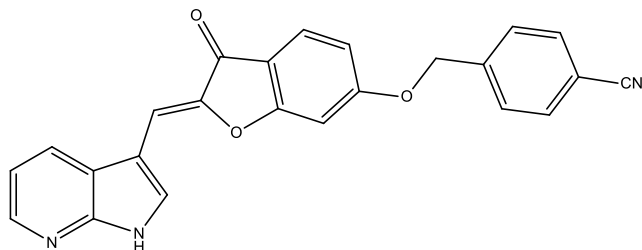
Yield: 70%; (EtoAC); mp 254-258 °C. ^{1}H NMR (600 MHz, DMSO) δ 12.96 (s, 1H), 8.78 (dd, *J* = 7.9, 1.1 Hz, 1H), 8.45 (dd, *J* = 4.9, 1.3 Hz, 1H), 8.33 (s, 1H), 7.94 (d, *J* = 8.3 Hz, 2H), 7.76 – 7.71 (m, 3H), 7.42 – 7.34 (m, 2H), 7.30 (s, 1H), 6.98 (dd, *J* = 8.5, 2.1 Hz, 1H), 5.45 (s, 2H). ^{13}C NMR (151 MHz, DMSO) δ 180.85, 167.09, 165.67, 146.90, 145.81, 142.37, 142.14, 132.87, 132.75, 130.84, 128.60, 125.60, 120.20, 119.02, 117.31, 115.67, 113.10, 111.15, 108.08, 105.42, 103.34, 98.52, 69.56, 40.40. APCI-HRMS m/z: calcld for $C_{24}H_{16}N_3O_3$ (MH[+]), 394.1186, found 394.1164. Purity (HPLC): 82.5%.

General procedure for the synthesis of disubstituted products (9a-b)

A mixture of previously prepared (Z)-2-((1*H*-pyrrolo[2,3-*b*]pyridin-3-yl)methylene)-6-hydroxybenzofuran-3(2H)-one (0.3 g, 1.08 mmol), N,N-dimethylformamide (DMF) and an appropriately substituted alkyl halide (1.08 mmol) was stirred in the presence of K_2CO_3 (0.298 mg, 2.16 mmol). The reaction products were precipitated with addition of ice-cold water (10 ml), collected by filtration and dried [36]. The target products were purified by recrystallisation with methanol.

(Z)-2-((1-benzyl-1H-pyrrolo[2,3-b]pyridin-3-yl)methylene)-6-(benzyloxy)benzofuran-3(2H)-one (9a)
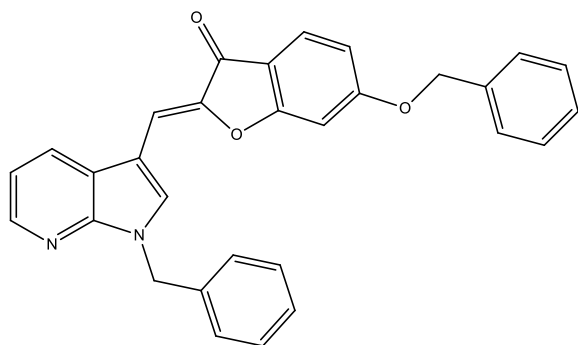
Yield: 60%; (acetonitrile); mp 189-192 °C. ^{1}H NMR (600 MHz, DMSO) δ 8.60 (d, *J* = 7.9 Hz, 1H), 8.45 (s, 1H), 8.39 (d, *J* = 4.5 Hz, 1H), 7.68 (d, *J* = 8.5 Hz, 1H), 7.49 (d, *J* = 7.8 Hz, 2H),

7.43 (t, *J* = 7.4 Hz, 2H), 7.37 (d, *J* = 7.3 Hz, 1H), 7.32 (d, *J* = 7.4 Hz, 2H), 7.31 – 7.25 (m, 4H), 7.24 (s, 1H), 7.21 (s, 1H), 6.91 (d, *J* = 8.5 Hz, 1H), 5.62 (s, 2H), 5.28 (s, 2H). ^{13}C NMR (151 MHz, DMSO) δ 180.9, 167.2, 166.2, 147.9, 145.8, 144.6, 138.1, 136.5, 134.6, 129.25, 129.18, 129.14, 129.04, 128.75, 128.66, 128.43, 128.33, 128.05, 127.7, 125.6, 119.6, 117.9, 115.6, 113.3, 107.2, 105.3, 98.3, 70.7, 48.1. APCI-HRMS m/z: calcld for $C_{30}H_{23}N_2O_3$ (MH[+]), 459.16, found 459.1691. Purity (HPLC): 92.2%.

(Z)-2-((1-(3-(trifluoromethyl)benzyl)-1H-pyrrolo[2,3-b]pyridin-3-yl)methylene)-6-((3-(trifluoromethyl)benzyl)oxy)benzofuran-3(2H)-one (9b)
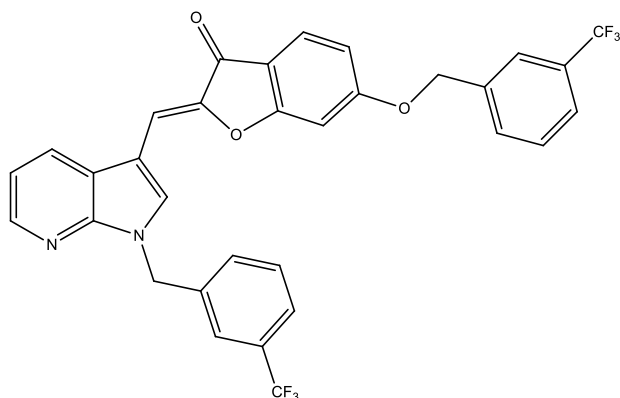
Yield: 48%; (methanol); mp 195-196 °C ^{1}H NMR (600 MHz, DMSO) δ 8.68 (d, *J* = 7.9 Hz, 1H), 8.56 (s, 1H), 8.44 (d, *J* = 4.6 Hz, 1H), 7.92 (s, 1H), 7.86 (d, *J* = 7.7 Hz, 1H), 7.74 (ddd, *J* = 28.0, 19.4, 7.3 Hz, 5H), 7.65 – 7.51 (m, 2H), 7.36 (dd, *J* = 7.9, 4.6 Hz, 1H), 7.30 (s, 1H), 7.26 (d, *J* = 1.8 Hz, 1H), 7.01 (dd, *J* = 8.5, 1.9 Hz, 1H), 5.77 (s, 2H), 5.45 (s, 2H). ^{13}C NMR (151 MHz, DMSO) δ 181.2, 167.4, 166.2, 148.2, 146.2, 145.1, 139.8, 138.3, 135.0, 132.62 6, 132.06, 130.62, 130.48, 130.15, 130.12, 129.94, 129.91, 129.78, 126.1, 125.66 (d, *J* = 3.9 Hz), 125.14 (d, *J* = 2.7 Hz), 125.03 (d, *J* = 3.6 Hz), 124.7 (d, *J* = 3.7 Hz), 119.9, 118.4, 116.1, 113.5, 107.8, 105.7, 98.7, 70.1, 48.0. APCI-HRMS m/z: calcld for $C_{30}H_{21}N_2O_3$ (MH[+]), 459.16, found 459.1691. Purity (HPLC): 80.3%.

Kinase inhibition assay

Kinase inhibition assays were carried out in 384-well plates following the ADP-Glo[TM] protocol (Promega, Madison, WI). Briefly, the reactions were carried out in a final volume of 6 µl for 30 min at 30°C in appropriate kinase buffer, with either protein or peptide as substrate in the presence of 10 µM ATP. After that, 6 µl of ADP-Glo[TM] Kinase Reagent was added to stop the kinase reaction. After incubating the reactions for 50 min at room temperature (RT), 12 µl of Kinase Detection Reagent was added for one hour at RT. The transmitted signal was measured using the Envision (PerkinElmer, Waltham, MA) microplate luminometer and

expressed in Relative Light Unit (RLU). The half maximal inhibitory concentration (IC_{50}) values were determined by performing assays in duplicate in the presence or absence of increasing doses of the tested compounds.

Buffer:

(A) 10 mM $MgCl_2$, 1 mM EGTA, 1 mM DTT, 25 mM Tris-HCl pH 7.5, 50 µg/ml heparin

Kinases:

*Hs*CDK2/CyclinA (cyclin-dependent kinase-2, human, kindly provided by Dr. A. Echalier-Glazer, Leicester, UK) was assayed in buffer A with 0.8 µg/µl of histone H1 as substrate;

*Hs*CDK5/p25 (human, recombinant, expressed in bacteria) was assayed in buffer A with 0.8 µg/µl of histone H1 as substrate;

*Hs*CDK9/CyclinT (human, recombinant, expressed by baculovirus in Sf9 insect cells) was assayed in buffer A with 0.27 µg/µl of the following peptide: YSPTSPSYSPTSPSYSPTSPSKKKK, as substrate;

*Hs*Haspin-kd (human, kinase domain, amino acids 470 to 798, recombinant, expressed in bacteria) was assayed in buffer A with 0.007 µg/µl of Histone H3 (1-21) peptide (ARTKQTARKSTGGKAPRKQLA) as substrate;

*Hs*Pim-1 (human proto-oncogene, recombinant, expressed in bacteria) was assayed in buffer A with 0.8 µg/µl of histone H1 (Sigma #H5505) as substrate;

*Lm*CK1 (from *Leishmania major*, recombinant, expressed in bacteria) was assayed in buffer A with 0.028 µg/µl of the following peptide: RRKHAAIGSpAYSITA as CK1-specific substrate;

*Hs*CK1ε (human casein kinase 1ε, recombinant expressed by baculovirus in Sf9 insect cells) was assayed in buffer A with 0.022 µg/µl of the following peptide: RRKHAAIGSpAYSITA ("Sp" stands for phosphorylated serine) as CK1-specific substrate;

*Hs*GSK-3β (human glycogen synthase kinase-3, recombinant expressed by baculovirus in Sf9 insect cells) was assayed in buffer A with 0.010 µg/µl of GS-1 peptide, a GSK-3-selective substrate (YRRAAVPPSPSLSRHSSPHQSpEDEEE).

To validate each kinase assay, the following model inhibitors were used under the same conditions than the tested compounds. Indirubin-3'-oxime for CDK2/CyclinA, CDK5/p25, CDK9/CyclinT and GSK-3β; SGI-1776 for Pim1; Staurosporine from *Streptomyces sp.* for CK1ε and LmCK1; Imatinib mesylate for ABL1; CHR-6494 for HASPIN.

In silico evaluation

SwissADME (http://www.swissadme.ch) was used to evaluate essential physicochemical parameters of small molecules such as pharmacokinetics, drug-likeness and medicinal chemistry friendliness. Pharmacokinetic parameters such as absorption, distribution, metabolism and excretion are predicted from molecular structures using the most relevant computational methods, therefore various physicochemical properties are explored [28].

Conflict of interest

Stéphane Bach is a founder and member of the scientific advisory board of SeaBeLife Biotech, which is developing novel therapies for treating liver and kidney acute disorders. This work was conducted in the absence of any commercial or financial relationships that could be construed as a potential conflict of interest.

References

[1]   P. Cohen, Protein kinases—the major drug targets of the twenty-first century?, Nat. Rev. Drug Discov 1(4) (2002) 309-315.

[2]   S.S. Taylor, A.P. Kornev, Protein kinases: evolution of dynamic regulatory proteins, Trends Biochem. Sci. 36(2) (2011) 65-77.

[3]   S.T. Nguyen, J.D. Williams, H. Majgier-Baranowska, B. Li, V.R. Neelagiri, H.-O. Kim, N.P. Peet, Concise synthesis of 6-Cyanobenzo[b]furan, a useful building block, Synth. Commun. 44(9) (2014) 1307-1313.

[4]   K.S. Bhullar, N.O. Lagaron, E.M. McGowan, I. Parmar, A. Jha, B.P. Hubbard, H.P.V. Rupasinghe, Kinase-targeted cancer therapies: progress, challenges and future directions, Mol. Cancer 17(1) (2018) 48.

[5]   L.J. Wilson, A. Linley, D.E. Hammond, F.E. Hood, J.M. Coulson, D.J. MacEwan, S.J. Ross, J.R. Slupsky, P.D. Smith, P.A. Eyers, New perspectives, opportunities, and challenges in exploring the human protein kinome, Cancer Res. 78(1) (2018) 15-29.

[6]   X. Zhou, K.J. Herbst-Robinson, J. Zhang, Visualizing dynamic activities of signaling enzymes using genetically encodable FRET-based biosensors: From designs to applications, Methods in enzymology, Elsevier2012, pp. 317-340.

[7]   M. Lawson, J. Rodrigo, B. Baratte, T. Robert, C. Delehouzé, O. Lozach, S. Ruchaud, S. Bach, J.-D. Brion, M. Alami, Synthesis, biological evaluation and molecular modeling studies of imidazo [1, 2-a] pyridines derivatives as protein kinase inhibitors, Eur. J. Med. Chem. 123 (2016) 105-114.

[8]   R. Roskoski Jr, A historical overview of protein kinases and their targeted small molecule inhibitors, Pharmacol. Res. 100 (2015) 1-23.

[9]   S. Gross, R. Rahal, N. Stransky, C. Lengauer, K.P. Hoeflich, Targeting cancer with kinase inhibitors, J Clin Invest 125(5) (2015) 1780-1789.

[10]   L.A. Smyth, I. Collins, Measuring and interpreting the selectivity of protein kinase inhibitors, J. Chem. Biol. 2(3) (2009) 131-151.

[11]   M.A. Qhobosheane, L.J. Legoabe, B. Josselin, S. Bach, S. Ruchaud, J.P. Petzer, R.M. Beteck, Synthesis and evaluation of 7-azaindole derivatives bearing benzocycloalkanone motifs as protein kinase inhibitors, Bioorg. Med. Chem. 28(11) (2020) 115468.

[12]   Z. Zhao, P.E. Bourne, Progress with covalent small-molecule kinase inhibitors, Drug Discov. Today 23 (3) (2018) 727-735.

[13]   T. Bello, T.S. Gujral, KInhibition: a kinase inhibitor selection portal, Iscience 8 (2018) 49-53.

[14]   M.A. Qhobosheane, L.J. Legoabe, B. Josselin, S. Bach, S. Ruchaud, R.M. Beteck, Synthesis and evaluation of C3 substituted chalcone-based derivatives of 7-azaindole as protein kinase inhibitors, Chem Biol Drug Des (2020)

[15]   Roskoski, R. 2020. Properties of FDA-approved small molecule protein kinase inhibitors: A 2020 update. Pharmacol. Res. 152:104609

[16]   R.W. Humphrey, L.M. Brockway-Lunardi, D.T. Bonk, K.M. Dohoney, J.H. Doroshow, S.J. Meech, M.J. Ratain, S.L. Topalian, D.M. Pardoll, Opportunities and challenges in the development of experimental drug combinations for cancer, J. Natl. Cancer Inst. 103(16) (2011) 1222-1226.

[17]   T. Stankovic, J. Dinic, A. Podolski-Renic, L. Musso, S. Buric, S. Dallavalle, M. Pesic, Dual inhibitors as a new challenge for cancer multidrug resistance treatment, Curr. Med. Chem. 25 (2018) 1-30.

[18]   R.R. Ramsay, M.R. Popovic-Nikolic, K. Nikolic, E. Uliassi, M.L. Bolognesi, A perspective on multi-target drug discovery and design for complex diseases, Clin Transl Sci. 7(1) (2018) 3

[19]   T. Irie, M. Sawa, 7-azaindole: a versatile scaffold for developing kinase inhibitors (Patent: WO 2012175168A1), Chem. Pharm. Bull. (2018), pp. 29-36.

[20]   L. Pieterse, L.J. Legoabe, R.M. Beteck, B. Josselin, S. Bach, S. Ruchaud, Synthesis and biological evaluation of selected 7-azaindole derivatives as CDK9/Cyclin T and Haspin inhibitors, Med. Chem. Res. 29 (2020) 1449-1462.

[21]   H. Nakano, N. Saito, L. Parker, Y. Tada, M. Abe, K. Tsuganezawa, S. Yokoyama, A. Tanaka, H. Kojima, T. Okabe, T. Nagano, Rational evolution of a novel type of potent and selective proviral integration site in Moloney murine leukemia virus kinase 1 (PIM1) inhibitor from a screening-hit compound, J. Med. Chem. 55(11) (2012) 5151-64.

[22]   H.R. Tsou, G. MacEwan, G. Birnberg, G. Grosu, M.G. Bursavich, J. Bard, N. Brooijmans, L. Toral-Barza, I. Hollander, T.S. Mansour, S. Ayral-Kaloustian, K. Yu, Discovery and optimization of 2-(4-substituted-pyrrolo[2,3-b]pyridin-3-yl)methylene-4-hydroxybenzofuran-3(2H)-ones as potent and selective ATP-competitive inhibitors of the mammalian target of rapamycin (mTOR), Bioorg. Med. Chem. Lett. 20(7) (2010) 2321-2325.

[23]   L.J. Legoabe, A. Petzer, J.P. Petzer, Inhibition of monoamine oxidase by selected C6-substituted chromone derivatives, Eur. J. Med. Chem. 49 (2012) 343-353.

[24]   W. Zeinyeh, Y.J. Esvan, B. Josselin, B. Baratte, S. Bach, L. Nauton, V. Théry, S. Ruchaud, F. Anizon, F. Giraud, Kinase inhibitions in pyrido [4, 3-h] and [3, 4-g] quinazolines: Synthesis, SAR and molecular modeling studies, Bioorg. Med. Chem. 27(10) (2019) 2083-2089.

[25]   D.O. Santos, C.E. Coutinho, M.F. Madeira, C.G. Bottino, R.T. Vieira, S.B. Nascimento, A. Bernardino, S.C. Bourguignon, S. Corte-Real, R.T. Pinho, Leishmaniasis treatment—a challenge that remains: a review, Parasitol. Res. 103(1) (2008) 1-10.

[26]   E. Torres-Guerrero, M.R. Quintanilla-Cedillo, J. Ruiz-Esmenjaud, R. Arenas, Leishmaniasis: a review, F1000Research 6 (2017) 750.

[27]   C. Merritt, L.E. Silva, A.L. Tanner, K. Stuart, M.P. Pollastri, Kinases as druggable targets in trypanosomatid protozoan parasites, Chem. Rev. 114(22) (2014) 11280-11304.

[28]   M. Bassetto, S. Ferla, F. Pertusati, Polyfluorinated groups in medicinal chemistry, Future Med. Chem. 7(4) (2015) 527-546.

[29]   A. Daina, O. Michielin, V. Zoete, SwissADME: a free web tool to evaluate pharmacokinetics, drug-likeness and medicinal chemistry friendliness of small molecules, Sci. Rep. 7 (2017) 42717.

[30]   F. Montanari, G.F. Ecker, Prediction of drug–ABC-transporter interaction—Recent advances and future challenges, Adv. Drug Deliv. Rev. 86 (2015) 17-26.

[31]   C.C. Ogu, J.L. Maxa, Drug interactions due to cytochrome P450, Baylor University medical center proceedings, Taylor & Francis, 2000, pp. 421-423.

[32]   Y.C. Martin, A bioavailability score, J. Med. Chem. 48(9) (2005) 3164-3170.

[33]   H.D. Janse van Rensburg, L.J. Legoabe, G. Terre'Blanche, J. Aucamp, Synthesis and evaluation of methoxy substituted 2-benzoyl-1-benzofuran derivatives as lead

compounds for the development adenosine A1 and/or A2A receptor antagonists, Bioorg. Chem. 94 (2020) 103459.

[34]   S.J. Teague, A.M. Davis, P.D. Leeson, T. Oprea, The design of leadlike combinatorial libraries, Angew. Chem. Int. Ed. 38(24) (1999) 3743-3748.

[35]   J.-S. Lan, S.-S. Xie, M. Huang, Y.-J. Hu, L.-Y. Kong, X.-B. Wang, Chromanones: selective and reversible monoamine oxidase B inhibitors with nanomolar potency, MedChemComm 6(7) (2015) 1293-1302.

[36]   M.A. Qhobosheane, A. Petzer, J.P. Petzer, L.J. Legoabe, Synthesis and evaluation of 2-substituted 4(3H)-quinazolinone thioether derivatives as monoamine oxidase inhibitors, Bioorg. Med. Chem. 26(20) (2018) 5531-5537.

CHAPTER 6
CONCLUSION

Protein phosphorylation is one of the most common reversible post-translational modifications that regulates protein functions in several physiological processes, including signal transduction pathways, proliferation, differentiation, metabolism, survival, motility and gene transcription (Sawyer, 2007; Fraschini *et al.*, 2012). Protein phosphorylation occurs through protein kinases, which transfer a phosphate group from ATP to a hydroxyl group of the lateral chain specific serine, threonine or tyrosine residues on peptide substrates (Fraschini *et al.*, 2012; Ardito *et al.*, 2017). About 30% of the human proteins contain covalently bound phosphate, and approximately 500 protein kinases are encoded by the human kinome, therefore, it is not surprising that aberrant phosphorylation causes various diseases (Cohen, 2001). Neurodegenerative disorders, cardiovascular disorders and cancer arise as a result of abnormal phosphorylation, hyperactivity or overexpression of protein kinases (Zhao & Bourne, 2018; Roskoski, 2019).

Cancer not only arises from genetic mutations, but it is also a consequence of epigenetic changes that lead to deregulation of signal transduction pathways with subsequent changes in normal cellular signalling (Ardito *et al.*, 2017). According to Ardito et al. (2017), protein kinases represent the largest group (almost 10%) of the nearly 300 cancer genes that have been reported to date. Furthermore, many cancers have been associated with somatic mutations of protein kinases (Sawyer, 2007). Oncogenic transformation of protein kinases may arise from the fusion products of genomic rearrangements (e.g. chromosomal translations), mutations (e.g. gain-of-function), deletions and overexpression resulting from gene amplifications (Sawyer, 2007). These transformations typically result in increased protein kinase activity, which consequently alters downstream signal transduction (Sawyer, 2007).

Because of their role in various pathological processes, protein kinases have gained great importance as drug targets (Kini *et al.*, 2017), and they are currently the target of many drug discovery programs (Roskoski, 2020). Kini *et al.* (2017) indicates that almost 25 to 30% of all targets screened in the pharmaceutical industry belong to the protein kinase family. Although protein kinases have mainly been exploited in oncology for development of anticancer drugs, they are gradually gaining attention in other diseases; this has led to an exponential increase in the development of kinase inhibitors as therapeutic agents for the treatment of several other diseases (Kini *et al.*, 2017).

Since the discovery of imatinib, several small molecule protein kinase inhibitors have been approved for clinical use (Griffith *et al.*, 2006). The US FDA approved four small molecule kinase inhibitors in 2019; entrecitinib, erdafitinib, pexidartinib and fedratinib (Roskoski, 2020). In total, the US FDA has approved 52 small molecule protein kinase inhibitors to date, the majority of which are for oral administration (Roskoski, 2020). Of the 52 approved drugs, eleven inhibit serine/threonine protein kinases, two are dual specificity protein kinase inhibitors, eleven block NRTKs while 28 inhibit RTKs (Roskoski, 2020). Moreover, 46 of the approved drugs are used in treatment of neoplastic diseases (eight against non-solid tumours such as leukaemias and 41 against solid tumours including breast and lung cancers; some drugs are used against both tumour types) (Roskoski, 2020).

Multi-kinase inhibitors are more effective than mono-kinase inhibitors in cancer chemotherapy (Petrelli & Giordano, 2008), the former represent a new perspective and an innovative approach to cancer treatment. Multi-target agents terminate tumour progression, while avoiding mechanisms of resistance that are commonly activated by the tumour (Daydé-Cazals *et al.*, 2016). In addition, multi-kinase inhibitors can be used to treat a wide range of cancers and they are effective as combination therapy, but lack the disadvantages associated with combination therapy such as drug-drug interactions and multiple side-effects (Daydé-Cazals *et al.*, 2016).

The 7-azaindole is known as a privileged scaffold for protein kinase binding, thus it has attracted great attention in the design of inhibitors of disease-related protein kinases (Pieterse *et al.*, 2020). Irie and Sawa (2018) reported that over 90 protein kinases are inhibited by 7-azaindole-based compounds. Several 7-azaindole-based compounds are currently in clinical use as protein kinase inhibitors; for instance, pexidartinib is a 7-azaindole-based TKI which was approved in 2019 for the treatment of symptomatic tenosynovial giant cell tumour (Gelderblom & Sande, 2020). On the other hand, chalcones exhibit a wide range of biological properties including anticancer (Mphahlele *et al.*, 2018). Several mechanisms of action such as induction of apoptosis, inhibition of angiogenesis, tubulin inhibition and kinase inhibition have been reported for chalcone-based compounds (Mphahlele *et al.*, 2018).

The present study aimed to investigate novel 7-azaindole-based chalcones and their analogues as inhibitors of tumorigenic protein kinases. So far, two articles have been published and a third manuscript is underway. In the first article, 7-azaindole was hybridized with various benzocycloalkanones, among which were α-tetralone, 1-indanone and 3-coumaranone to afford a series of novel compounds which were evaluated against a panel of eight protein kinases. All active compounds in this series inhibited Haspin kinase, and (Z)-2-((1H-pyrrolo[2,3-b]pyridin-3-yl)methylene)-6-hydroxybenzofuran-3(2H)-one (**8l**) was notable

as the most potent inhibitor (IC_{50} = 14 nM). Furthermore, an interesting observation was made that active derivatives bearing α-tetralone (**8g** and **8h**) were dual inhibitors of Haspin and CDK9/CyclinT, and they exhibit similar potencies for CDK9/CyclinT (IC_{50} = 424 nM and 495 nM, respectively).

The second paper evaluated a series of novel 7-azaindole-chalcones against the same panel of protein kinases, and two compounds were active against Haspin and CDK9/CyclinT. Compound **5q** which bears a *para*-hydroxyphenyl substituent was the most potent Haspin inhibitor (IC_{50} = 410 nM), while **5f** was a dual inhibitor of Haspin (IC_{50} = 470 nM) and CDK9/CyclinT (IC_{50} = 2260 nM).

The third series was inspired by the excellent activity of compound **8l**. In this series, various substituted and unsubstituted aryl-alkyl groups were attached to 6-OH of 3-coumaranone and N-1 of the 7-azaindole ring of **8l** to evaluate how this derivatisation would affect the inhibitors' activity. Eight hits were established from this series, all of which were dual inhibitors of either Haspin and GSK-3β, or GSK-3β and *Lm*CK1. Among the evaluated compounds, **7h**, which bears a *meta*-nitrobenzyloxy substituent was identified as the most potent Haspin inhibitor (IC_{50} = 0.15 μM). Furthermore, attaching a *para*-fluorosubstituted aryl-alkyl to 6-OH of 3-coumaranone led to synthesis of a dual inhibitor (**7b**), which is equipotent to Haspin and GSK-3β. Interestingly, disubstituted compounds exhibited good potencies for *Lm*CK1, in addition to GSK-3β.

In summary, the following conclusions were made from this study:

- With the exception of **9a** and **9b**, all active compounds reported in this study are Haspin inhibitors; derivatisation of 7-azaindole at position C3 with various substituted and unsubstituted benzocycloalkanones and benzaldehydes generated novel single and dual selectivity protein kinase inhibitors.
- Some of the potent Haspin inhibitors synthesised in this study bear a hydroxyl group side chain (e.g. **5q, 8h** and **8l**), and this suggests that the –OH group is crucial for the binding of inhibitors into the active side of Haspin.
- In addition, all active compounds bearing α-tetralone (**8g** and **8h**) are dual inhibitors of CDK9/CyclinT and Haspin. Although the binding modes are unknown, it may be assumed that α-tetralone is an optimum substituent for the development of dual CDK9/CyclinT – Haspin inhibitors.
- Attaching an aryl-alkyl group to the OH of **8l** led to synthesis of several dual inhibitors of Haspin and GSK-3β, as well as GSK-3β and *Lm*CK1, with micromolar to submicromolar IC_{50} values.

- The nitrobenzyloxy substituted derivative (**7h**) is 3-fold more selective for Haspin, contrary to GSK-3β, and this implies that the presence of the nitro group within the inhibitor is ideal for Haspin inhibition.

- Furthermore, derivatisation at position N-1 of the 7-azaindole and 6-OH of the 3-coumaranon demonstrated good activity against *Lm*CK1 while also displaying a decrease in activity towards GSK-3β.

In conclusion, this study has successfully identified several novel 7-azaindole-chalcones and related compounds as potent Haspin inhibitors, as well as dual inhibitors of mammalian CDK9/CyclinT and Haspin, Haspin and GSK-3β, and finally GSK-3β and *Lm*CK1. Dual protein kinase inhibitors slow the onset of resistance to anticancer agents, and they provide optimal effects in cancer treatment. Potent Haspin inhibitors have a potential to act as antimitotic agents, with an ability to terminate cancer cell proliferation (Pieterse *et al.*, 2020). Haspin is essential in the regulation of mitosis, and its RNA interference in tumour cells disrupts chromosome alignment and completion of the normal mitotic process (Pieterse *et al.*, 2020); therefore, Haspin is a susceptible target to anticancer drugs. Moreover, *Lm*CK1 has been validated as a drug target for antileishmanial therapy because of its essential role in parasite survival (Bazin *et al.*, 2020). Targeting *Lm*CK1 not only kills the parasite but it also limits the emergence of parasite resistance (Bazin *et al.*, 2020). Compounds synthesised in this study may thus provide valuable candidates for the development of anticancer and antileishmanial drugs.

Future perspective

Great progress has been made in the development of small molecule protein kinase inhibitors in the past two decades, however, this field still needs further exploration. Most of the FDA approved therapeutics are directed towards treatment of various cancers and inflammatory diseases. Despite numerous advances in cancer therapy, treatment of cancer is complicated by a plethora of protein kinase mutations, which lead to drug resistance. These challenges may be overcome by multiple kinase inhibition as well as combination therapy.

The hybridisation of 7-azaindole and 3-coumaranone proved to be an effective approach to the synthesis of potent single and dual kinase inhibitors. These derivatives may be a starting point for future design of potent Haspin inhibitors. Haspin has only one substrate, therefore these inhibitors may have potential therapeutic advantage, with fewer side effects. Because of their ability to inhibit multiple kinases, these inhibitors can be more efficient in cancer therapy, contrary to single target inhibitors. Disubstitution of 7-azaindole at positions N1 and C3 may lead to synthesis of compounds with leishmanicidal activity. This derivatisation may

further be exploited to improve activity of inhibitors against *Lm*CK1. The 7-azaindole-coumanone pharmacophore may also be derivatised at other position to synthesise compounds with improved kinase activity and a potential to inhibit other classes of protein kinases.

References

Ardito, F., Giuliani, M., Perrone, D., Troiano, G. & Lo Muzio, L. 2017. The crucial role of protein phosphorylation in cell signaling and its use as targeted therapy. *International journal of molecular medicine*, 40(2):271-280.

Bazin, M.-A., Cojean, S., Pagniez, F., Bernadat, G., Cavé, C., Ourliac-Garnier, I., Nourrisson, M.-R., Morgado, C., Picot, C., Leclercq, O., Baratte, B., Robert, T., Späth, G.F., Rachidi, N., Bach, S., Loiseau, P.M., Le Pape, P. & Marchand, P. 2020. In vitro identification of imidazo[1,2-a]pyrazine-based antileishmanial agents and evaluation of L. major casein kinase 1 inhibition. *European journal of medicinal chemistry*:112956.

Cohen, P. 2001. The role of protein phosphorylation in human health and disease. *European journal of biochemistry*, 268(19):5001-5010.

Daydé-Cazals, B., Fauvel, B., Singer, M., Feneyrolles, C., Bestgen, B., Gassiot, F., Spenlinhauer, A., Warnault, P., Van Hijfte, N., Borjini, N., Chevé, G. & Yasri, A. 2016. Rational design, synthesis, and biological evaluation of 7-azaindole derivatives as potent focused multi-targeted kinase inhibitors. *Journal of medicinal chemistry*, 59(8):3886-3905.

Fraschini, R., Raspelli, E. & Cassani, C. 2012. Protein phosphorylation is an important tool to change the fate of key players in the control of cell cycle progression in saccharomyces cerevisiae. *Protein phosphorylation in human health*:377-394.

Gelderblom, H. & Sande, M.v.d. 2020. Pexidartinib: first approved systemic therapy for patients with tenosynovial giant cell tumor. *Future oncology*, 16(29):2345-2356.

Griffith, R., Brown, M., McCluskey, A. & Ashman, L. 2006. Small molecule inhibitors of protein kinases in cancer-how to overcome resistance. *Mini reviews in medicinal chemistry*, 6(10):1101-1110.

Irie, T. & Sawa, M. 2018. 7-azaindole: a versatile scaffold for developing kinase inhibitors (Patent: WO 2012175168A1).

Kini, S.G., Garg, V., Prasanna, S., Rajappan, R. & Mubeen, M. 2017. Protein kinases as drug targets in human and animal diseases. *Current enzyme inhibition*, 13(2):99-106.

Mphahlele, M., Maluleka, M., Parbhoo, N. & Malindisa, S. 2018. Synthesis, evaluation for cytotoxicity and molecular docking studies of benzo [c] furan-chalcones for potential to inhibit tubulin polymerization and/or EGFR-tyrosine kinase phosphorylation. *International journal of molecular sciences*, 19(9):2552.

Petrelli, A. & Giordano, S. 2008. From single-to multi-target drugs in cancer therapy: when aspecificity becomes an advantage. *Current medicinal chemistry*, 15(5):422-432.

Pieterse, L., Legoabe, L.J., Beteck, R.M., Josselin, B., Bach, S. & Ruchaud, S. 2020. Synthesis and biological evaluation of selected 7-azaindole derivatives as CDK9/Cyclin T and Haspin inhibitors. *Medicinal chemistry research*, 29:1449-1462.

Roskoski, R. 2019. Properties of FDA-approved small molecule protein kinase inhibitors. *Pharmacological research*, 144:19-50.

Roskoski, R. 2020. Properties of FDA-approved small molecule protein kinase inhibitors: A 2020 update. *Pharmacological research*, 152:104609.

Sawyer, T. 2007. Protein kinases and protein phosphatases in signal transduction pathways. *(In* Taylor, J.B. & Triggle D.J., *eds.* Comprehensive medicinal chemistry II Elsevier Ltd.

Zhao, Z. & Bourne, P.E. 2018. Progress with covalent small-molecule kinase inhibitors. *Drug discovery today*, 23 (3):727-735.

APPENDIX A:
SUPPORTING DATA FOR CHAPTER 3

^{1}H NMR, ^{13}C NMR and HPLC

Malikotsi A. Qhobosheane,[1] Lesetja J. Legoabe [1,*], Béatrice Josselin[2,3], Stéphane Bach[2,3], Sandrine Ruchaud[2], Jacobus P. Petzer[1,4], Richard M Beteck[1]

[1]   *Centre of Excellence for Pharmaceutical Sciences, North-West University, Private Bag X6001, Potchefstroom 2520, South Africa*

[2]   *Sorbonne Université, CNRS, UMR 8227, Integrative Biology of Marine Models, Station Biologique de Roscoff, CS 90074, 29688 Roscoff Cedex, France*
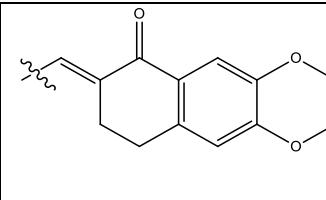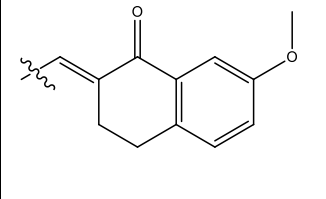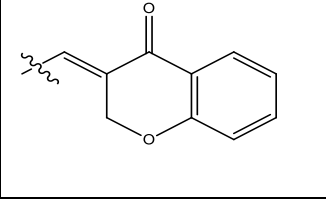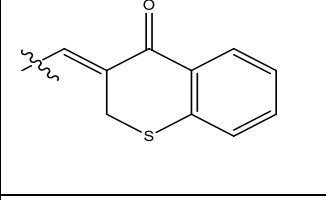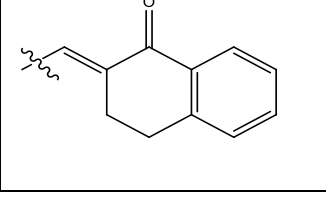
[3]   *Sorbonne Université, CNRS, FR2424, Plateforme de criblage KISSf (Kinase Inhibitor Specialized Screening facility), Station Biologique de Roscoff, Place Georges Teissier, 29682 Roscoff, France*
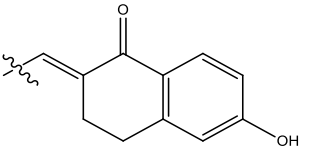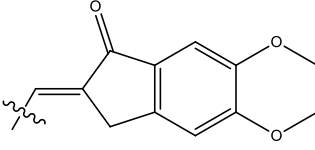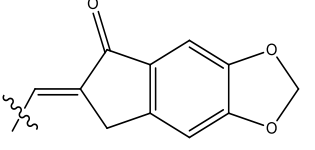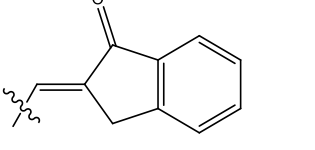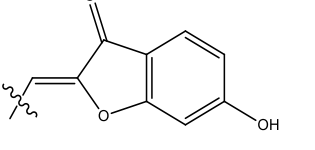
[4]   *Pharmaceutical Chemistry, School of Pharmacy, North-West University, Private Bag X6001, Potchefstroom 2520, South Africa*

Table 2a: Percentage of kinase inhibition of hybrids (**7 and 8a-l**). The table displays the remaining activities detected after treatment with 10µM of the tested compounds.

Compound	R	% residual activity measured at 10 µM of analytes							
		CDK2/Cyclin A	CDK5/p25	CDK9/CyclinT	HASPIN	PIM1	*Ssc*_CK1δ/ε	*Ssc*_GSK3α/β	*Lm*_CK1
7		≥100	89	34	23	≥100	49	82	57
8a		48	55	15	34	≥100	63	32	35
8b		≥100	80	36	19	91	75	30	13

8c		≥100	95	32	62	85	76	65	88
8d		≥100	≥100	26	55	77	75	65	65
8e		79	93	30	39	71	63	32	75
8f		91	62	27	40	81	57	9	46
8g		44	43	-2	6	41	37	8	35

8h		61	≥100	3	2	55	41	10	31
8i		87	≥100	30	12	59	53	17	48
8j		≥100	91	64	20	67	66	20	49
8k		69	62	34	13	28	62	27	43
8l		61	53	17	9	7	41	18	28

1H-pyrrolo[2,3-b]pyridine-3-carbaldehyde (7)

^{1}H NMR

^{13}C NMR

110

HPLC

DAD1 A, Sig=210,4 Ref=off (C:\CHEM32\1\DATA\FCH\PUR22OCT 2018-10-22 10-16-46\22Oct000017.D)
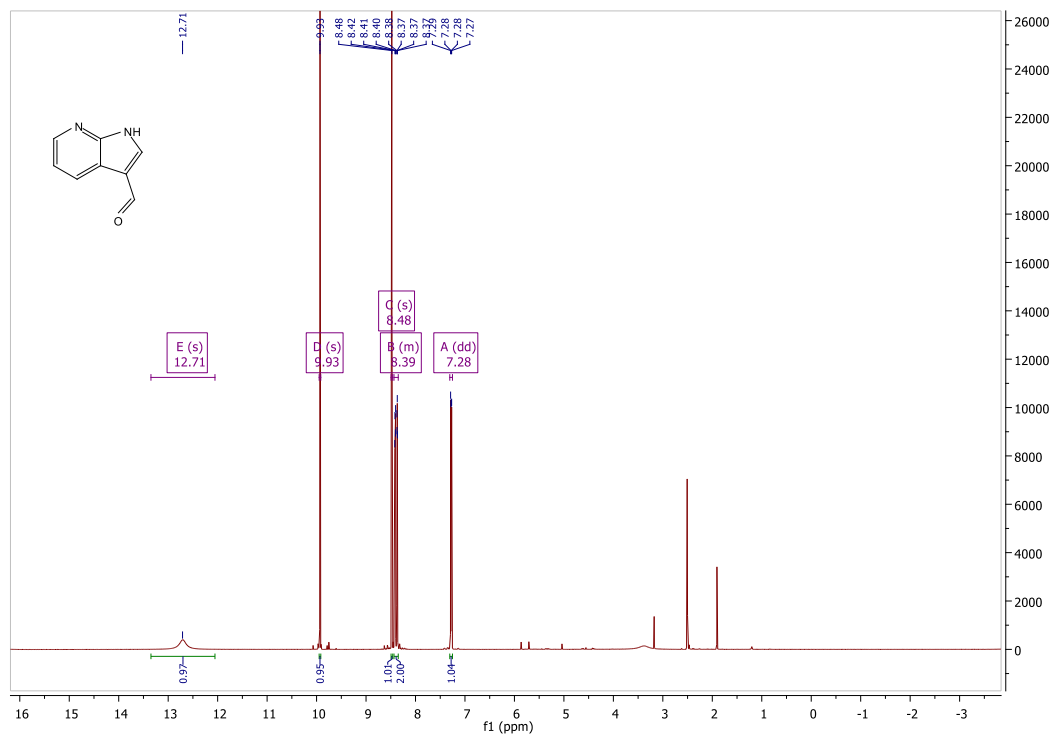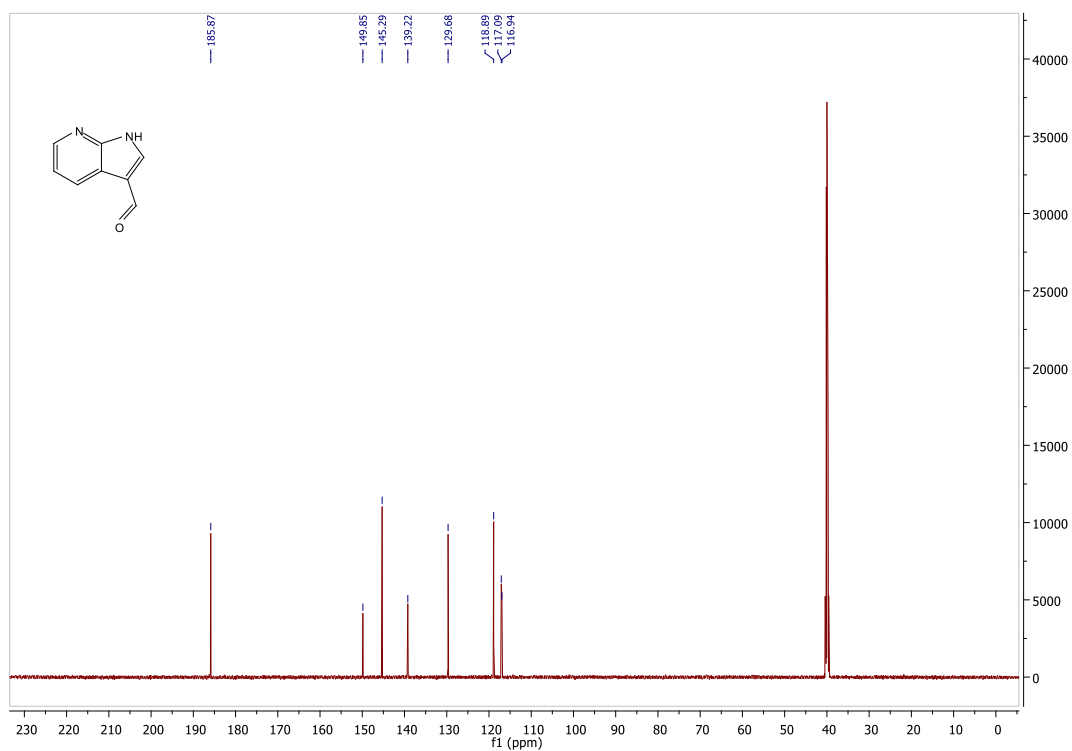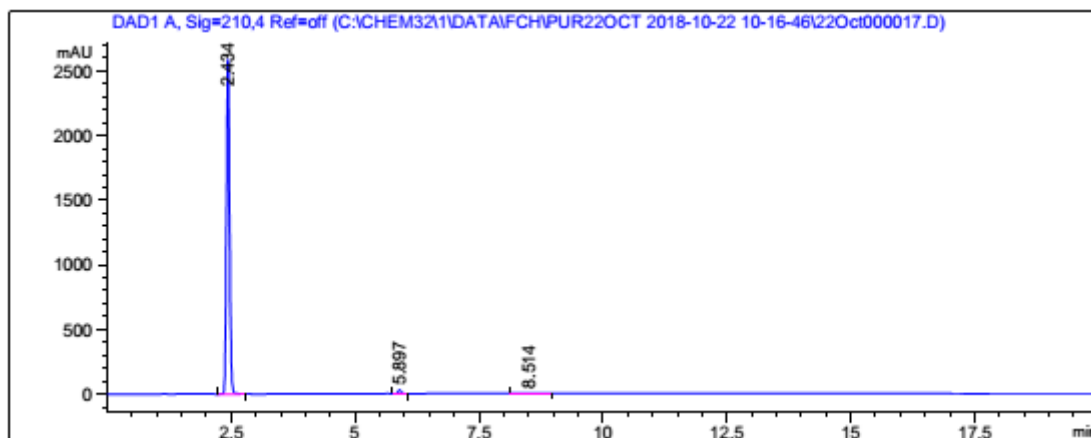
2-((1H-pyrrolo[2,3-b]pyridin-3-yl)methyl)-6-methoxy-3,4-dihydronaphthalen-1(2H)-one (8a)

¹H NMR

¹³C NMR

HPLC

DAD1 A, Sig=210,4 Ref=off (C:\CHEM32\1\DATA\FCH\PUR22OCT 2018-10-22 10-16-46\22Oct000020.D)
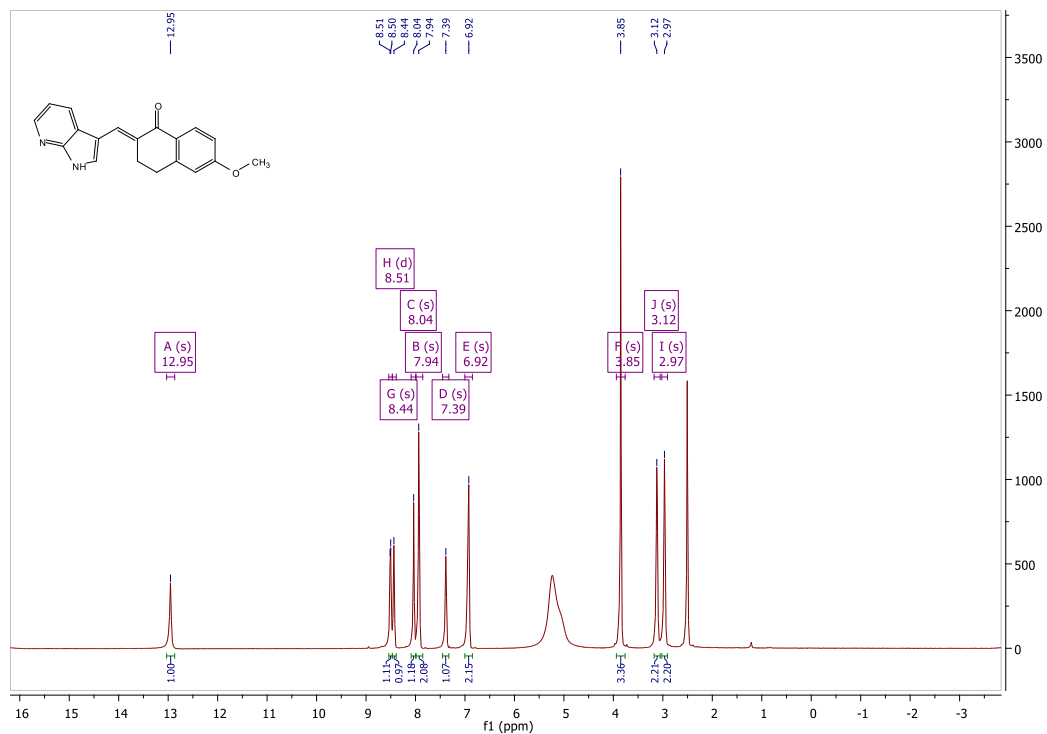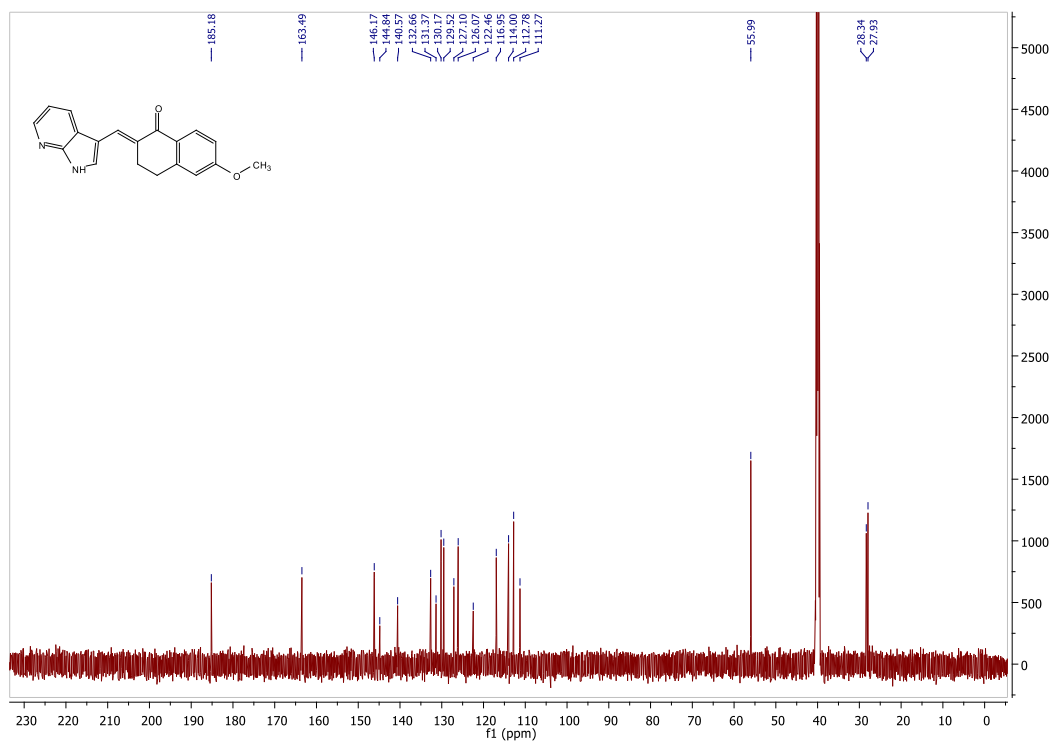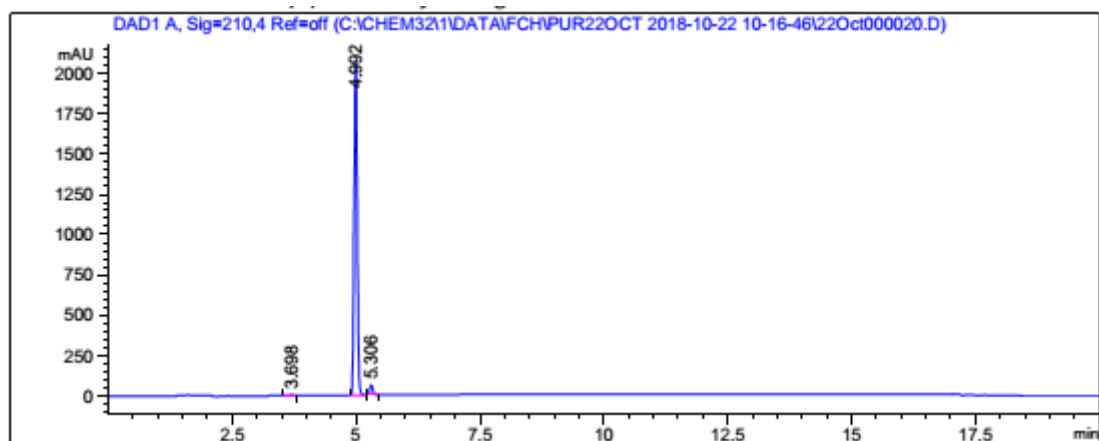
2-((1H-pyrrolo[2,3-b]pyridin-3-yl)methyl)-5-methoxy-2,3-dihydro-1H-inden-1-one (8b)

^{1}H NMR

^{13}C NMR

HPLC

DAD1 A, Sig=210,4 Ref=off (C:\CHEM32\1\DATA\FCH\PUR22OCT 2018-10-22 10-16-46\22Oct000021.D)
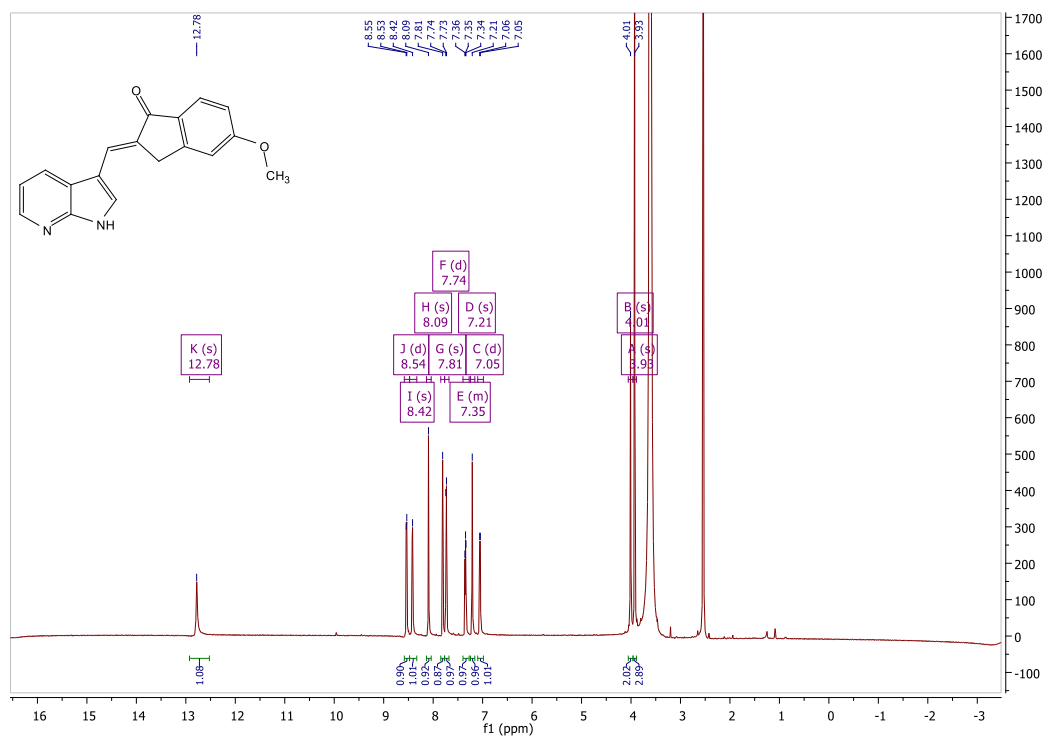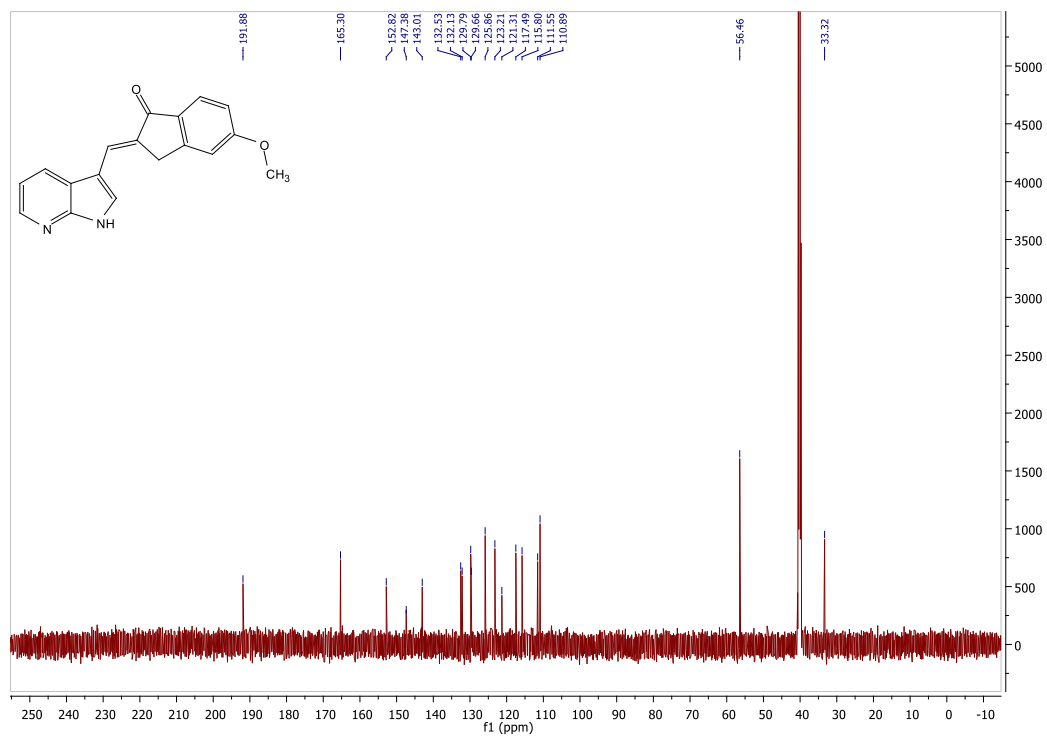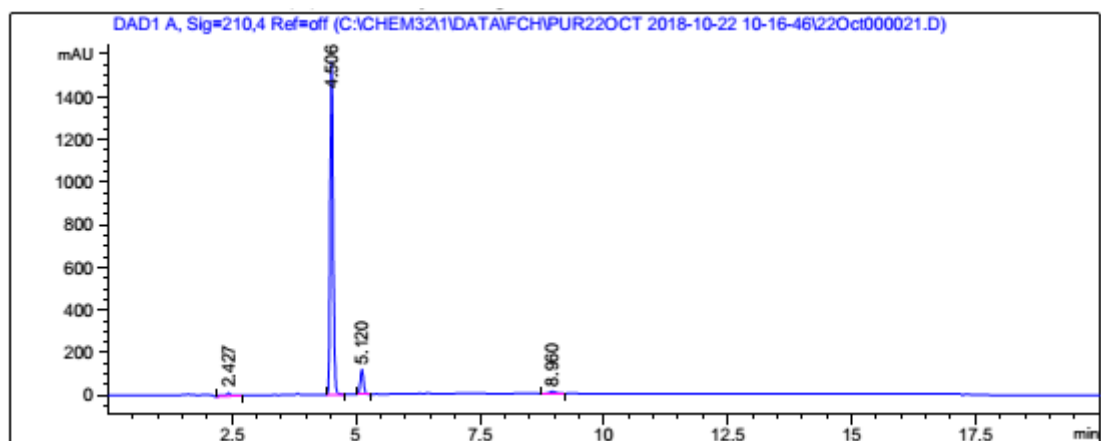
2-((1H-pyrrolo[2,3-b]pyridin-3-yl)methyl)-6,7-dimethoxy-3,4-dihydronaphthalen-1(2H)-one (8c)

¹H NMR

¹³C NMR

HPLC

DAD1 A, Sig=210,4 Ref=off (C:\CHEM32\1\DATA\FCH\PUR22OCT 2018-10-22 10-16-46\22Oct000022.D)
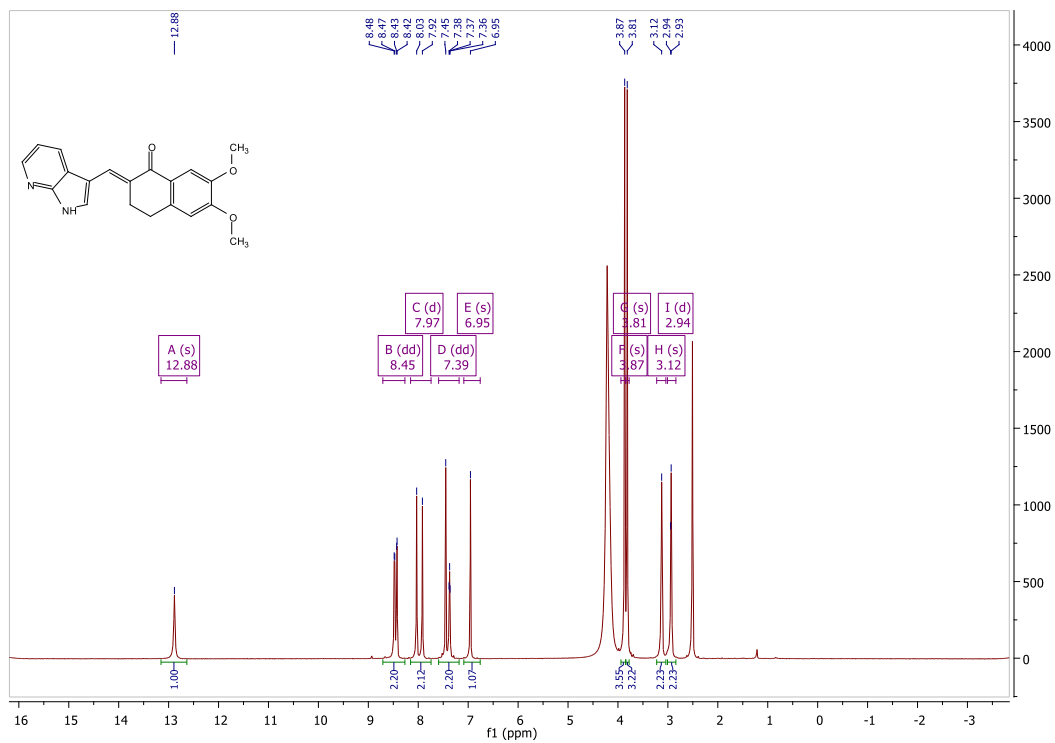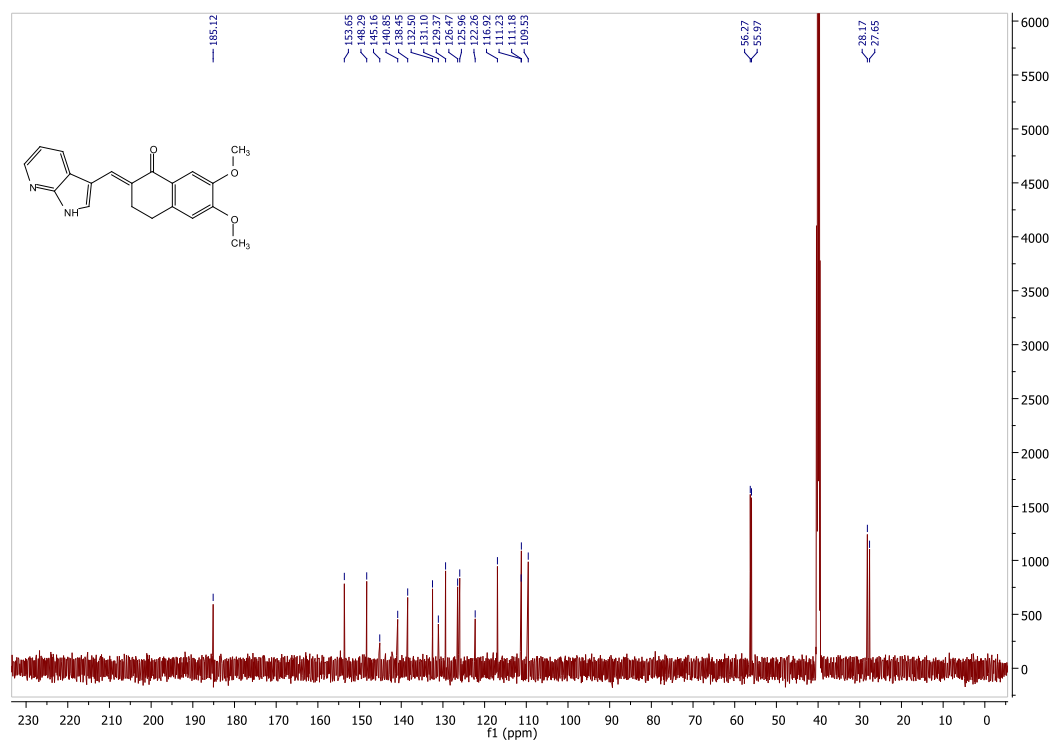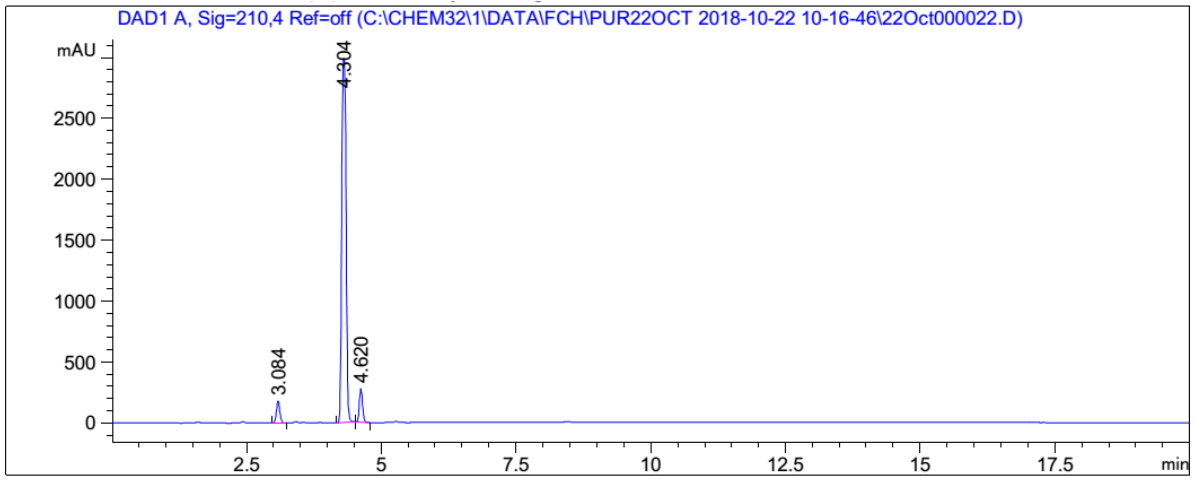
2-((1H-pyrrolo[2,3-b]pyridin-3-yl)methyl)-7-methoxy-3,4-dihydronaphthalen-1(2H)-one (8d)

<div align="center">

¹H NMR

</div>

<div align="center">

³C NMR

</div>

HPLC

119
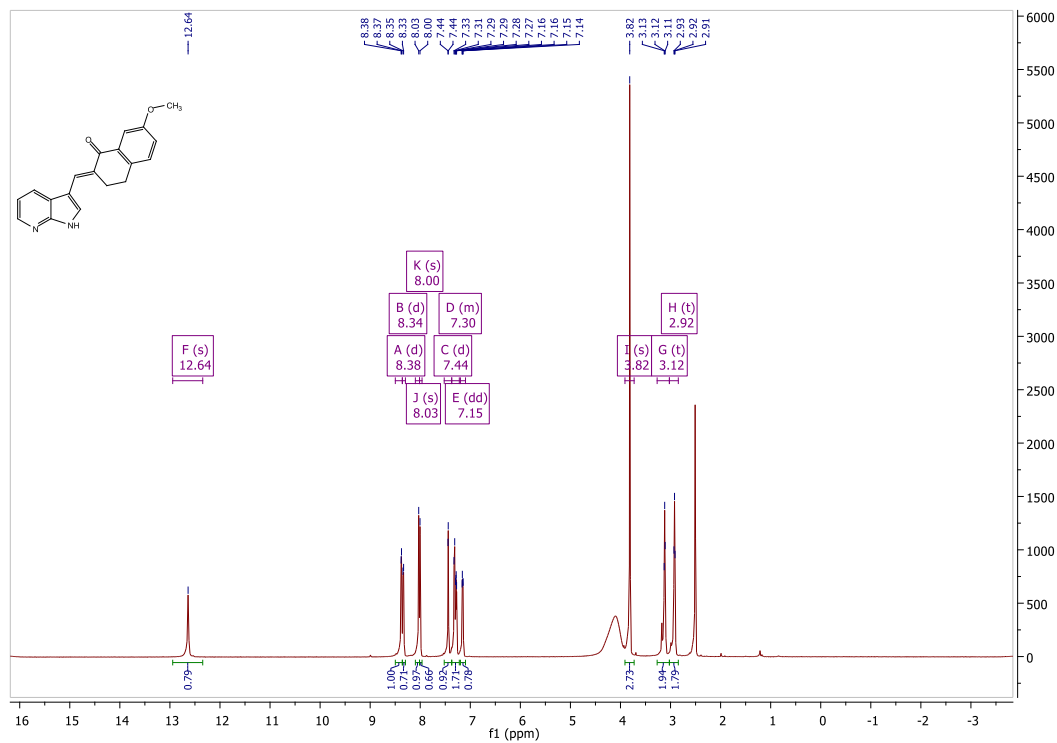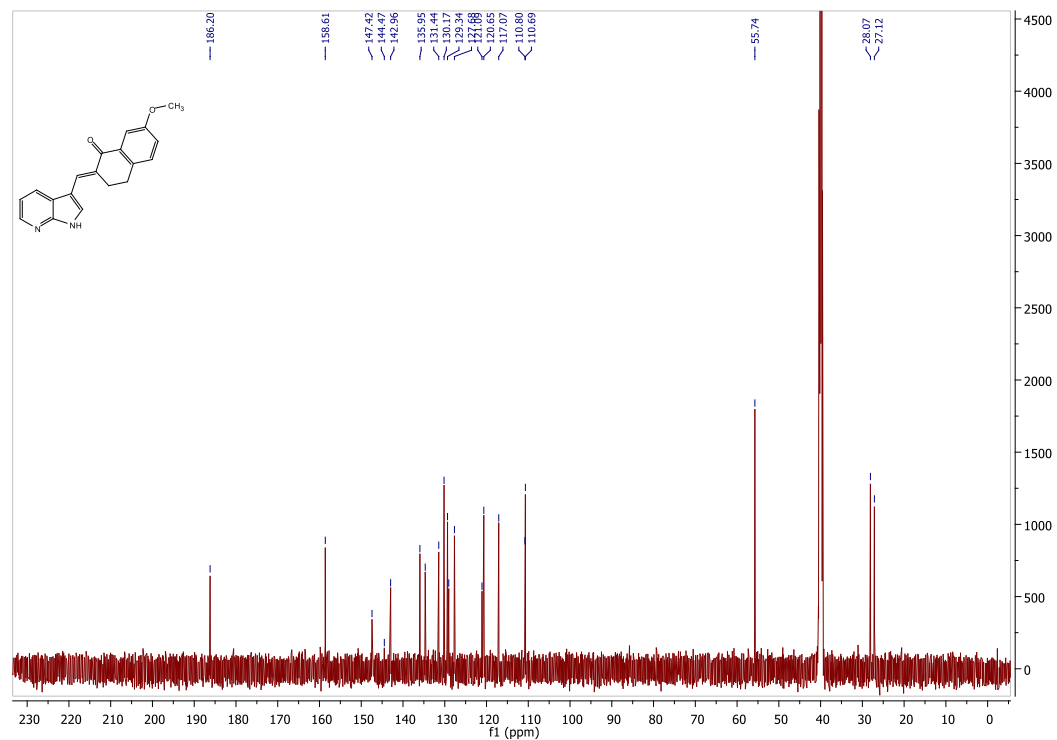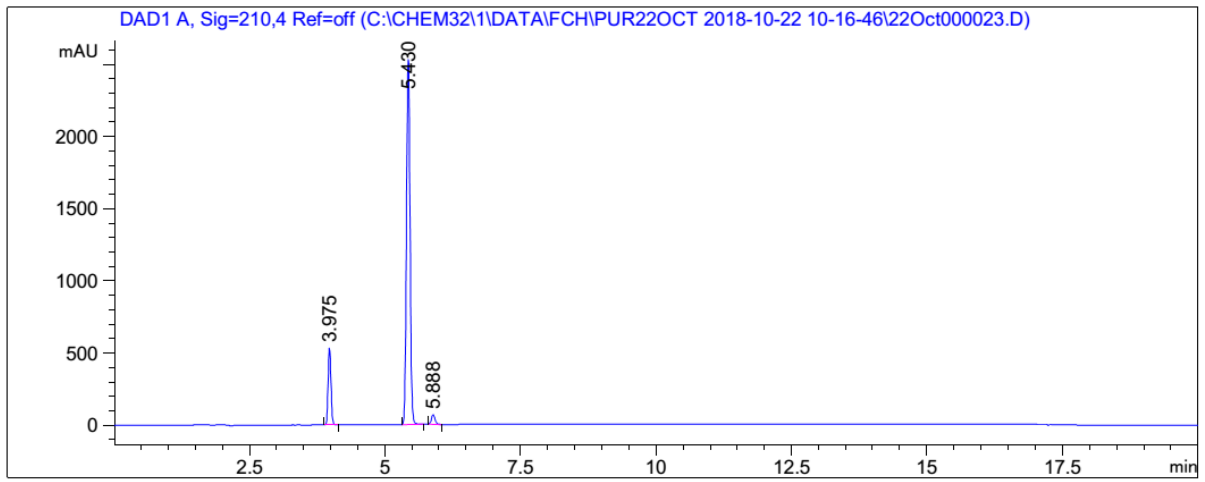
3-((1H-pyrrolo[2,3-b]pyridin-3-yl)methyl)chroman-4-one (8e)

^{1}H NMR

^{13}C NMR

HPLC

DAD1 A, Sig=210,4 Ref=off (C:\CHEM32\1\DATA\FCH\PUR22OCT 2018-10-22 10-16-46\22Oct000024.D)
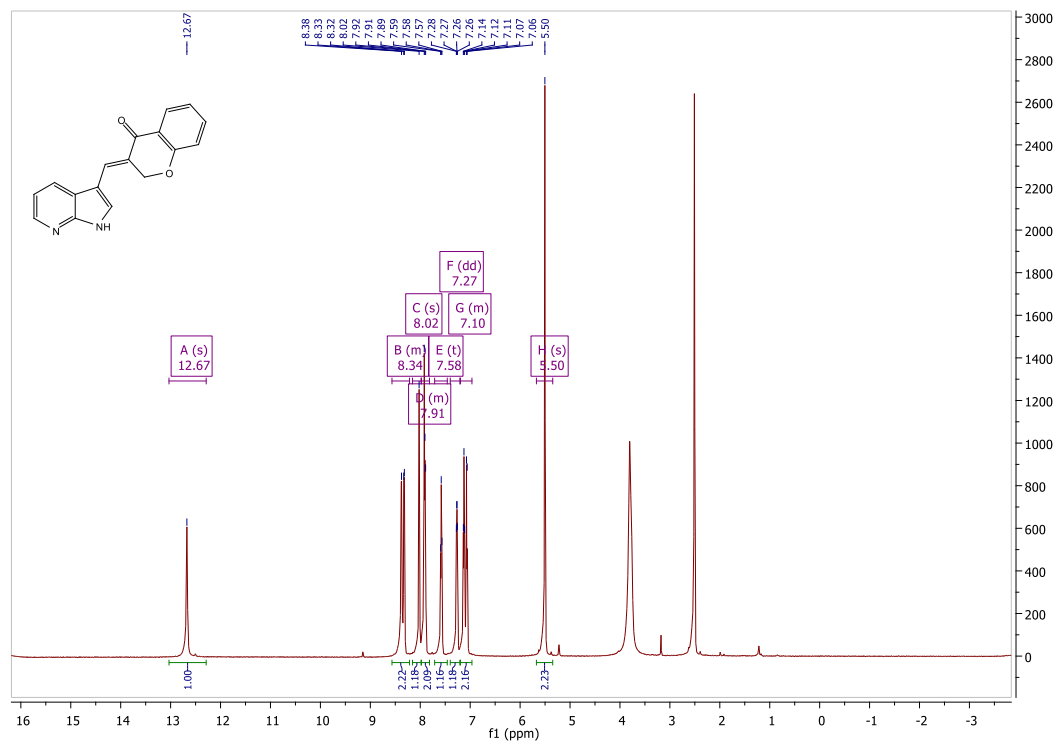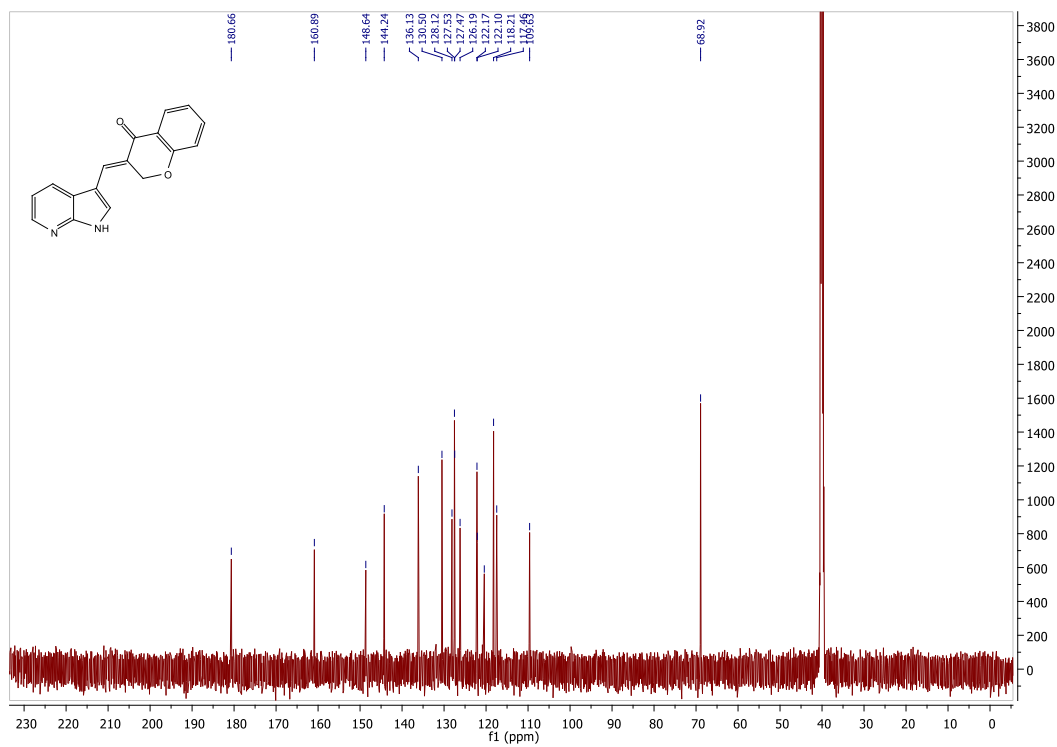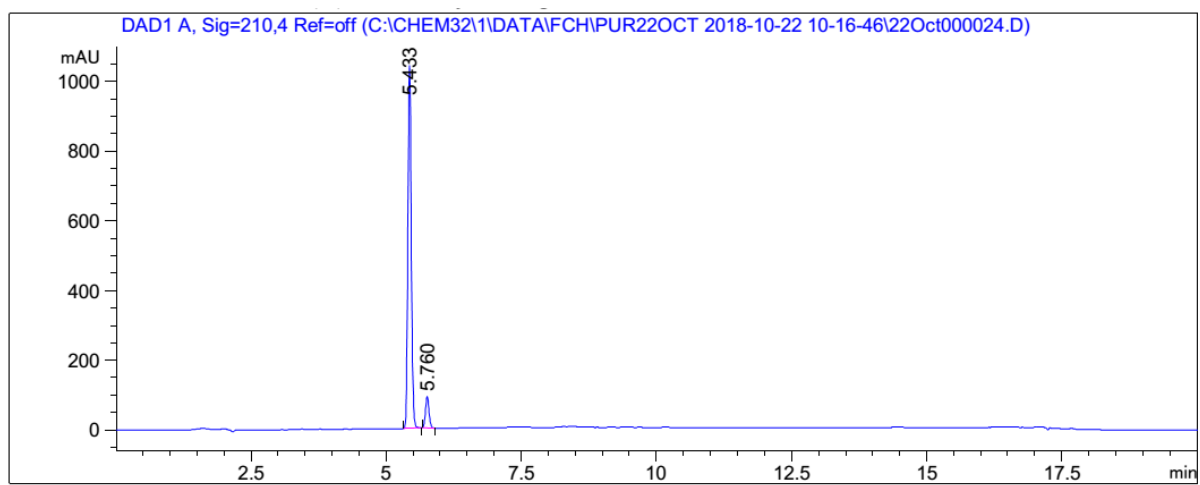
3-((1H-pyrrolo[2,3-b]pyridin-3-yl)methyl)thiochroman-4-one (8f)

^{1}H NMR

^{13}C NMR

HPLC

DAD1 A, Sig=210,4 Ref=off (C:\CHEM32\1\DATA\FCH\PUR22OCT 2018-10-22 10-16-46\22Oct000025.D)
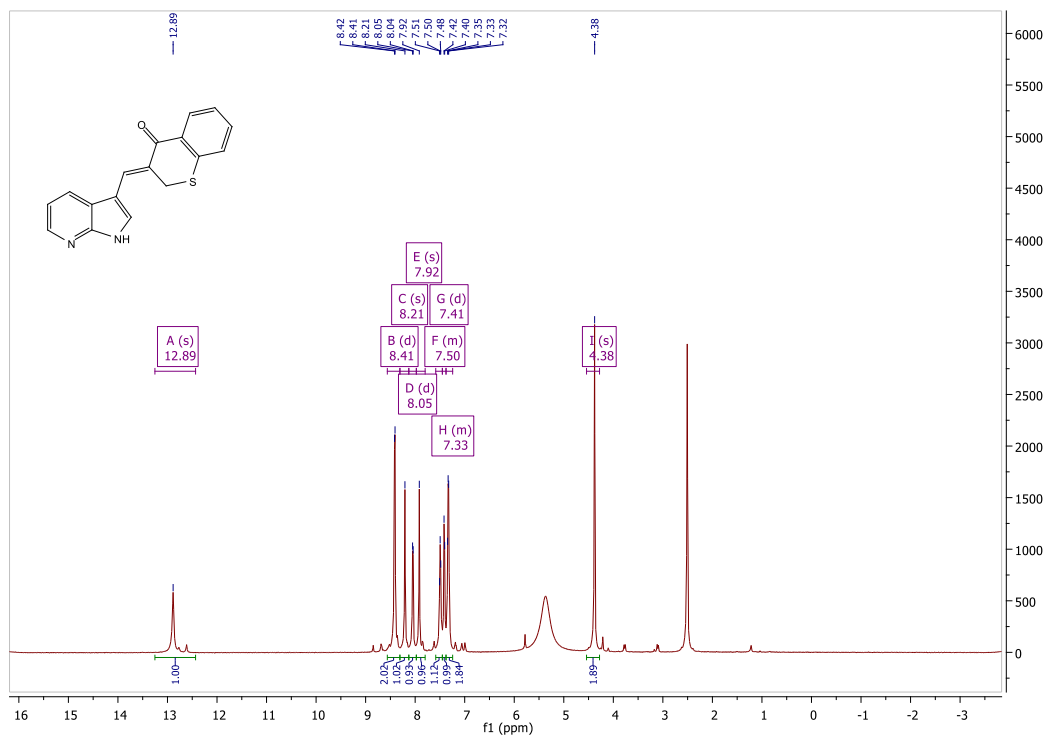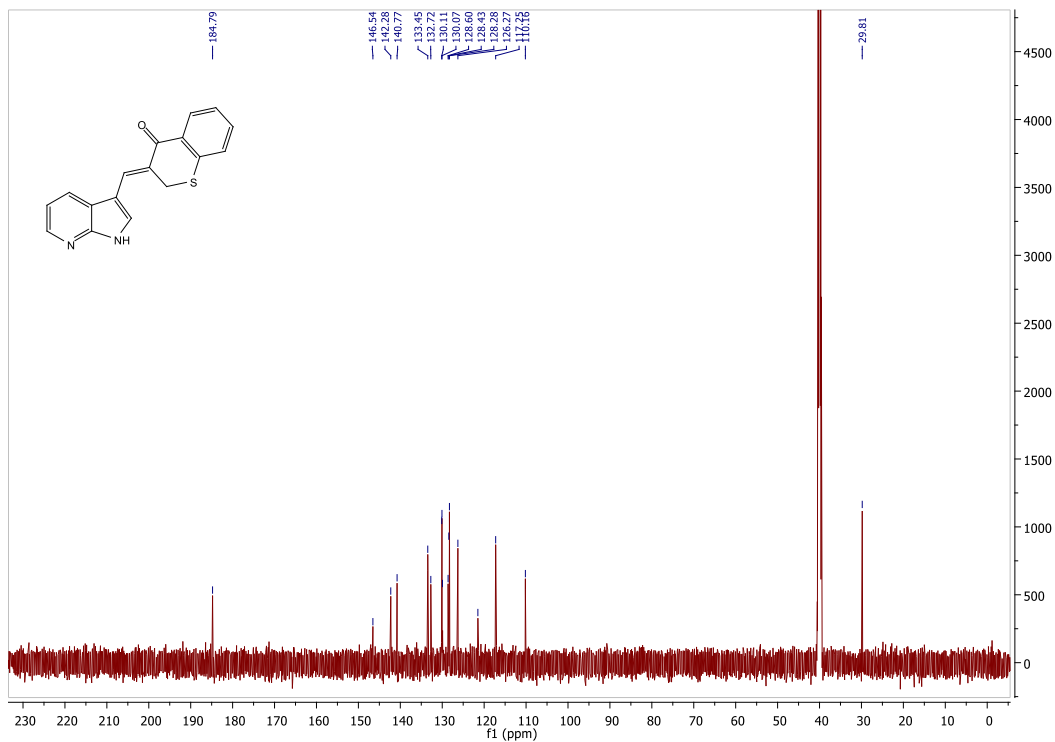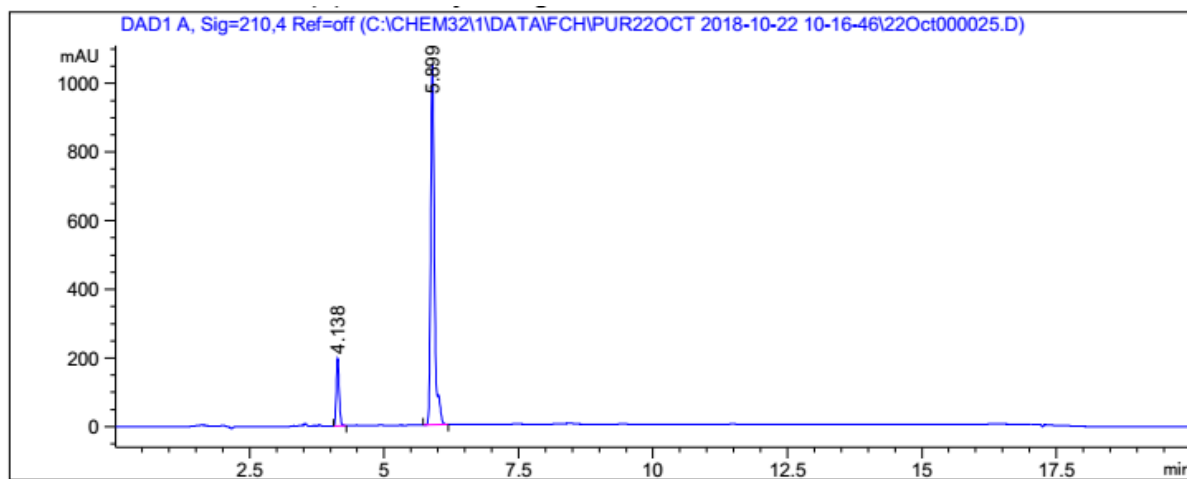
2-((1H-pyrrolo[2,3-b]pyridin-3-yl)methyl)-3,4-dihydronaphthalen-1(2H)-one (8g)

^{1}H NMR

^{13}C NMR

HPLC

DAD1 A, Sig=210,4 Ref=off (C:\CHEM32\1\DATA\FCH\PUR22OCT 2018-10-22 10-16-46\22Oct000026.D)
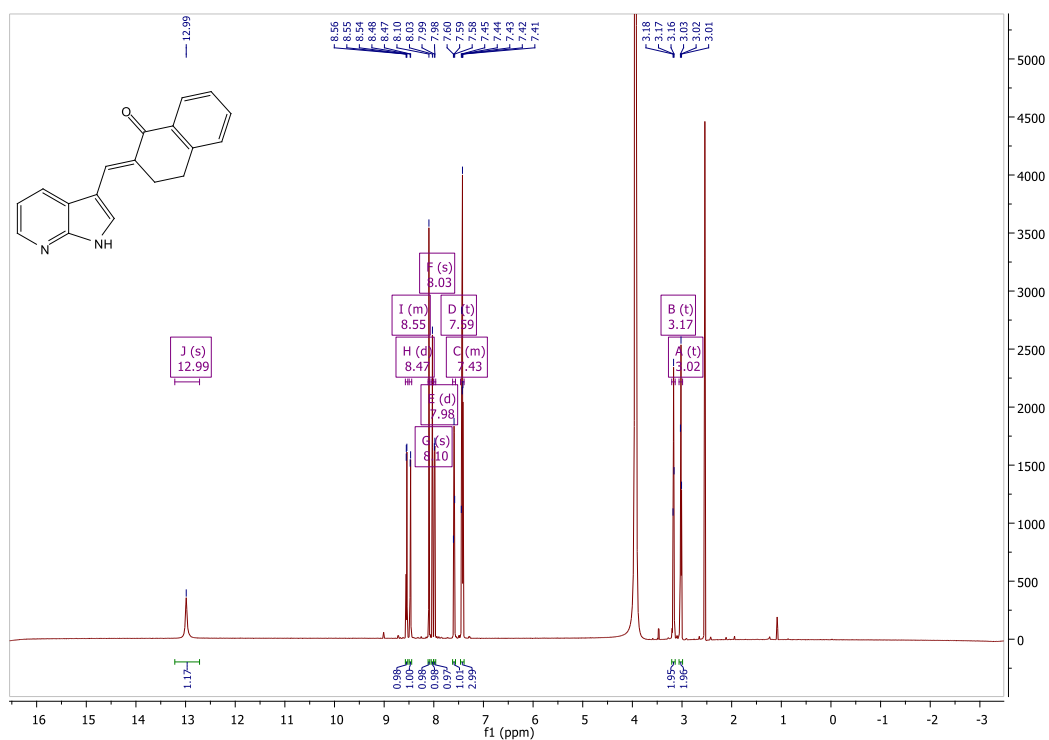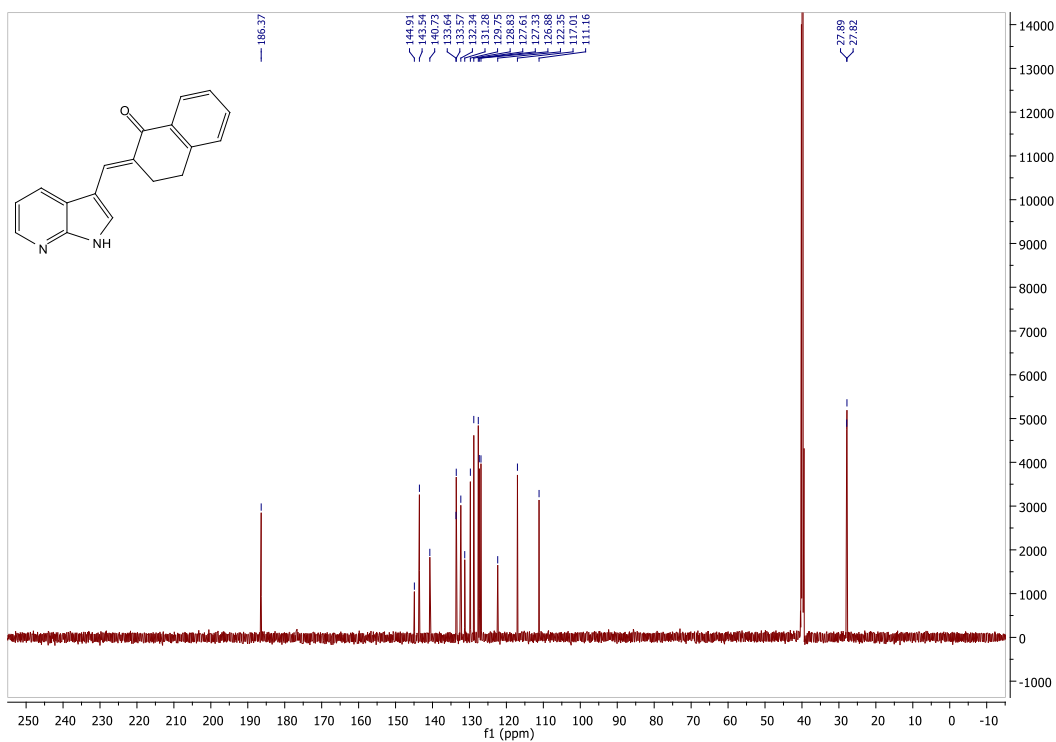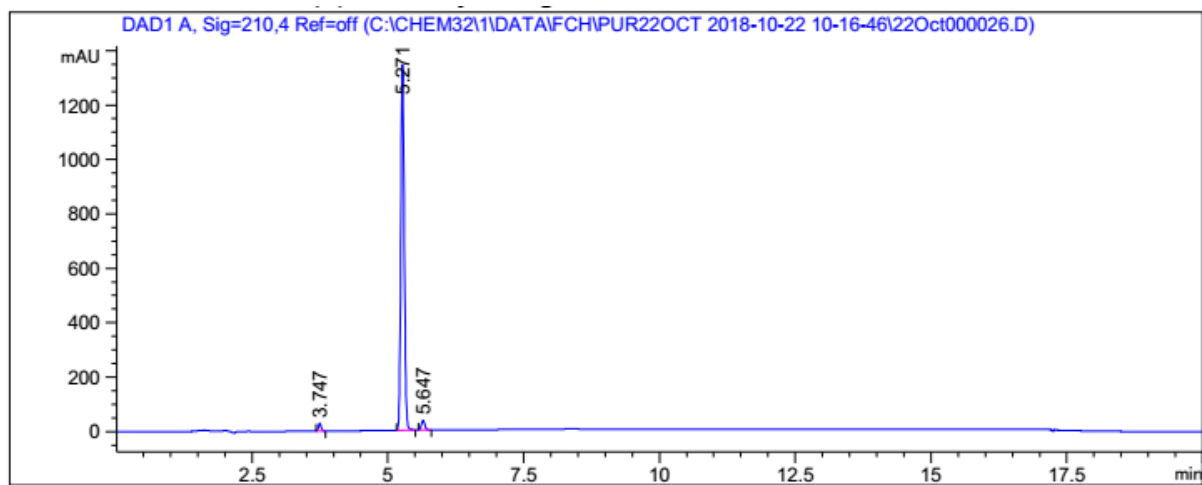
2-((1H-pyrrolo[2,3-b]pyridin-3-yl)methyl)-6-hydroxy-3,4-dihydronaphthalen-1(2H)-one (8h)

¹H NMR

¹³C NMR

HPLC

DAD1 A, Sig=210,4 Ref=off (C:\CHEM32\1\DATA\FCH\PUR22OCT 2018-10-22 10-16-46\22Oct000027.D)
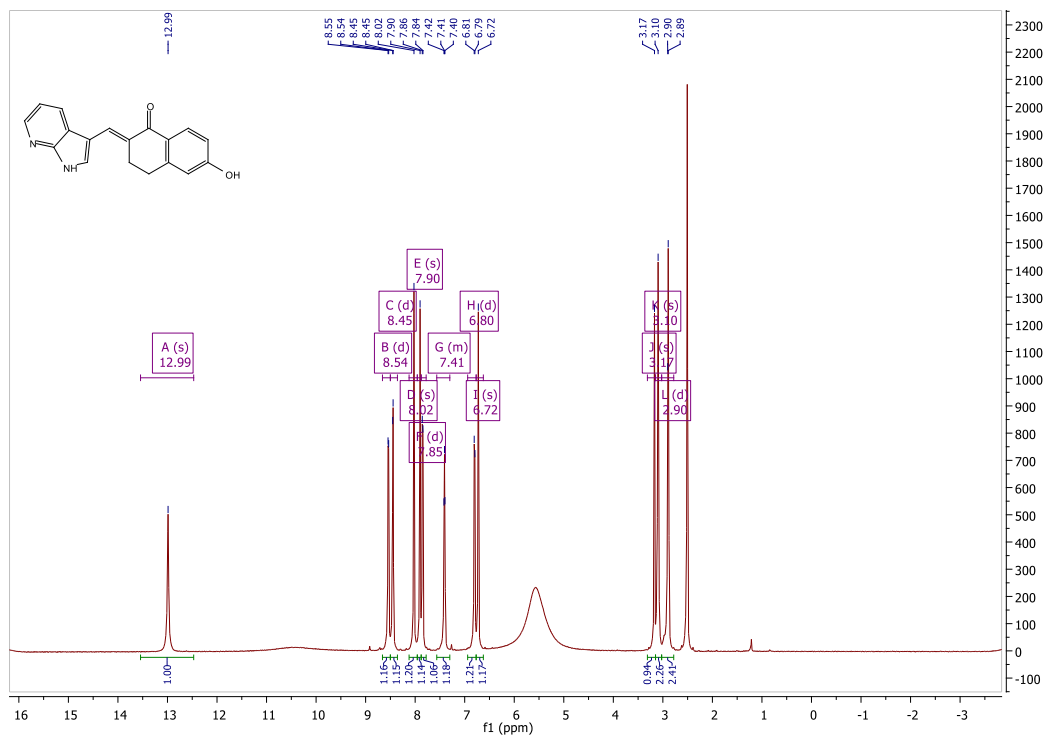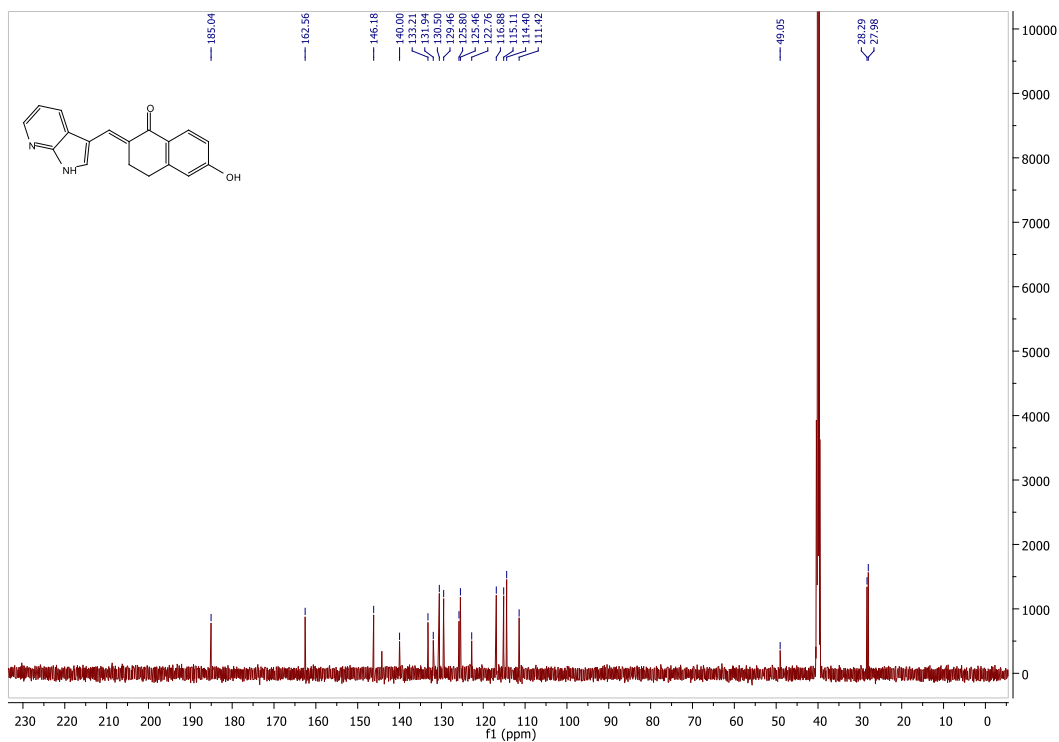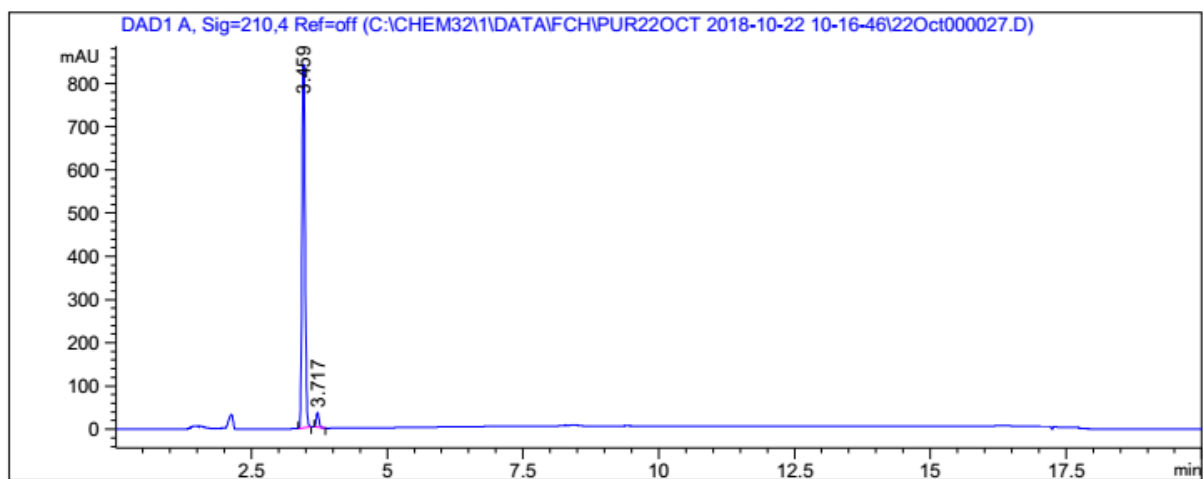
2-((1H-pyrrolo[2,3-b]pyridin-3-yl)methyl)-5,6-dimethoxy-2,3-dihydro-1H-inden-1-one (8i)

^{1}H NMR

^{13}C NMR

HPLC

DAD1 A, Sig=210,4 Ref=off (C:\CHEM32\1\DATA\FCH\PUR22OCT 2018-10-22 10-16-46\22Oct000028.D)
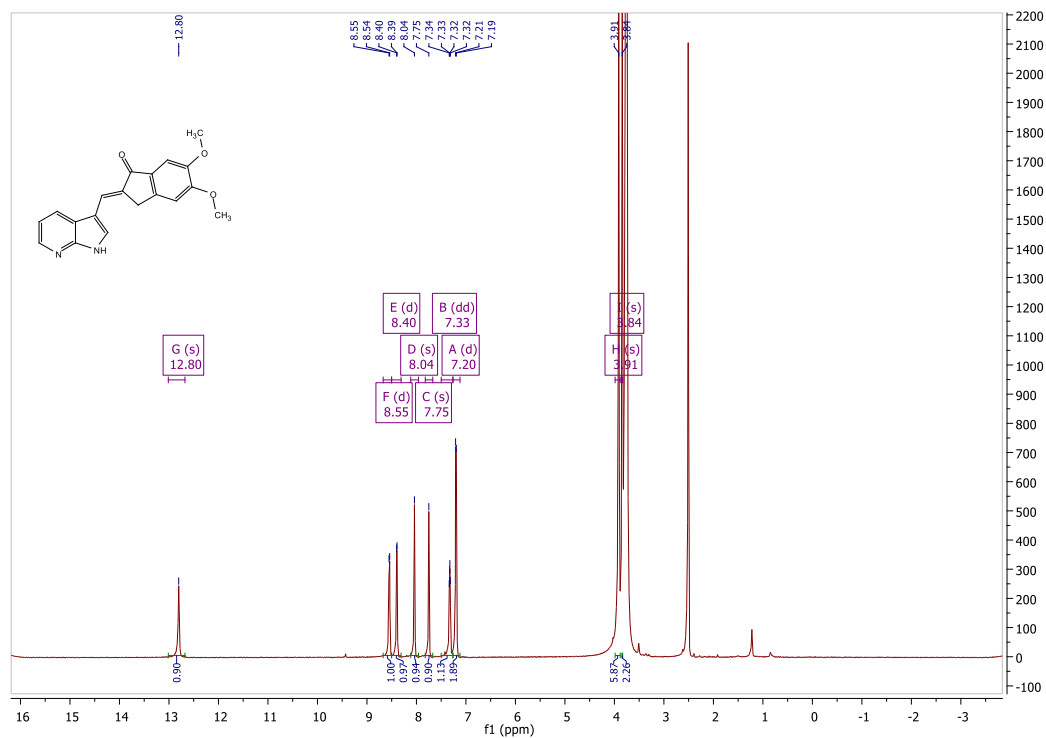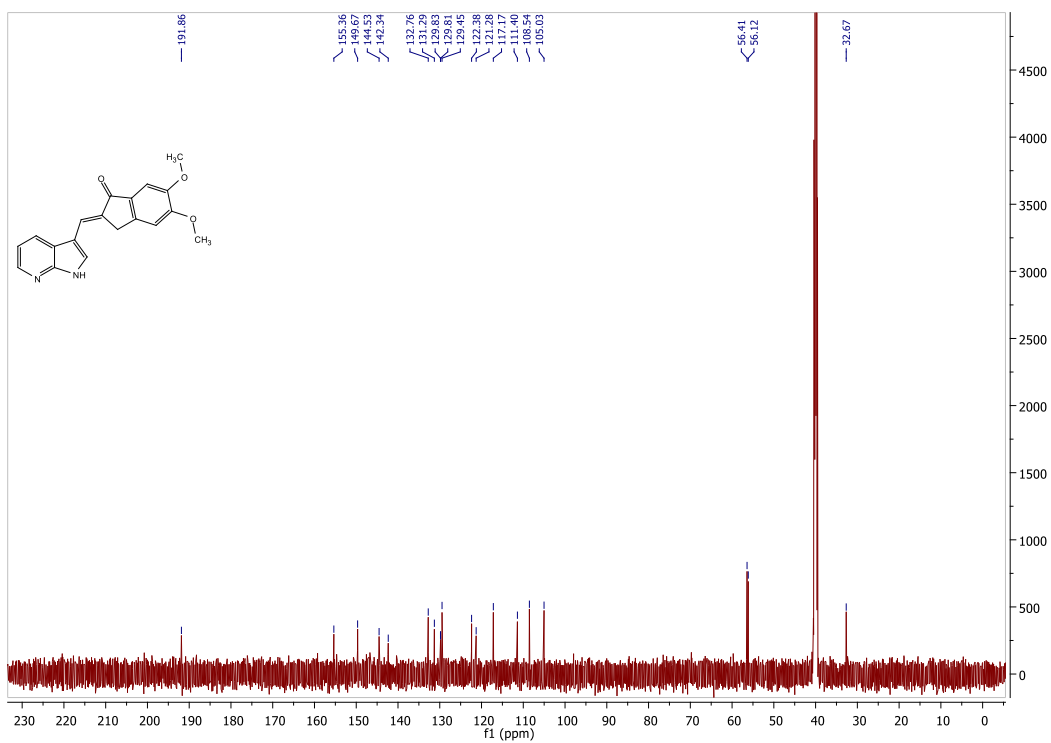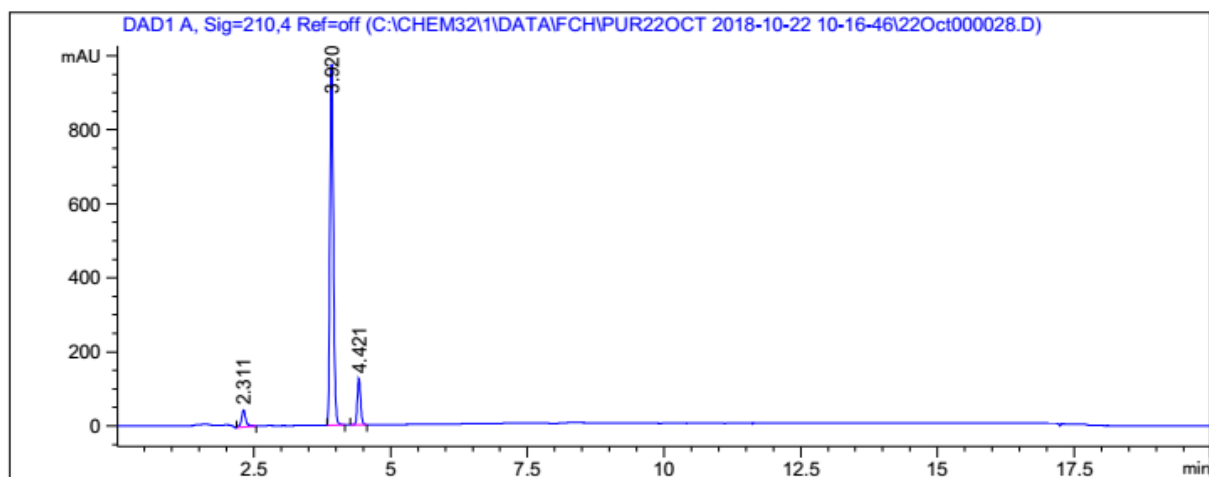
6-((1H-pyrrolo[2,3-b]pyridin-3-yl)methyl)-6,7-dihydro-5H-indeno[5,6-d][1,3]dioxol-5-one (8j)

^{1}H NMR

^{13}C NMR

HPLC

DAD1 A, Sig=210,4 Ref=off (C:\CHEM32\1\DATA\FCH\PUR22OCT 2018-10-22 10-16-46\22Oct000029.D)
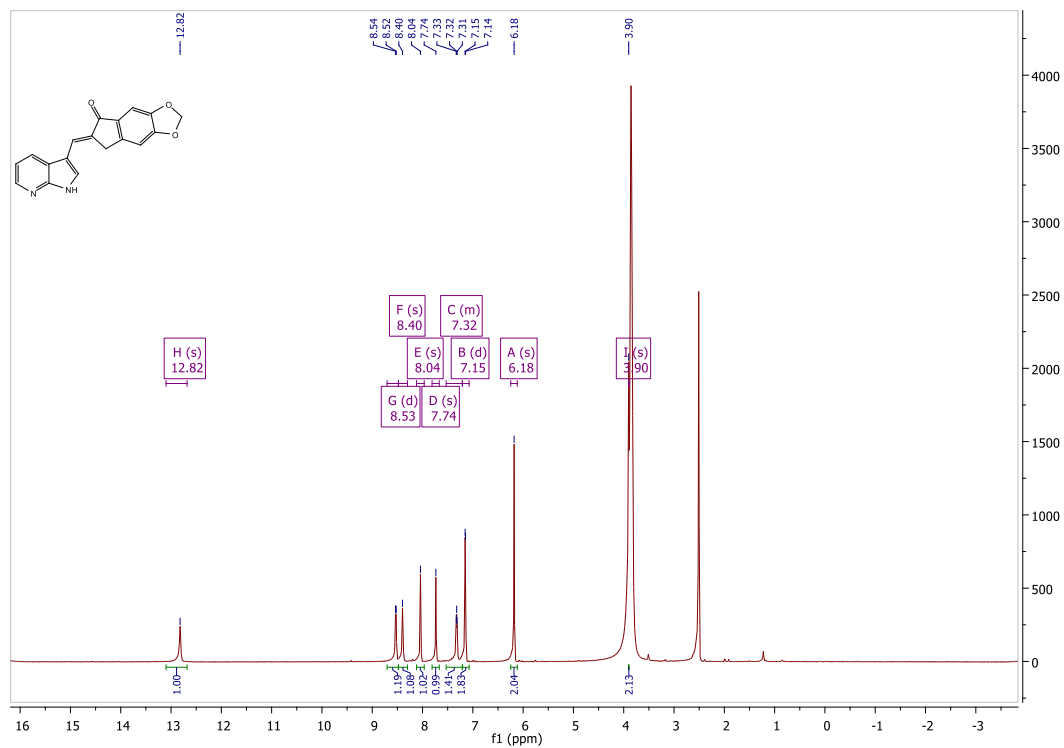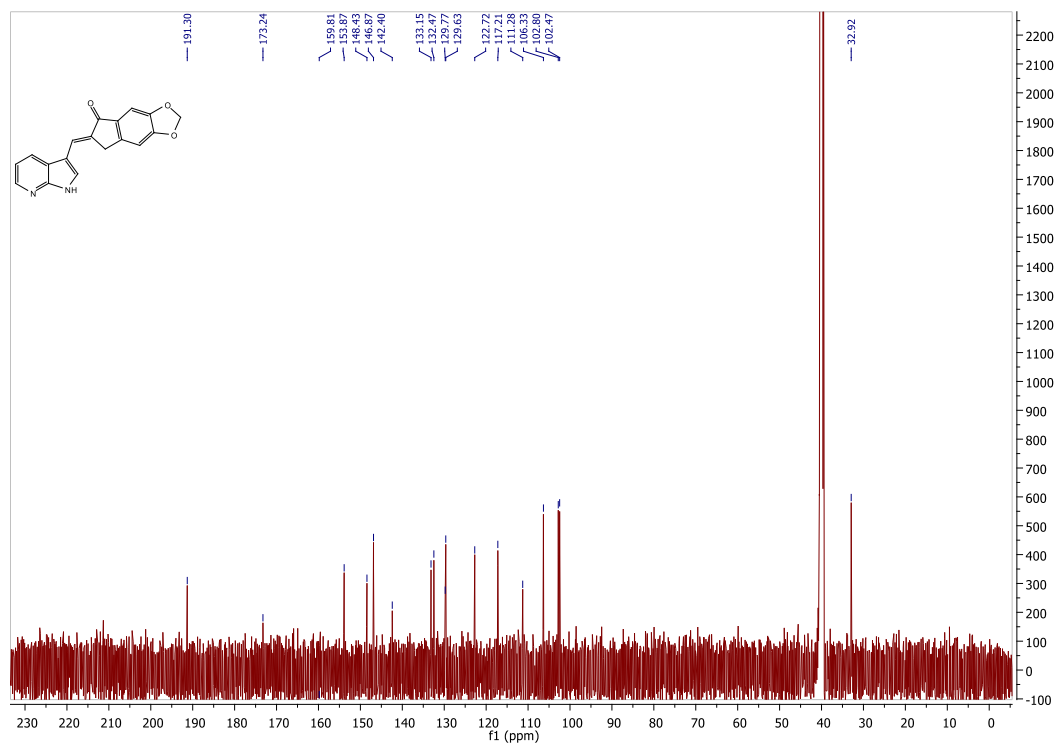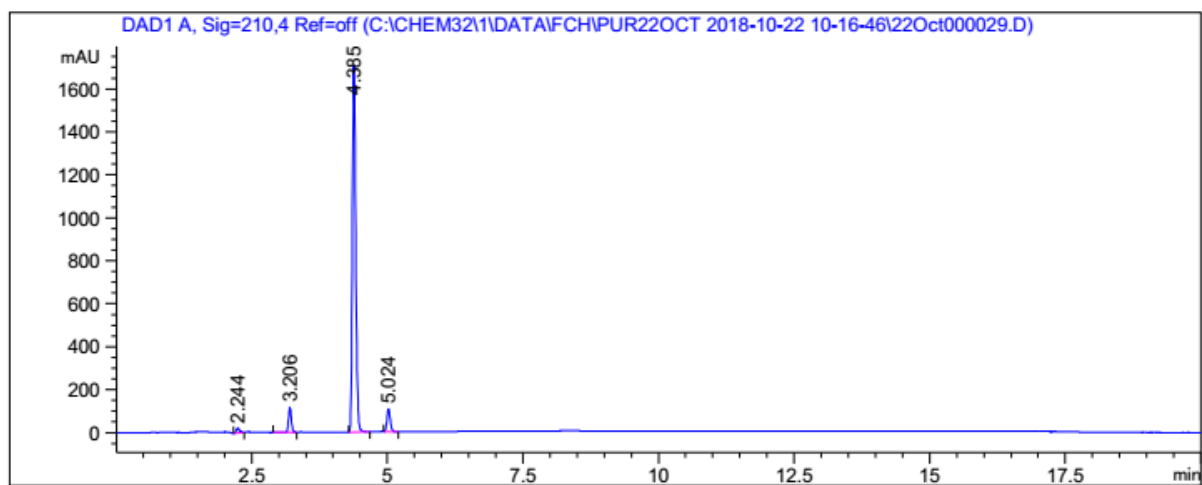
2-((1H-pyrrolo[2,3-b]pyridin-3-yl)methyl)-2,3-dihydro-1H-inden-1-one (8k)

^{1}H NMR

^{13}C NMR

HPLC

DAD1 A, Sig=210,4 Ref=off (C:\CHEM32\1\DATA\FCH\PUR22OCT 2018-10-22 10-16-46\22Oct000031.D)
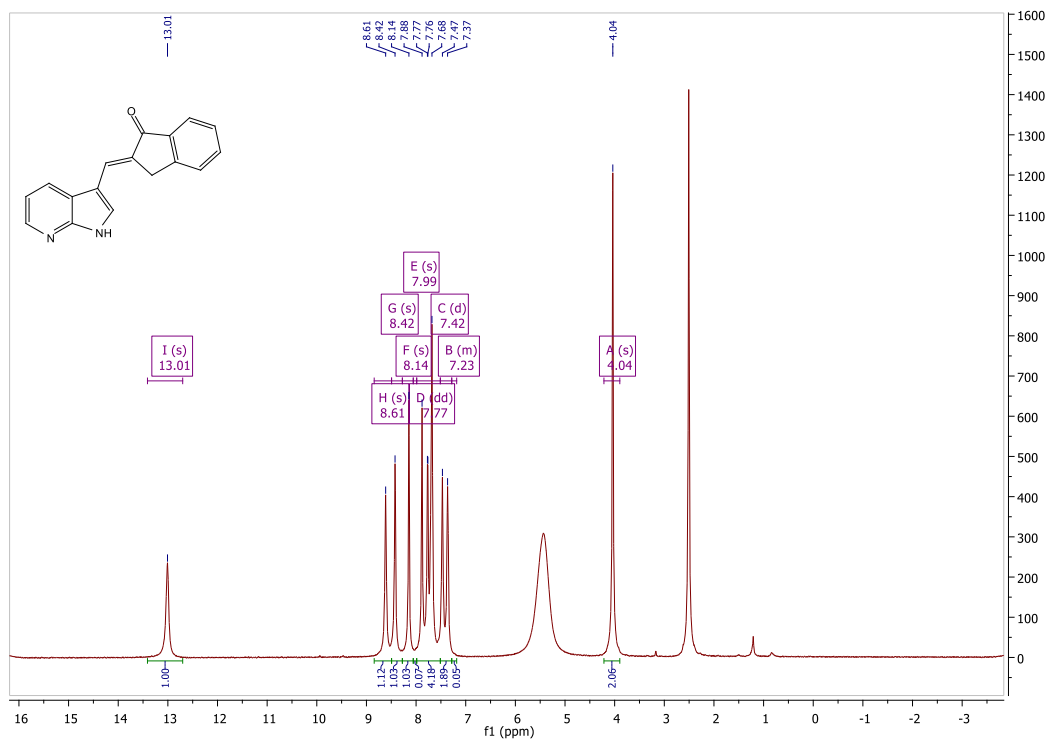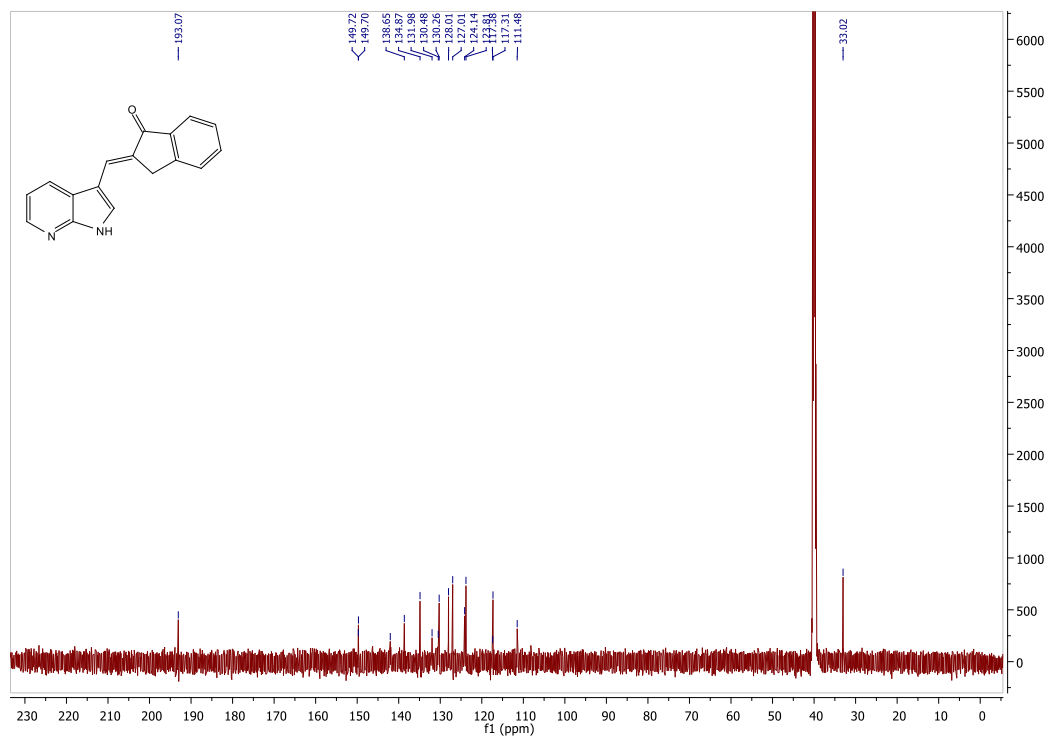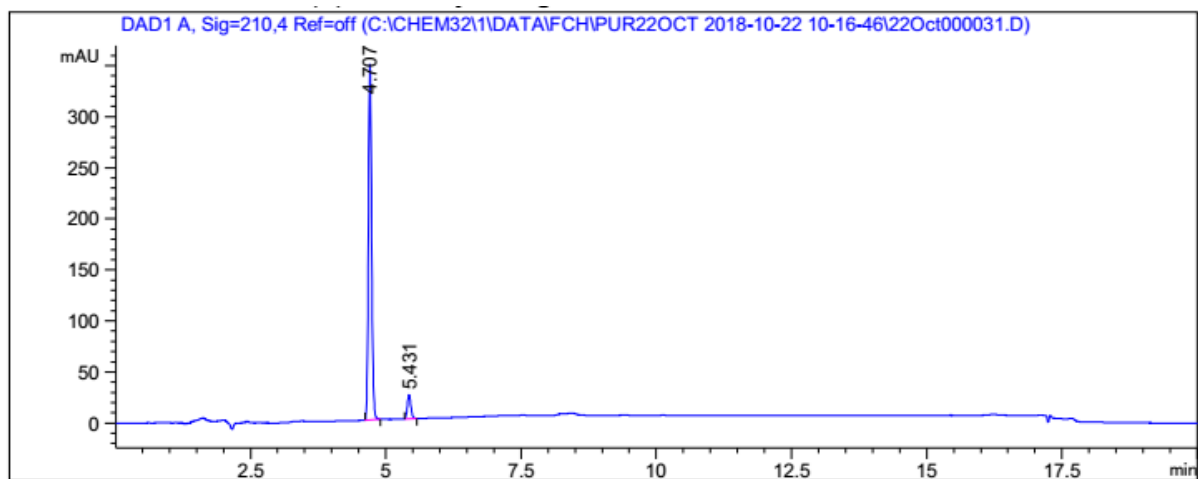
2-((1H-pyrrolo[2,3-b]pyridin-3-yl)methyl)-6-hydroxybenzofuran-3(2H)-one (8l)

^{1}H NMR

^{13}C NMR

HPLC

DAD1 A, Sig=210,4 Ref=off (C:\CHEM32\1\DATA\FCH\PUR22OCT 2018-10-22 10-16-46\22Oct000032.D)
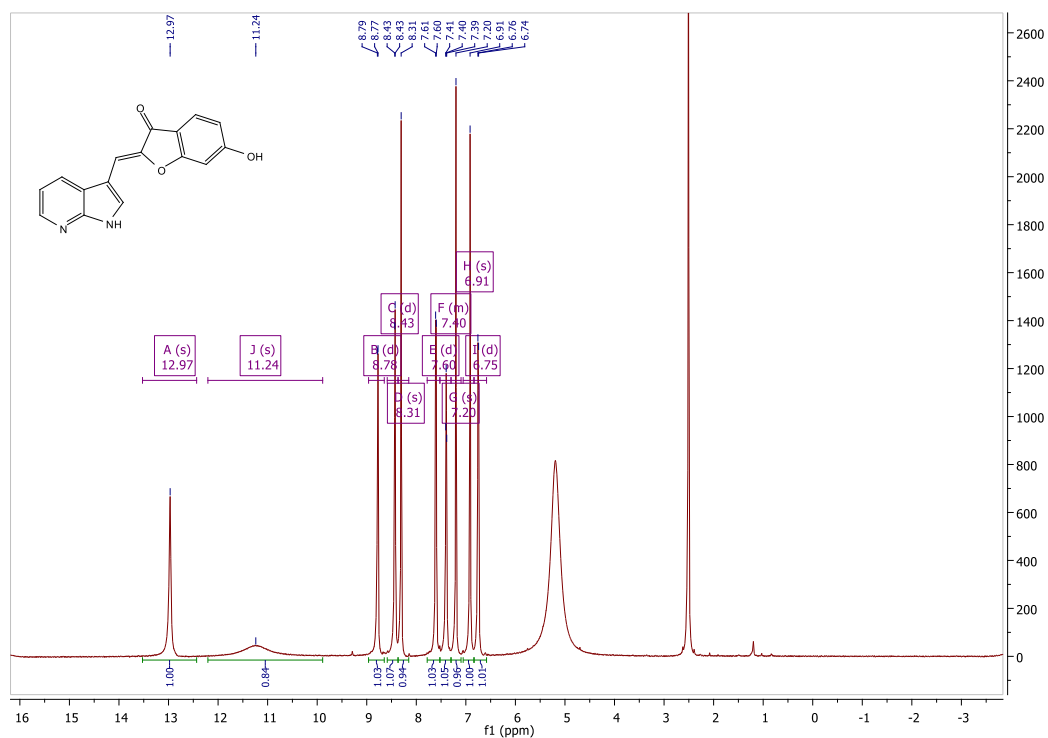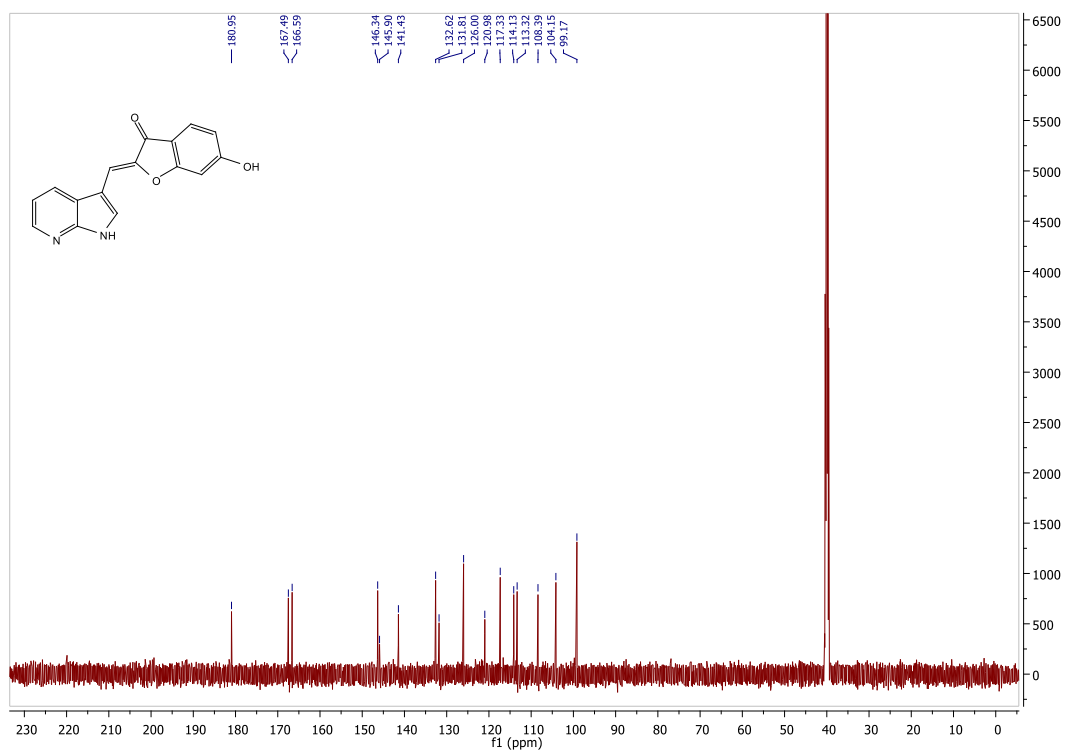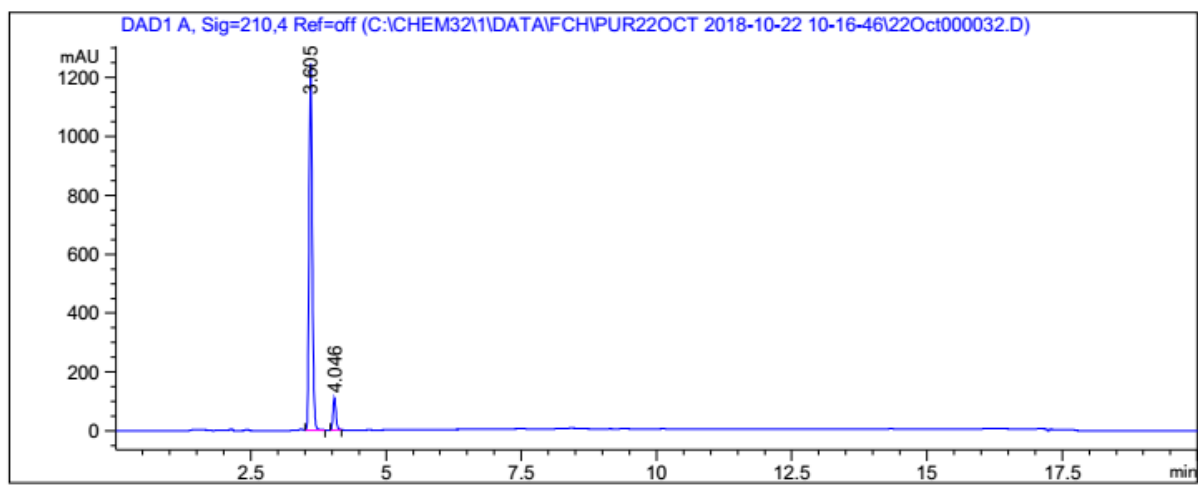
APPENDIX B:
SUPPORTING DATA FOR CHAPTER 4

Malikotsi A. Qhobosheane[1], Lesetja J. Legoabe[1,*], Béatrice Josselin[2,3], Stéphane Bach[2,3], Sandrine Ruchaud[2], Richard M. Beteck[1]

[1]   *Centre of Excellence for Pharmaceutical Sciences, North-West University, Private Bag X6001, Potchefstroom 2520, South Africa*

[2]   *Sorbonne Université, CNRS, UMR 8227, Integrative Biology of Marine Models, Station Biologique de Roscoff, CS 90074, 29688 Roscoff Cedex, France*

[3]   *Sorbonne Université, CNRS, FR2424, Plateforme de criblage KISSf (Kinase Inhibitor Specialized Screening facility), Station Biologique de Roscoff, Place Georges Teissier, 29682 Roscoff, France*

1. Experimental section

1.1. General Procedures

Unless otherwise stated, all starting materials and reagents were purchased from Sigma-Aldrich or AK Scientific and used without further purification. Proton (^{1}H) and carbon (^{13}C) Nuclear Magnetic Resonance (NMR) spectra were recorded on a Bruker Avance III 600 spectrometer at frequencies of 600 MHz and 151 MHz, respectively, with DMSO-*d*6 serving as NMR solvent. All chemical shifts (δ) are reported in parts per million (ppm) and were referenced to the residual solvent signal (DMSO-d6: 2.50 and 39.52 ppm for ^{1}H and ^{13}C, respectively). Spin multiplicities are given as follows: s (singlet), d (doublet), dd (doublet of doublets), t (triplet), (td) triplets of doublets, q (quartet), and m (multiplet). High resolution mass spectra (HRMS) were recorded on a Bruker micrOTOF-Q II mass spectrometer in atmospheric-pressure chemical ionisation (APCI) mode.

Chemical purities were determined by HPLC (Agilent 1200 system) with a Venusil XBP C18 column (4.60 × 150 mm, 5 μm) and a mobile phase of 30% acetonitrile and 70% MilliQ water at a flow rate of 1 mL/min. At the start of each injection, a solvent gradient program was initiated by linearly increasing the percentage of acetonitrile to 85% over a period of 5 min. Each run lasted 15 min, 20 μL of the test compounds in acetonitrile (1 mM) was injected into the HPLC system and the eluent was monitored at wavelengths of 210 and 254 nm. Melting points (mp) were determined with a Buchi B-545 melting point apparatus and are uncorrected. Thin layer chromatography (TLC) was carried out using silica gel 60 F254 pre-coated aluminium sheets (0.25 mm, Merck), while column chromatography was carried out with silica gel 60 (Fluka, particle size 0.063–0.200 mm). Full-length kinases were used unless specified. Peptide substrates were obtained from Proteogenix (Schiltigheim, France).

1.2. Synthesis

Synthesis of 1-(1H-pyrrolo[2,3-b]pyridin-3-yl)ethanone (4)

To a suspension of aluminium chloride (AlCl$_3$) (16.93 g, 127 mmol) in dichloromethane (DCM) (100 ml) was added 7-azaindole (5 g, 42.3 mmol). Acetyl chloride (9.03 ml, 127 mmol) was added to the mixture at room temperature and stirred for 1h. The work up was done by quenching the reaction with methanol (60 ml) and evaporating to dryness. The resultant residue was triturated with saturated aqueous sodium bicarbonate/EtOAc (3:4). The aqueous

layer was washed several times with EtOAc, and the combined organic layers were dried over MgSO$_4$ and then evaporated to dryness to afford compound **4** in 77% yield.

Yield: 77%; white solid; mp 51 °C. ^{1}H NMR (600 MHz, DMSO) δ 12.51 (s, 1H), 8.50 – 8.45 (m, 2H), 8.32 (dd, J = 4.7, 1.6 Hz, 1H), 7.24 (dd, J = 7.8, 4.7 Hz, 1H), 2.47 (s, 3H). ^{13}C NMR (151 MHz, DMSO) δ 193.36, 149.30, 144.46, 135.20, 130.19, 118.48, 118.16, 115.96, 27.41. APCI-HRMS m/z: calcld for C$_9$H$_9$N$_2$O (MH$^+$), 161.0709, found, 161.0712. Purity (HPLC): 97.2%

Synthesis of 7-azaindole- chalcones

An appropriately substituted aromatic aldehyde (1.873 mmol) and 1-(1H-pyrrolo[2,3-b]pyridine-3-yl)ethan-1-one (0.3 g, 1.873 mmol) were stirred in 32% HCl/methanol (1.5:1 v/v) and refluxed for 24 h at 100 °C. The progress of the reaction was monitored by TLC with ethyl acetate as mobile phase. The target products were precipitated with ice-cold water or extracted and recrystallised from appropriate solvents.

1.2.1. (E)-3-phenyl-1-(1H-pyrrolo[2,3-b]pyridin-3-yl)prop-2-en-1-one (5a)

Yield: 78%; off-white solid; mp 294-295 °C. ^{1}H NMR (600 MHz, DMSO) δ 13.05 (s, 1H), 9.01 (s, 1H), 8.76 (dd, J = 7.8, 1.5 Hz, 1H), 8.43 (dd, J = 4.9, 1.5 Hz, 1H), 7.96 – 7.86 (m, 3H), 7.68 (d, J = 15.6 Hz, 1H), 7.49 – 7.37 (m, 4H). ^{13}C NMR (151 MHz, DMSO) δ 184.21, 147.34, 142.76, 141.10, 136.18, 135.44, 132.57, 130.57, 129.32, 129.10, 124.21, 119.96, 118.69, 117.01. APCI-HRMS m/z: calcld for C$_{16}$H$_{13}$N$_2$O (MH$^+$), 249.1022, found, 249.1009. Purity (HPLC): 98.1%

1.2.2. (E)-3-(2-chlorophenyl)-1-(1H-pyrrolo[2,3-b]pyridin-3-yl)prop-2-en-1-one (5b)

Yield: 88%; off-white solid; mp 231 °C. ^{1}H NMR (600 MHz, DMSO) δ 13.01 (s, 1H), 9.01 (s, 1H), 8.71 (dd, J = 7.8, 1.3 Hz, 1H), 8.42 (dd, J = 4.8, 1.2 Hz, 1H), 8.32 – 8.19 (m, 1H), 7.99 (q, J = 15.5 Hz, 2H), 7.56 (dd, J = 5.9, 3.3 Hz, 1H), 7.46 (dd, J = 5.6, 3.8 Hz, 2H), 7.38 (dd, J = 7.8, 4.9 Hz, 1H). ^{13}C NMR (151 MHz, DMSO) δ 183.74, 148.00, 143.45, 136.47, 136.26, 135.67, 134.60, 133.03, 131.97, 130.44, 128.79, 128.04, 126.84, 119.57, 118.79, 116.83. APCI-HRMS m/z: calcld for C$_{16}$H$_{12}$ClN$_2$O (MH$^+$), 283.0633, found, 283.0613. Purity (HPLC): 97.0%

1.2.3. (E)-3-(3-oxo-3-(1H-pyrrolo[2,3-b]pyridin-3-yl)prop-1-en-1-yl)-4H-chromen-4-one (5c)

Yield: 88%; off-white solid; mp 285-287 °C. ^{1}H NMR (600 MHz, DMSO) δ 12.83 (s, 1H), 9.07 (s, 1H), 8.71 – 8.63 (m, 2H), 8.40 (dd, J = 4.8, 1.5 Hz, 1H), 8.26 – 8.15 (m, 2H), 7.86 (dd, J = 7.1, 1.5 Hz, 1H), 7.74 (d, J = 8.4 Hz, 1H), 7.64 – 7.54 (m, 2H), 7.35 (dd, J = 7.8, 4.8 Hz, 1H).^{13}C NMR (151 MHz, DMSO) δ 184.31, 175.82, 159.27, 155.80, 148.55, 143.97, 135.17, 135.02, 132.23, 131.42, 126.57, 125.92, 125.59, 123.93, 119.43, 119.19, 119.10, 118.69, 116.69. APCI-HRMS m/z: calcld for $C_{19}H_{13}N_2O_3$ (MH$^+$), 317.0921, found, 317.0918. Purity (HPLC): 71.5%

1.2.4. (E)-3-(4-(piperidin-1-yl)phenyl)-1-(1H-pyrrolo[2,3-b]pyridin-3-yl)prop-2-en-1-one (5d)

Yield: 92%; dark-brown solid; mp 168 °C. ^{1}H NMR (600 MHz, DMSO) δ 12.75 (s, 1H), 8.92 (s, 1H), 8.64 (d, J = 7.8 Hz, 1H), 8.46 – 8.22 (m, 1H), 8.15 – 7.79 (m, 3H), 7.64 (d, J = 15.5 Hz, 3H), 7.30 (dd, J = 7.7, 4.8 Hz, 1H), 3.62 – 3.29 (m, 4H), 2.18 – 1.75 (m, 4H), 1.75 – 1.52 (m, 2H). ^{13}C NMR (151 MHz, DMSO) δ 184.07, 178.98, 168.73, 154.35, 149.08, 144.34, 139.73, 135.62, 131.01, 130.40, 119.47, 119.02, 118.63, 116.88, 100.96, 40.53, 24.00. APCI-HRMS m/z: calcld for $C_{21}H_{22}N_3O$ (MH$^+$), 332.1757, found, 332.1744. Purity (HPLC): 71.0%

1.2.5. (E)-4-(3-oxo-3-(1H-pyrrolo[2,3-b]pyridin-3-yl)prop-1-en-1-yl)benzoic acid (5e)

Yield: 44%; off-white solid; mp 312 °C. ^{1}H NMR (600 MHz, DMSO) δ 12.84 (s, 1H), 8.98 (s, 1H), 8.67 (d, J = 6.6 Hz, 1H), 8.39 (d, J = 3.5 Hz, 1H), 8.15 – 7.88 (m, J = 9.0 Hz, 5H), 7.71 (d, J = 15.6 Hz, 1H), 7.34 (dd, J = 7.5, 4.8 Hz, 1H), 5.35 (s, 1H). ^{13}C NMR (151 MHz, DMSO) δ 184.31, 175.82, 159.27, 155.80, 148.55, 135.17, 135.02, 132.23, 131.42, 126.57, 125.92, 123.93, 119.10, 118.69, 116.69. APCI-HRMS m/z: calcld for $C_{17}H_{13}N_2O_3$ (MH$^+$), 293.0921, found, 293.0893. Purity (HPLC): 66.3%

1.2.6. (E)-1-(1H-pyrrolo[2,3-b]pyridin-3-yl)-3-(thiophen-2-yl)prop-2-en-1-one (5f)

Yield: 26%; light yellow solid; mp 213 °C. ^{1}H NMR (600 MHz, DMSO) δ 12.61 (s, 1H), 8.84 (s, 1H), 8.61 (d, J = 7.8 Hz, 1H), 8.36 (d, J = 4.5 Hz, 1H), 7.83 (d, J = 15.3 Hz, 1H), 7.73 (d, J = 4.8 Hz, 1H), 7.63 (d, J = 3.0 Hz, 1H), 7.54 (d, J = 15.3 Hz, 1H), 7.28 (dd, J = 7.8, 4.7 Hz, 1H), 7.23 – 7.13 (m, 1H). ^{13}C NMR (151 MHz, DMSO) δ 183.26, 149.22, 144.41, 140.02, 134.82,

133.06, 131.50, 129.95, 129.28, 128.46, 122.40, 118.20, 118.11, 116.05. APCI-HRMS m/z: calcld for $C_{14}H_{11}N_2O$ (MH$^+$), 255.0587, found, 255.0584. Purity (HPLC): 79.6%

1.2.7. (E)-3-(4-isopropylphenyl)-1-(1H-pyrrolo[2,3-b]pyridin-3-yl)prop-2-en-1-one (5g)

Yield: 68%; light yellow solid; mp 293-294 °C. ^{1}H NMR (600 MHz, DMSO) δ 12.99 (s, 1H), 8.98 (s, 1H), 8.74 (dd, J = 7.8, 1.5 Hz, 1H), 8.42 (dd, J = 4.9, 1.5 Hz, 1H), 7.87 (d, J = 15.6 Hz, 1H), 7.80 (d, J = 8.2 Hz, 2H), 7.65 (d, J = 15.5 Hz, 1H), 7.38 (dd, J = 7.8, 4.9 Hz, 1H), 7.32 (d, J = 8.2 Hz, 2H), 3.13 – 2.75 (m, 1H), 1.22 (d, J = 6.9 Hz, 6H). ^{13}C NMR (151 MHz, DMSO) δ 184.29, 151.28, 147.59, 142.96, 141.09, 135.94, 133.15, 132.34, 129.21, 127.28, 123.32, 119.84, 118.65, 117.02, 33.88, 24.15. APCI-HRMS m/z: calcld for $C_{19}H_{19}N_2O$ (MH$^+$), 291.1492, found, 291.1489. Purity (HPLC): 91.1%

1.2.8. (E)-3-(4-(tert-butyl)phenyl)-1-(1H-pyrrolo[2,3-b]pyridin-3-yl)prop-2-en-1-one (5h)

Yield: 56%; off-white solid; mp 287-289 °C. ^{1}H NMR (600 MHz, DMSO) δ 12.98 (s, 1H), 8.97 (s, 1H), 8.74 (dd, J = 7.8, 1.5 Hz, 1H), 8.42 (dd, J = 4.9, 1.5 Hz, 1H), 7.87 (d, J = 15.6 Hz, 1H), 7.80 (d, J = 8.3 Hz, 2H), 7.66 (d, J = 15.5 Hz, 1H), 7.47 (d, J = 8.4 Hz, 2H), 7.38 (dd, J = 7.8, 4.9 Hz, 1H), 1.30 (s, 9H). ^{13}C NMR (151 MHz, DMSO) δ 184.30, 153.45, 147.65, 143.03, 140.96, 135.92, 132.75, 132.29, 128.94, 126.11, 123.45, 119.81, 118.65, 117.00, 40.52, 35.09, 31.43. APCI-HRMS m/z: calcld for $C_{20}H_{21}N_2O$ (MH$^+$), 305.1648, found, 305.1637. Purity (HPLC): 99.1%

1.2.9. (E)-3-(4-nitrophenyl)-1-(1H-pyrrolo[2,3-b]pyridin-3-yl)prop-2-en-1-one (5i)

Yield: 44%; off-white solid; mp 158-159 °C. ^{1}H NMR (600 MHz, DMSO) δ 12.82 (s, 1H), 9.00 (s, 1H), 8.64 (dd, J = 7.8, 1.6 Hz, 1H), 8.39 (dd, J = 4.7, 1.5 Hz, 1H), 8.30 (d, J = 8.8 Hz, 2H), 8.16 (d, J = 8.8 Hz, 2H), 8.09 (d, J = 15.6 Hz, 1H), 7.75 (d, J = 15.6 Hz, 1H), 7.33 (dd, J = 7.8, 4.7 Hz, 1H). ^{13}C NMR (151 MHz, DMSO) δ 183.61, 149.28, 148.22, 144.67, 142.16, 138.15, 136.36, 130.89, 129.98, 128.33, 124.40, 118.86, 118.82, 116.81. APCI-HRMS m/z: calcld for $C_{16}H_{12}N_3O_3$ (MH$^+$), 294.0873, found, 294.0857. Purity (HPLC): 86.2%
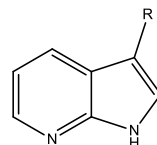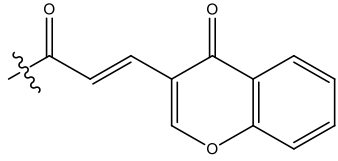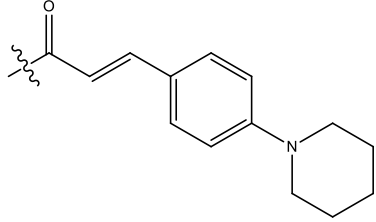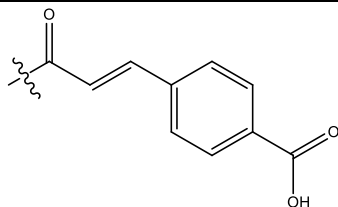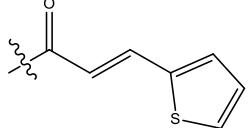
1.2.10. (E)-3-(3-methoxyphenyl)-1-(1H-pyrrolo[2,3-b]pyridin-3-yl)prop-2-en-1-one (5j)

Yield: 96%; light brown solid; mp 261-263 °C. ^{1}H NMR (600 MHz, DMSO) δ 13.01 (s, 1H), 9.02 (s, 1H), 8.74 (dd, J = 7.8, 1.4 Hz, 1H), 8.42 (dd, J = 4.9, 1.4 Hz, 1H), 7.91 (d, J = 15.6 Hz, 1H), 7.65 (d, J = 15.5 Hz, 1H), 7.49 (s, 1H), 7.46 – 7.32 (m, 3H), 7.01 (dd, J = 8.1, 2.0 Hz, 1H), 3.84 (s, 3H). ^{13}C NMR (151 MHz, DMSO) δ 184.19, 160.12, 147.66, 143.05, 141.05, 136.85, 136.17, 132.31, 130.34, 124.44, 121.93, 119.80, 118.69, 116.98, 116.47, 113.75, 55.79. APCI-HRMS m/z: calcld for $C_{17}H_{15}N_2O_2$ (MH$^+$), 279.1128, found, 279.1126. Purity (HPLC): 100%

1.2.11. (E)-3-(3,4-dimethoxyphenyl)-1-(1H-pyrrolo[2,3-b]pyridin-3-yl)prop-2-en-1-one (5k)

Yield: 19%; white solid; mp 216 °C. ^{1}H NMR (600 MHz, DMSO) δ 12.63 (s, 1H), 8.90 (s, 1H), 8.62 (dd, J = 7.8, 1.3 Hz, 1H), 8.36 (dd, J = 4.6, 1.3 Hz, 1H), 7.74 (d, J = 15.5 Hz, 1H), 7.62 (d, J = 15.5 Hz, 1H), 7.52 (d, J = 1.3 Hz, 1H), 7.36 (dd, J = 8.2, 1.4 Hz, 1H), 7.28 (dd, J = 7.8, 4.7 Hz, 1H), 7.02 (d, J = 8.3 Hz, 1H), 3.88 (s, 3H), 3.82 (s, 3H). ^{13}C NMR (151 MHz, DMSO) δ 184.27, 151.21, 149.72, 149.46, 144.85, 141.06, 135.13, 130.48, 128.30, 123.69, 121.94, 118.75, 118.54, 116.85, 112.04, 111.05, 56.20, 56.04. APCI-HRMS m/z: calcld for $C_{18}H_{17}N_2O_3$ (MH$^+$), 309.1234, found, 309.1231. Purity (HPLC): 87.2%

1.2.12. (E)-3-(2-fluorophenyl)-1-(1H-pyrrolo[2,3-b]pyridin-3-yl)prop-2-en-1-one (5l)

Yield: 62%; light pink solid; mp 301 °C. ^{1}H NMR (600 MHz, DMSO) δ 12.98 (s, 1H), 8.98 (s, 1H), 8.71 (dd, J = 7.8, 1.5 Hz, 1H), 8.42 (dd, J = 4.9, 1.5 Hz, 1H), 8.21 – 8.13 (m, 1H), 7.96 (d, J = 15.7 Hz, 1H), 7.81 (d, J = 15.7 Hz, 1H), 7.55 – 7.46 (m, 1H), 7.40 – 7.29 (m, 3H). ^{13}C NMR (151 MHz, DMSO) δ 183.80, 161.21 (d, J = 250.6 Hz), 148.03, 143.48, 136.29, 132.59 (d, J = 8.7 Hz), 131.98, 131.92 (d, J = 4.8 Hz), 128.96, 126.18 (d, J = 2.7 Hz), 125.32 (d, J = 3.2 Hz), 123.05 (d, J = 11.5 Hz), 119.56, 118.78, 116.82, 116.50 (d, J = 21.5 Hz). APCI-HRMS m/z: calcld for $C_{16}H_{12}FN_2O$ (MH$^+$), 267.0928, found, 267.0945. Purity (HPLC): 98.9%

1.2.13. (E)-3-(3-fluorophenyl)-1-(1H-pyrrolo[2,3-b]pyridin-3-yl)prop-2-en-1-one (5m)

Yield: 53%; off-white solid; mp 270-272 °C. ^{1}H NMR (600 MHz, DMSO) δ 13.09 (s, 1H), 9.03 (s, 1H), 8.75 (dd, J = 7.8, 1.5 Hz, 1H), 8.43 (dd, J = 4.9, 1.5 Hz, 1H), 7.97 (d, J = 15.6 Hz, 1H), 7.88 – 7.82 (m, 1H), 7.67 (t, J = 10.8 Hz, 2H), 7.49 (td, J = 7.9, 6.2 Hz, 1H), 7.40 (dd, J = 7.8, 5.0 Hz, 1H), 7.29 – 7.25 (m, 1H). ^{13}C NMR (151 MHz, DMSO) δ 183.98, 163.01 (d, J = 243.4

Hz), 147.31, 142.79, 139.68, 138.06 (d, J = 7.9 Hz), 136.47, 132.58, 131.26 (d, J = 8.4 Hz), 125.88, 125.61, 119.92, 118.75, 117.23 (d, J = 21.4 Hz), 117.00, 114.75 (d, J = 21.8 Hz). APCI-HRMS m/z: calcld for $C_{16}H_{12}FN_2O$ (MH$^+$), 267.0928, found, 267.0951. Purity (HPLC): 98.0%

1.2.14. (E)-3-(4-fluorophenyl)-1-(1H-pyrrolo[2,3-b]pyridin-3-yl)prop-2-en-1-one (5n)

Yield: 55%; off-white solid; mp 279-281 °C. ^{1}H NMR (600 MHz, DMSO) δ 12.98 (s, 1H), 8.98 (s, 1H), 8.73 (d, J = 7.7 Hz, 1H), 8.42 (d, J = 4.7 Hz, 1H), 7.97 (dd, J = 8.0, 5.8 Hz, 2H), 7.88 (d, J = 15.6 Hz, 1H), 7.67 (d, J = 15.6 Hz, 1H), 7.38 (dd, J = 7.7, 4.9 Hz, 1H), 7.31 (t, J = 8.6 Hz, 2H). ^{13}C NMR (151 MHz, DMSO) δ 184.12, 163.58 (d, J = 248.1 Hz), 147.71, 143.11, 139.79, 136.09, 132.19 (d, J = 11.7 Hz), 131.34 (d, J = 8.4 Hz), 124.15, 119.74, 118.68, 116.97, 116.32 (d, J = 21.6 Hz). APCI-HRMS m/z: calcld for $C_{16}H_{12}FN_2O$ (MH$^+$), 267.0928, found, 267.0923. Purity (HPLC): 100.0%

1.2.15. (E)-3-(4-chlorophenyl)-1-(1H-pyrrolo[2,3-b]pyridin-3-yl)prop-2-en-1-one (5o)

Yield: 55%; light brown solid; mp 281 °C. ^{1}H NMR (600 MHz, DMSO) δ 12.98 (s, 1H), 8.99 (s, 1H), 8.72 (dd, J = 7.8, 1.6 Hz, 1H), 8.42 (dd, J = 4.9, 1.5 Hz, 1H), 7.97 – 7.90 (m, 3H), 7.66 (d, J = 15.6 Hz, 1H), 7.56 – 7.50 (m, 2H), 7.37 (dd, J = 7.8, 4.9 Hz, 1H). ^{13}C NMR (151 MHz, DMSO) δ 184.02, 147.85, 143.25, 139.56, 136.20, 134.98, 134.46, 132.11, 130.76, 129.34, 124.99, 119.66, 118.71, 116.95. APCI-HRMS m/z: calcld for $C_{16}H_{12}ClN_2O$ (MH$^+$), 283.0633, found, 283.0609. Purity (HPLC): 97.2%

1.2.16. (E)-3-(4-bromophenyl)-1-(1H-pyrrolo[2,3-b]pyridin-3-yl)prop-2-en-1-one (5p)

Yield: 52%; off-white solid; mp 295-296 °C. ^{1}H NMR (600 MHz, DMSO) δ 12.99 (s, 1H), 8.99 (s, 1H), 8.72 (dd, J = 7.8, 1.5 Hz, 1H), 8.42 (dd, J = 4.9, 1.5 Hz, 1H), 7.95 (d, J = 15.6 Hz, 1H), 7.86 (d, J = 8.5 Hz, 2H), 7.65 (dd, J = 13.5, 12.2 Hz, 3H), 7.38 (dd, J = 7.8, 4.9 Hz, 1H). ^{13}C NMR (151 MHz, DMSO) δ 184.02, 147.79, 143.22, 139.67, 136.24, 134.79, 132.27, 132.16, 131.00, 125.04, 123.82, 119.68, 118.72, 116.96. APCI-HRMS m/z: calcld for $C_{16}H_{12}BrN_2O$ (MH$^+$), 327.0127, found, 327.0132. Purity (HPLC): 99.0%

1.2.17. (E)-3-(4-hydroxyphenyl)-1-(1H-pyrrolo[2,3-b]pyridin-3-yl)prop-2-en-1-one (5q)

Yield: 93%; light brown solid; mp 257 °C. ^{1}H NMR (600 MHz, DMSO) δ 12.89 (s, 1H), 8.91 (s, 1H), 8.74 (dd, J = 7.8, 1.5 Hz, 1H), 8.41 (dd, J = 4.9, 1.5 Hz, 1H), 7.77 – 7.66 (m, 3H), 7.61 (d, J = 15.5 Hz, 1H), 7.37 (dd, J = 7.8, 4.9 Hz, 1H), 6.86 (d, J = 8.6 Hz, 2H), 6.63 (s, 1H). ^{13}C NMR (151 MHz, DMSO) δ 184.37, 160.13, 147.59, 142.90, 141.41, 135.43, 132.32, 131.01, 126.47, 120.78, 119.86, 118.54, 117.10, 116.21. APCI-HRMS m/z: calcld for $C_{16}H_{13}N_2O_2$ (MH$^+$), 265.0972, found, 265.0972. Purity (HPLC): 100%

1.2.18. (E)-3-(4-methoxyphenyl)-1-(1H-pyrrolo[2,3-b]pyridin-3-yl)prop-2-en-1-one (5r)

Yield: 76%; off-white solid; mp 339 °C. ^{1}H NMR (600 MHz, DMSO) δ 12.60 (s, 1H), 8.88 (d, J = 2.4 Hz, 1H), 8.62 (dd, J = 7.8, 1.4 Hz, 1H), 8.36 (dd, J = 4.6, 1.5 Hz, 1H), 7.83 (d, J = 8.7 Hz, 2H), 7.76 (d, J = 15.5 Hz, 1H), 7.64 (d, J = 15.5 Hz, 1H), 7.28 (dd, J = 7.8, 4.7 Hz, 1H), 7.02 (d, J = 8.7 Hz, 2H), 3.82 (s, 3H). ^{13}C NMR (151 MHz, DMSO) δ 184.30, 161.32, 149.66, 144.80, 140.57, 135.13, 130.75, 130.51, 128.14, 121.95, 118.77, 118.55, 116.87, 114.79, 55.81. APCI-HRMS m/z: calcld for $C_{17}H_{15}N_2O_2$ (MH$^+$), 279.1128, found, 279.1130. Purity (HPLC): 93.2%

1.2.19. (2E,5E)-6-phenyl-1-(1H-pyrrolo[2,3-b]pyridin-3-yl)hexa-2,5-dien-1-one (5s)

Yield: 92%; brown solid; mp 333 °C. ^{1}H NMR (600 MHz, DMSO) δ 12.88 (s, 1H), 8.72 – 8.66 (m, 2H), 8.40 (dd, J = 4.9, 1.5 Hz, 1H), 7.58 (d, J = 7.3 Hz, 2H), 7.53 – 7.44 (m, 1H), 7.44 – 7.31 (m, 5H), 7.20 – 7.15 (m, 2H). ^{13}C NMR (151 MHz, DMSO) δ 184.32, 147.90, 143.34, 141.25, 140.72, 140.64, 136.64, 135.16, 131.98, 129.40, 127.84, 127.60, 127.51, 119.53, 118.64, 116.88. APCI-HRMS m/z: calcld for $C_{18}H_{15}N_2O$ (MH$^+$), 275.1179, found, 275.1153. Purity (HPLC): 96.5%.

1.2.20. (E)-1-(1H-pyrrolo[2,3-b]pyridin-3-yl)-3-(p-tolyl)prop-2-en-1-one (5t)

Yield: 91%; off-white solid; mp 299-300 °C. ^{1}H NMR (600 MHz, DMSO) δ 12.97 (s, 1H), 8.97 (s, 1H), 8.74 (d, J = 7.7 Hz, 1H), 8.42 (d, J = 4.3 Hz, 1H), 7.86 (d, J = 15.5 Hz, 1H), 7.78 (d, J = 7.7 Hz, 2H), 7.65 (d, J = 15.5 Hz, 1H), 7.50 – 7.27 (m, 2H), 7.27 (s, 1H), 2.35 (s, 3H). ^{13}C NMR (151 MHz, DMSO) δ 184.27, 147.63, 143.00, 141.07, 140.48, 135.91, 132.72, 132.30,

129.94, 129.10, 123.20, 119.81, 118.64, 117.02, 21.55. APCI-HRMS m/z: calcld for C$_{17}$H$_{15}$N$_2$O (MH$^+$), 263.1179, found, 263.1161. Purity (HPLC): 97.1%.

1.2.21. (E)-3-(5-nitrofuran-2-yl)-1-(1H-pyrrolo[2,3-b]pyridin-3-yl)prop-2-en-1-one (5u)

Yield: 10%; dark brown solid; mp 187 °C. ^{1}H NMR (600 MHz, DMSO) δ 12.68 (s, 1H), 8.84 (s, 1H), 8.50 (d, J = 7.6 Hz, 1H), 8.29 (s, 1H), 7.75 (dd, J = 15.1, 9.7 Hz, 2H), 7.44 (d, J = 15.5 Hz, 1H), 7.30 (d, J = 3.4 Hz, 1H), 7.22 (dd, J = 7.5, 4.7 Hz, 1H). ^{13}C NMR (151 MHz, DMSO) δ 182.68, 154.41, 152.25, 149.78, 145.17, 136.43, 130.47, 127.80, 125.94, 118.89, 118.58, 117.02, 116.44, 115.47. APCI-HRMS m/z: calcld for C$_{14}$H$_{10}$N$_3$O$_4$ (MH$^+$), 284.0666, found, 284.0671. Purity (HPLC): 45.9%

1.2.22. (E)-3-(3-nitrophenyl)-1-(1H-pyrrolo[2,3-b]pyridin-3-yl)prop-2-en-1-one (5v)

Yield: 69%; off-white solid; mp 305 °C. ^{1}H NMR (600 MHz, DMSO) δ 12.71 (s, 1H), 8.99 (s, 1H), 8.74 (s, 1H), 8.61 (dd, J = 7.7, 1.2 Hz, 1H), 8.37 (d, J = 3.3 Hz, 1H), 8.29 (d, J = 7.6 Hz, 1H), 8.23 (d, J = 6.5 Hz, 1H), 8.06 (d, J = 15.6 Hz, 1H), 7.75 (dd, J = 19.8, 11.8 Hz, 2H), 7.29 (dd, J = 7.7, 4.7 Hz, 1H). ^{13}C NMR (151 MHz, DMSO) δ 183.27, 149.15, 148.43, 144.42, 144.34, 137.85, 136.99, 135.67, 134.86, 130.26, 130.08, 126.51, 124.10, 122.48, 118.25, 116.26. APCI-HRMS m/z: calcld for C$_{16}$H$_{12}$N$_3$O$_3$ (MH$^+$), 294.0873, found, 294.0860. Purity (HPLC): 82.1%

1.2.23. (E)-3-(2-nitrophenyl)-1-(1H-pyrrolo[2,3-b]pyridin-3-yl)prop-2-en-1-one (5w)

Yield: 68%; light brown solid; mp 261-263 °C. ^{1}H NMR (600 MHz, DMSO) δ 12.98 (s, 1H), 8.98 (s, 1H), 8.76 – 8.63 (m, 1H), 8.42 (d, J = 3.6 Hz, 1H), 8.24 (d, J = 7.7 Hz, 1H), 8.08 (d, J = 8.1 Hz, 1H), 7.92 (s, 2H), 7.84 (t, J = 7.4 Hz, 1H), 7.69 (t, J = 7.3 Hz, 1H), 7.38 (dd, J = 7.7, 4.9 Hz, 1H). ^{13}C NMR (151 MHz, DMSO) δ 183.57, 149.35, 148.22, 143.70, 136.59, 135.20, 134.01, 131.79, 131.12, 130.26, 129.70, 128.62, 125.07, 119.42, 118.84, 116.66. APCI-HRMS m/z: calcld for C$_{16}$H$_{12}$N$_3$O$_3$ (MH$^+$), 294.0873, found, 294.0863. Purity (HPLC): 98.9%.
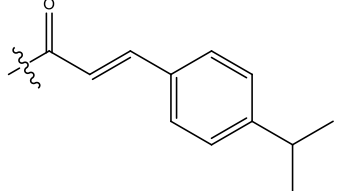
1.3. Kinase inhibition assay
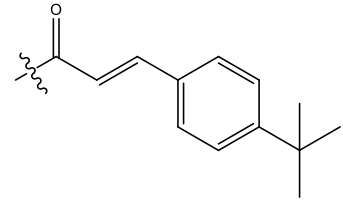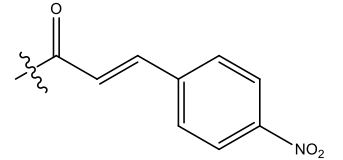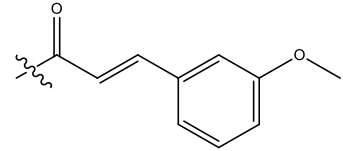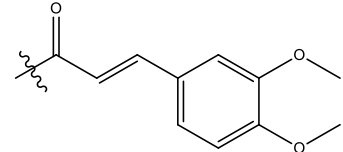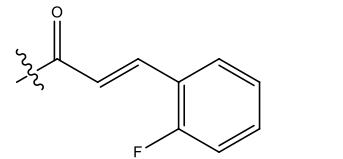
Kinase activities were measured using the bioluminescent, homogeneous ADP-Glo™ assay (Promega, Madison, WI) performed in 96-well plates. The kinase assays are described in Nguyen *et al* (Nguyen *et al.*, 2019 except for the following kinases: (i) *Lm*CK1 (from *Leishmania major*, recombinant, expressed in bacteria) was assayed in buffer A with 0.028 µg/µl of the following peptide: RRKHAAIGSpAYSITA as CK1-specific substrate; (ii) *Ssc*CK1δ/ε (casein kinase 1δ/ε, porcine brain, native, affinity purified) was assayed in buffer A with 0.022 µg/µl of the following peptide: RRKHAAIGSpAYSITA ("Sp" stands for phosphorylated serine) as CK1-specific substrate; (iii) *Ssc*GSK-3α/β (glycogen synthase kinase-3, porcine brain, native, affinity purified) isoforms were assayed in buffer A with 0.010 µg/µl of GS-1 peptide, a GSK-3-selective substrate (YRRAAVPPSPSLSRHSSPHQSpEDEEE). The buffer "A" is composed of 10 mM $MgCl_2$, 1 mM EGTA, 1 mM DTT, 25 mM Tris-HCl pH 7.5 and 50 µg/ml heparin.
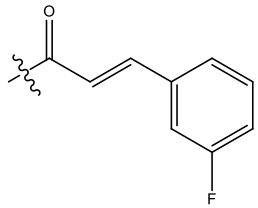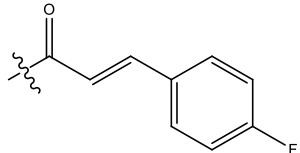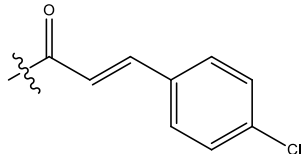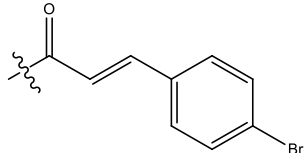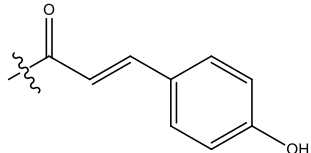
Table 2a: Percentage of kinase inhibition of hybrids (**4** and **5a-w**). The table displays the remaining activities detected after treatment with 10µM of the tested compounds.
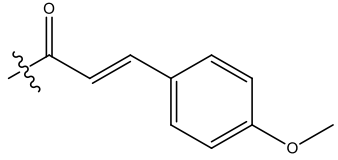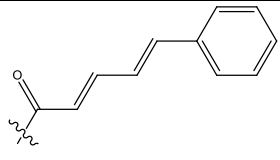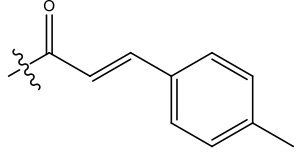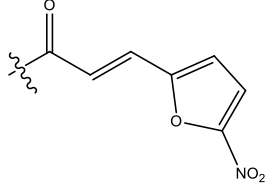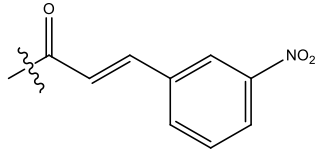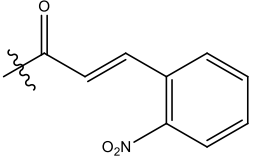
Compound	R	% residual activity measured at 10 µM of analytes							
		CDK2/Cyclin A	CDK5/p25	CDK9/CyclinT	HASPIN	PIM1	*Ssc*_CK1δ/ε	*Ssc*_GSK3α/β	*Lm*_CK1
4		≥100	89	34	23	≥100	49	82	57
5a		91	79	14	20	95	40	44	30
5b		94	86	34	33	61	53	67	26

5c		83	76	≥100	47	18	59	54	26
5d		83	62	14	41	55	54	72	17
5e		≥100	84	40	68	40	50	81	25
5f		84	≥100	3	4	43	31	37	50
5g		84	83	43	22	75	34	54	47

5h		≥100	84	48	50	95	52	80	50
5i		91	≥100	71	44	68	67	82	17
5j		≥100	88	25	19	59	46	53	46
5k		75	73	21	34	83	30	37	51
5l		≥100	≥100	40	26	65	70	55	55

5m		47	96	44	50	78	45	69	51
5n		63	≥100	42	36	93	64	75	62
5o		83	≥100	42	45	73	42	68	16
5p		88	88	42	59	79	38	79	27
5q		79	81	35	16	55	61	55	54

149

5r		≥100	≥100	61	40	87	74	82	42
5s		99	≥100	38	37	85	35	76	45
5t		≥100	≥100	32	41	70	66	68	59
5u		76	91	26	18	55	66	57	56
5v		≥100	≥100	≥100	76	59	86	89	72

5w		81	99	57	83	≥100	97	≥100	≥100

3-acetyl-7-azaindole (4)

^{1}H NMR
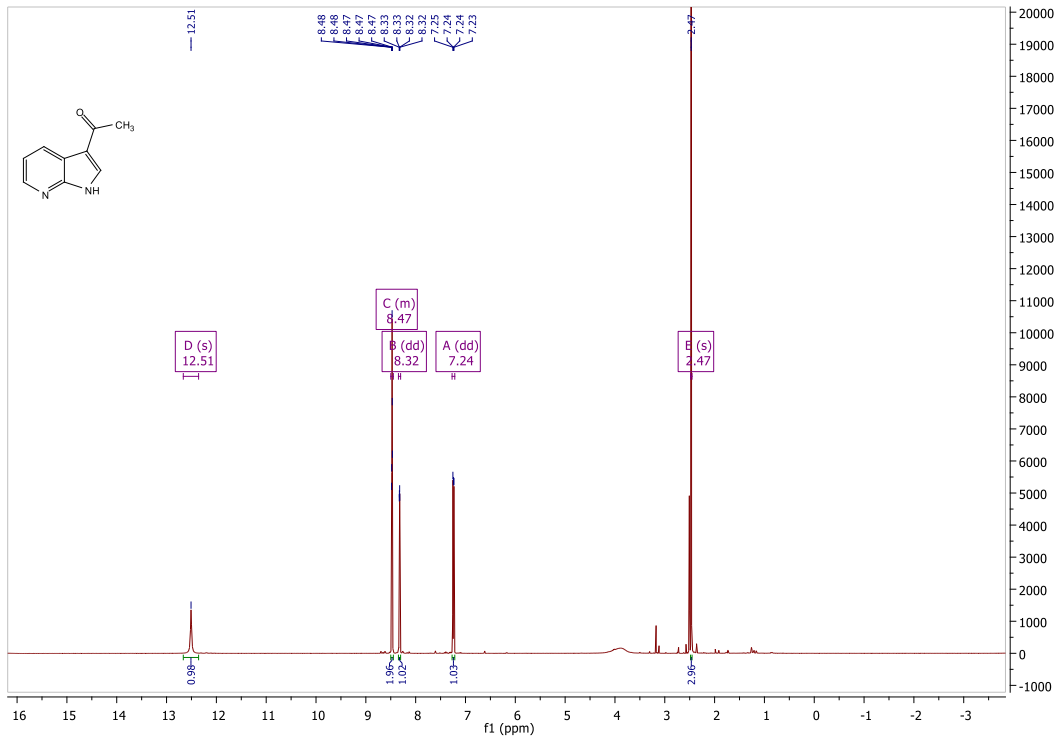
^{13}C NMR
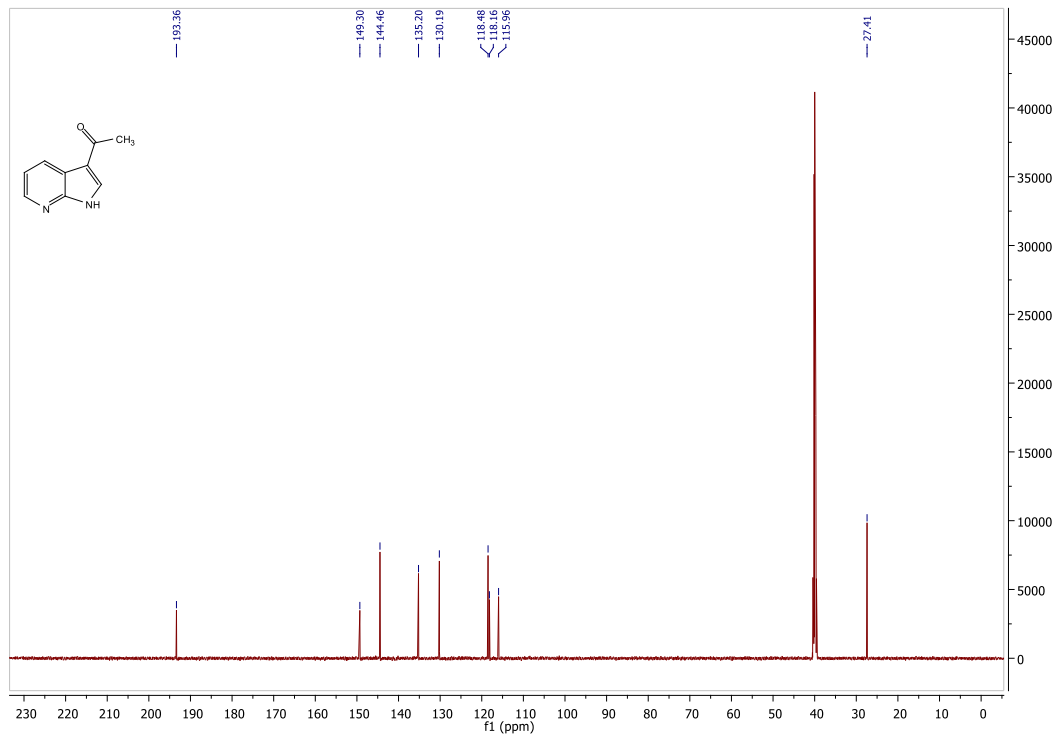
(E)-3-phenyl-1-(1H-pyrrolo[2,3-b]pyridin-3-yl)prop-2-en-1-one (5a)

^{1}H NMR
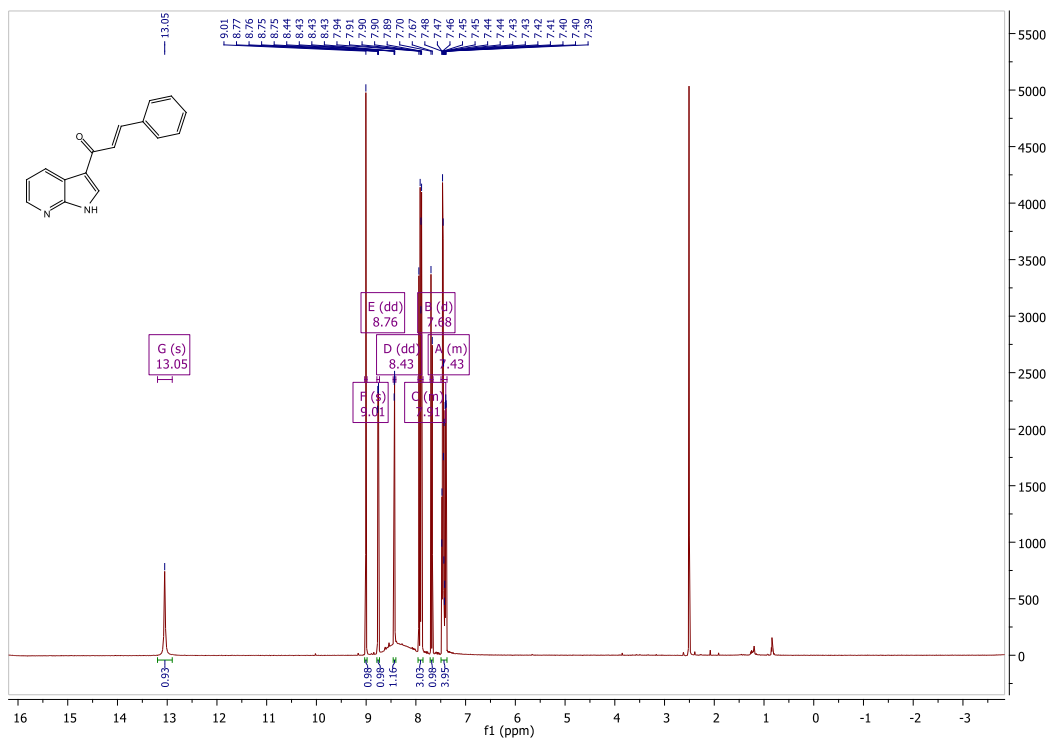
^{13}C NMR
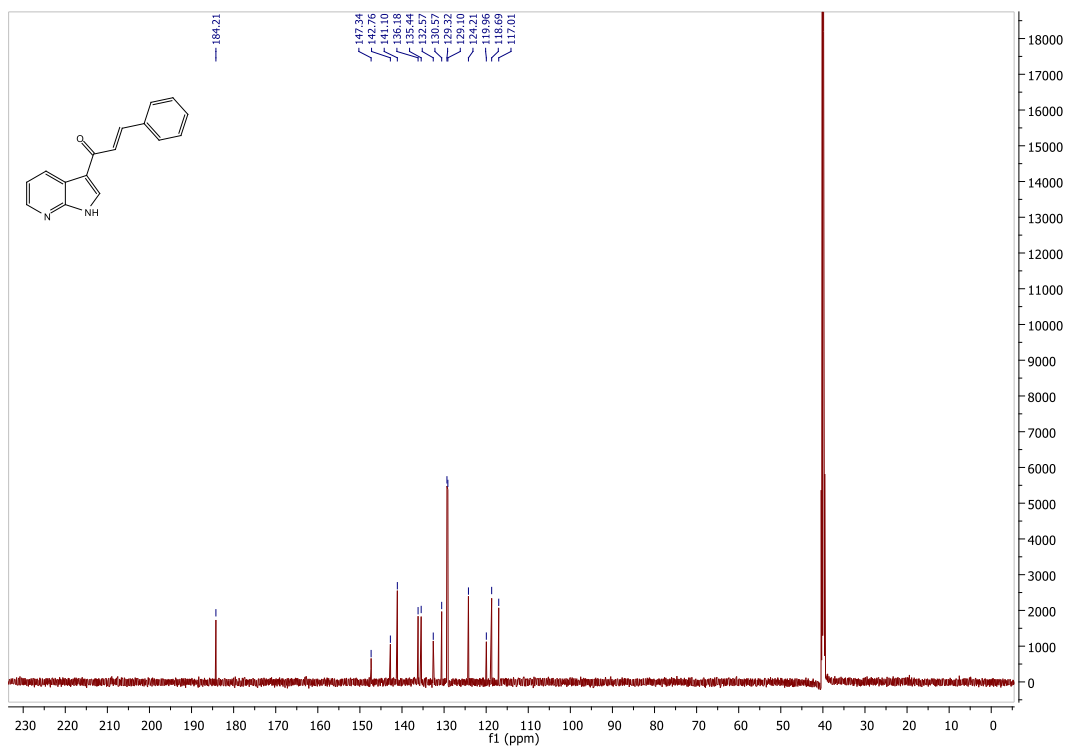
(E)-3-(2-chlorophenyl)-1-(1H-pyrrolo[2,3-b]pyridin-3-yl)prop-2-en-1-one (5b)

^{1}H NMR
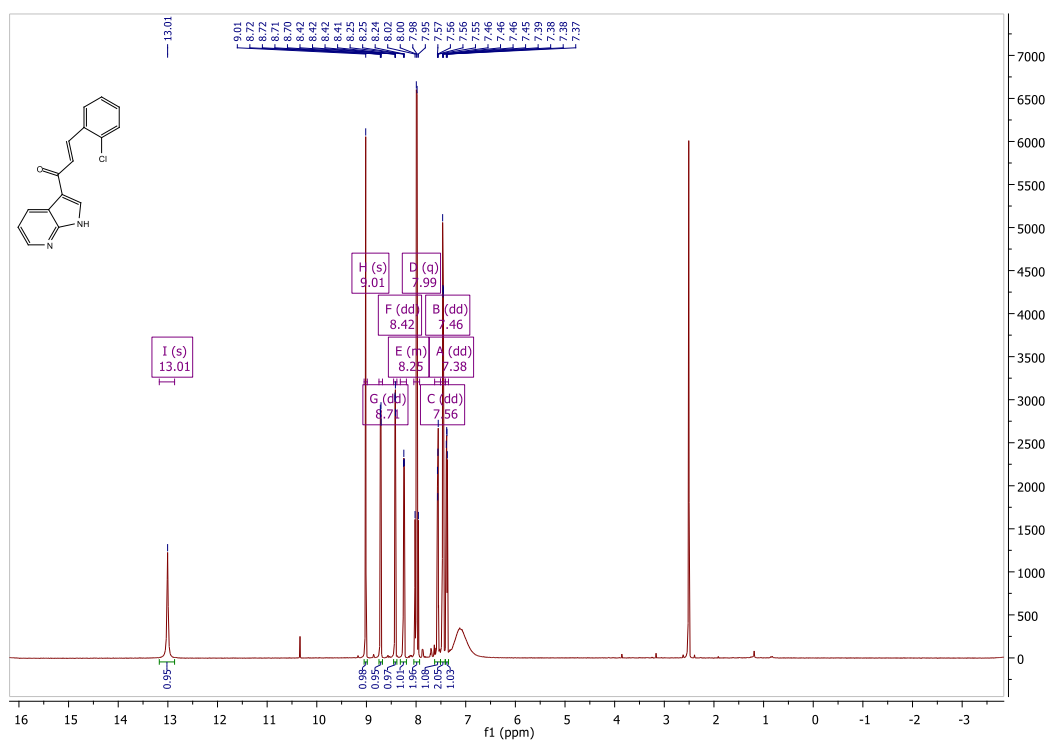
^{13}C NMR
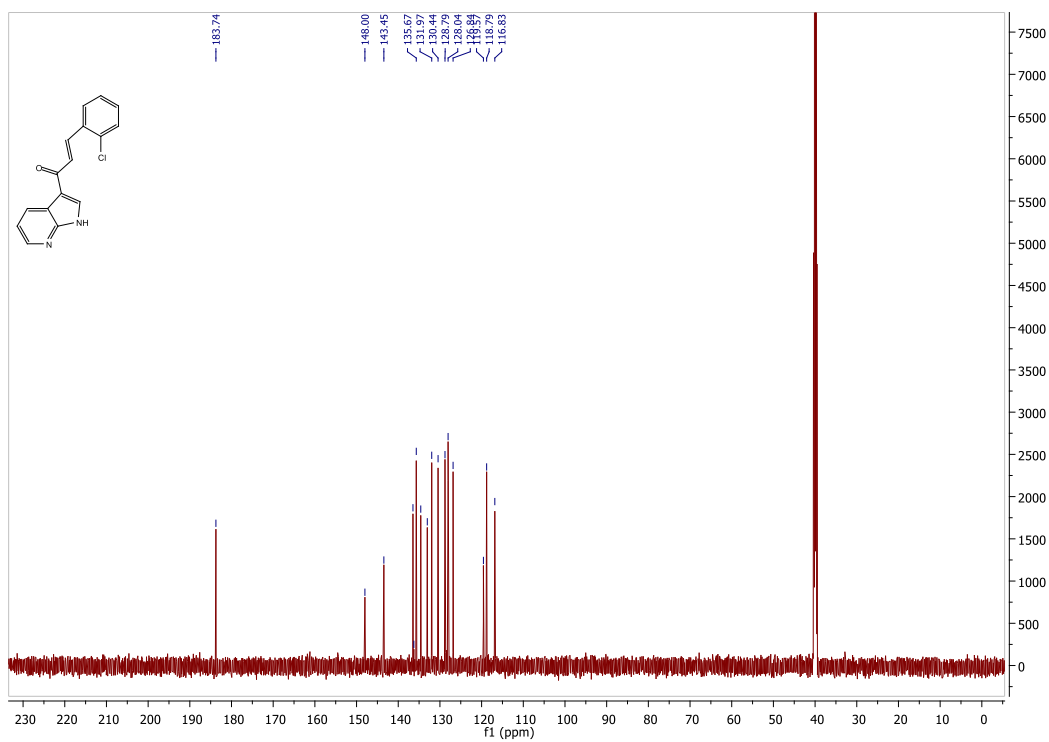
(E)-3-(3-oxo-3-(1H-pyrrolo[2,3-b]pyridin-3-yl)prop-1-en-1-yl)-4H-chromen-4-one (5c)

^{1}H NMR
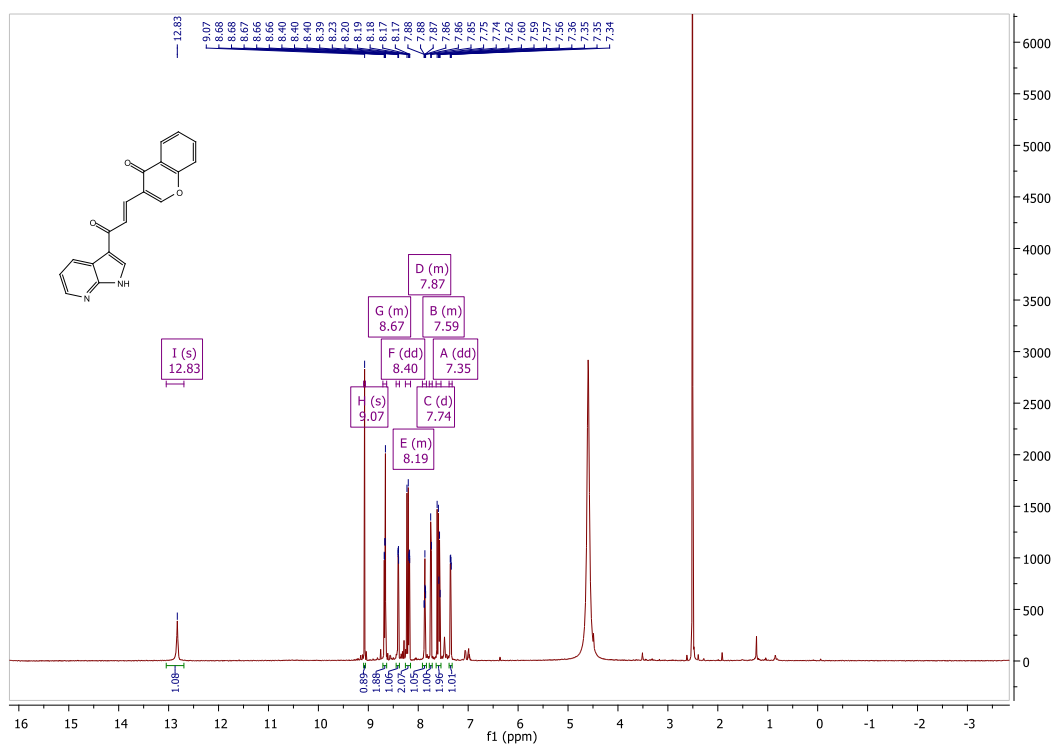
^{13}C NMR
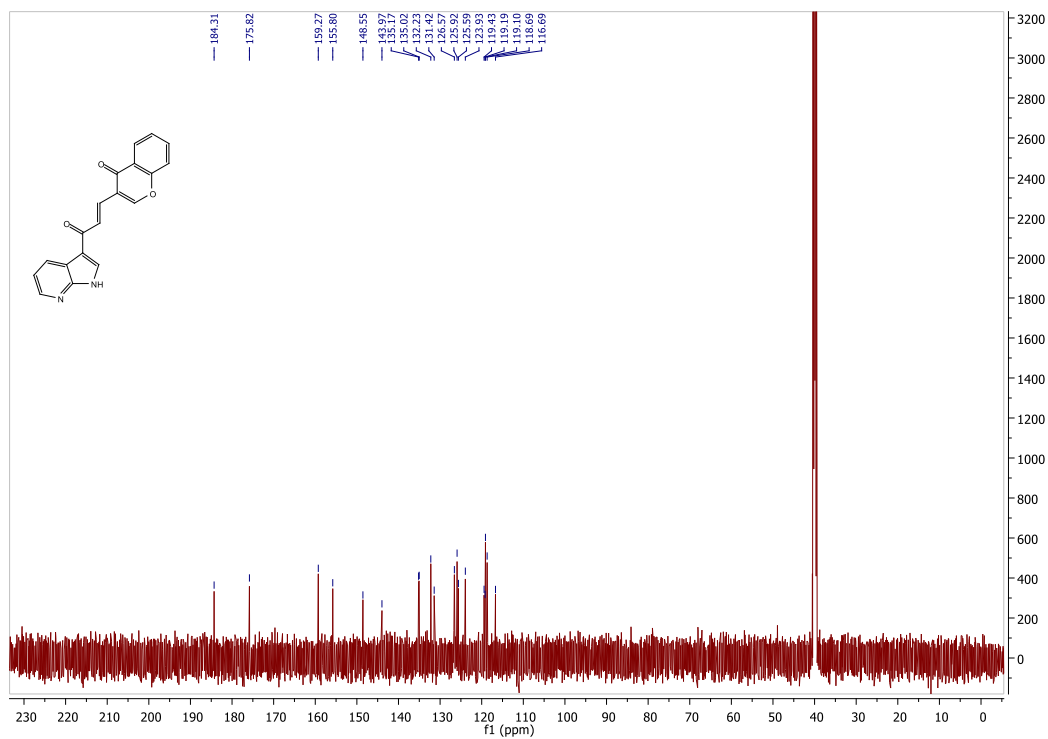
(E)-3-(4-(piperidin-1-yl)phenyl)-1-(1H-pyrrolo[2,3-b]pyridin-3-yl)prop-2-en-1-one (5d)

^{1}H NMR
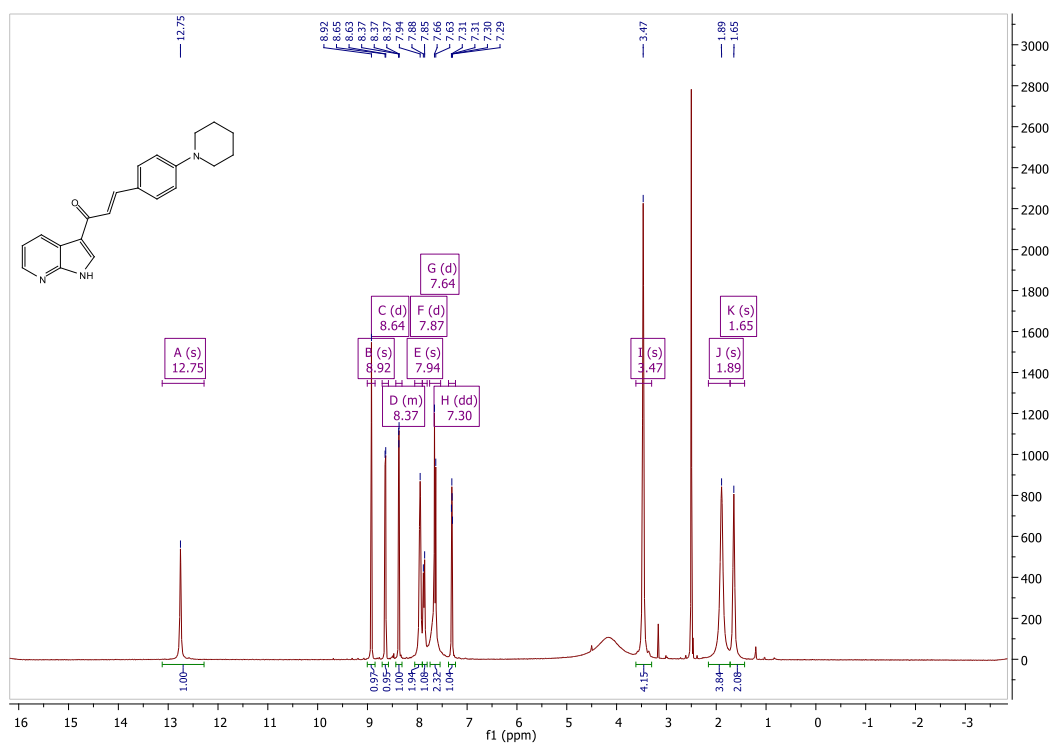
^{13}C NMR
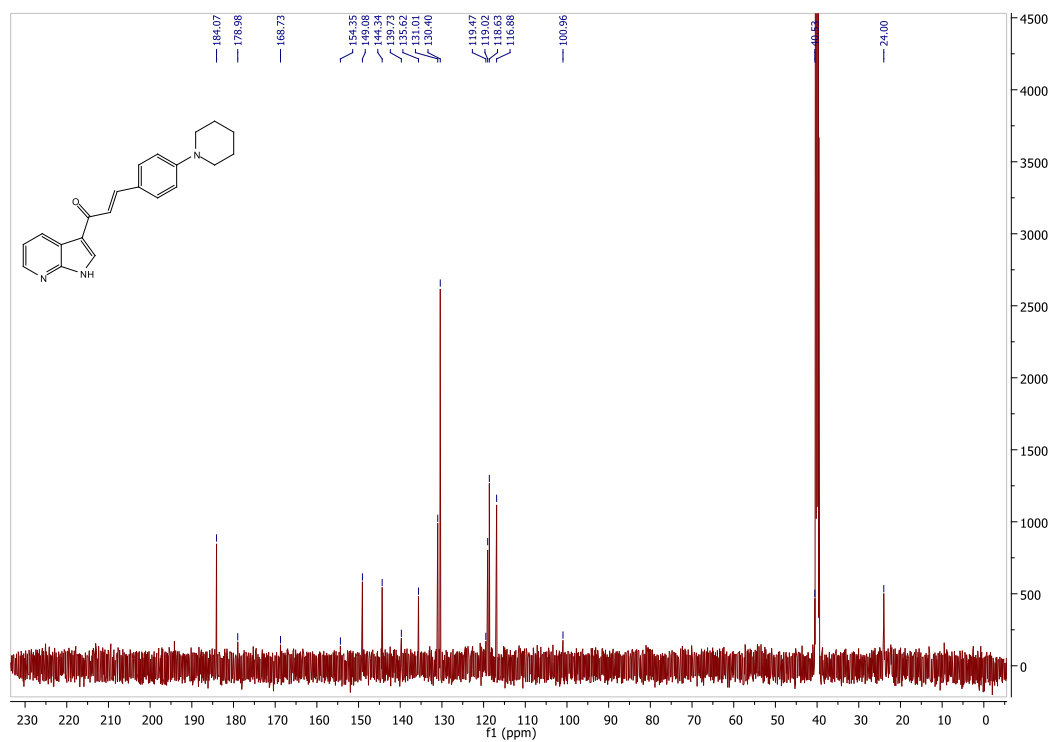
(E)-4-(3-oxo-3-(1H-pyrrolo[2,3-b]pyridin-3-yl)prop-1-en-1-yl)benzoic acid (5e)

^{1}H NMR
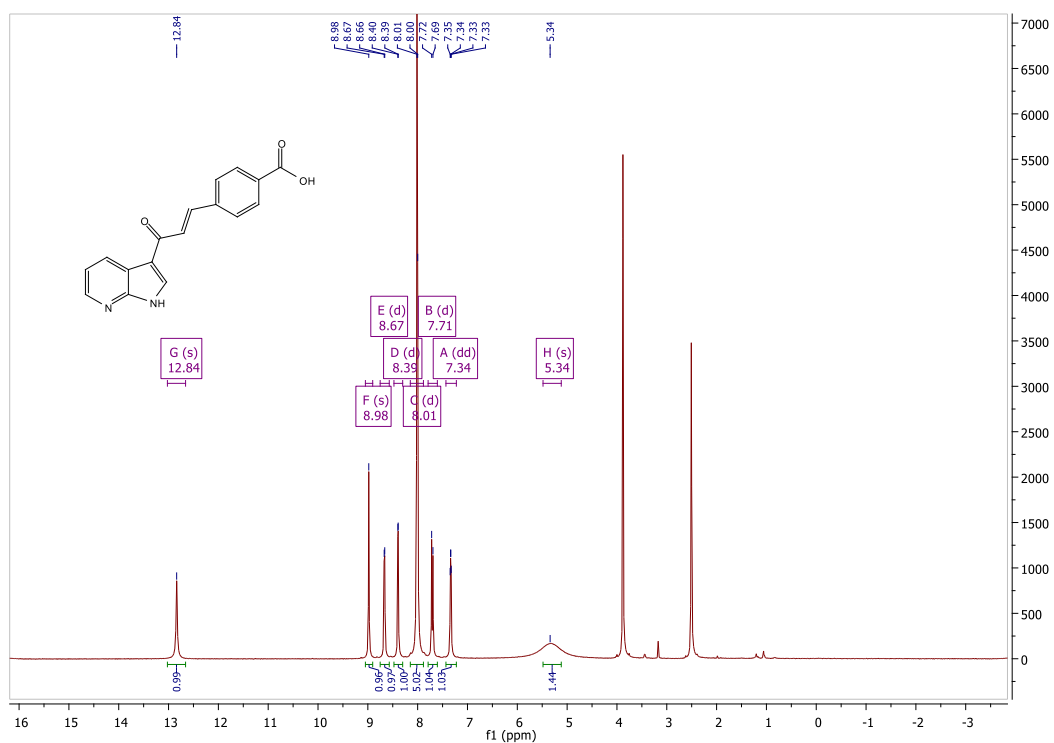
^{13}C NMR
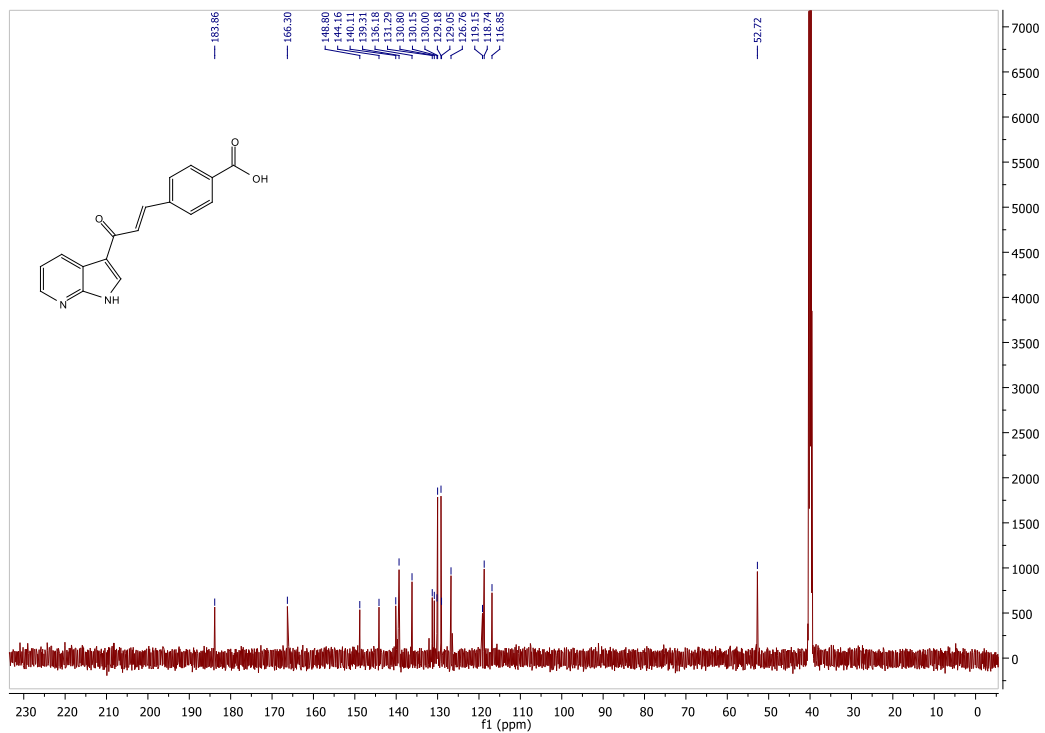
(E)-1-(1H-pyrrolo[2,3-b]pyridin-3-yl)-3-(thiophen-2-yl)prop-2-en-1-one (5f)

^{1}H NMR
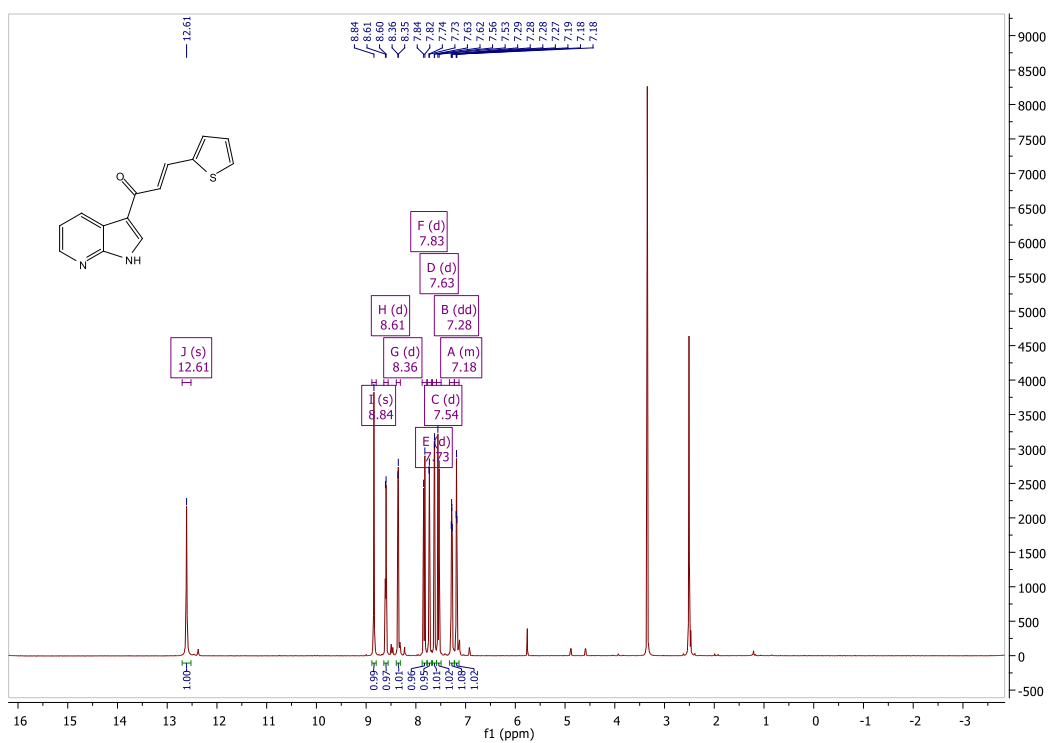
^{13}C NMR
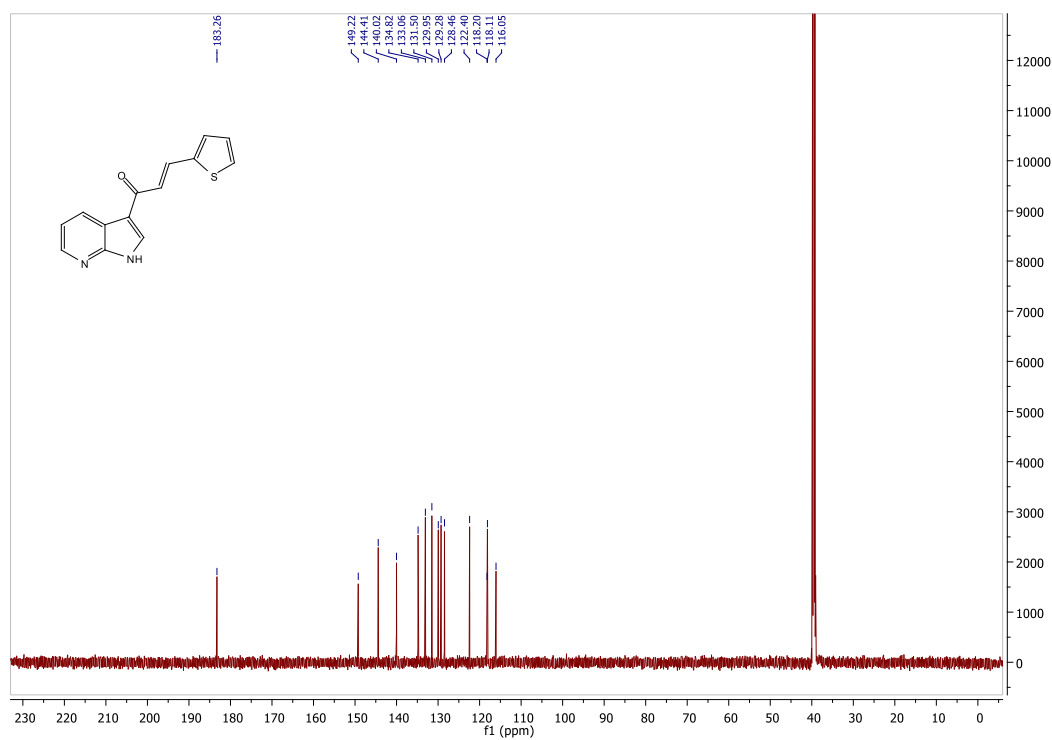
(E)-3-(4-isopropylphenyl)-1-(1H-pyrrolo[2,3-b]pyridin-3-yl)prop-2-en-1-one (5g)

^{1}H NMR
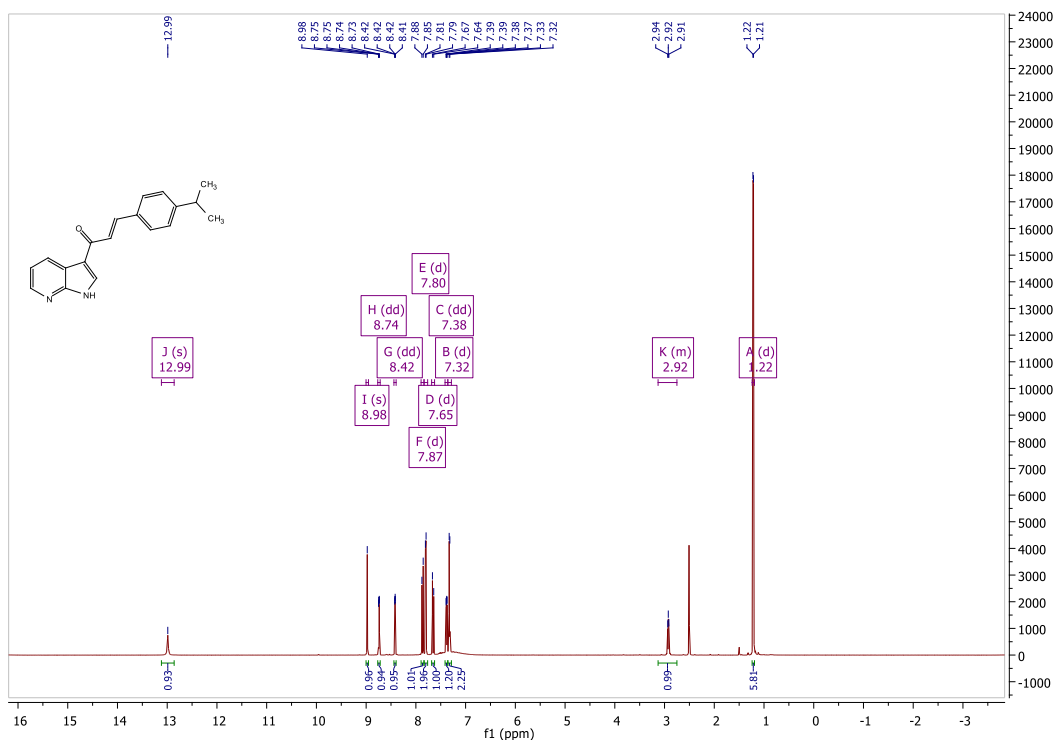
^{13}C NMR
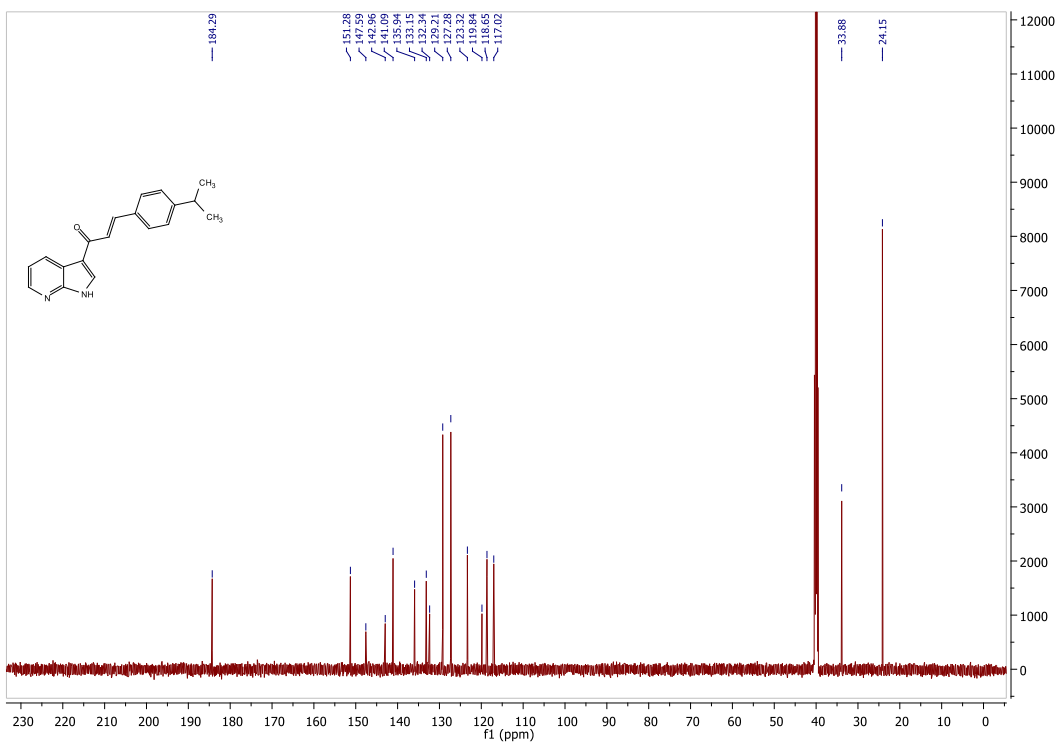
(E)-3-(4-(tert-butyl)phenyl)-1-(1H-pyrrolo[2,3-b]pyridin-3-yl)prop-2-en-1-one (5h)

^{1}H NMR
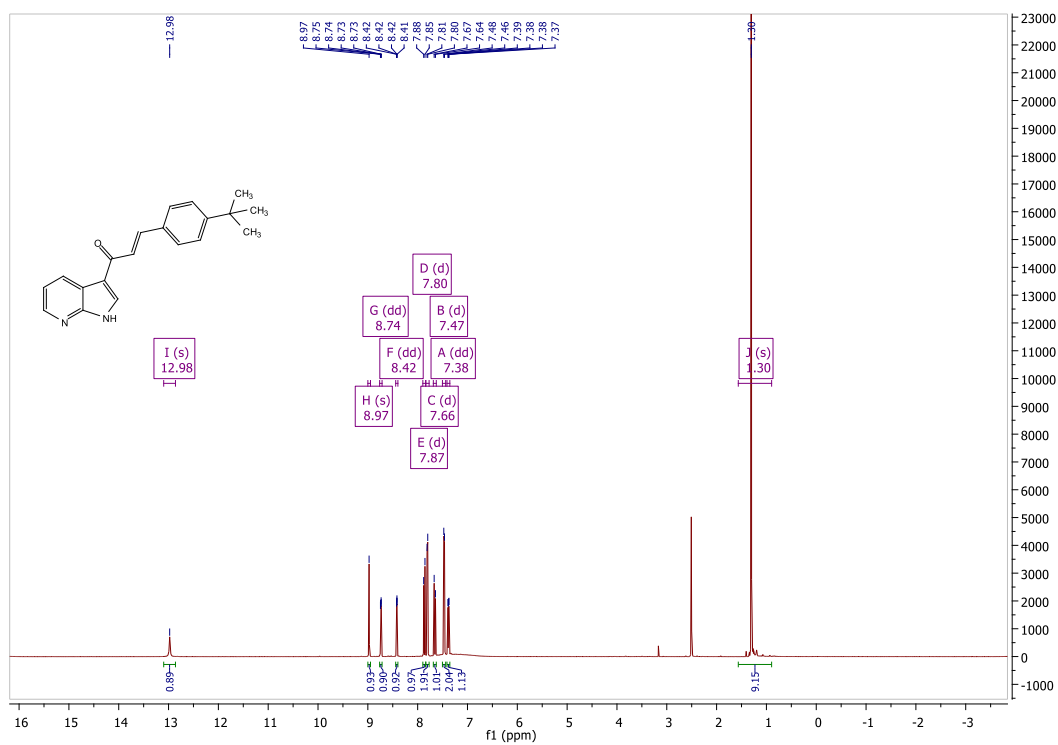
^{13}C NMR
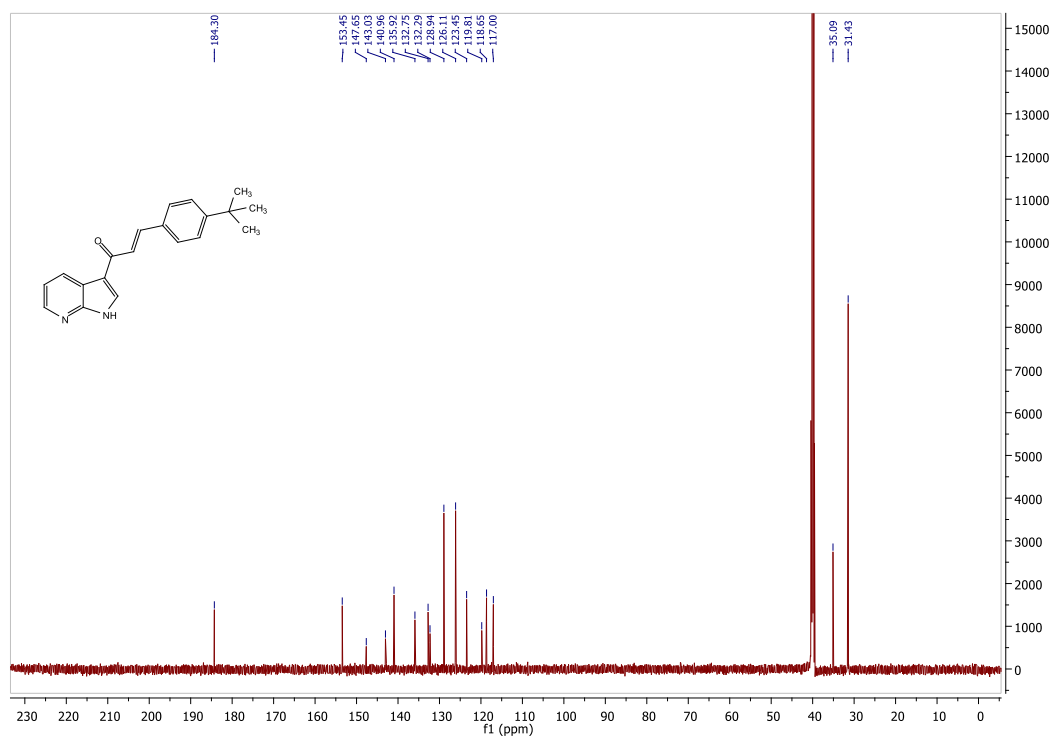
(E)-3-(4-nitrophenyl)-1-(1H-pyrrolo[2,3-b]pyridin-3-yl)prop-2-en-1-one (5i)
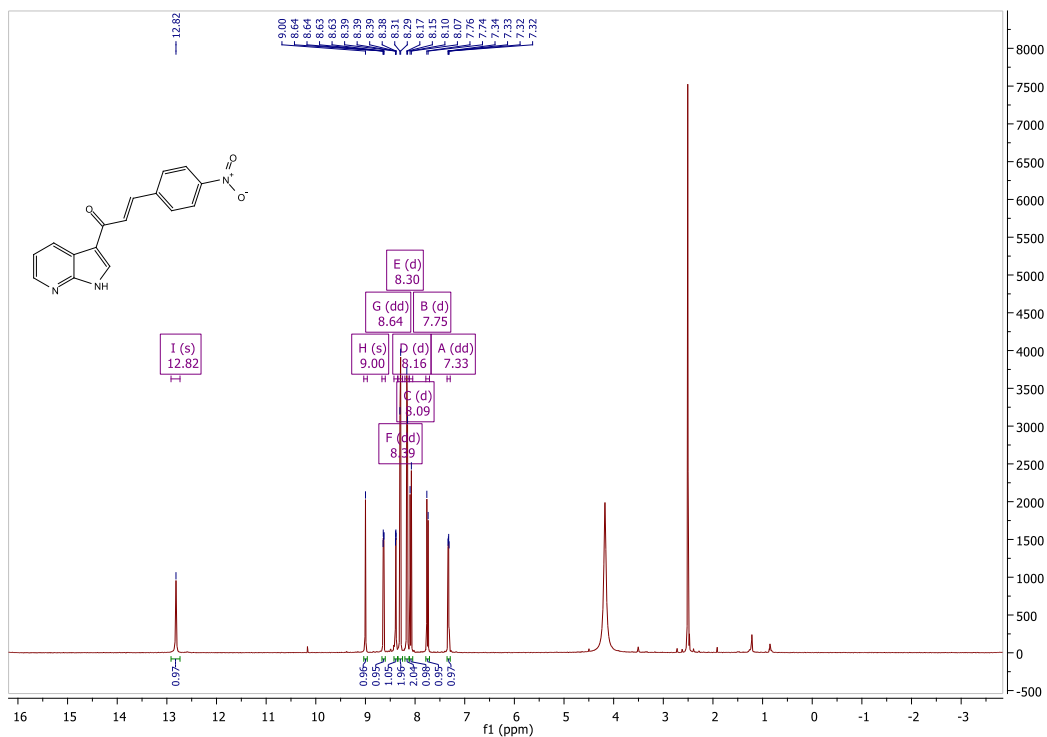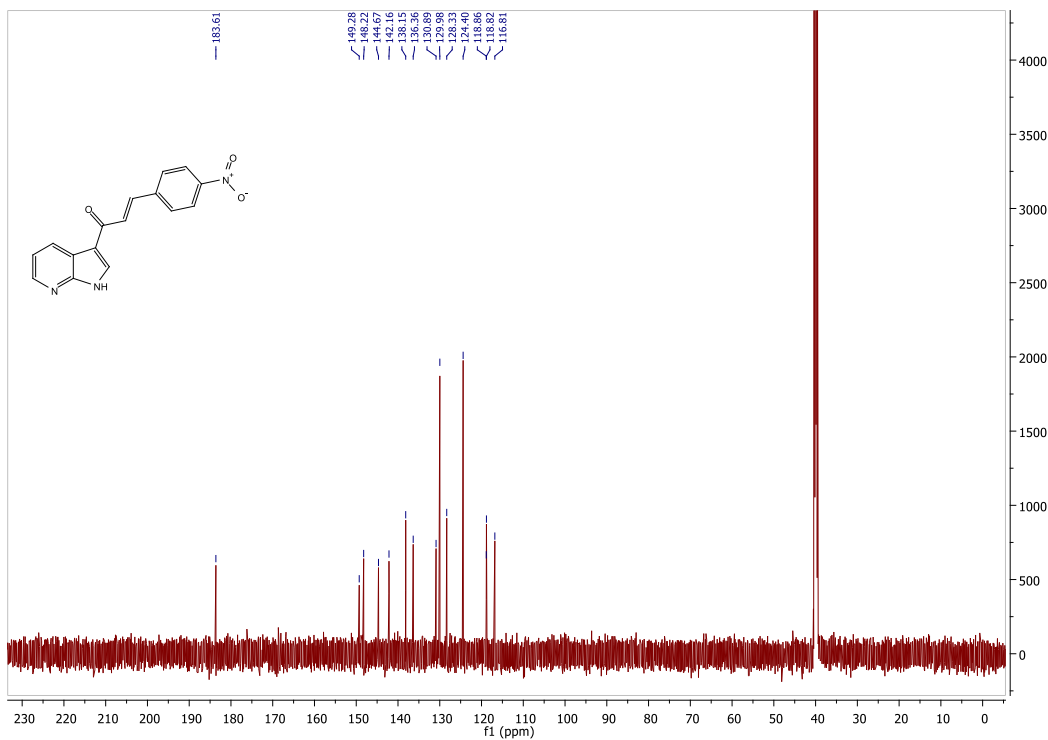
^{1}H NMR

^{13}C NMR

(E)-3-(3-methoxyphenyl)-1-(1H-pyrrolo[2,3-b]pyridin-3-yl)prop-2-en-1-one (5j)

^{1}H NMR
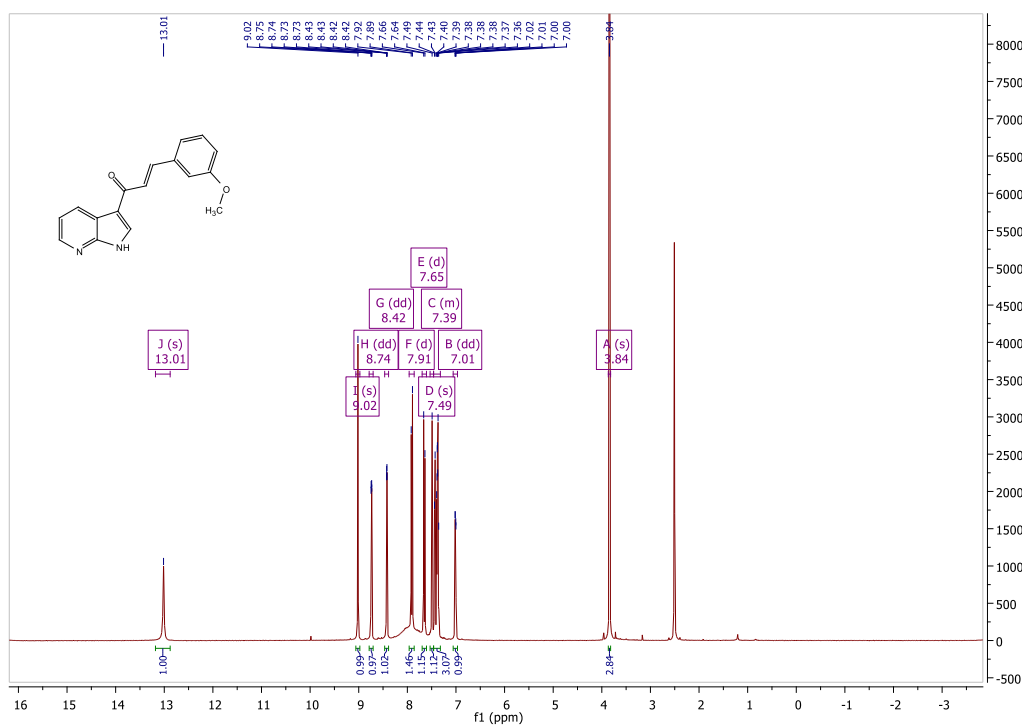
^{13}C NMR
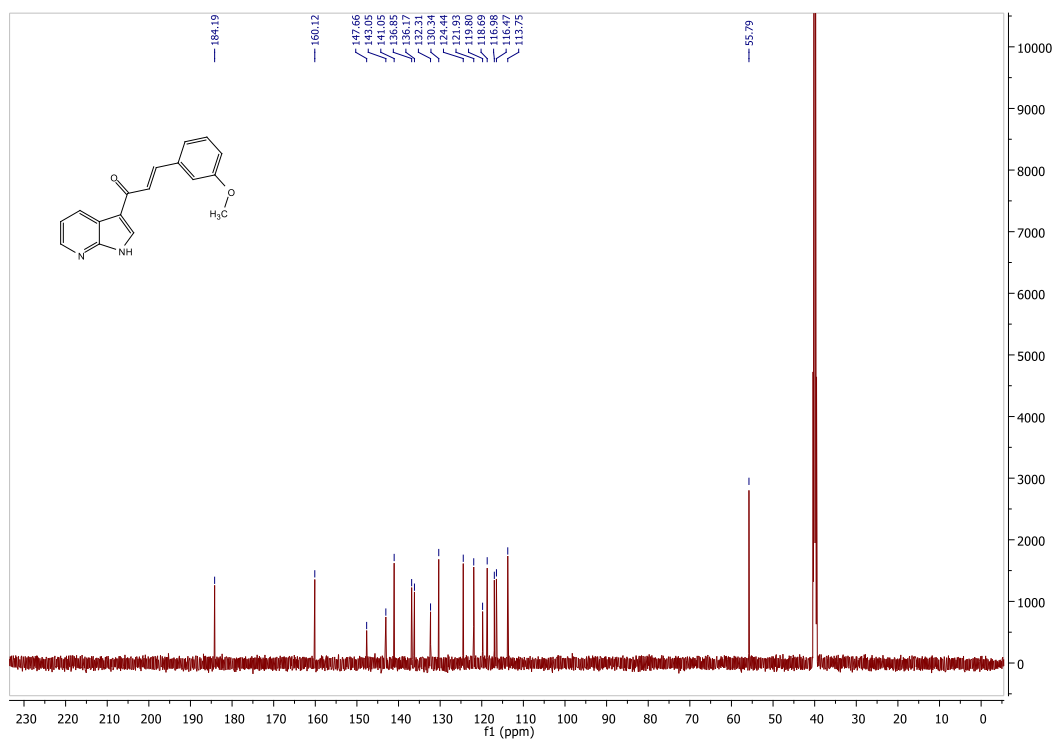
(E)-3-(3,4-dimethoxyphenyl)-1-(1H-pyrrolo[2,3-b]pyridin-3-yl)prop-2-en-1-one (5k)

^{1}H NMR
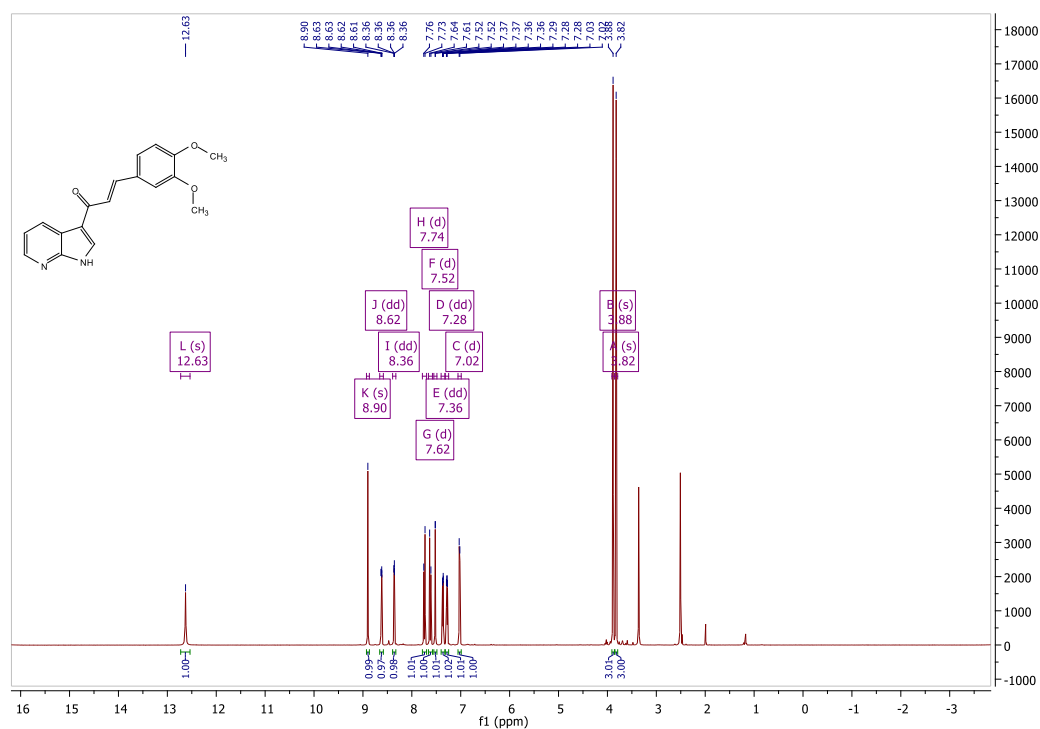
^{13}C NMR
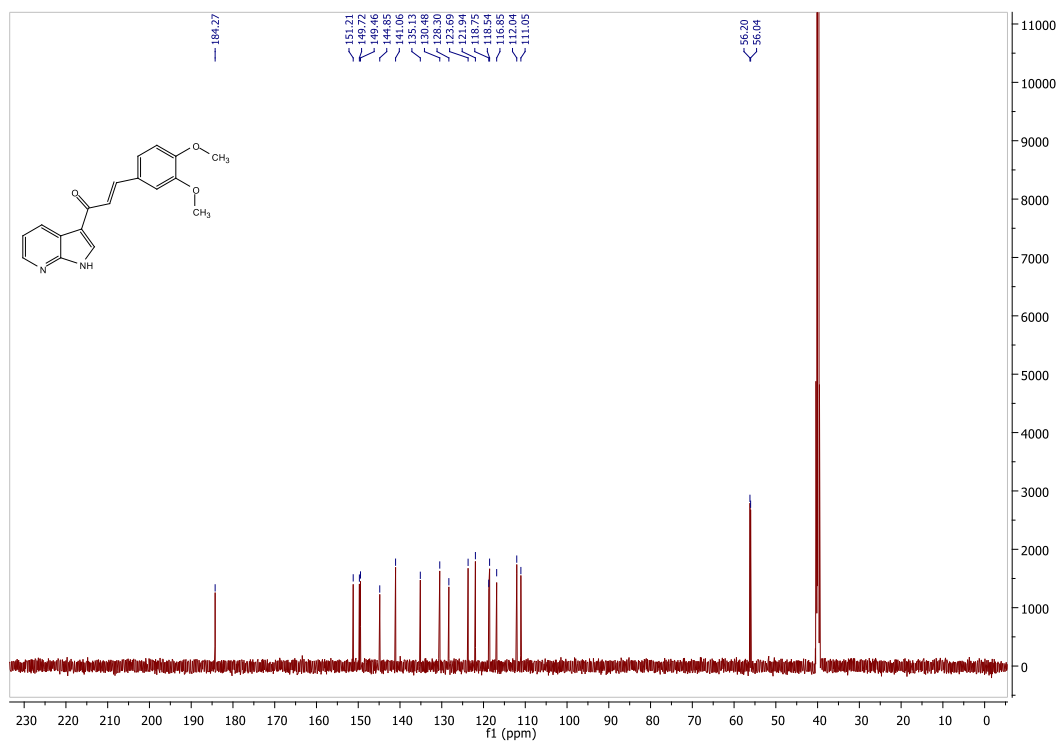
(E)-3-(2-fluorophenyl)-1-(1H-pyrrolo[2,3-b]pyridin-3-yl)prop-2-en-1-one (5I)
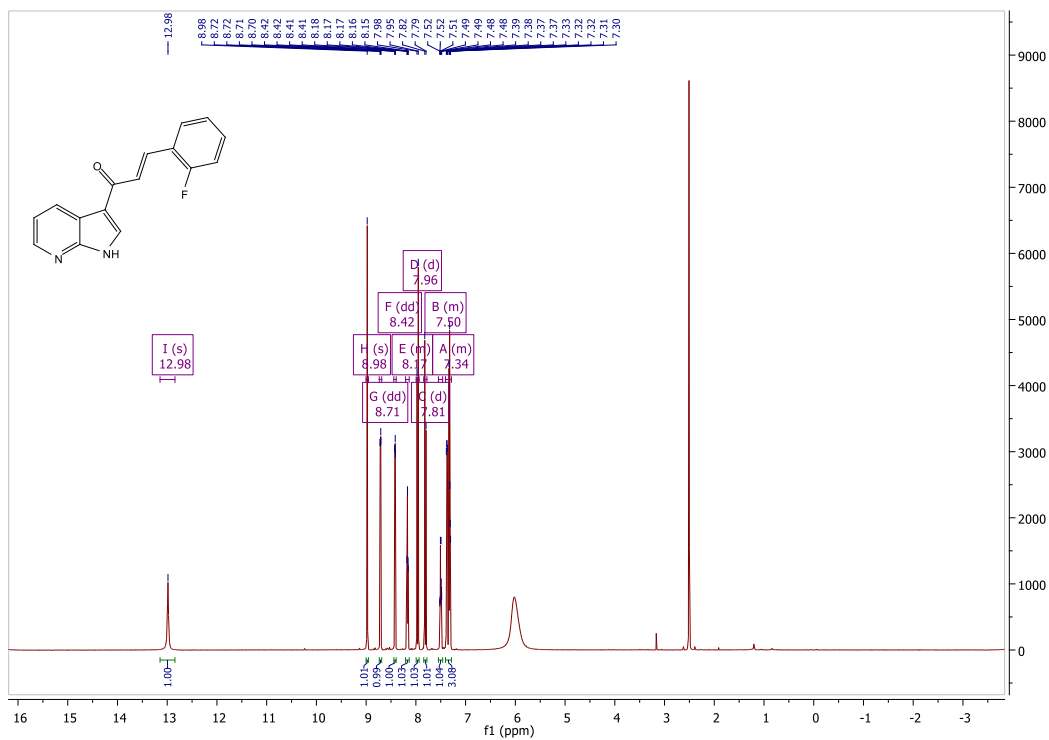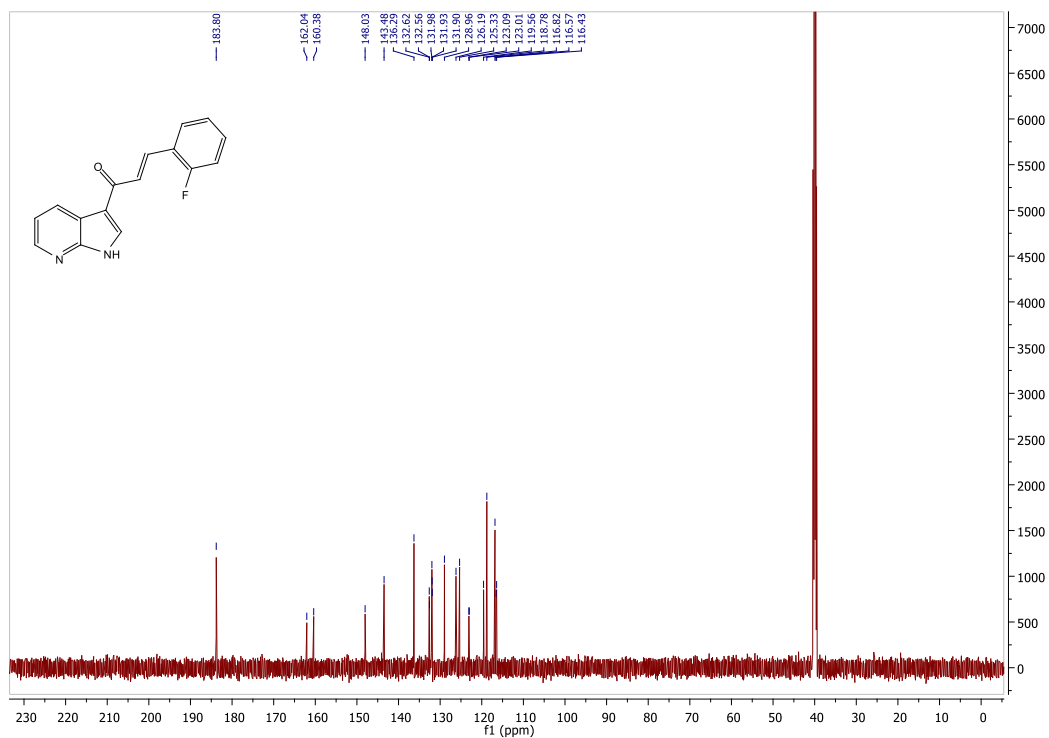
^{1}H NMR

^{13}C NMR

(E)-3-(3-fluorophenyl)-1-(1H-pyrrolo[2,3-b]pyridin-3-yl)prop-2-en-1-one (5m)

^{1}H NMR
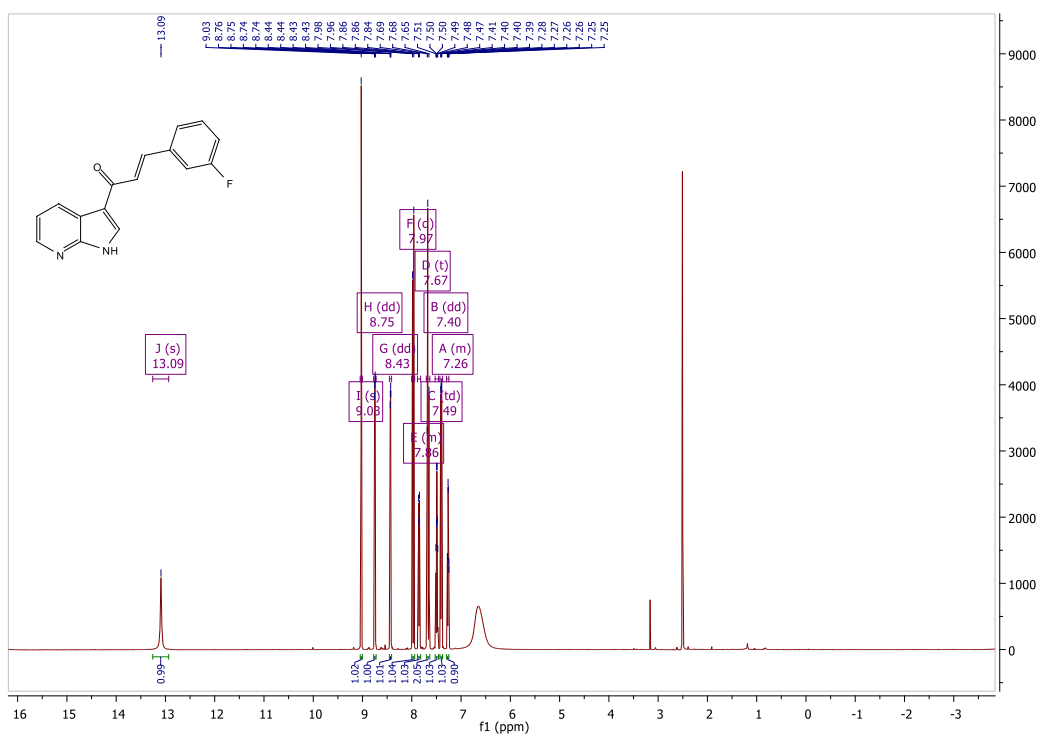
^{13}C NMR
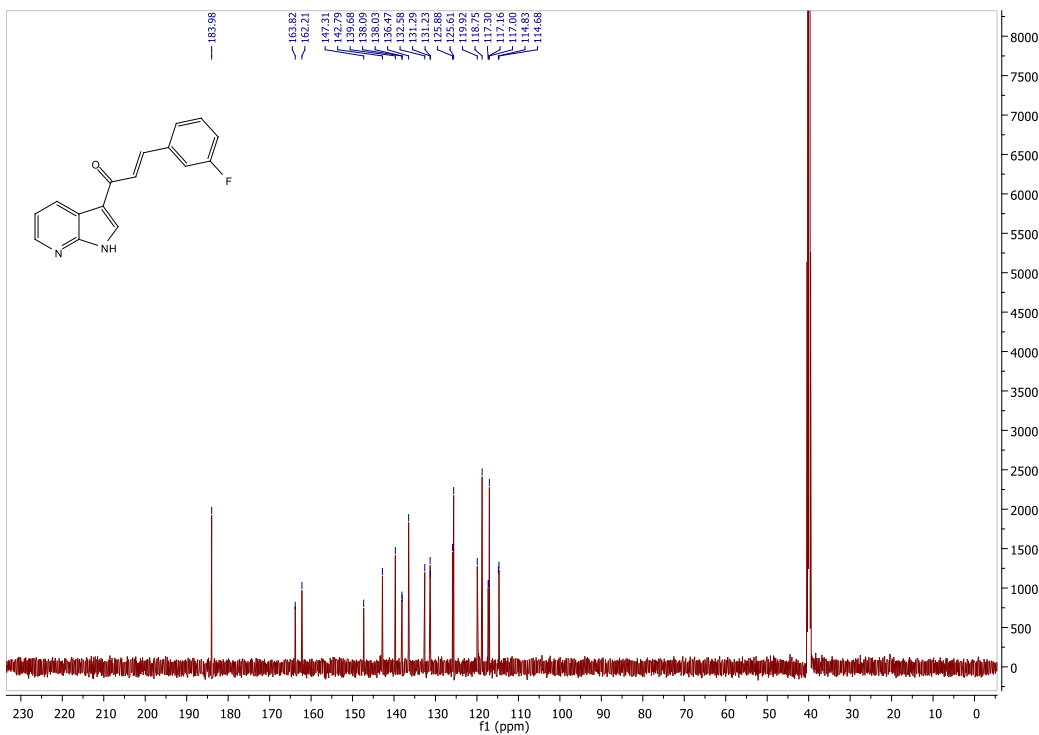
(E)-3-(4-fluorophenyl)-1-(1H-pyrrolo[2,3-b]pyridin-3-yl)prop-2-en-1-one (5n)

^{1}H NMR
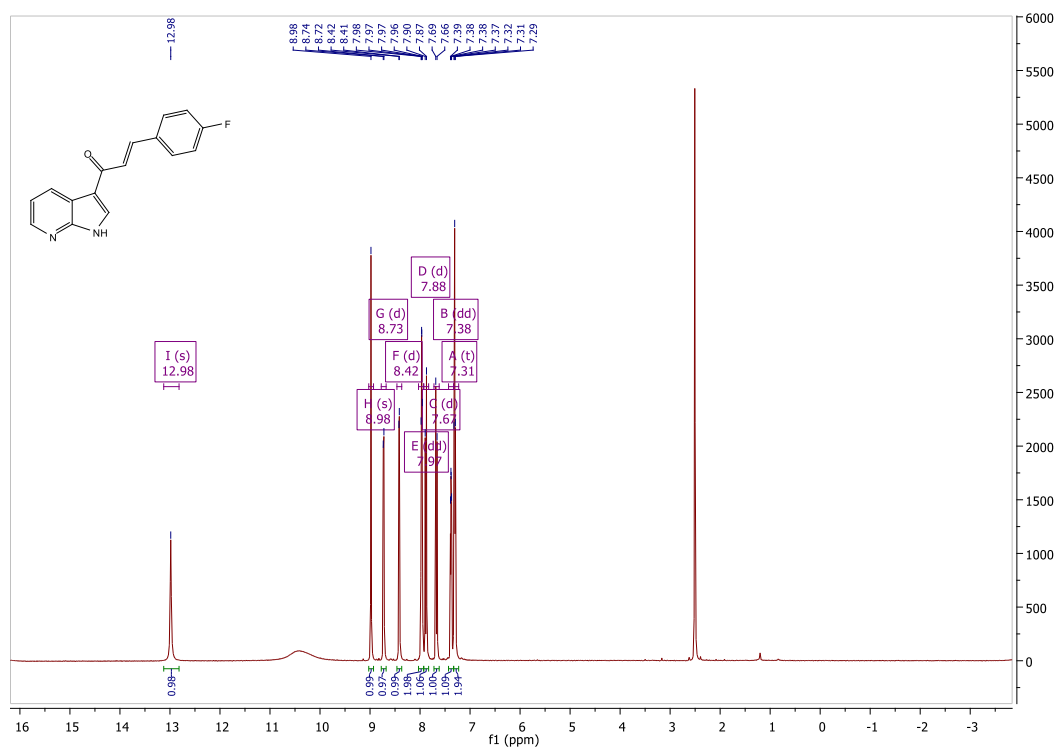
^{13}C NMR
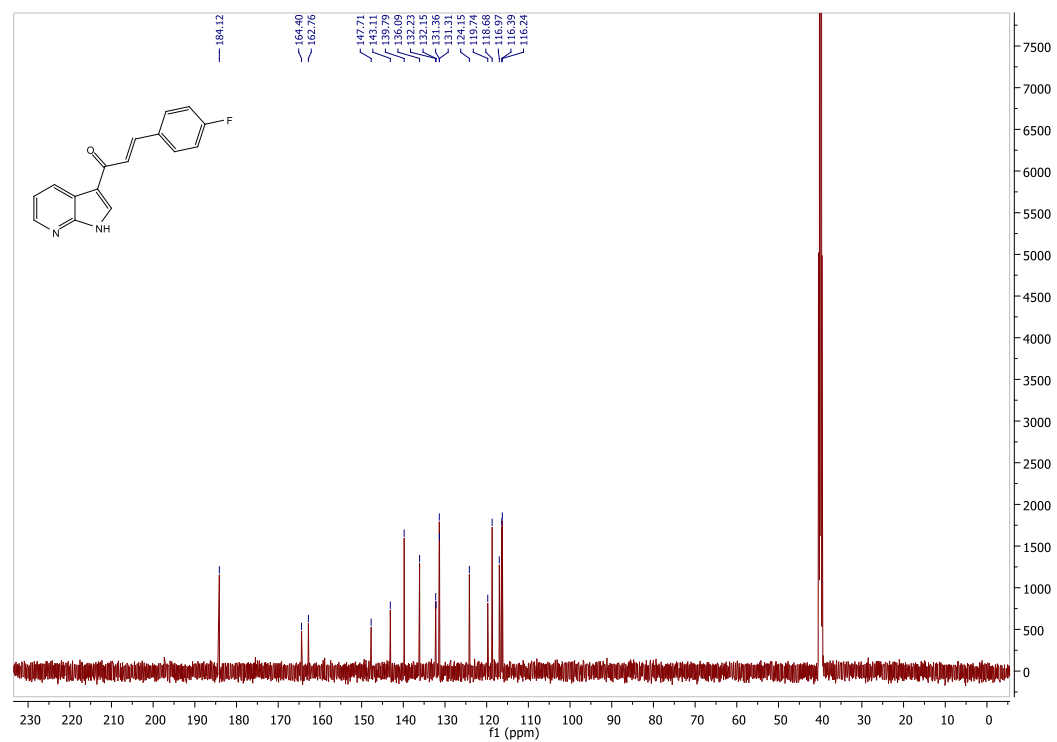
(E)-3-(4-chlorophenyl)-1-(1H-pyrrolo[2,3-b]pyridin-3-yl)prop-2-en-1-one (5o)

^{1}H NMR
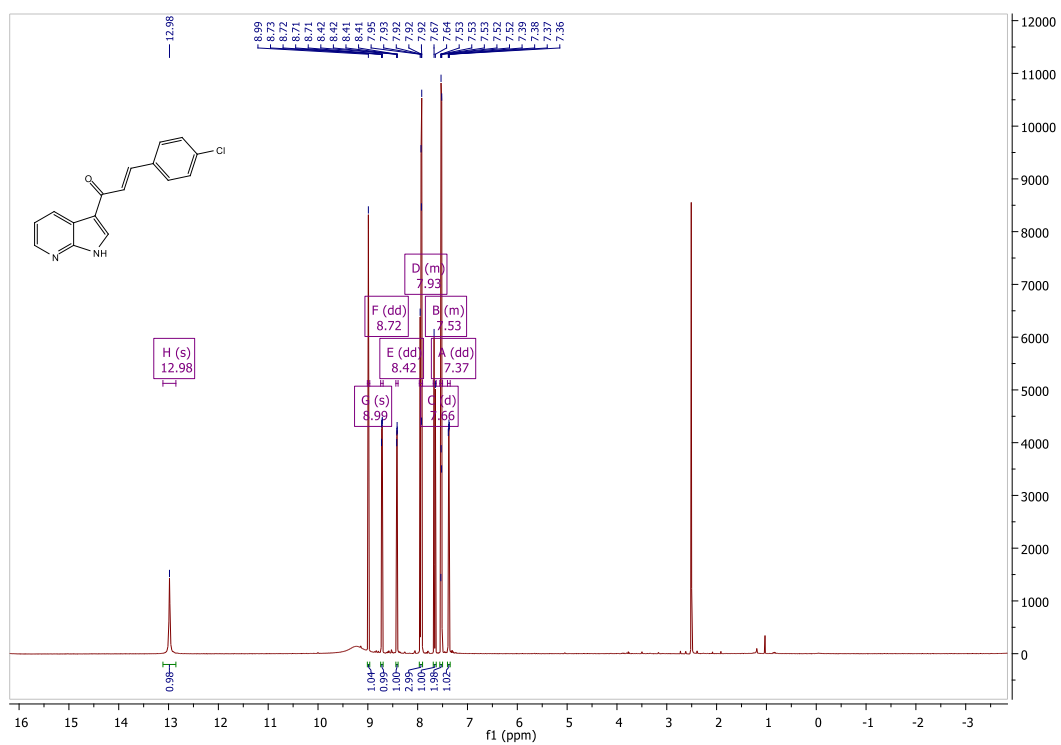
^{13}C NMR
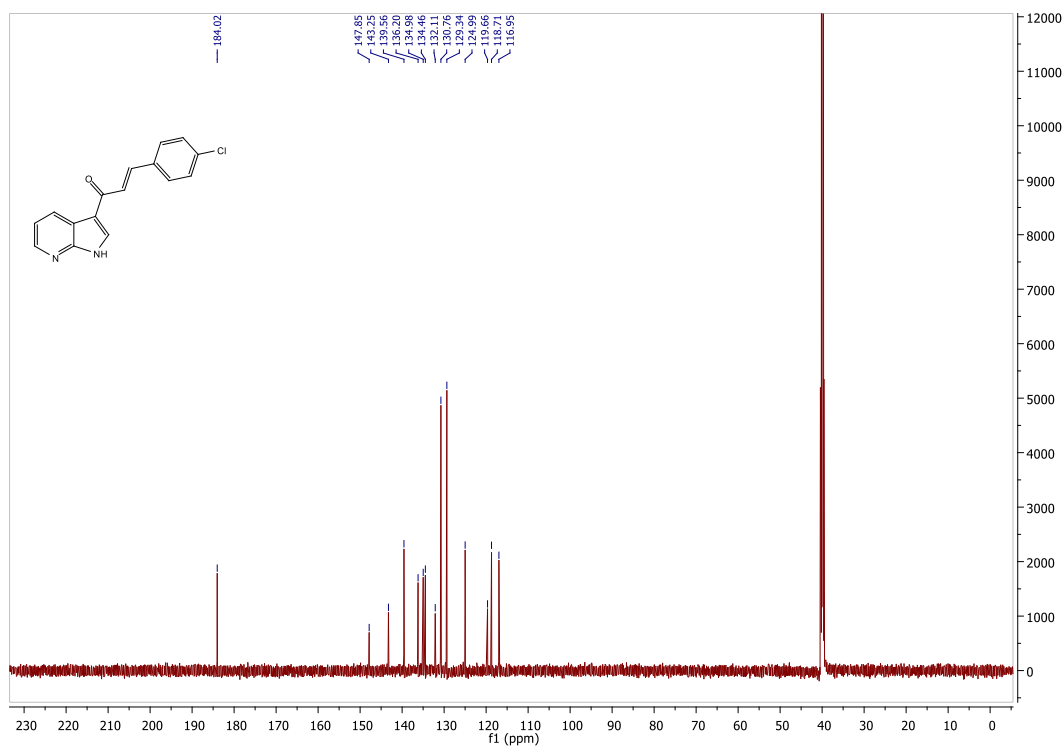
(E)-3-(4-bromophenyl)-1-(1H-pyrrolo[2,3-b]pyridin-3-yl)prop-2-en-1-one (5p)

¹H NMR
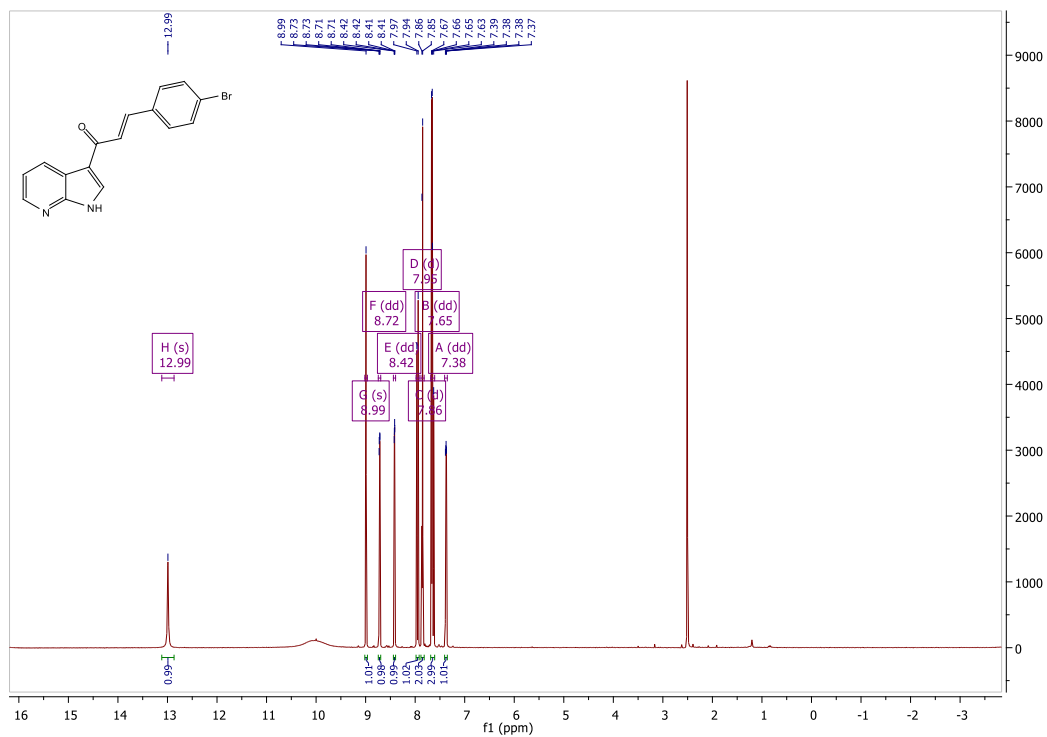
¹³C NMR
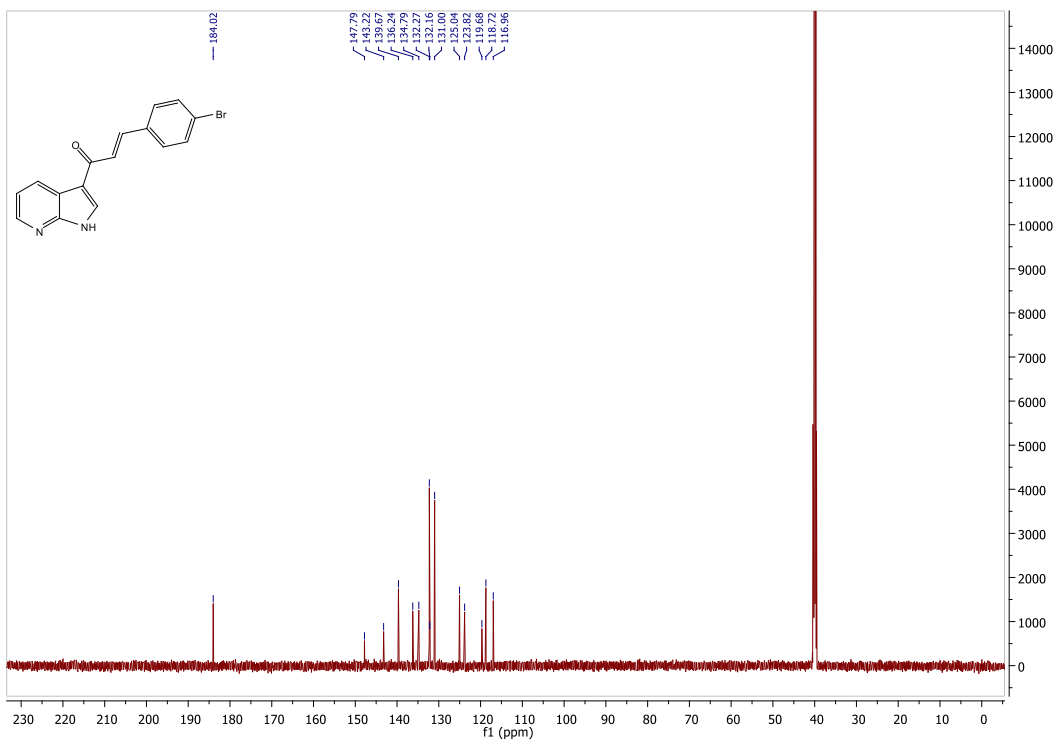
(E)-3-(4-hydroxyphenyl)-1-(1H-pyrrolo[2,3-b]pyridin-3-yl)prop-2-en-1-one (5q)

^{1}H NMR
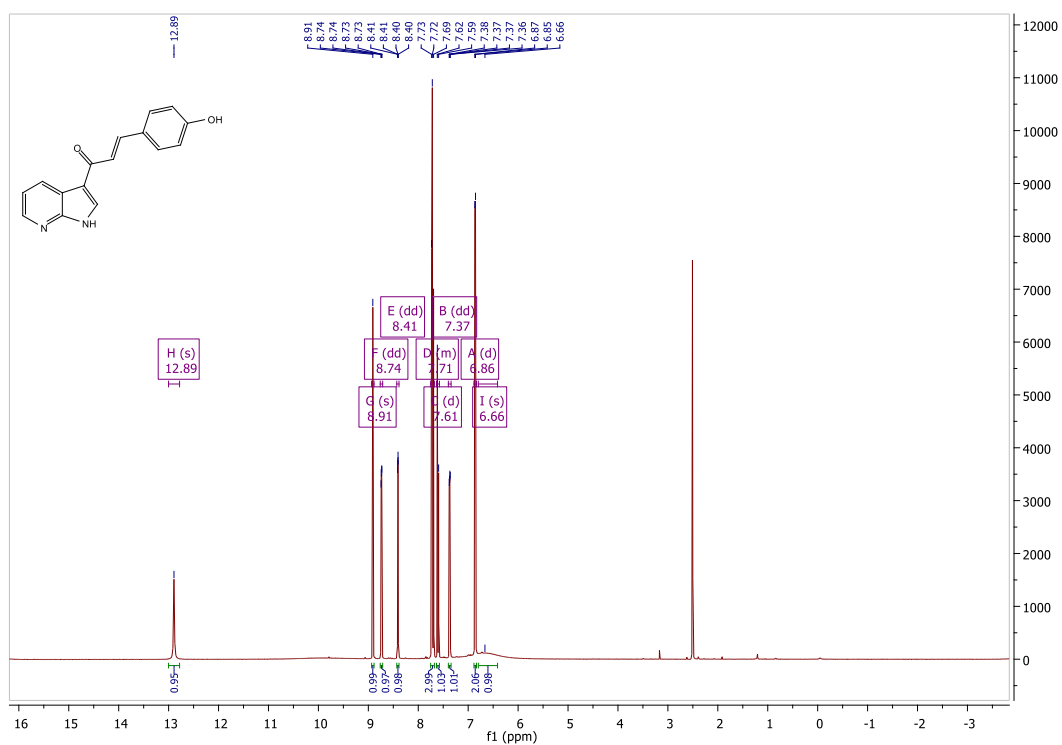
^{13}C NMR
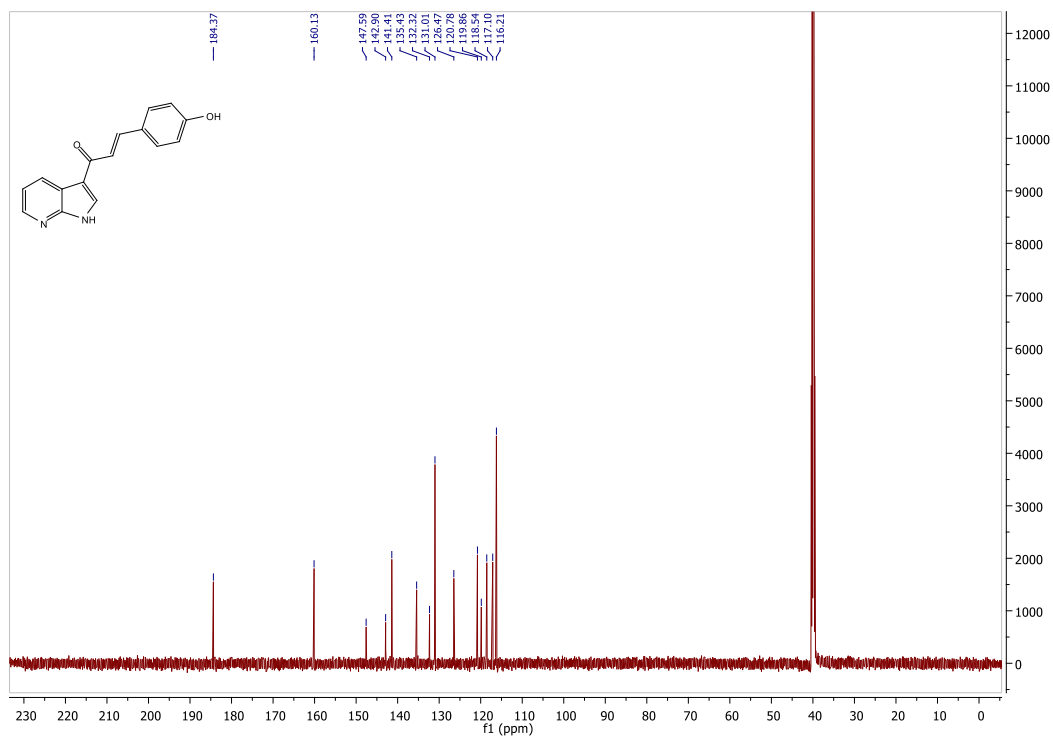
(E)-3-(4-methoxyphenyl)-1-(1H-pyrrolo[2,3-b]pyridin-3-yl)prop-2-en-1-one (5r)

¹H NMR
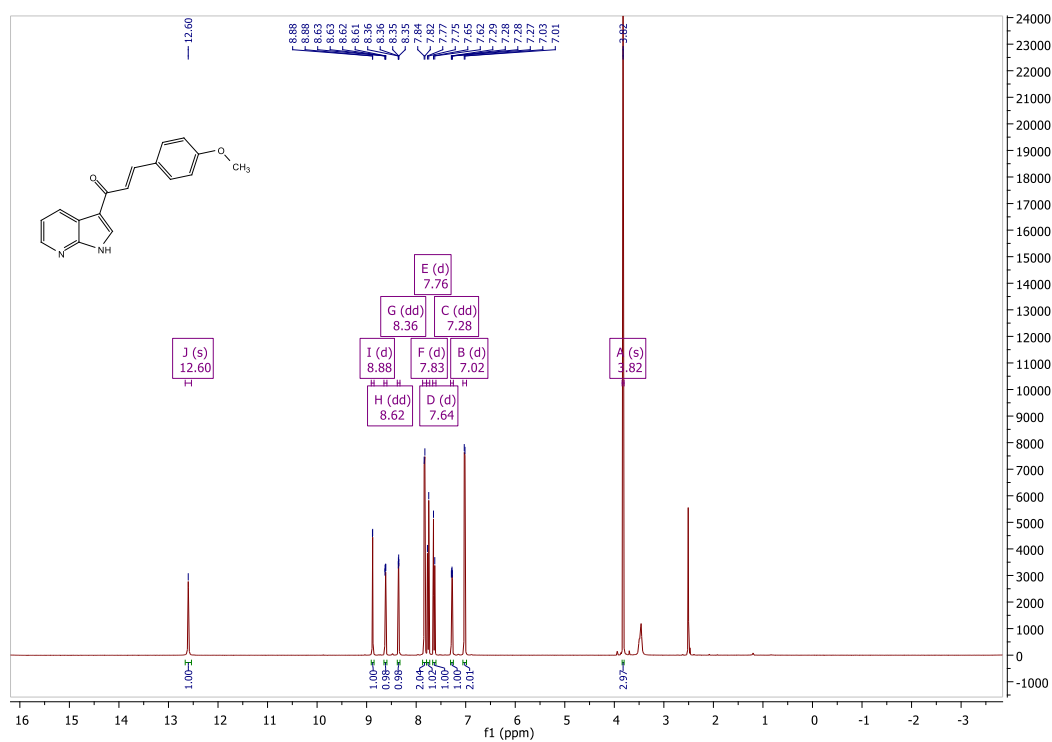
¹³C NMR
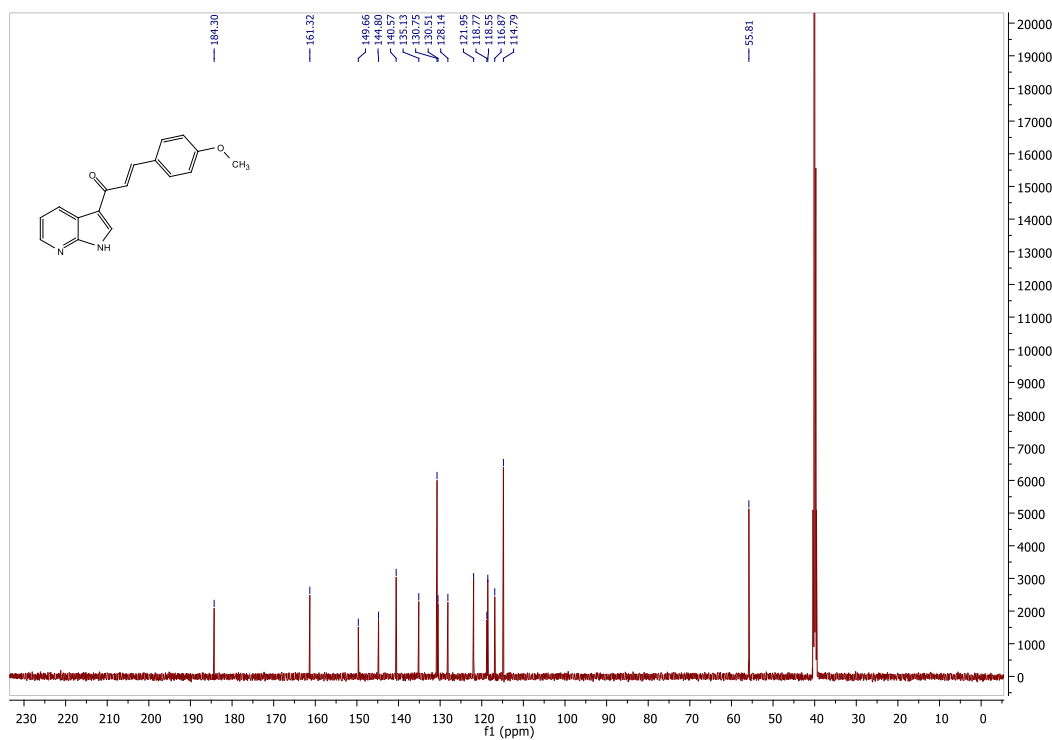
(2E,5E)-6-phenyl-1-(1H-pyrrolo[2,3-b]pyridin-3-yl)hexa-2,5-dien-1-one (5s)

^{1}H NMR

^{13}C NMR

171
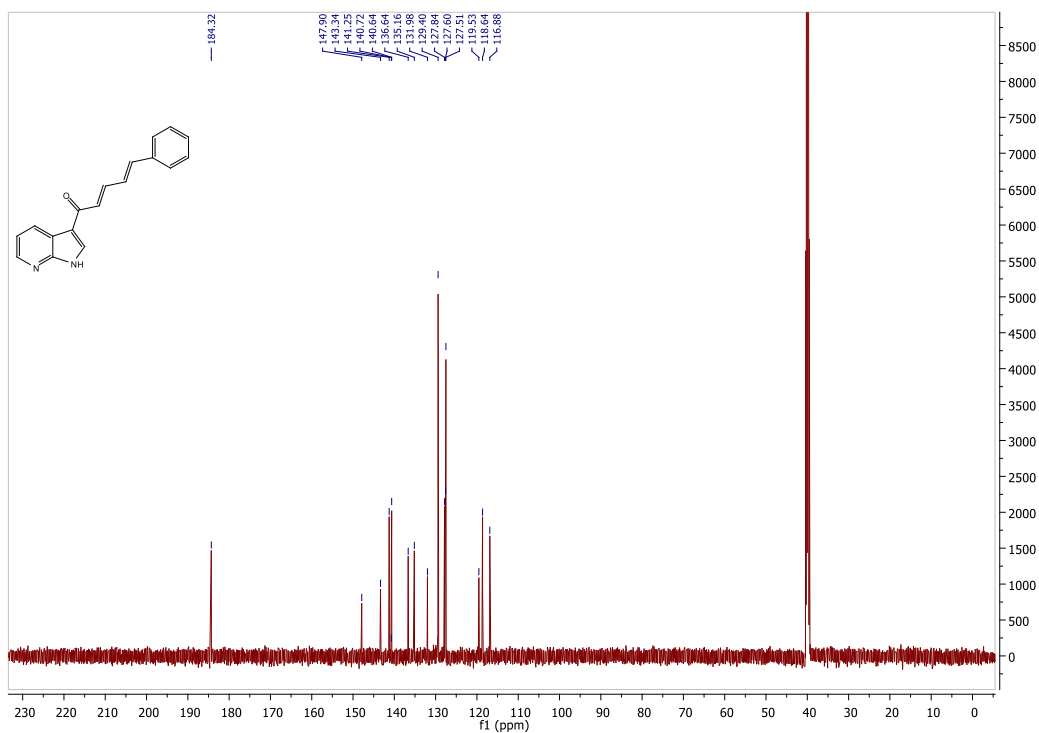
(E)-1-(1H-pyrrolo[2,3-b]pyridin-3-yl)-3-(p-tolyl)prop-2-en-1-one (5t)

^{1}H NMR

^{13}C NMR

172
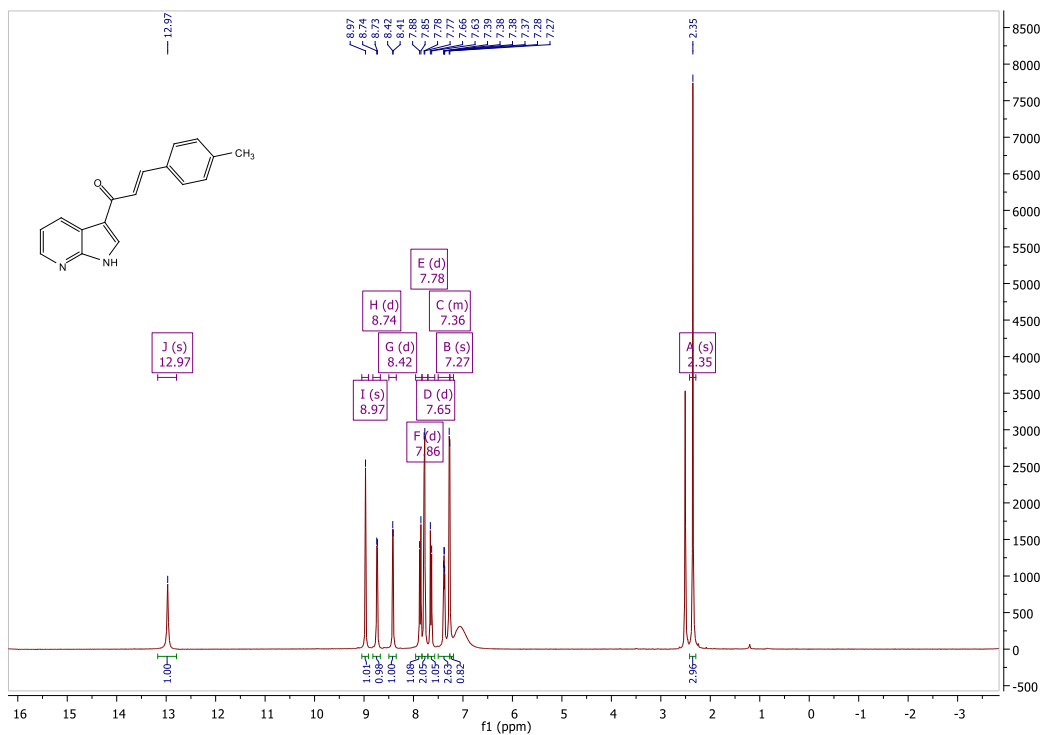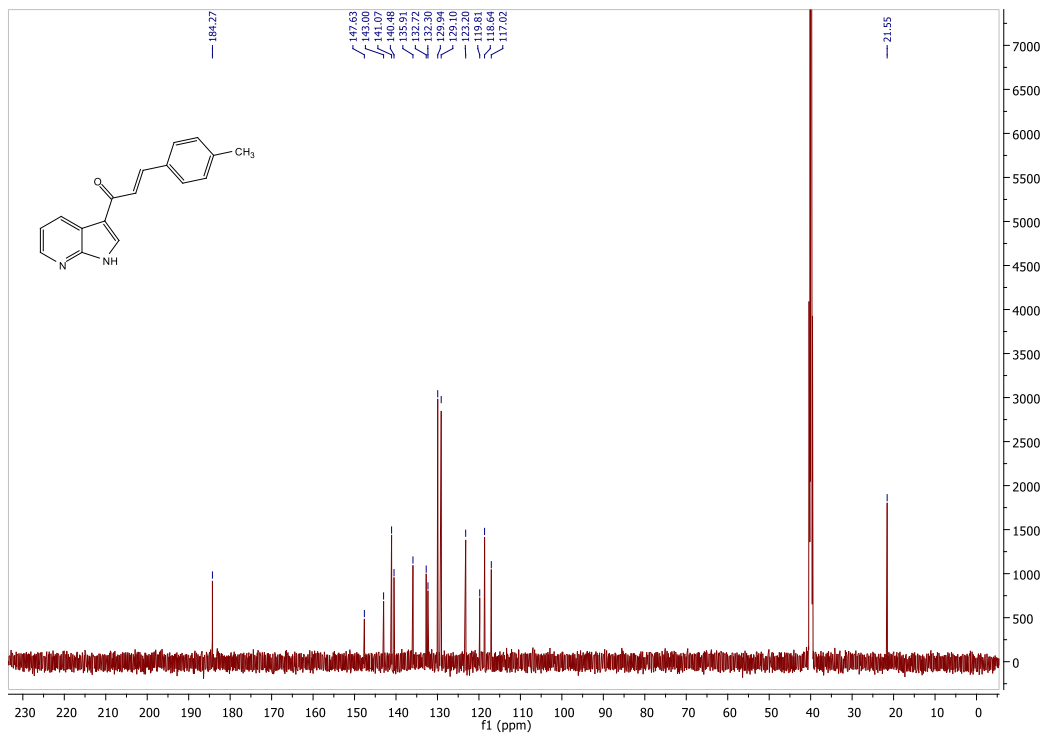
(E)-3-(5-nitrofuran-2-yl)-1-(1H-pyrrolo[2,3-b]pyridin-3-yl)prop-2-en-1-one (5u)

^{1}H NMR
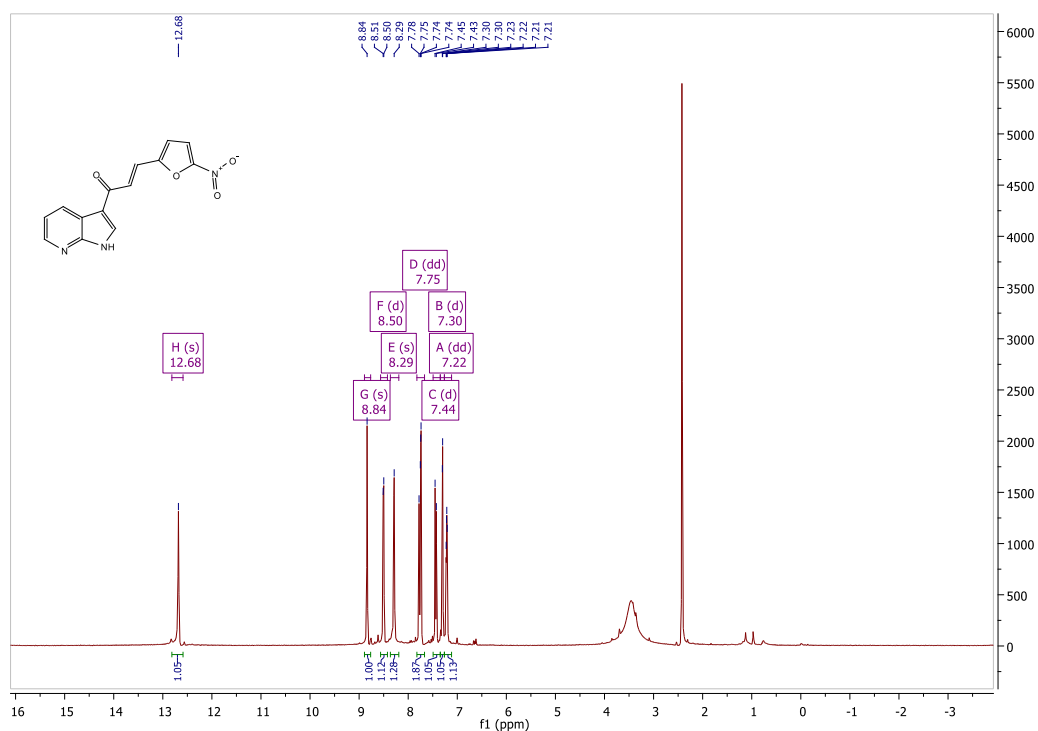
^{13}C NMR
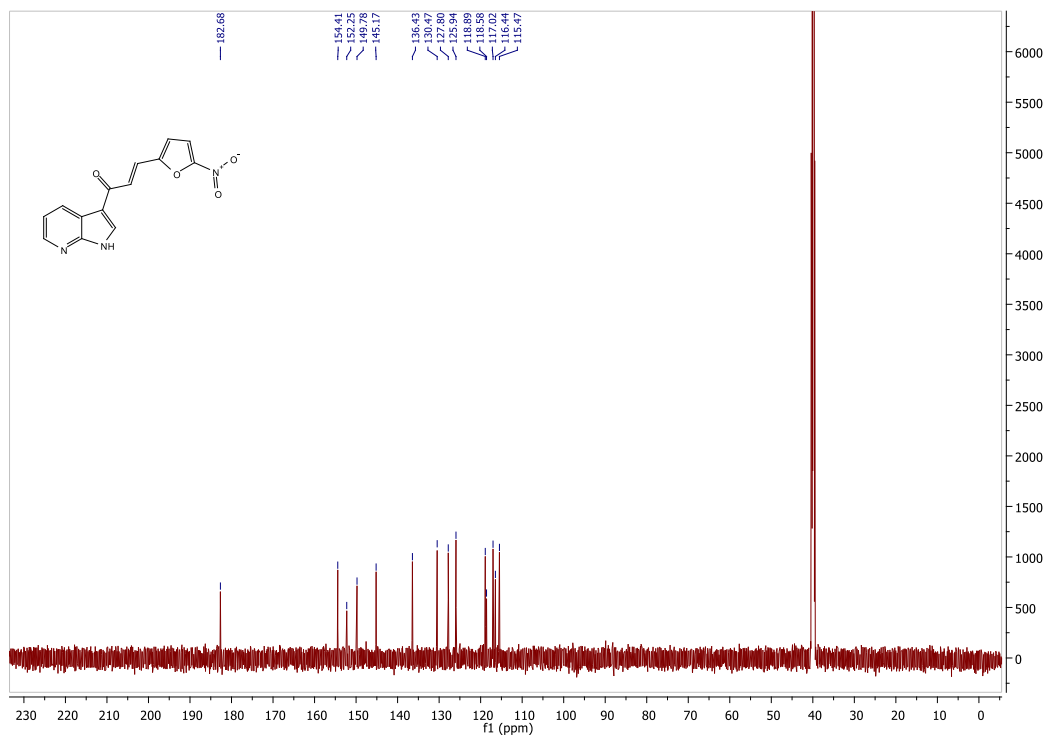
(E)-3-(3-nitrophenyl)-1-(1H-pyrrolo[2,3-b]pyridin-3-yl)prop-2-en-1-one (5v)

^{1}H NMR
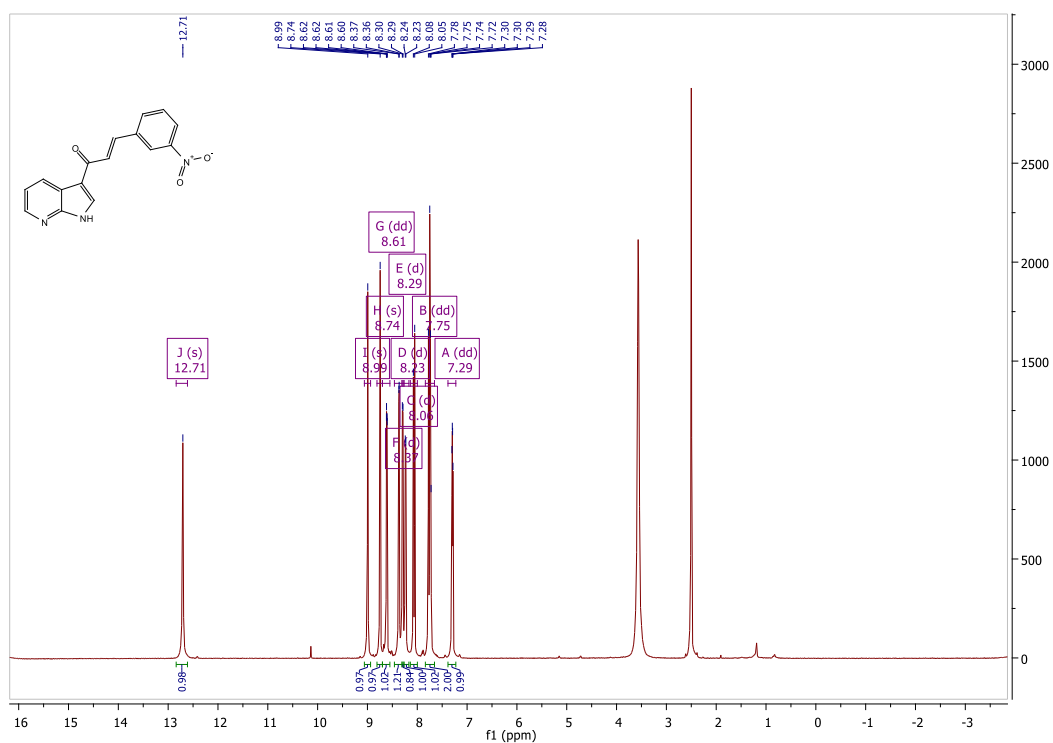
^{13}C NMR
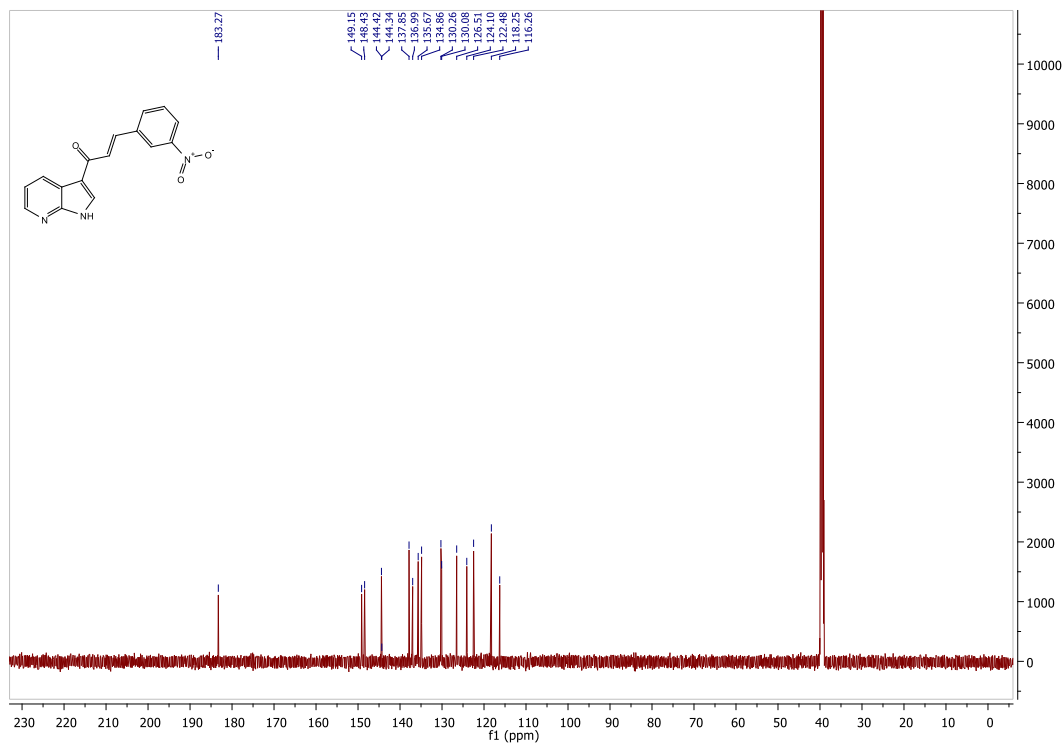
(E)-3-(2-nitrophenyl)-1-(1H-pyrrolo[2,3-b]pyridin-3-yl)prop-2-en-1-one (5w)

^{1}H NMR
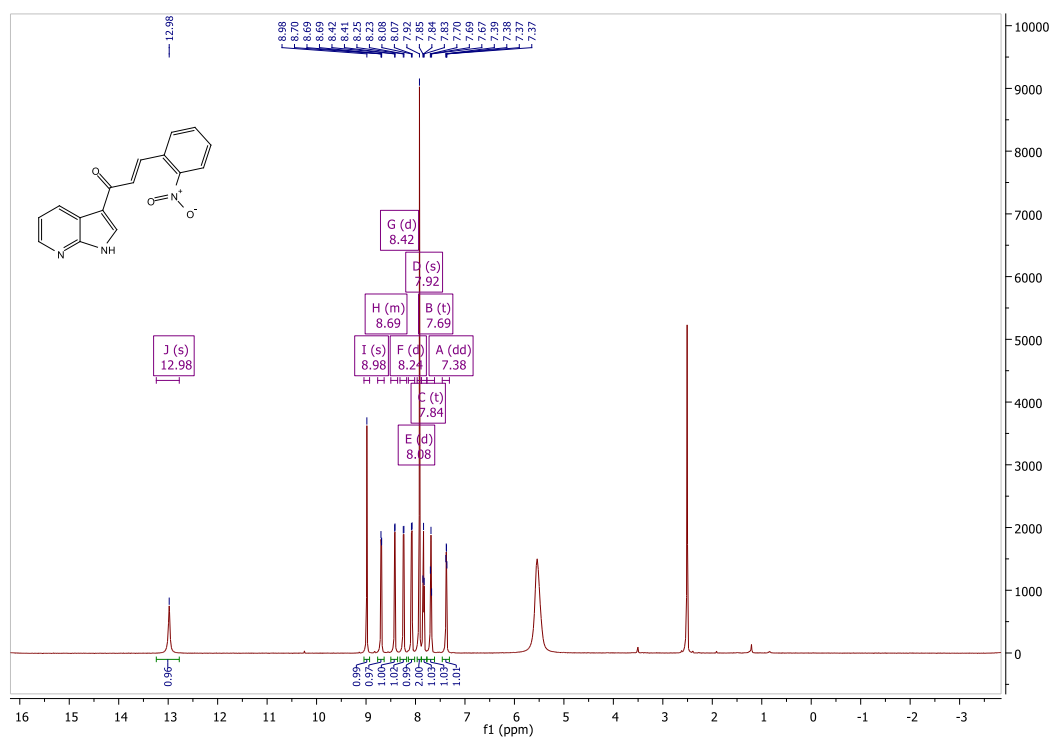
^{13}C NMR
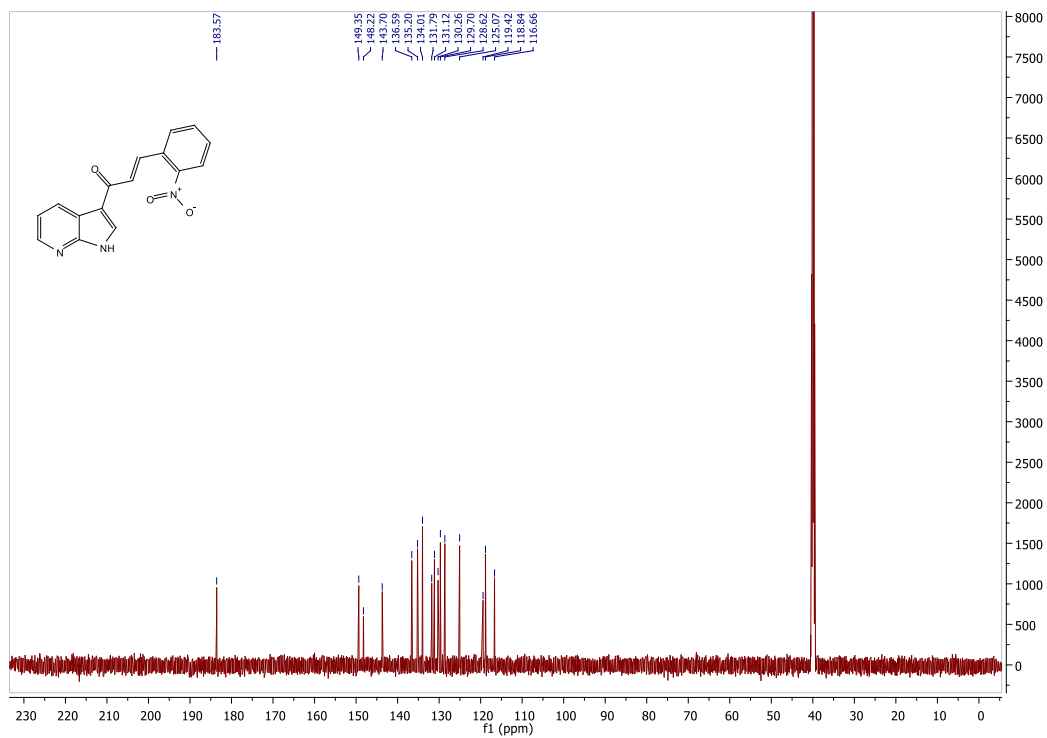
1.6. Molecular Docking

Docking was done using Glide Ligand Docking as implemented in Maestro in the Schrödinger package. Crystal structure of DprE1 enzyme (PDB code: 4KW5) was obtained from RSC protein data bank (PDB). Enzyme refinement and docking protocol are as reported by Gawad and Bonde (2018).

APPENDIX C:
SUPPORTING DATA FOR CHAPTER 5

^{1}H NMR, ^{13}C NMR, MS and HPLC

Malikotsi A Qhobosheane[1], Richard M. Beteck[1], Blandine Baratte[2,3], Thomas Robert[2,3], Sandrine Ruchaud[2], Stéphane Bach[1,2,3], Lesetja J. Legoabe[1]*

[1] *Centre of Excellence for Pharmaceutical Sciences, North-West University, Private Bag X6001, Potchefstroom 2520, South Africa*

[2] *Sorbonne Université, CNRS, UMR8227, Integrative Biology of Marine Models Laboratory (LBI2M), Station Biologique de Roscoff, 29680 Roscoff, France*

[3] *Sorbonne Université, CNRS, FR2424, Plateforme de criblage KISSf (Kinase Inhibitor Specialized Screening facility), Station Biologique de Roscoff, 29680 Roscoff Cedex, France*
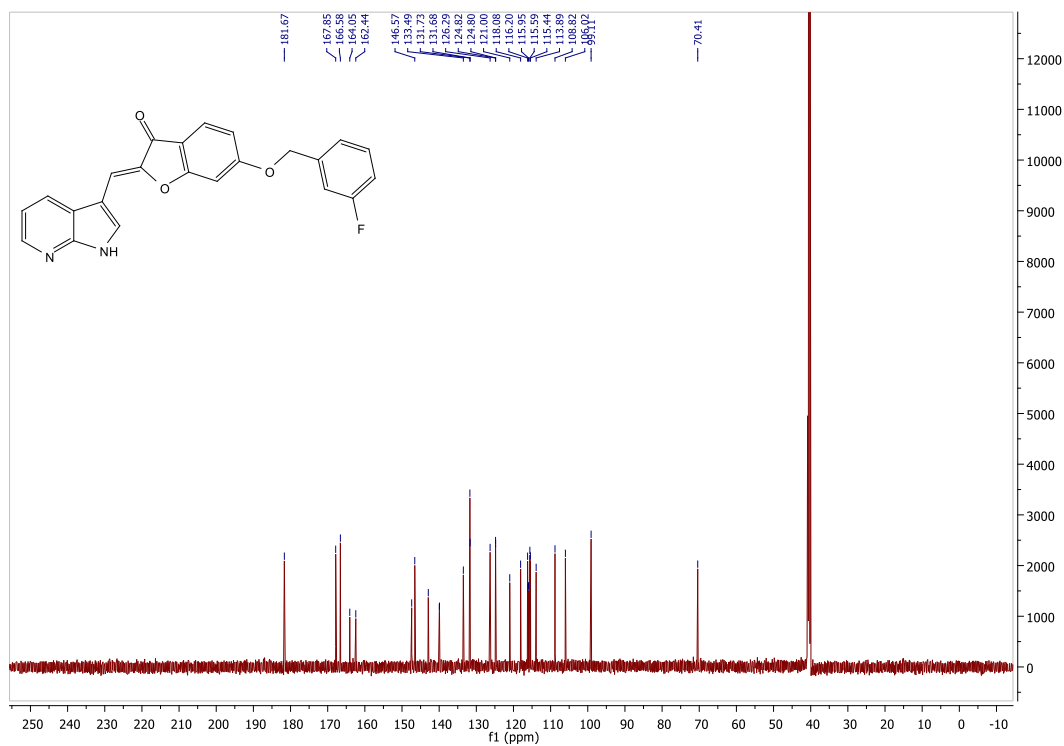
(2*Z*)-6-(benzyloxy)-2-[(1*H*-pyrrolo[2,3-*b*]pyridin-3-yl)methylidene]-1-benzofuran-3(2*H*)-one (7a)

¹HNMR

¹³CNMR

MS
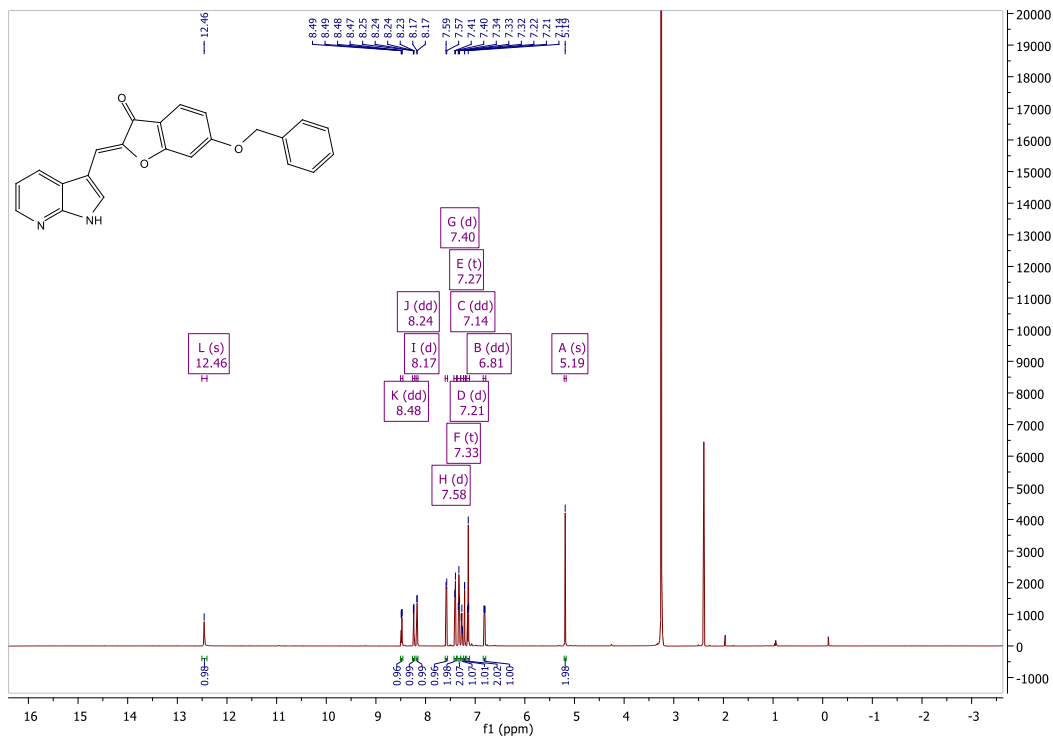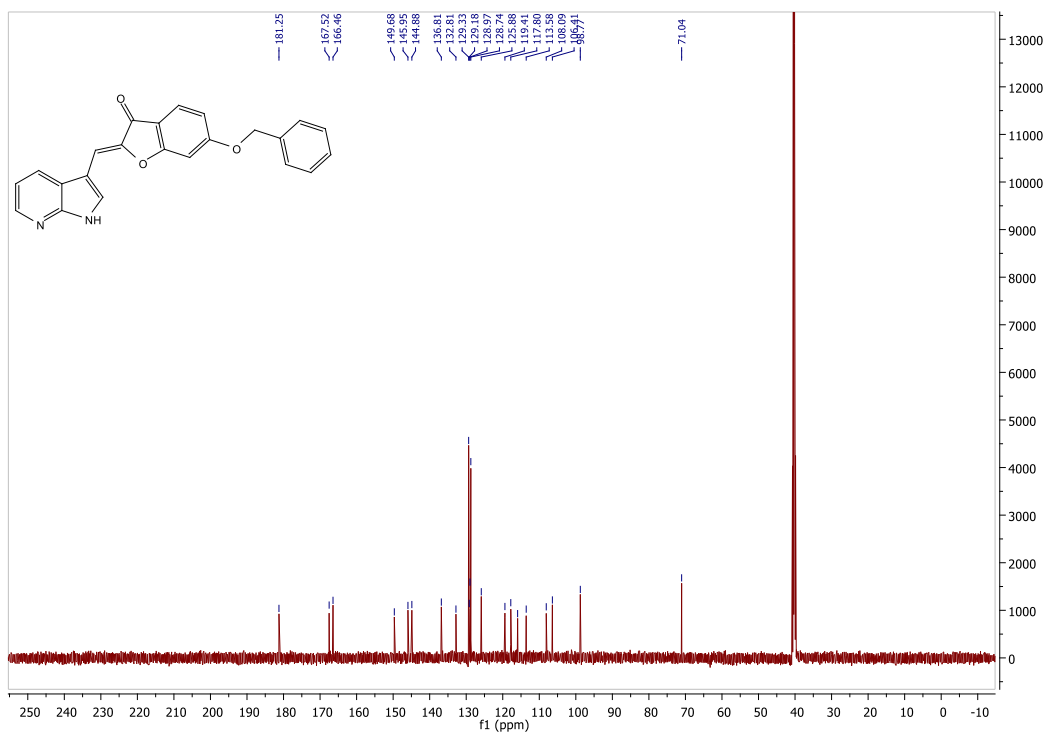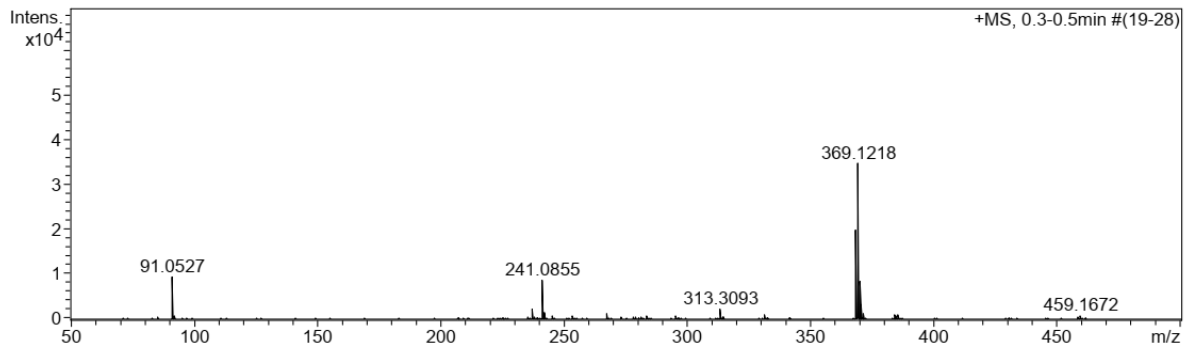
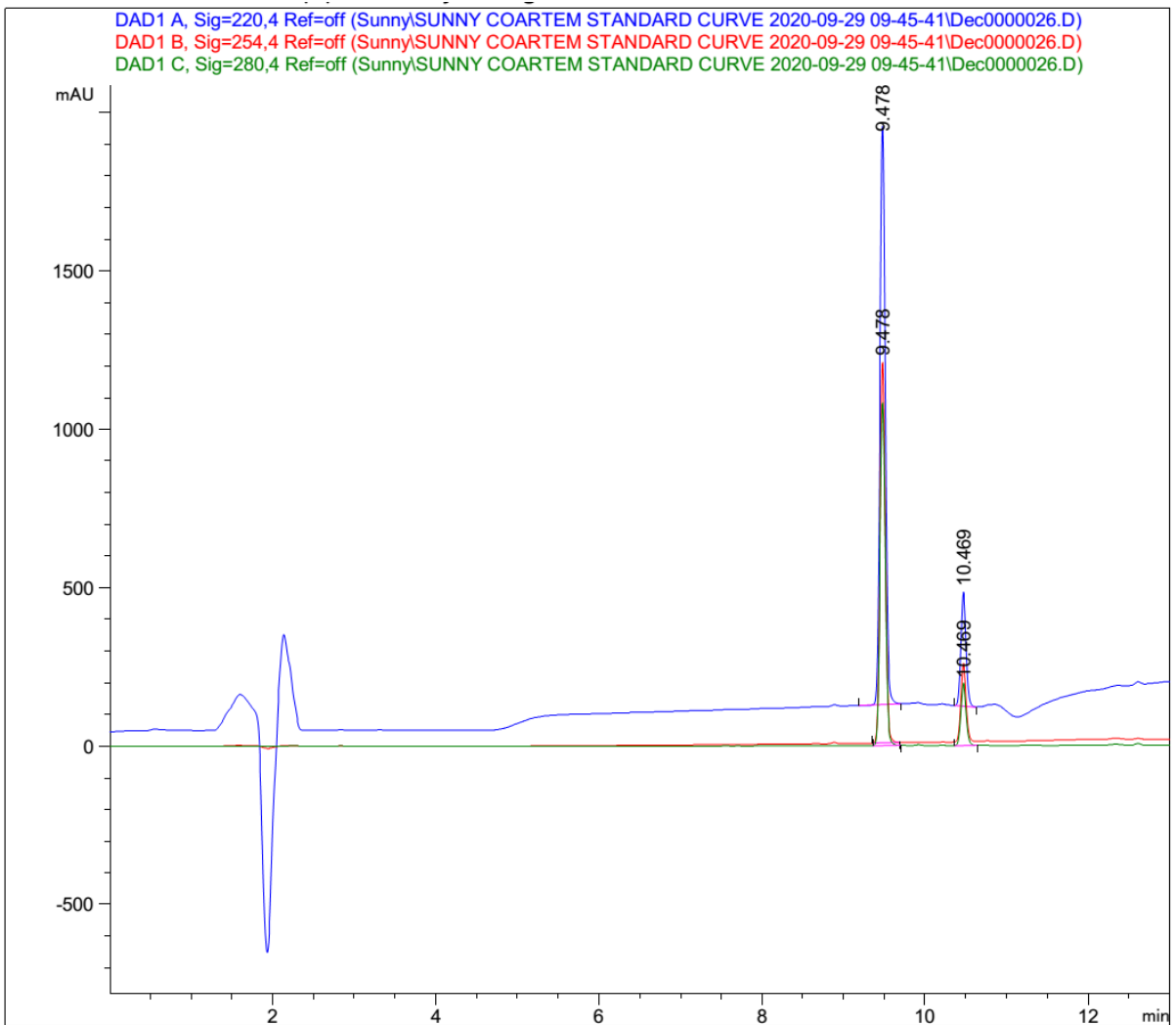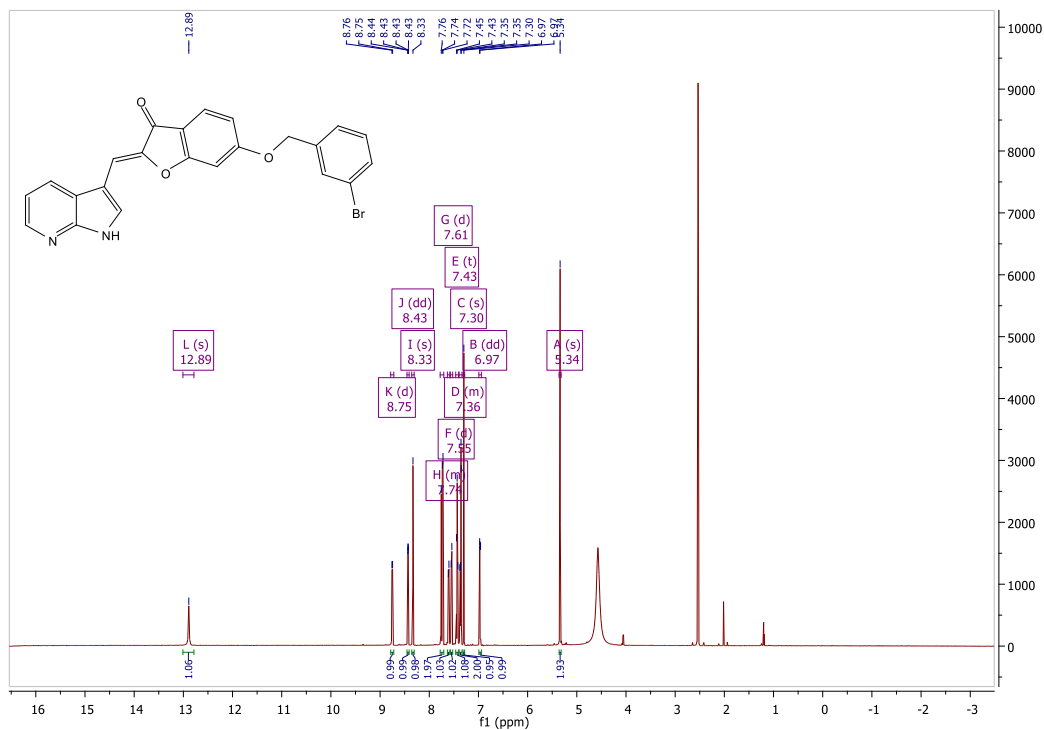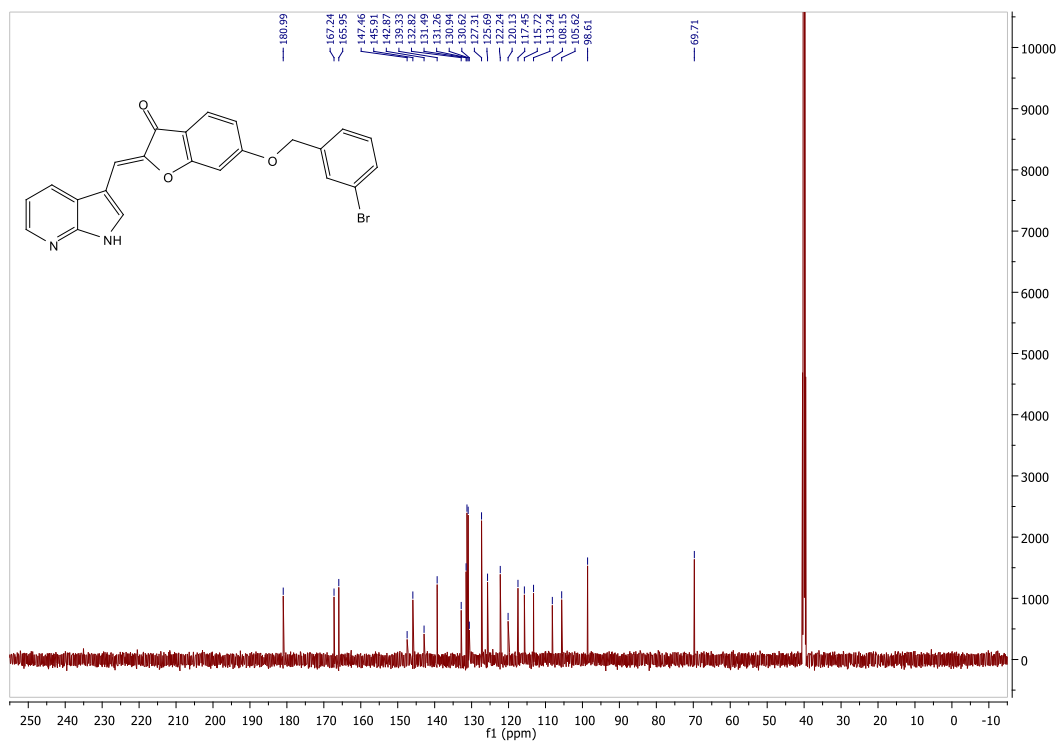| Meas. m/z	#	Formula	Score	m/z	err [mDa]	err [ppm]	mSigma	rdb	e⁻ Conf	N-Rule
91.0527	1	C 7 H 7	100.00	91.0542	1.5	16.9	0.3	4.5	even	ok
241.0855	1	C 15 H 13 O 3	100.00	241.0859	0.4	1.9	6.7	9.5	even	ok
	2	C 10 H 13 N 2 O 5	5.30	241.0819	-3.6	-14.8	31.7	5.5	even	ok
369.1218	1	C 23 H 17 N 2 O 3	100.00	369.1234	1.6	4.3	8.3	16.5	even	ok
	2	C 18 H 17 N 4 O 5	43.23	369.1193	-2.4	-6.6	19.0	12.5	even	ok

HPLC

179
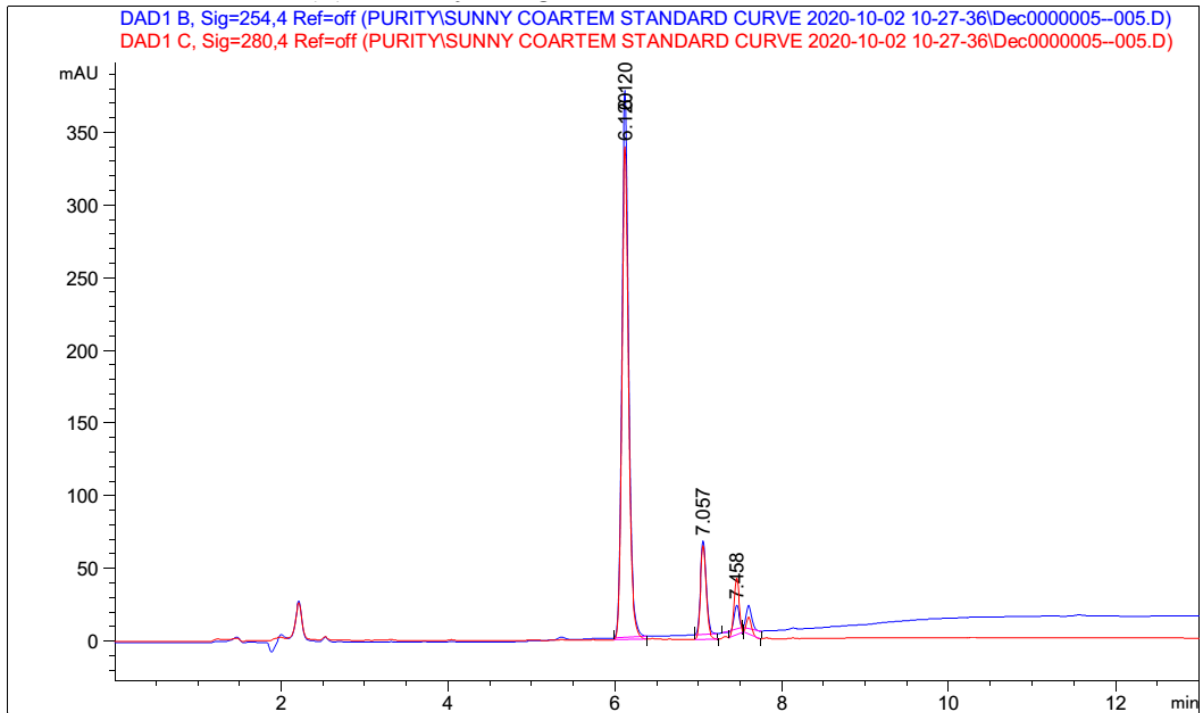
(2*Z*)-6-[(4-fluorobenzyl)oxy]-2-(1*H*-pyrrolo[2,3-*b*]pyridin-3-ylmethylidene)-1-benzofuran-3(2*H*)-one (7b)

¹HNMR

¹³CNMR

MS

+MS, 0.5-0.5min #(30-31)
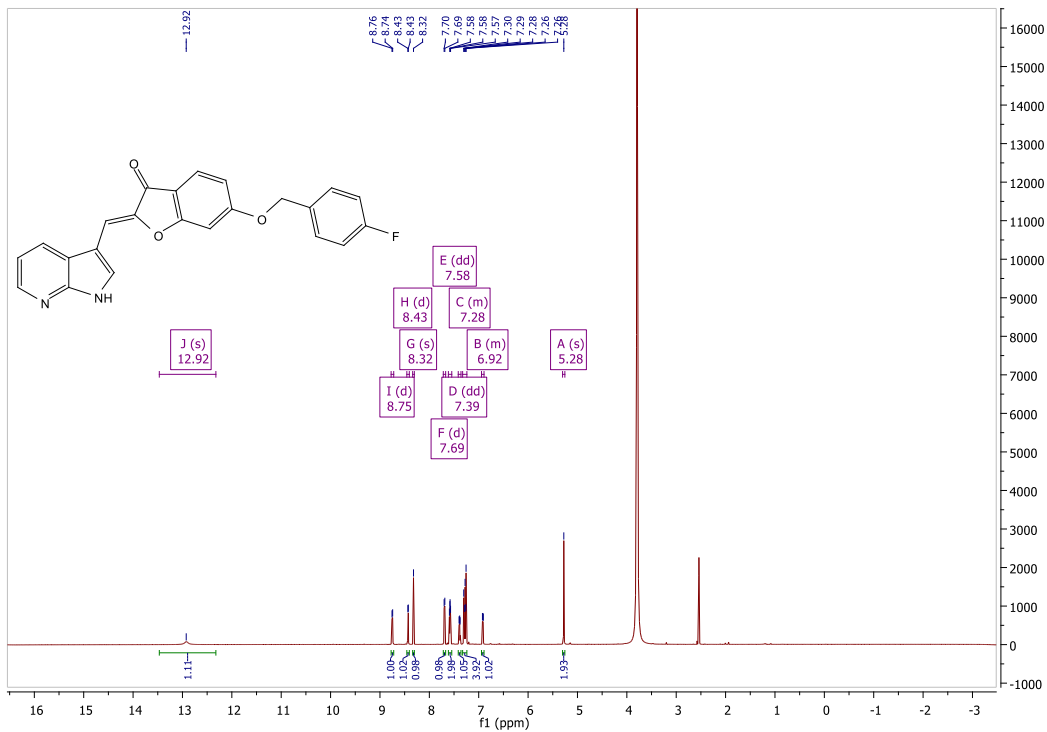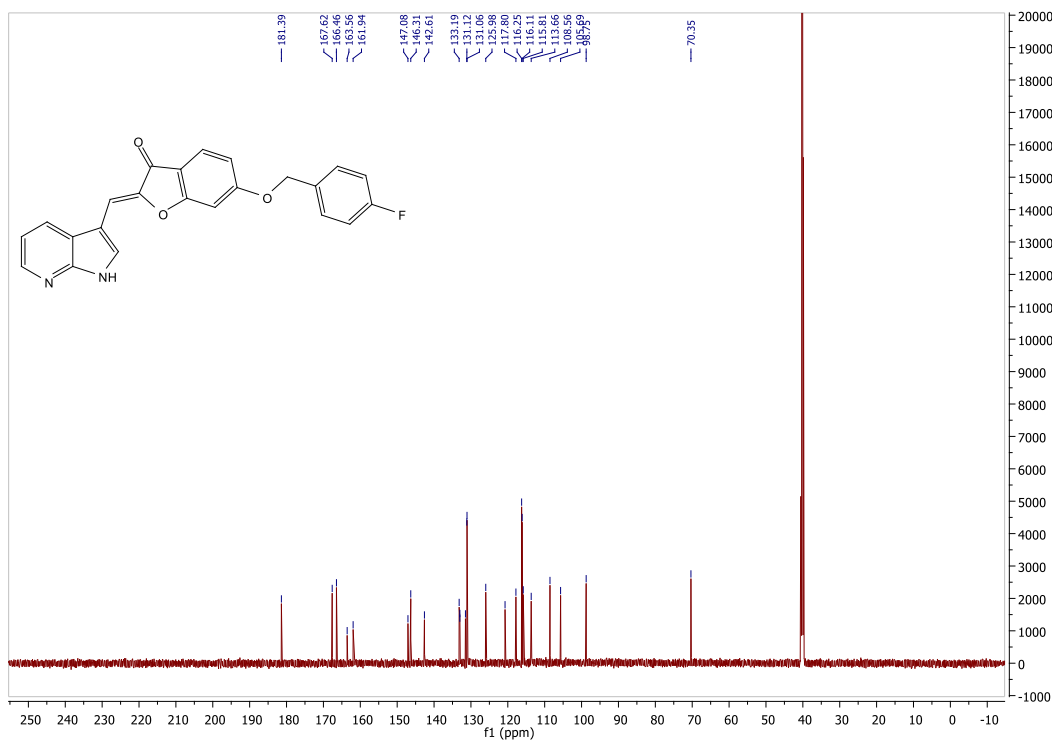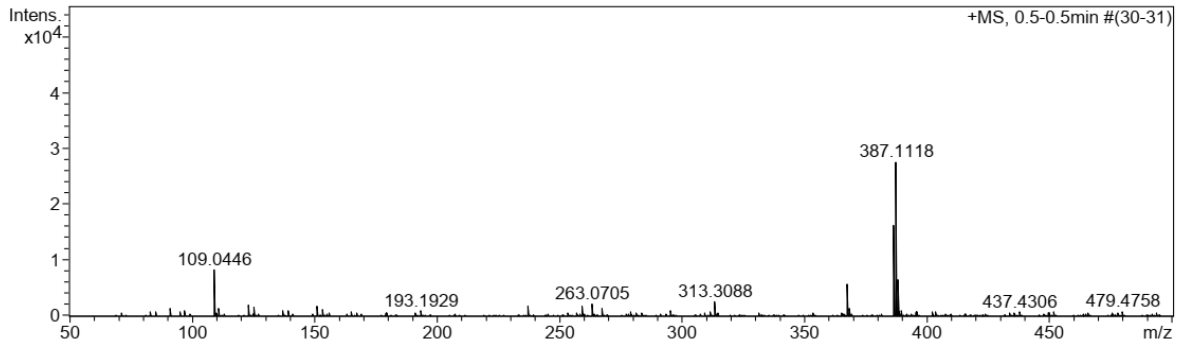
Meas. m/z	#	Formula	Score	m/z	err [mDa]	err [ppm]	mSigma	rdb	e⁻ Conf	N-Rule
109.0446	1	C 7 H 6 F	100.00	109.0448	0.2	2.0	4.1	4.5	even	ok
	2	C 2 H 6 F N 2 O 2	3.58	109.0408	-3.8	-34.9	31.1	0.5	even	ok
367.1119	1	C 25 H 16 F O 2	100.00	367.1129	1.0	2.7	26.0	17.5	even	ok
	2	C 20 H 16 F N 2 O 4	18.60	367.1089	-3.0	-8.3	30.6	13.5	even	ok
387.1118	1	C 23 H 16 F N 2 O 3	100.00	387.1139	2.2	5.6	10.7	16.5	even	ok

HPLC

DAD1 A, Sig=220,4 Ref=off (Sunny\SUNNY COARTEM STANDARD CURVE 2020-09-29 09-45-41\Dec0000024.D)
DAD1 B, Sig=254,4 Ref=off (Sunny\SUNNY COARTEM STANDARD CURVE 2020-09-29 09-45-41\Dec0000024.D)
DAD1 C, Sig=280,4 Ref=off (Sunny\SUNNY COARTEM STANDARD CURVE 2020-09-29 09-45-41\Dec0000024.D)

181
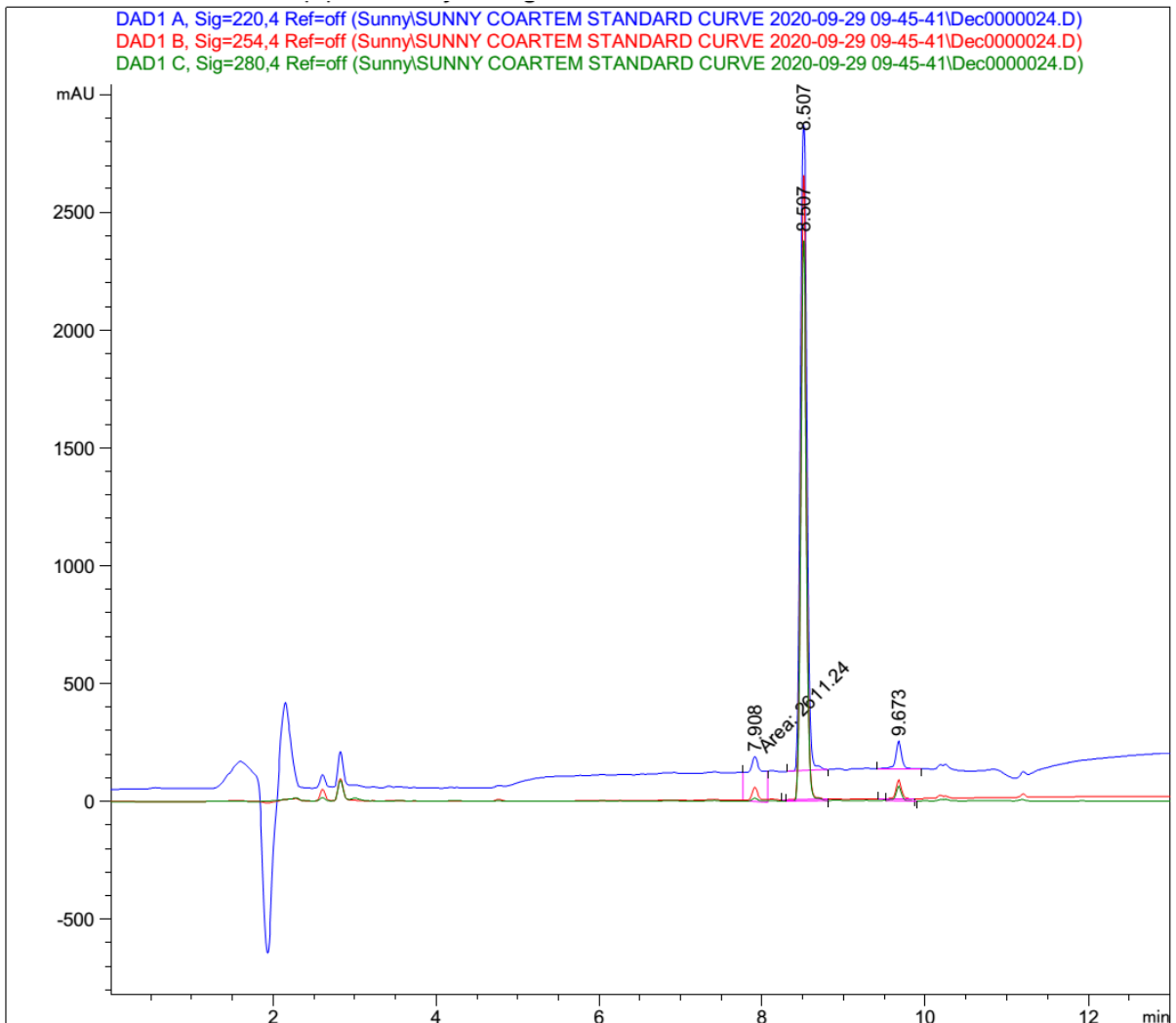
(2*Z*)-6-[(3-fluorobenzyl)oxy]-2-(1*H*-pyrrolo[2,3-*b*]pyridin-3-ylmethylidene)-1-benzofuran-3(2*H*)-one (7c)

¹HNMR

¹³CNMR

MS

Meas. m/z	#	Formula	Score	m/z	err [mDa]	err [ppm]	mSigma	rdb	e⁻ Conf	N-Rule
387.1118	1	C 23 H 16 F N 2 O 3	100.00	387.1139	2.2	5.6	12.3	16.5	even	ok

HPLC

183

(2*Z*)-2-[(1*H*-pyrrolo[2,3-*b*]pyridin-3-yl)methylidene]-6-{[3-(trifluoromethyl)phenyl]methoxy}-1-benzofuran-3(2*H*)-one (7d)

¹HNMR

¹³CNMR

MS

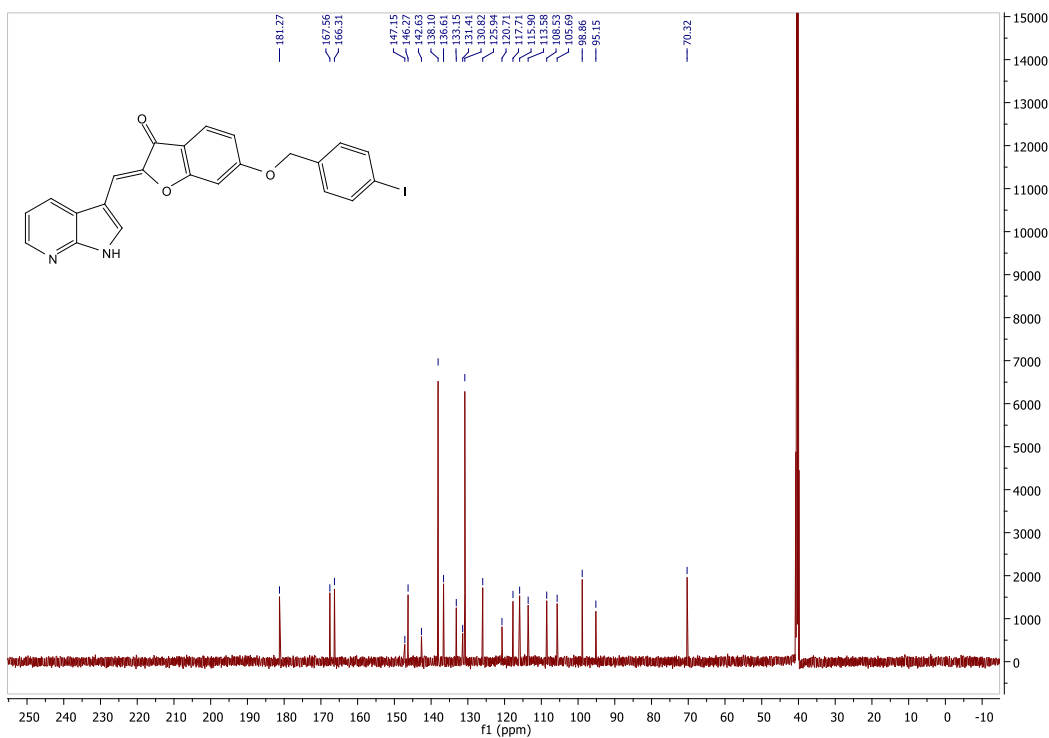| Meas. m/z	#	Formula	Score	m/z	err [mDa]	err [ppm]	mSigma	rdb	e⁻ Conf	N-Rule
437.1088	1	C 24 H 16 F 3 N 2 O 3	100.00	437.1108	1.9	4.4	8.3	16.5	even	ok
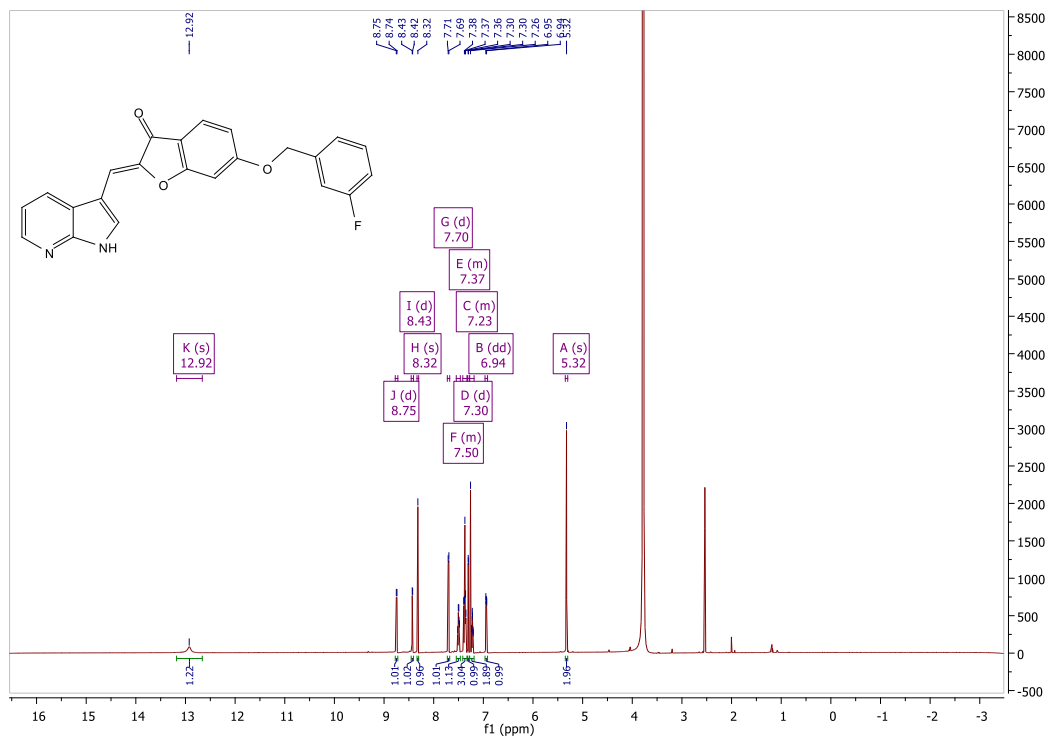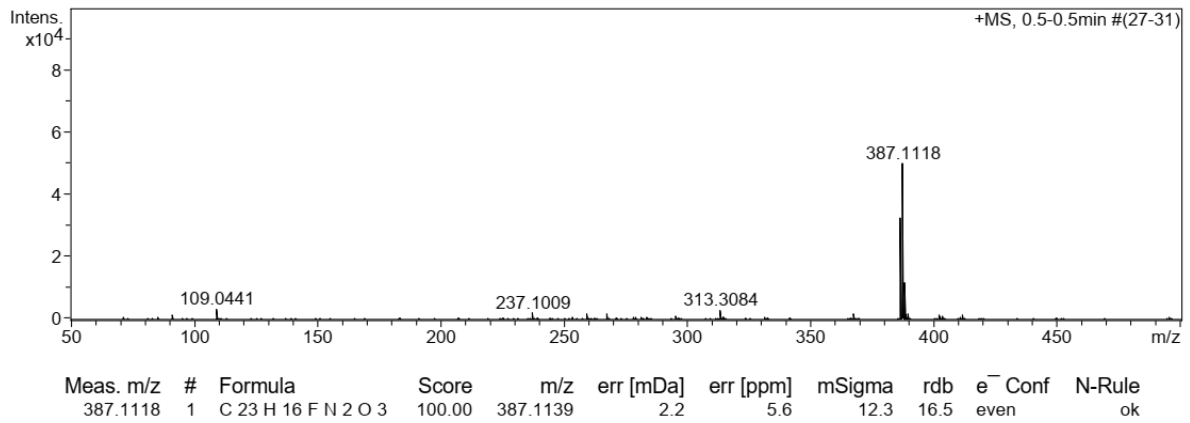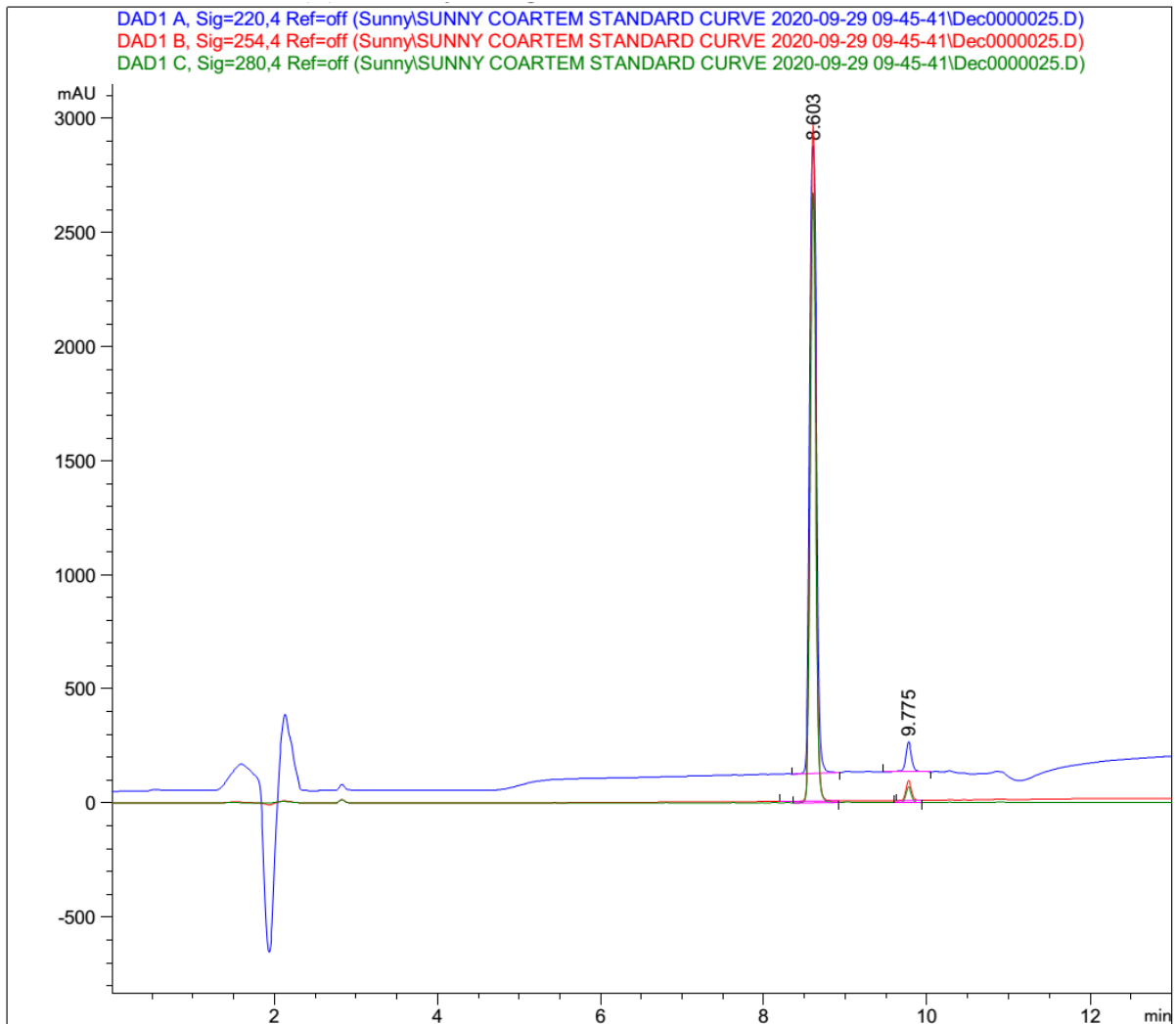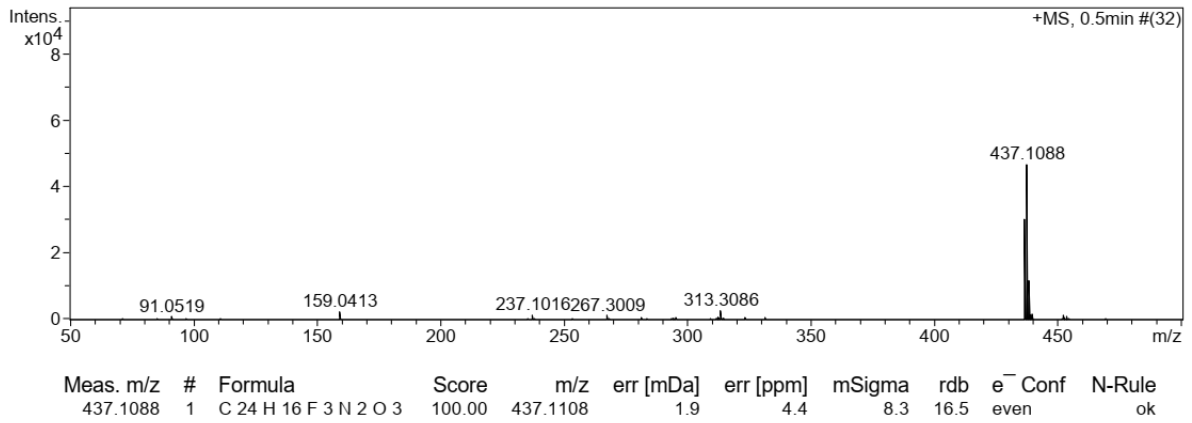
HPLC

(2*Z*)-6-[(3-bromophenyl)methoxy]-2-[(1*H*-pyrrolo[2,3-*b*]pyridin-3-yl)methylidene]-1-benzofuran-3(2*H*)-one (7e)

¹HNMR

¹³CNMR

MS

+MS, 0.1-0.1min #(5-7)
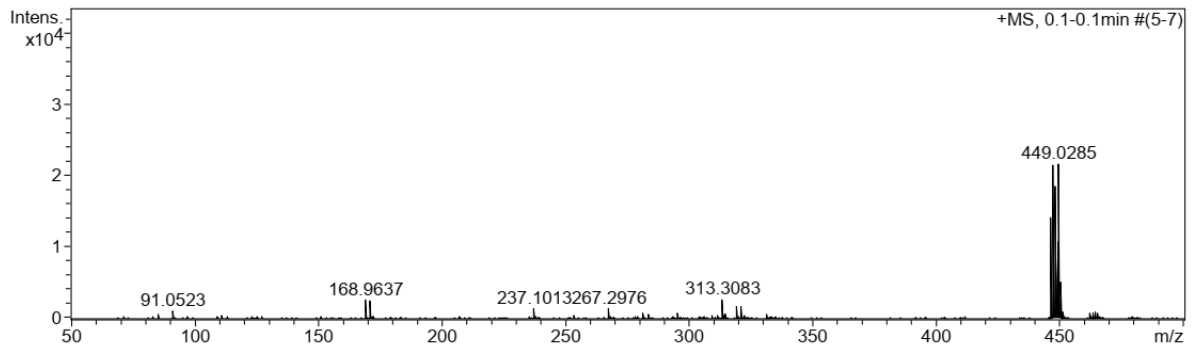
Meas. m/z	#	Formula	Score	m/z	err [mDa]	err [ppm]	mSigma	rdb	e⁻ Conf	N-Rule
446.0233	1	C 23 H 15 Br N 2 O 3	100.00	446.0261	2.8	6.2	505.9	17.0	odd	ok
447.0304	1	C 24 H 16 Br O 4	0.16	447.0226	-7.7	-17.3	265.8	16.5	even	ok
	2	C 23 H 16 Br N 2 O 3	100.00	447.0339	3.5	7.8	266.9	16.5	even	ok

HPLC

DAD1 A, Sig=220,4 Ref=off (Sunny\SUNNY COARTEM STANDARD CURVE 2020-09-29 09-45-41\Dec0000027.D)
DAD1 B, Sig=254,4 Ref=off (Sunny\SUNNY COARTEM STANDARD CURVE 2020-09-29 09-45-41\Dec0000027.D)
DAD1 C, Sig=280,4 Ref=off (Sunny\SUNNY COARTEM STANDARD CURVE 2020-09-29 09-45-41\Dec0000027.D)
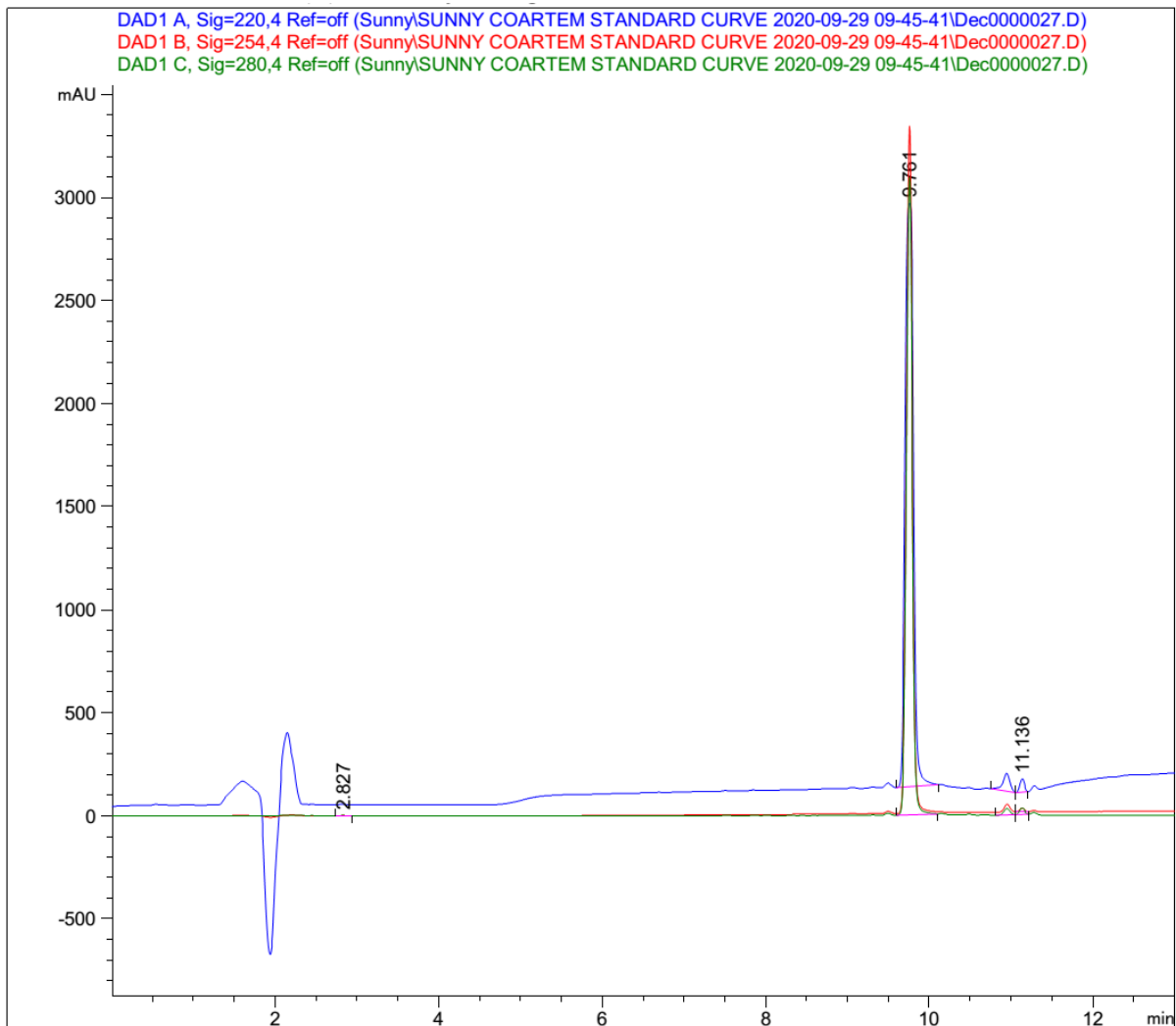
(2Z)-6-[(3-chlorophenyl)methoxy]-2-[(1H-pyrrolo[2,3-b]pyridin-3-yl)methylidene]-1-benzofuran-3(2H)-one (7f)

¹HNMR

¹³CNMR

188

MS

+MS, 1.0-1.0min #(60-62)
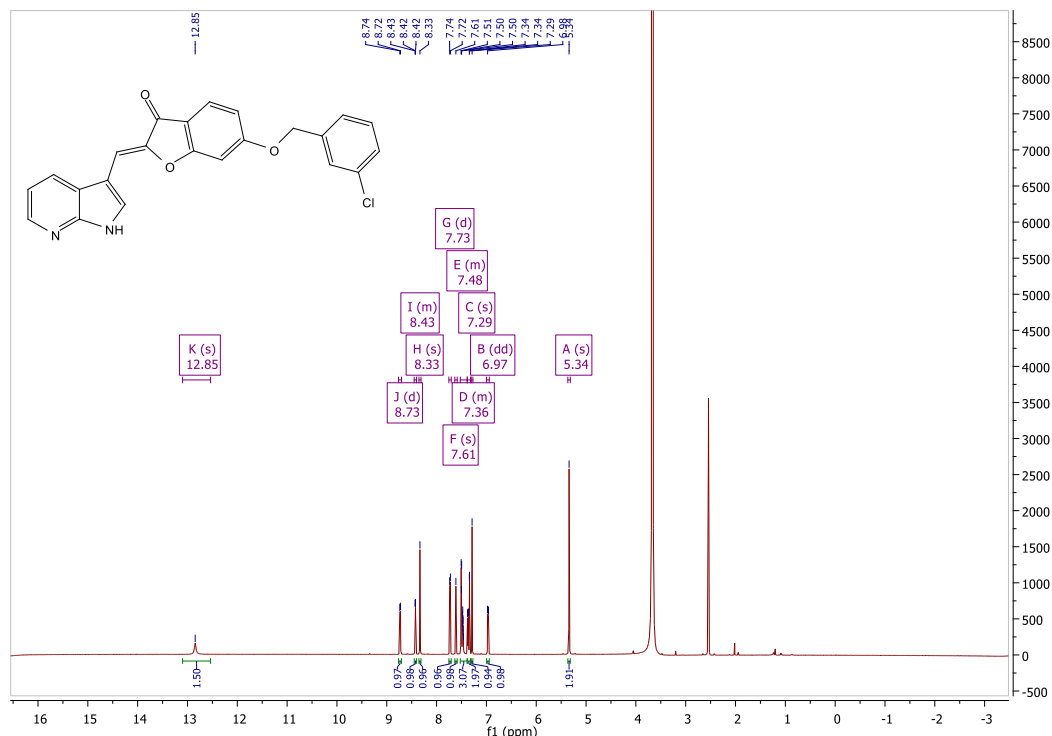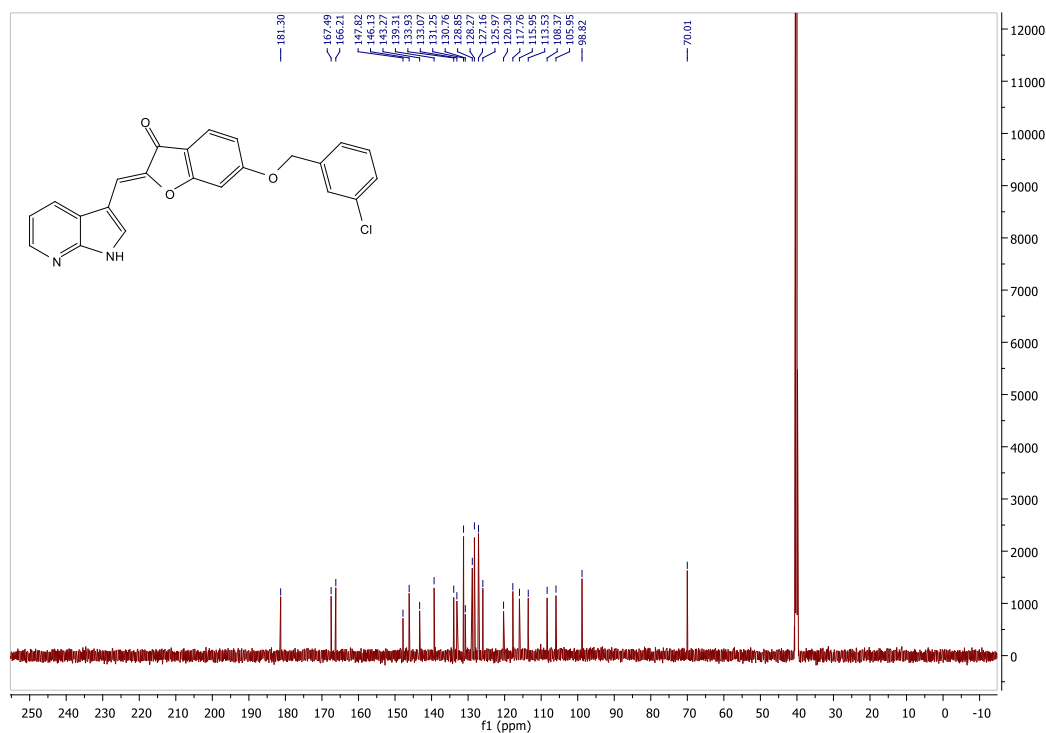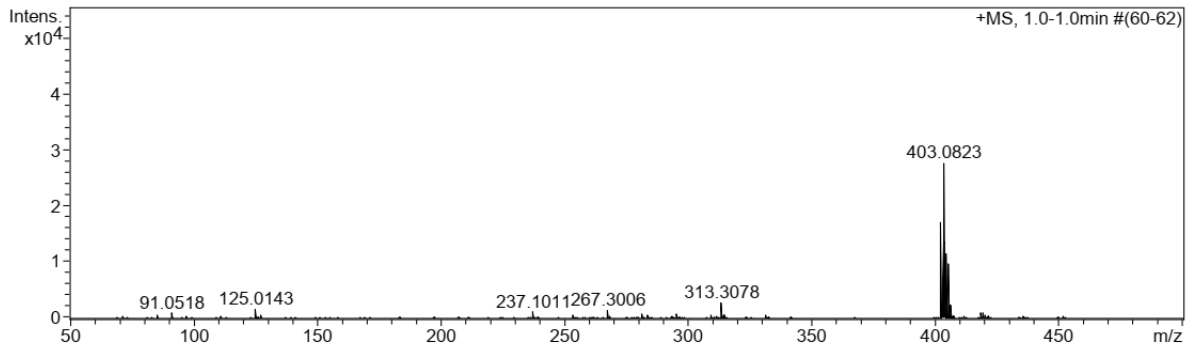
Meas. m/z	#	Formula	Score	m/z	err [mDa]	err [ppm]	mSigma	rdb	e⁻ Conf	N-Rule
402.0745	1	C 23 H 15 Cl N 2 O 3	100.00	402.0766	2.0	5.0	395.0	17.0	odd	ok
403.0823	1	C 23 H 16 Cl N 2 O 3	100.00	403.0844	2.1	5.1	70.1	16.5	even	ok

HPLC

DAD1 A, Sig=220,4 Ref=off (Sunny\SUNNY COARTEM STANDARD CURVE 2020-09-29 09-45-41\Dec0000028.D)
DAD1 B, Sig=254,4 Ref=off (Sunny\SUNNY COARTEM STANDARD CURVE 2020-09-29 09-45-41\Dec0000028.D)
DAD1 C, Sig=280,4 Ref=off (Sunny\SUNNY COARTEM STANDARD CURVE 2020-09-29 09-45-41\Dec0000028.D)

189
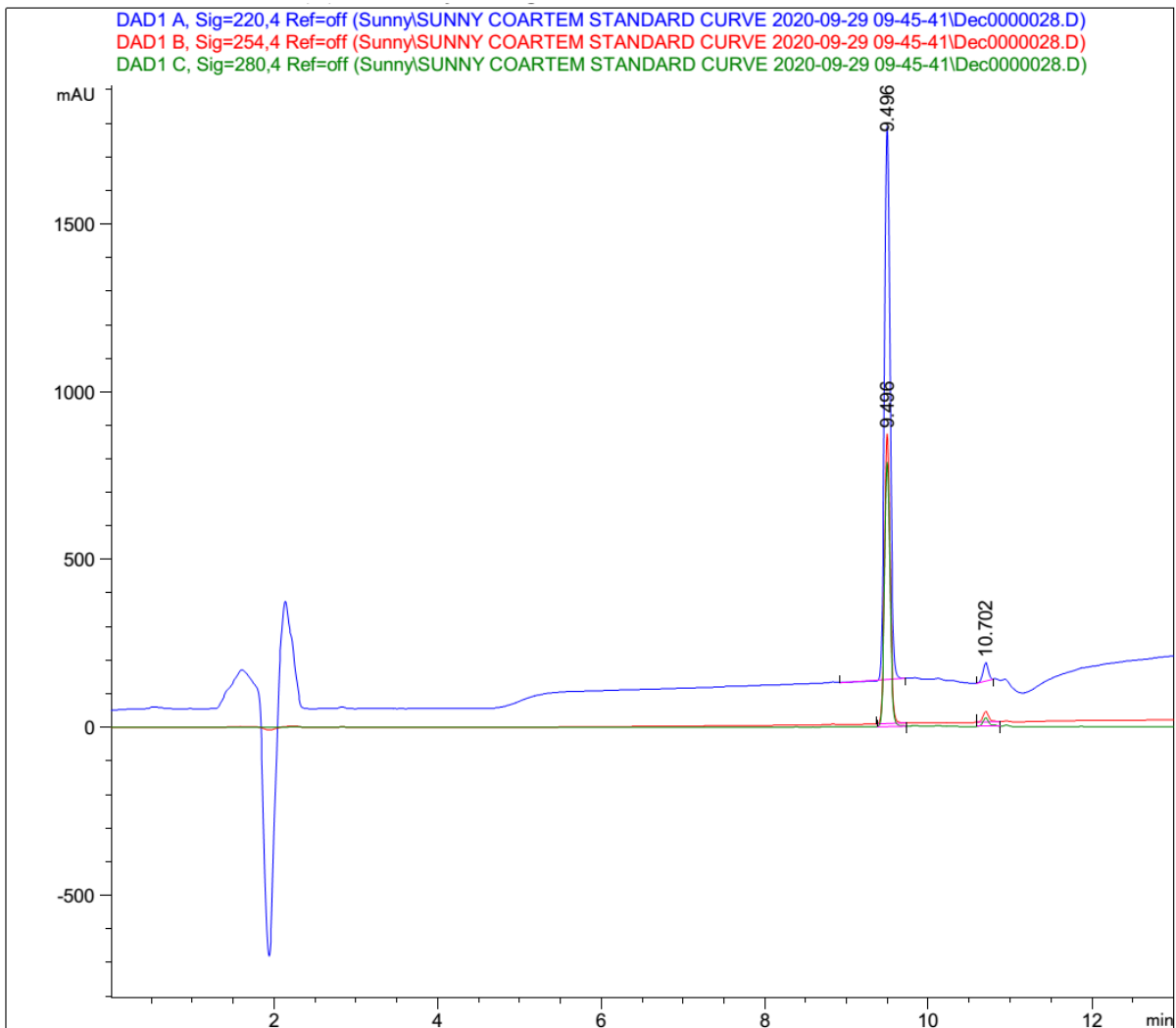
(2*Z*)-6-[(4-iodophenyl)methoxy]-2-[(1*H*-pyrrolo[2,3-*b*]pyridin-3-yl)methylidene]-1-benzofuran-3(2*H*)-one (7g)

¹HNMR

¹³CNMR

MS

+MS, 0.4-0.4min #(22-24)
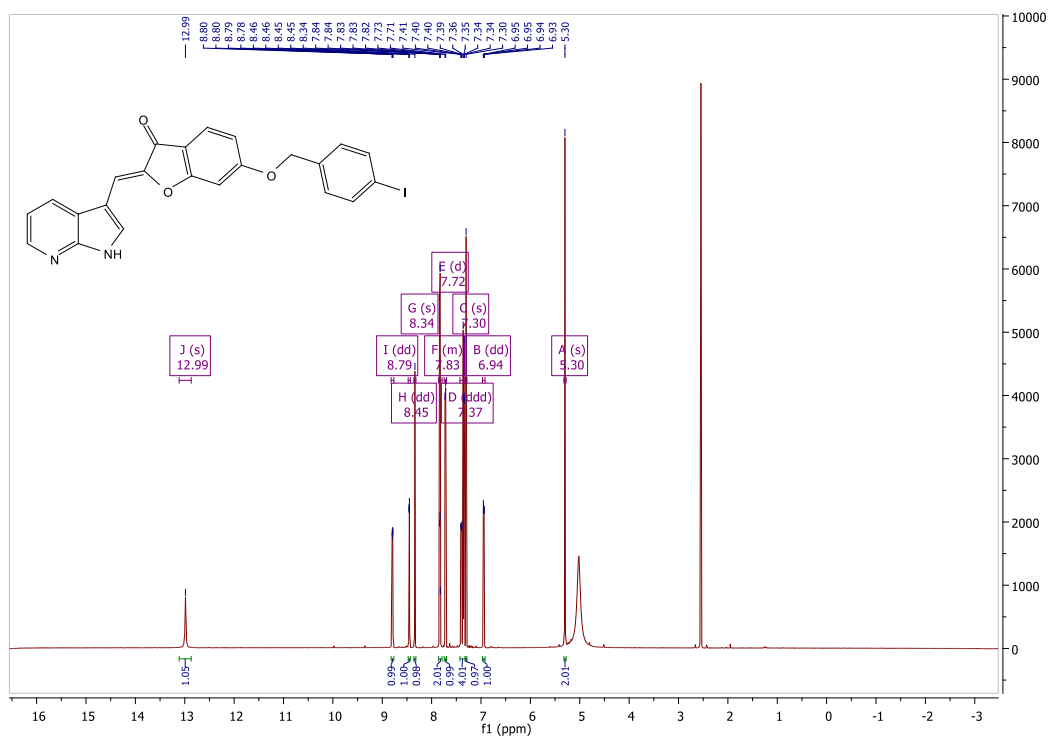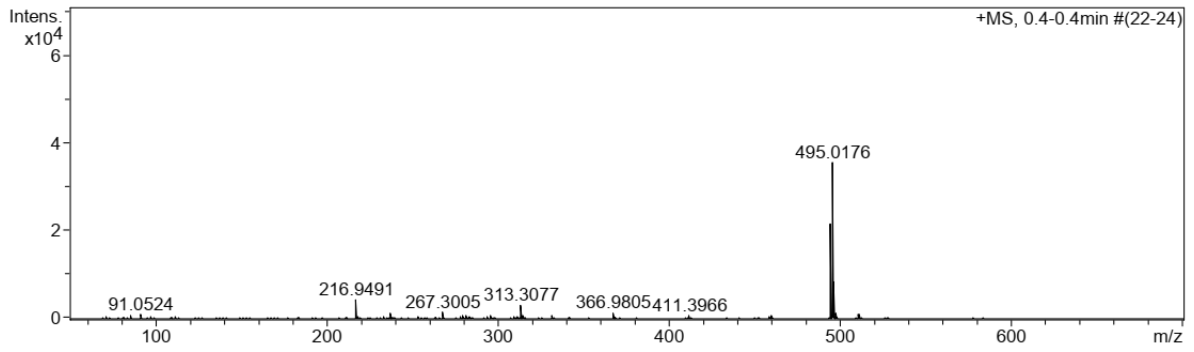
Meas. m/z	#	Formula	Score	m/z	err [mDa]	err [ppm]	mSigma	rdb	e⁻ Conf	N-Rule
495.0176	1	C 23 H 16 I N 2 O 3	100.00	495.0200	2.4	4.8	13.7	16.5	even	ok

HPLC

DAD1 A, Sig=220,4 Ref=off (Sunny\SUNNY COARTEM STANDARD CURVE 2020-09-29 09-45-41\Dec0000029.D)
DAD1 B, Sig=254,4 Ref=off (Sunny\SUNNY COARTEM STANDARD CURVE 2020-09-29 09-45-41\Dec0000029.D)
DAD1 C, Sig=280,4 Ref=off (Sunny\SUNNY COARTEM STANDARD CURVE 2020-09-29 09-45-41\Dec0000029.D)
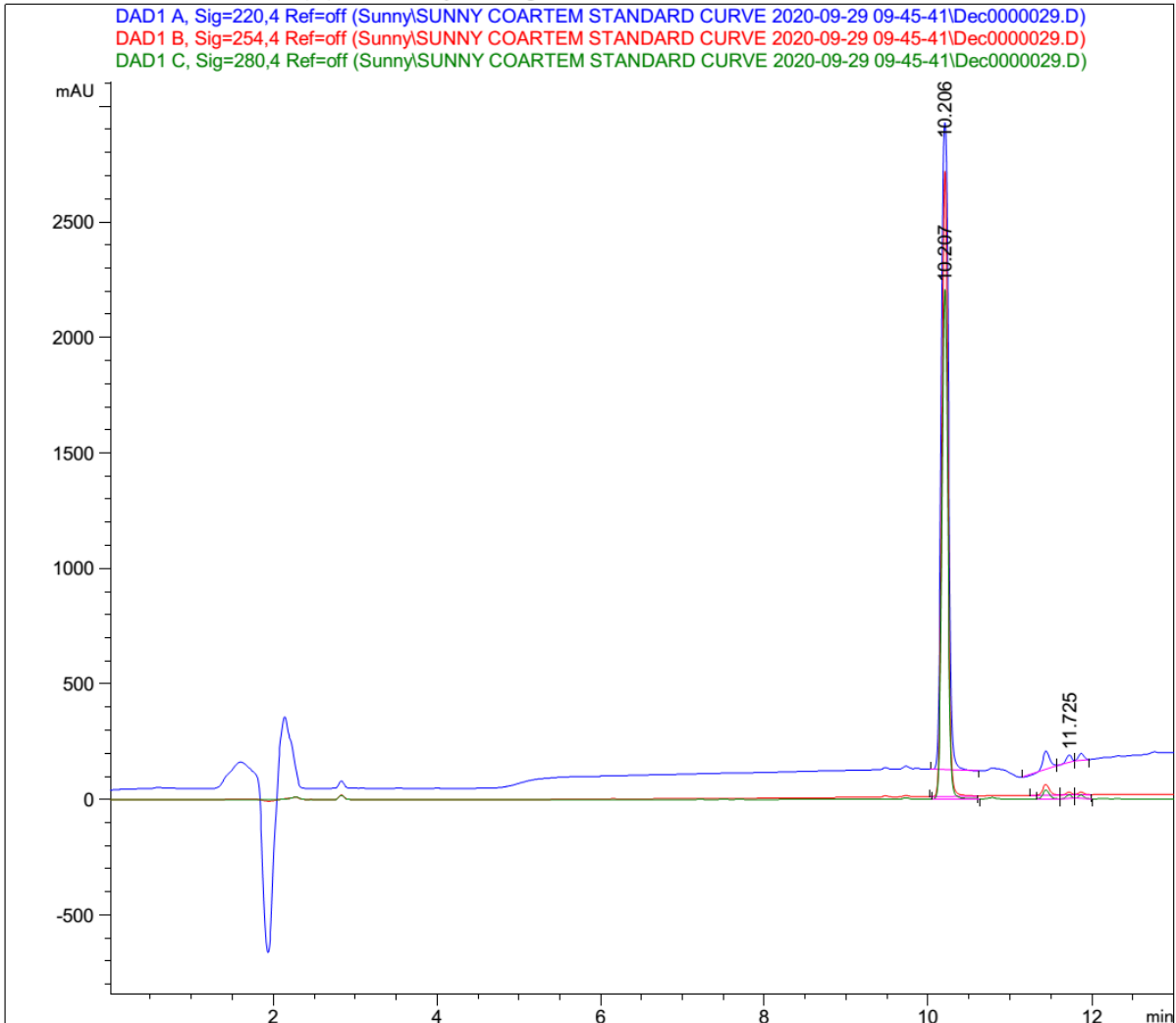
(2*Z*)-6-[(3-nitrobenzyl)oxy]-2-(1*H*-pyrrolo[2,3-*b*]pyridin-3-ylmethylidene)-1-benzofuran-3(2*H*)-one (7h)

¹HNMR

¹³CNMR

192

MS

+MS, 0.8-0.8min #(45-47)
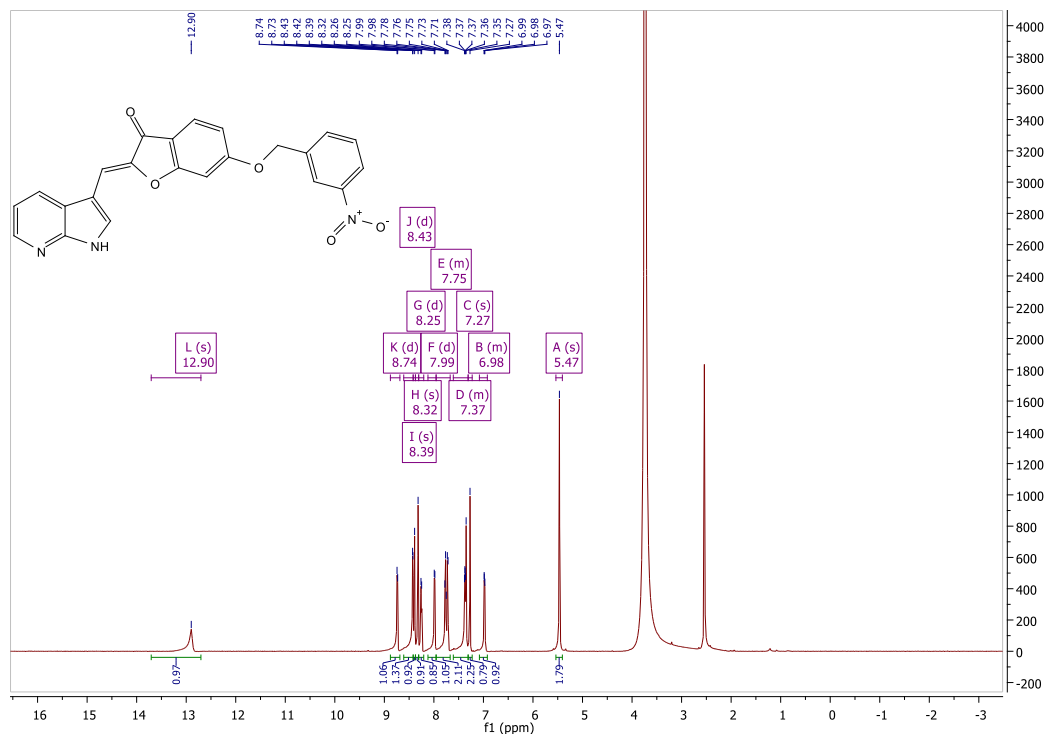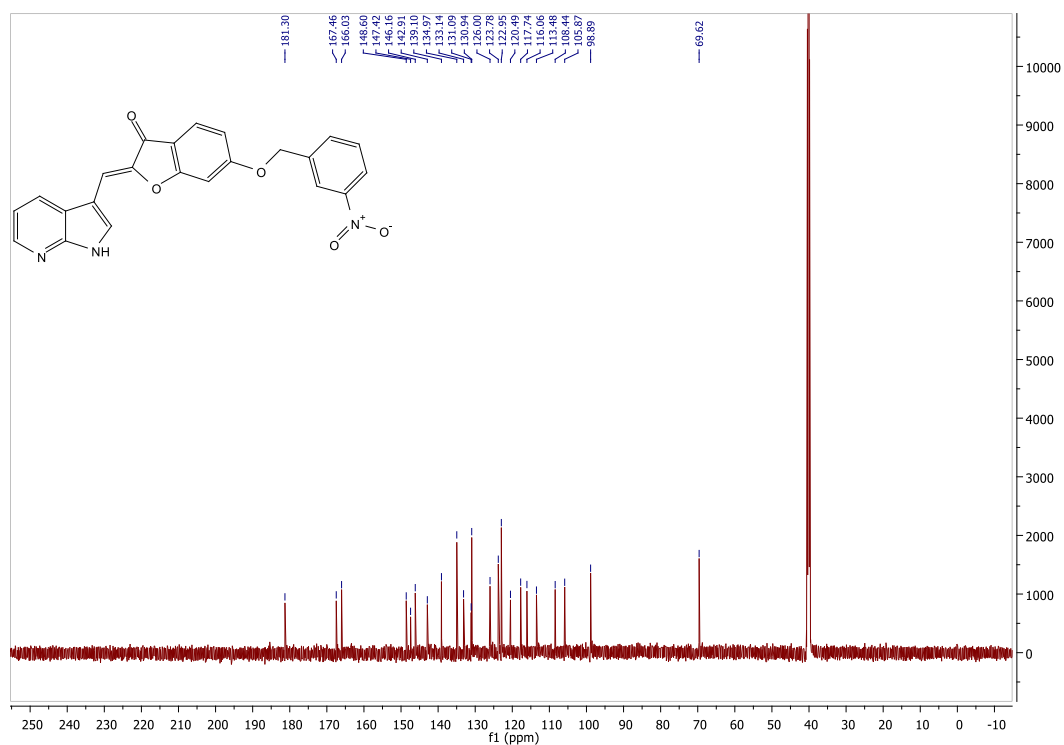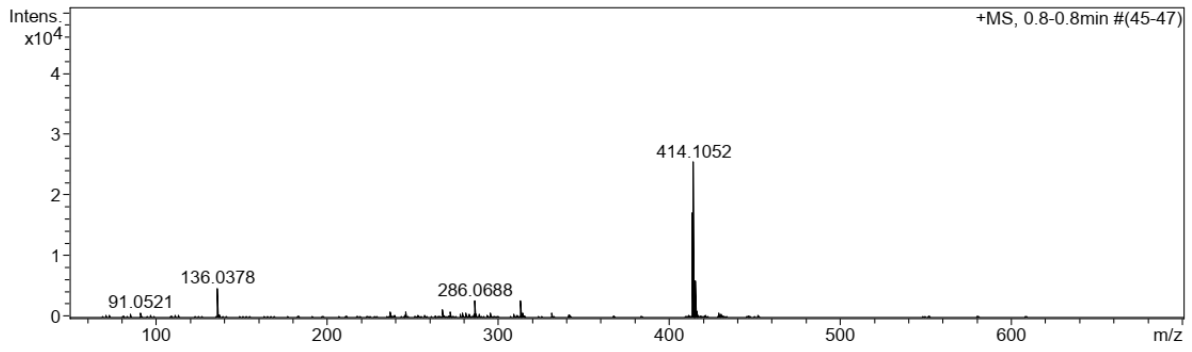
Meas. m/z	#	Formula	Score	m/z	err [mDa]	err [ppm]	mSigma	rdb	e⁻ Conf	N-Rule
414.1052	1	C 23 H 16 N 3 O 5	100.00	414.1084	3.3	7.9	15.1	17.5	even	ok

HPLC

DAD1 A, Sig=220,4 Ref=off (Sunny\SUNNY COARTEM STANDARD CURVE 2020-09-29 09-45-41\Dec0000030.D)
DAD1 B, Sig=254,4 Ref=off (Sunny\SUNNY COARTEM STANDARD CURVE 2020-09-29 09-45-41\Dec0000030.D)
DAD1 C, Sig=280,4 Ref=off (Sunny\SUNNY COARTEM STANDARD CURVE 2020-09-29 09-45-41\Dec0000030.D)
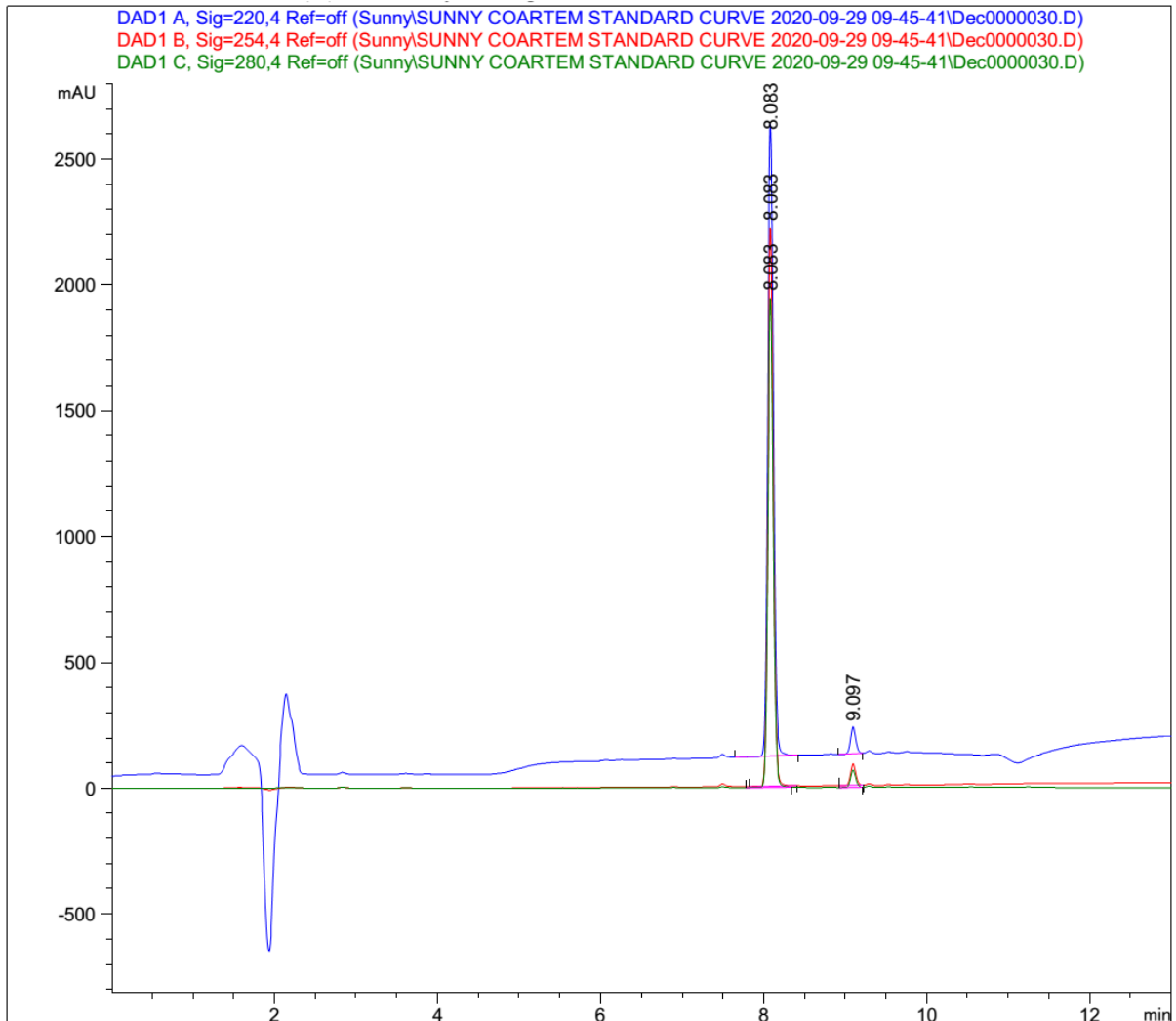
(2Z)-6-(3-phenylpropoxy)-2-[(1H-pyrrolo[2,3-b]pyridin-3-yl)methylidene]-1-benzofuran-3(2H)-one (7i)

¹HNMR

¹³CNMR

MS

+MS, 0.3-0.4min #(19-22)
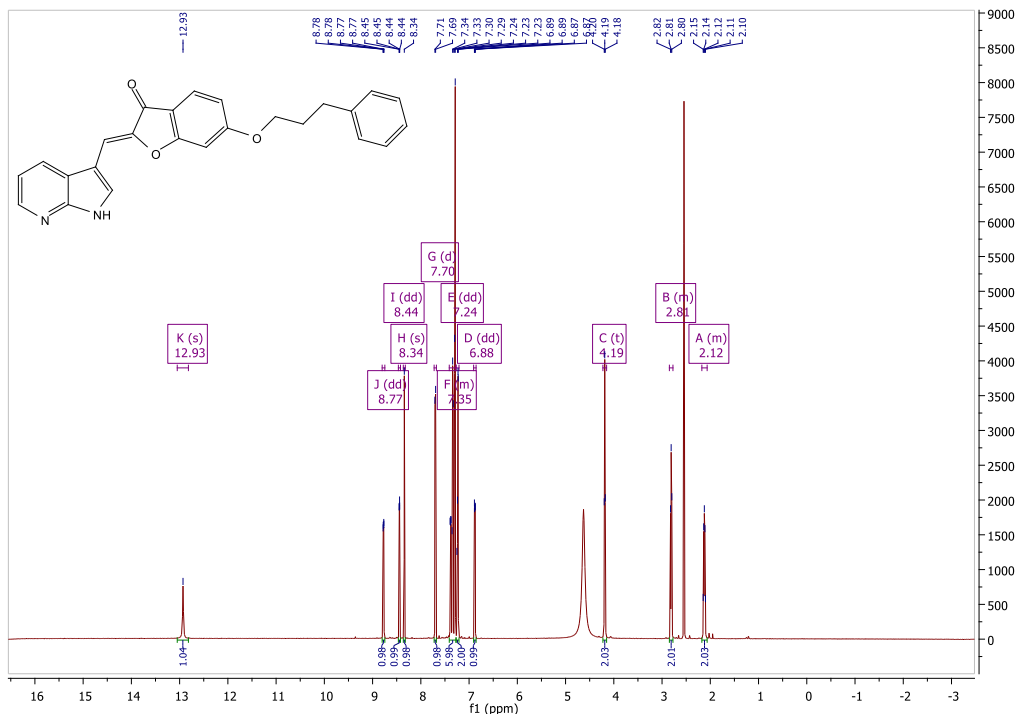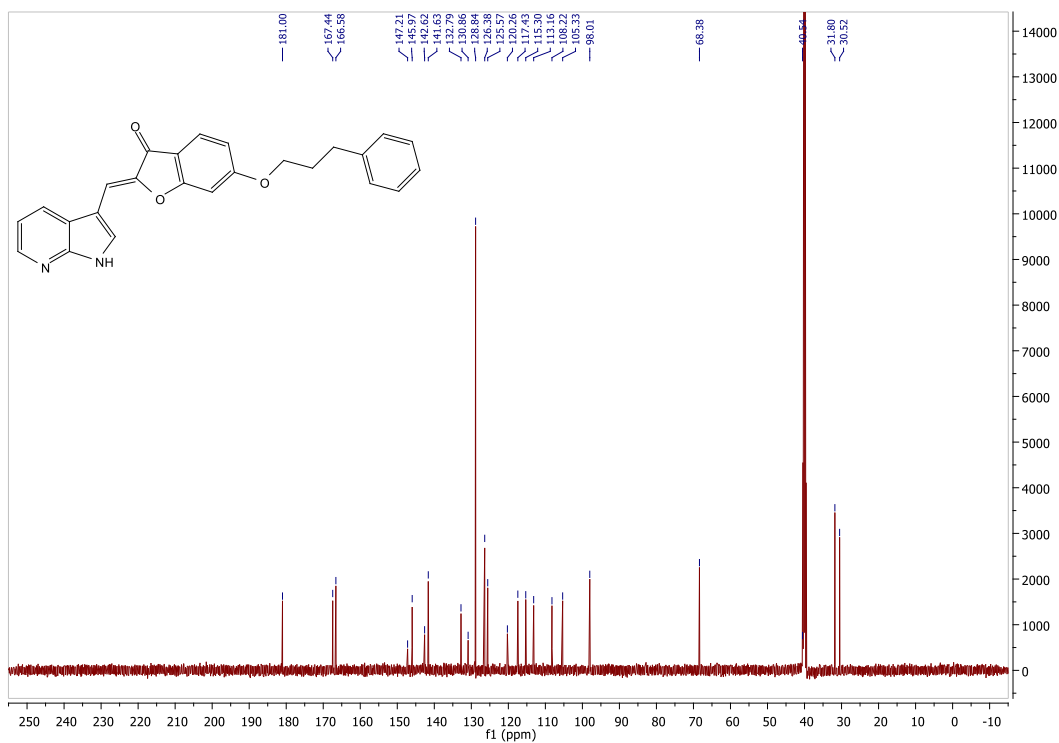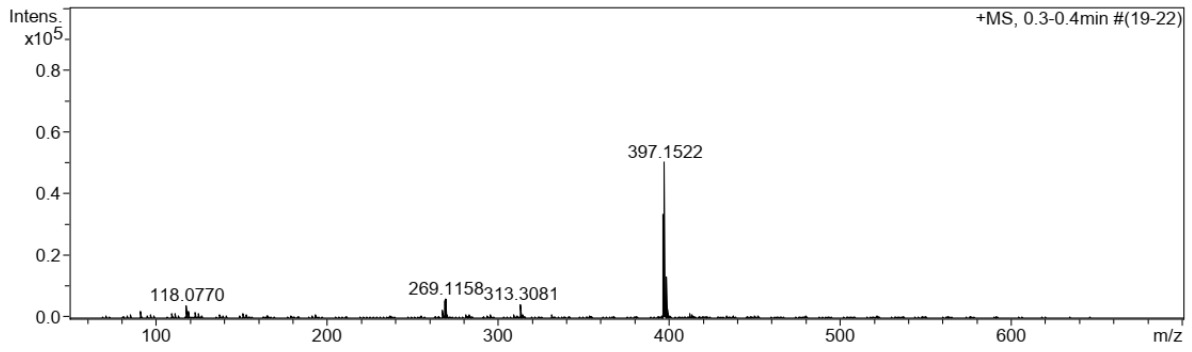
Meas. m/z	#	Formula	Score	m/z	err [mDa]	err [ppm]	mSigma	rdb	e⁻ Conf	N-Rule
397.1522	1	C 25 H 21 N 2 O 3	100.00	397.1547	2.5	6.2	11.4	16.5	even	ok

HPLC
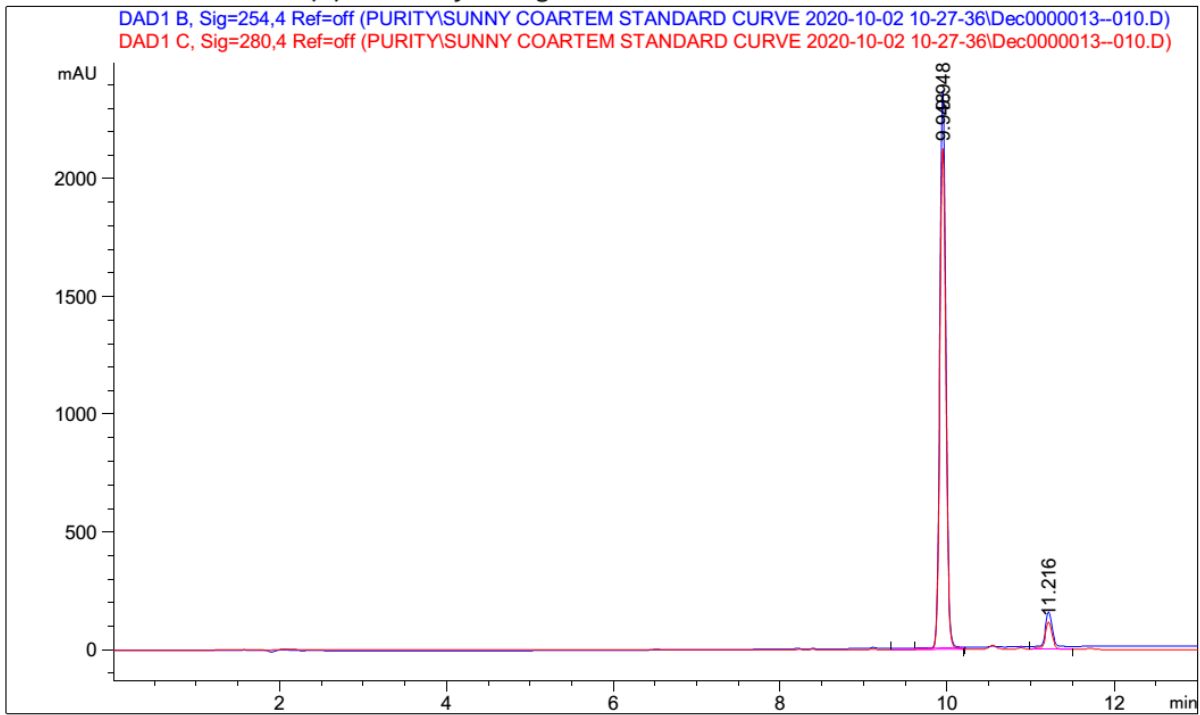
195

(2*Z*)-6-[(4-ethoxyphenyl)methoxy]-2-[(1*H*-pyrrolo[2,3-*b*]pyridin-3-yl)methylidene]-1-benzofuran-3(2*H*)-one (7j)

¹HNMR

¹³CNMR

MS

+MS, 0.3-0.4min #(20-24)
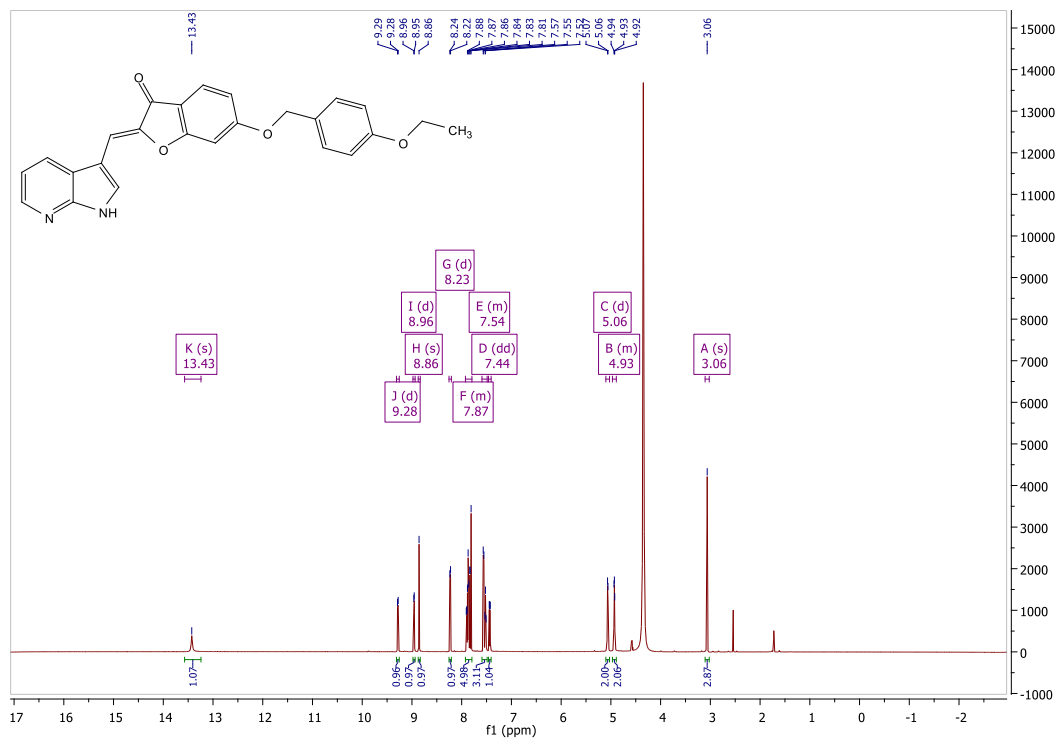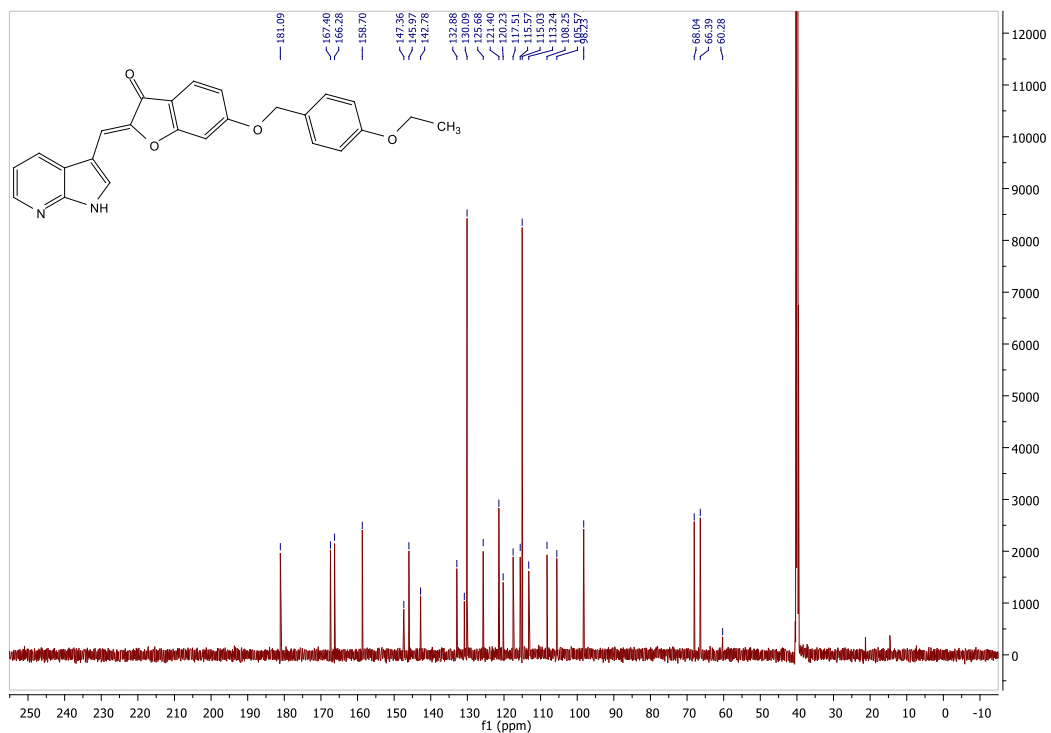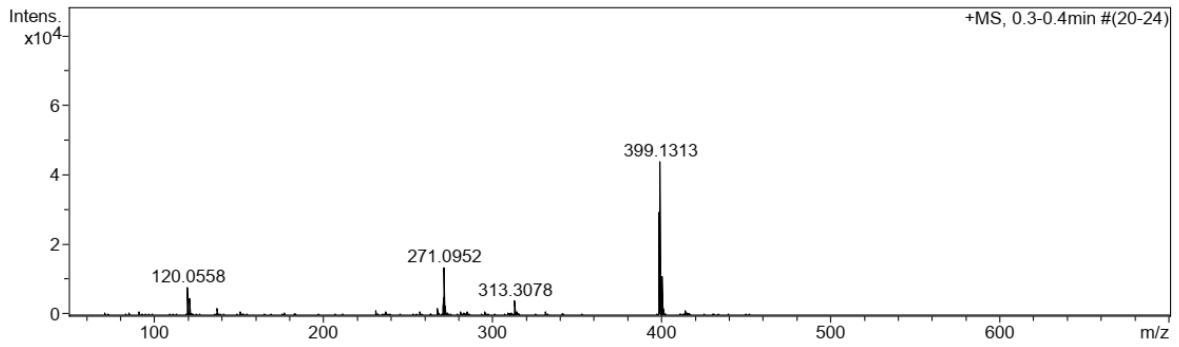
Meas. m/z	#	Formula	Score	m/z	err [mDa]	err [ppm]	mSigma	rdb	e⁻ Conf	N-Rule
120.0558	1	C 8 H 8 O	100.00	120.0570	1.2	9.6	294.5	5.0	odd	ok
	2	C 6 H 6 N 3	78.10	120.0556	-0.2	-1.6	300.6	5.5	even	ok
	3	C 3 H 8 N 2 O 3	0.94	120.0529	-2.9	-23.9	321.1	1.0	odd	ok
271.0952	1	C 16 H 15 O 4	58.44	271.0965	1.3	4.7	14.8	9.5	even	ok
	2	C 14 H 13 N 3 O 3	100.00	271.0951	-0.1	-0.3	18.2	10.0	odd	ok
	3	C 19 H 13 N O	4.26	271.0992	3.9	14.5	25.9	14.0	odd	ok
399.1313	1	C 24 H 19 N 2 O 4	100.00	399.1339	2.6	6.6	11.6	16.5	even	ok

HPLC

DAD1 A, Sig=220,4 Ref=off (Sunny\SUNNY COARTEM STANDARD CURVE 2020-09-29 09-45-41\Dec0000032.D)
DAD1 B, Sig=254,4 Ref=off (Sunny\SUNNY COARTEM STANDARD CURVE 2020-09-29 09-45-41\Dec0000032.D)
DAD1 C, Sig=280,4 Ref=off (Sunny\SUNNY COARTEM STANDARD CURVE 2020-09-29 09-45-41\Dec0000032.D)

197
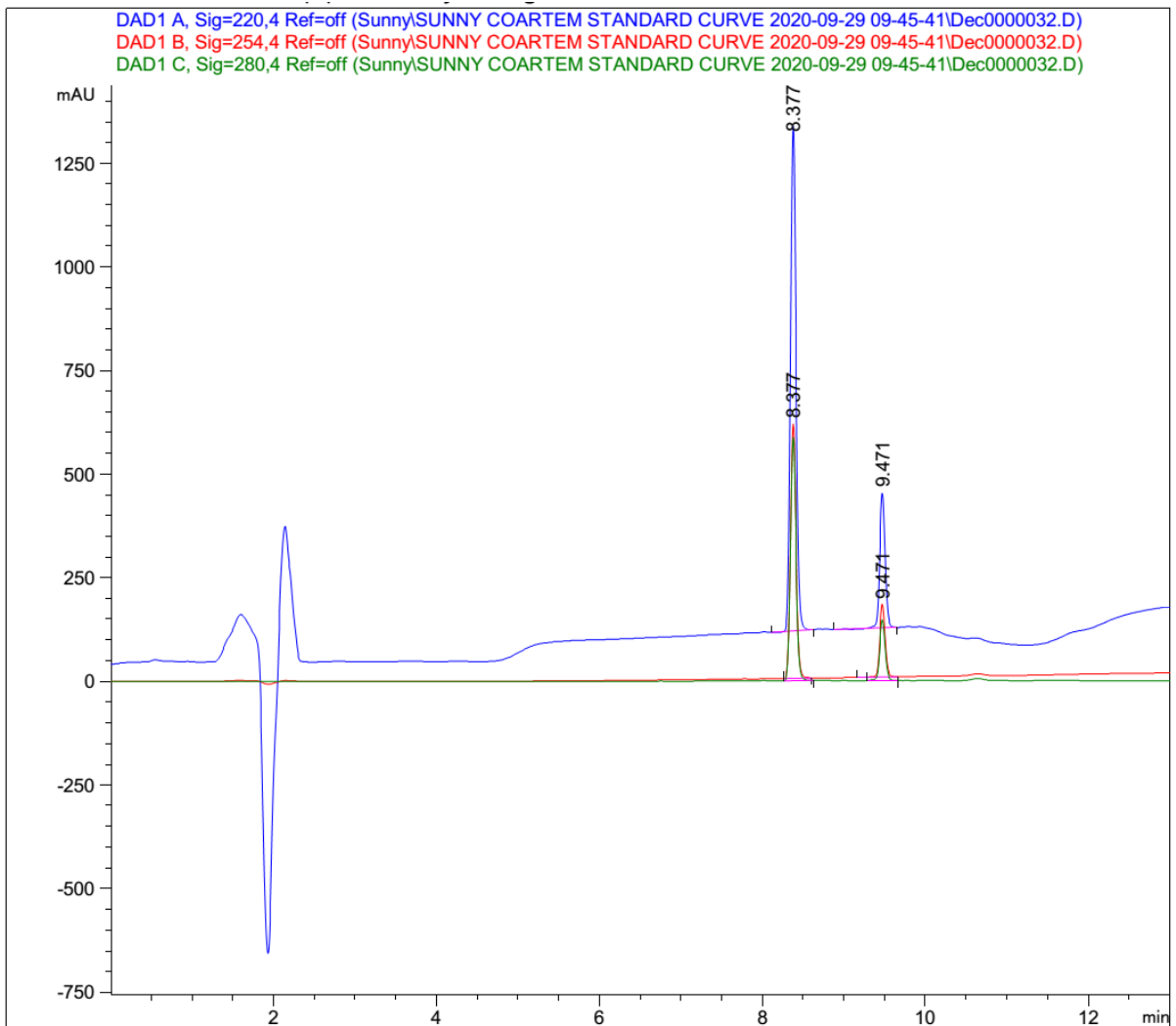
4-[({(2Z)-3-oxo-2-[(1H-pyrrolo[2,3-b]pyridin-3-yl)methylidene]-2,3-dihydro-1-benzofuran-6-yl}oxy)methyl]benzonitrile (7k)
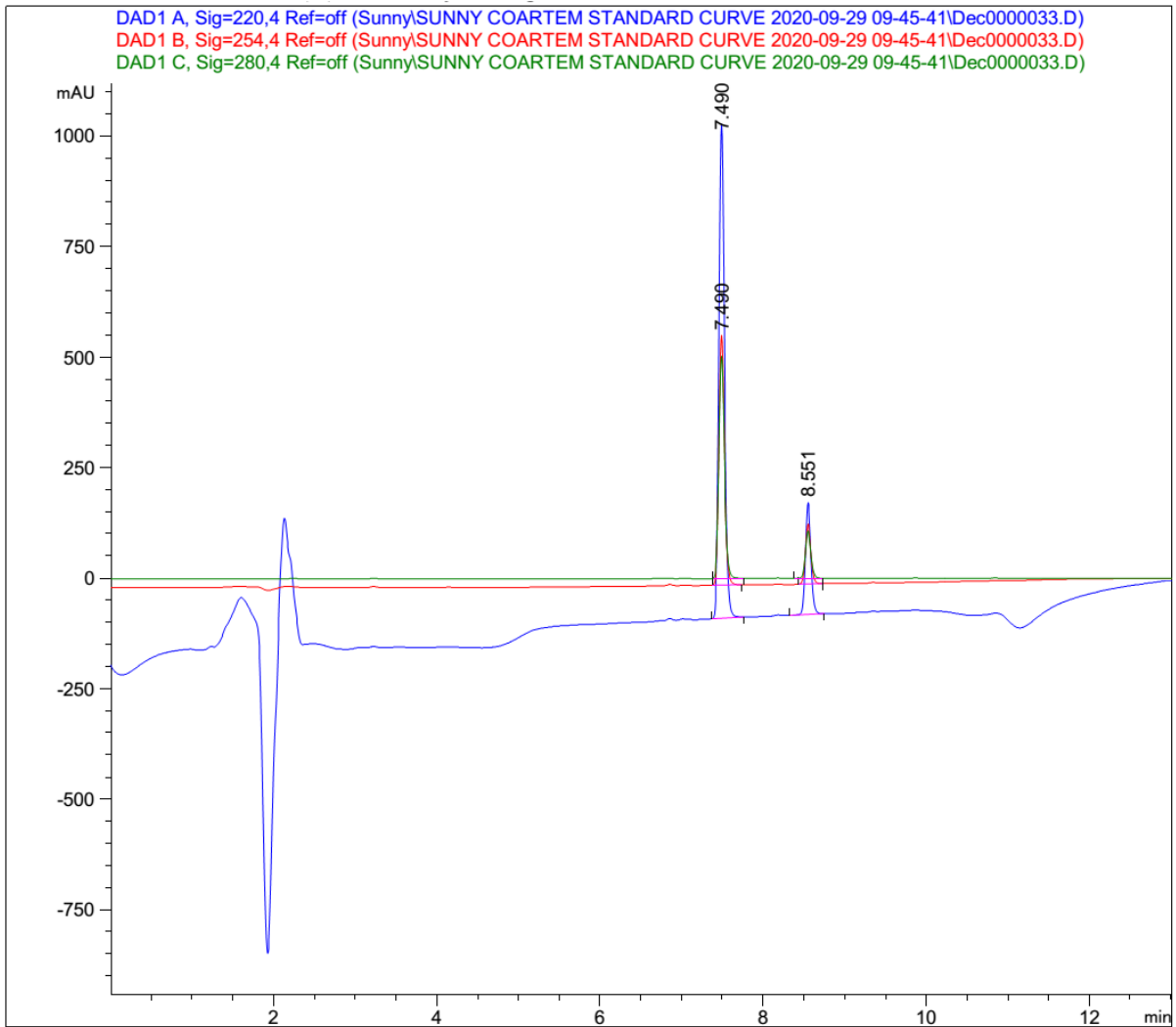
1HNMR

13CNMR

MS

+MS, 0.4-0.5min #(24-27)
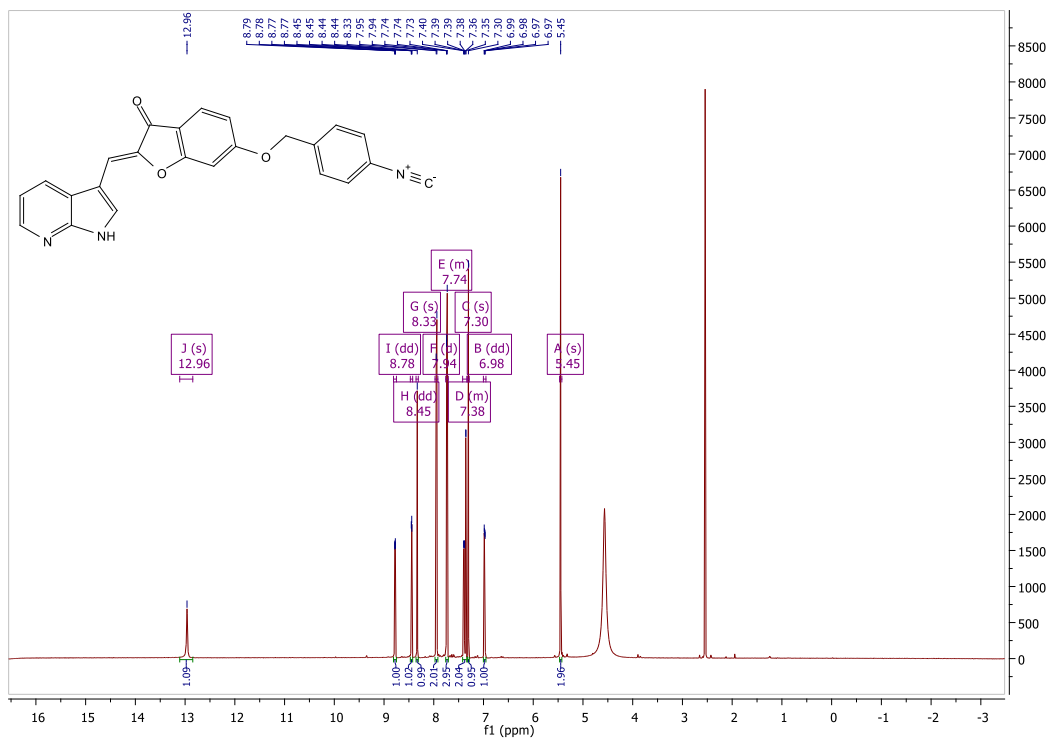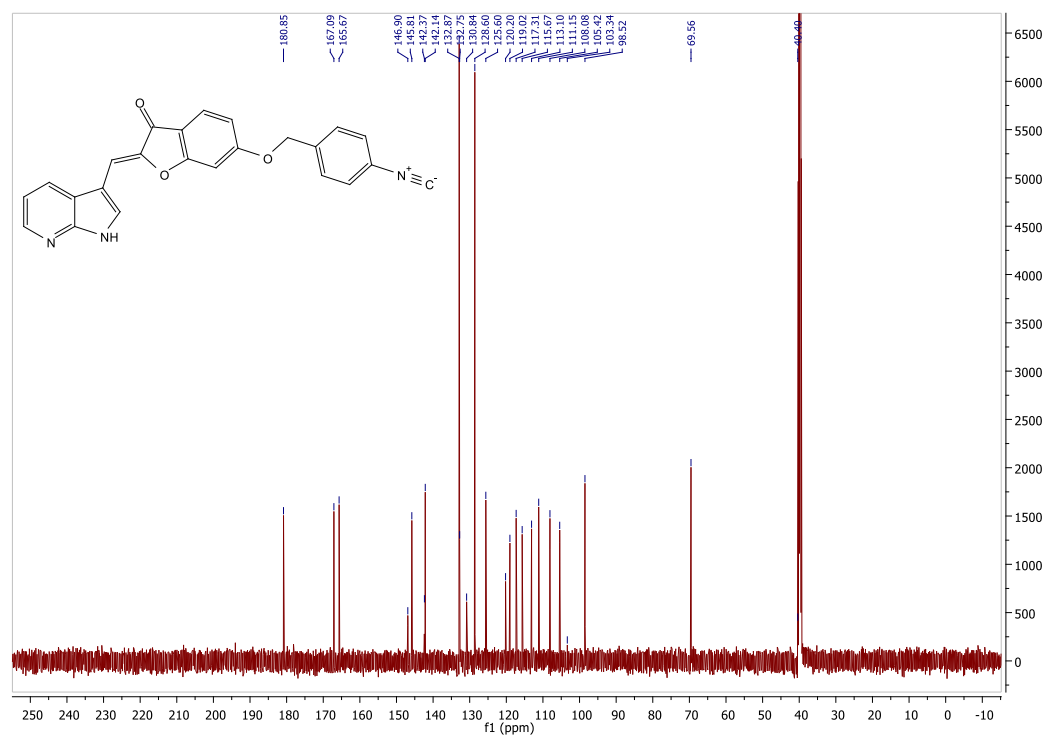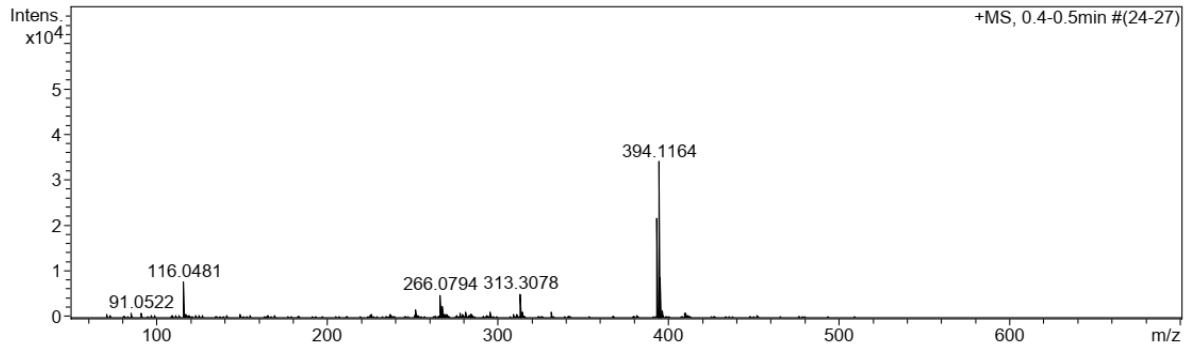
Meas. m/z	#	Formula	Score	m/z	err [mDa]	err [ppm]	mSigma	rdb	e¯ Conf	N-Rule
116.0481	1	C 8 H 6 N	100.00	116.0495	1.4	12.0	5.5	6.5	even	ok
	2	C 5 H 8 O 3	69.22	116.0468	-1.3	-11.1	26.6	2.0	odd	ok
266.0794	1	C 16 H 12 N O 3	100.00	266.0812	1.8	6.7	66.0	11.5	even	ok
313.3078	1	C 20 H 41 O 2	45.02	313.3101	2.3	7.3	8.1	0.5	even	ok
	2	C 18 H 39 N 3 O	100.00	313.3088	1.0	3.1	14.9	1.0	odd	ok
394.1164	1	C 24 H 16 N 3 O 3	100.00	394.1186	2.2	5.7	9.4	18.5	even	ok

HPLC

DAD1 A, Sig=220,4 Ref=off (Sunny\SUNNY COARTEM STANDARD CURVE 2020-09-29 09-45-41\Dec0000033.D)
DAD1 B, Sig=254,4 Ref=off (Sunny\SUNNY COARTEM STANDARD CURVE 2020-09-29 09-45-41\Dec0000033.D)
DAD1 C, Sig=280,4 Ref=off (Sunny\SUNNY COARTEM STANDARD CURVE 2020-09-29 09-45-41\Dec0000033.D)

(Z)-2-((1-benzyl-1H-pyrrolo[2,3-b]pyridin-3-yl)methylene)-6-(benzyloxy)benzofuran-3(2H)-one (9a)

^{1}HNMR

^{13}CNMR

MS

+MS, 1.7-2.4min #(103-144)
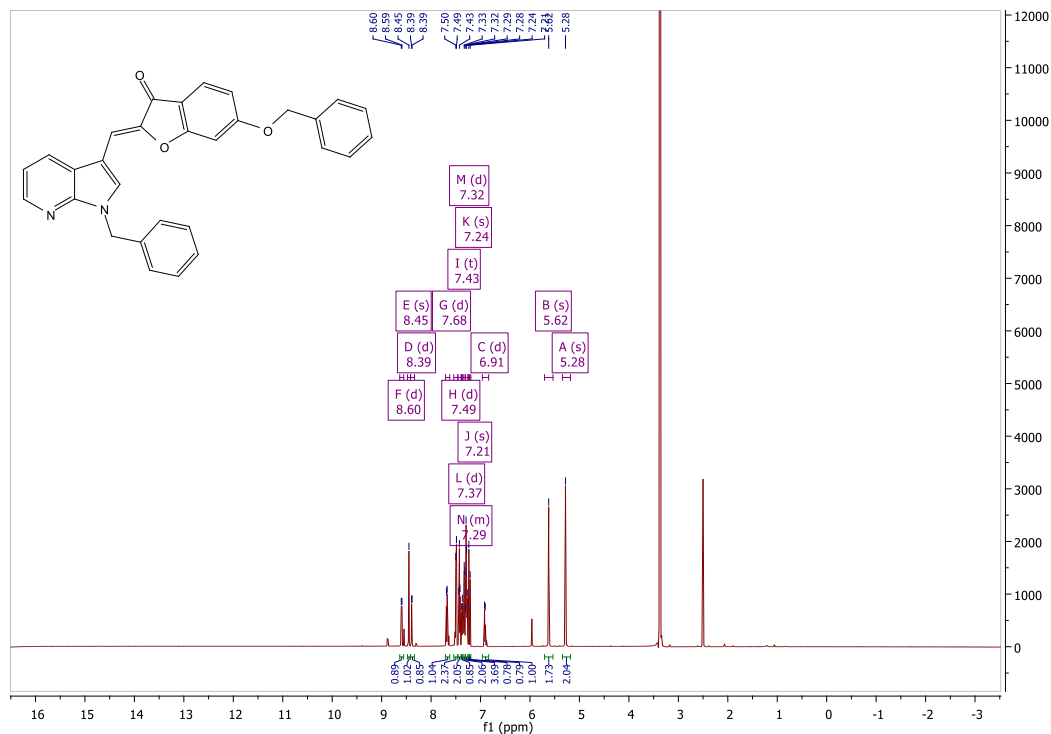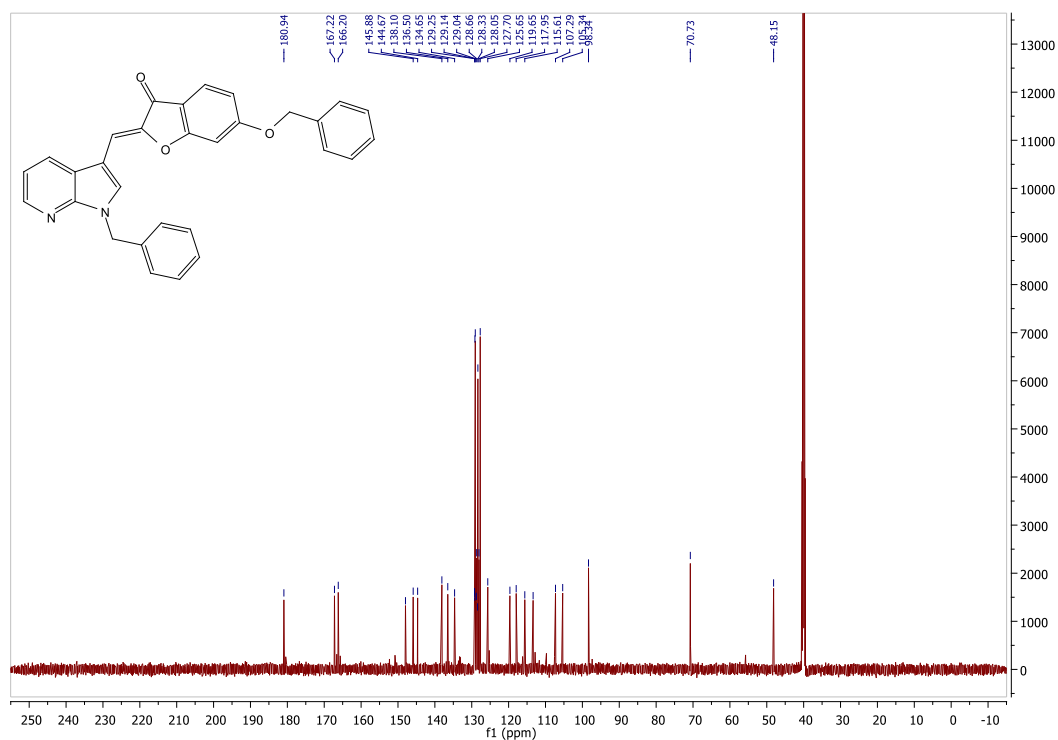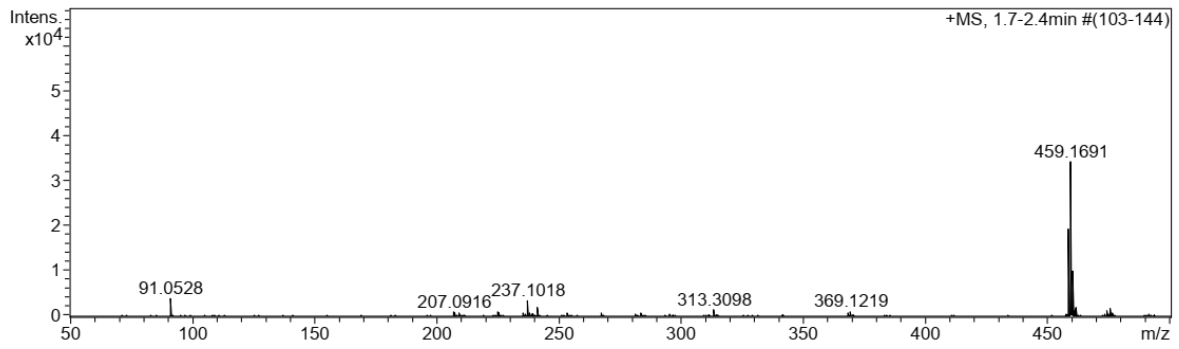
Meas. m/z	#	Formula	Score	m/z	err [mDa]	err [ppm]	mSigma	rdb	e⁻ Conf	N-Rule
458.1617	1	C 27 H 24 N O 6	100.00	458.1598	-1.9	-4.2	431.7	16.5	even	ok
	2	C 26 H 24 N 3 O 5	0.00	458.1710	9.3	20.3	499.9	16.5	even	ok
459.1691	1	C 25 H 23 N 4 O 5	44.16	459.1663	-2.8	-6.0	3.6	16.5	even	ok
	2	C 30 H 23 N 2 O 3	100.00	459.1703	1.3	2.7	21.1	20.5	even	ok

HPLC
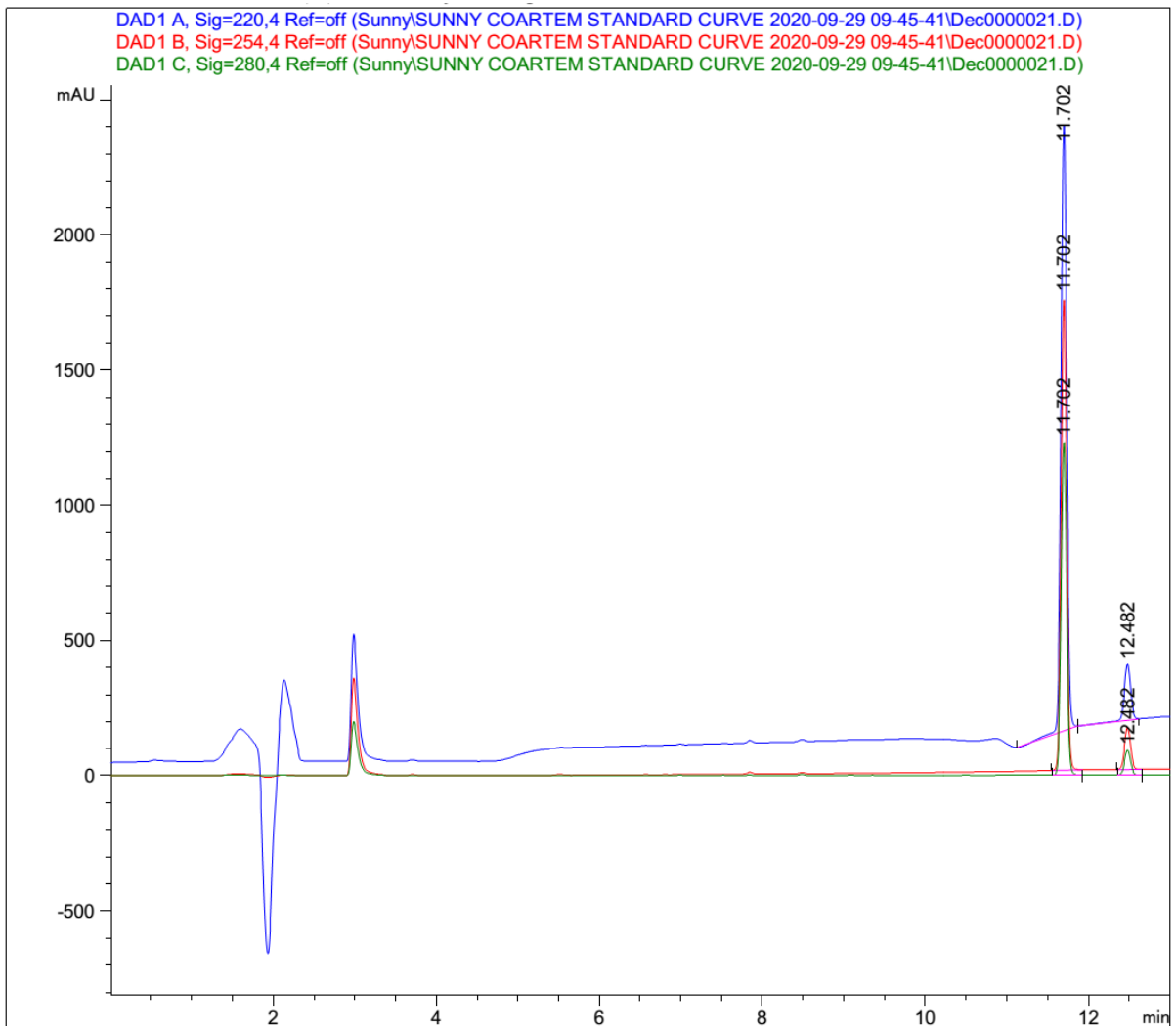
(Z)-2-((1-(3-(trifluoromethyl)benzyl)-1H-pyrrolo[2,3-b]pyridin-3-yl)methylene)-6-((3-(trifluoromethyl)benzyl)oxy)benzofuran-3(2H)-one (9b)

¹HNMR

¹³CNMR

MS

+MS, 0.3-0.4min #(20-23)

Meas. m/z	#	Formula	Score	m/z	err [mDa]	err [ppm]	mSigma	rdb	e⁻ Conf	N-Rule
595.1430	1	C 32 H 21 F 6 N 2 O 3	100.00	595.1451	2.1	3.5	13.9	20.5	even	ok
	2	C 33 H 21 F 6 O 4	0.00	595.1339	-9.2	-15.4	15.6	20.5	even	ok

HPLC

DAD1 A, Sig=220,4 Ref=off (PURITY\SUNNY COARTEM STANDARD CURVE 2020-10-02 10-27-36\Dec0000004.D)
DAD1 B, Sig=254,4 Ref=off (PURITY\SUNNY COARTEM STANDARD CURVE 2020-10-02 10-27-36\Dec0000004.D)
DAD1 C, Sig=280,4 Ref=off (PURITY\SUNNY COARTEM STANDARD CURVE 2020-10-02 10-27-36\Dec0000004.D)

APPENDIX D:

PERMISSION TO REPRODUCE FIGURE 1.2

ACS Publications
Most Trusted. Most Cited. Most Read.

Rational Design, Synthesis, and Biological Evaluation of 7-Azaindole Derivatives as Potent Focused Multi-Targeted Kinase Inhibitors

Author: Bénédicte Daydé-Cazals, Bénédicte Fauvel, Mathilde Singer, et al

Publication: Journal of Medicinal Chemistry

Publisher: American Chemical Society

Date: Apr 1, 2016

Copyright © 2016, American Chemical Society

PERMISSION/LICENSE IS GRANTED FOR YOUR ORDER AT NO CHARGE

This type of permission/license, instead of the standard Terms & Conditions, is sent to you because no fee is being charged for your order. Please note the following:

- Permission is granted for your request in both print and electronic formats, and translations.
- If figures and/or tables were requested, they may be adapted or used in part.
- Please print this page for your records and send a copy of it to your publisher/graduate school.
- Appropriate credit for the requested material should be given as follows: "Reprinted (adapted) with permission from (COMPLETE REFERENCE CITATION). Copyright (YEAR) American Chemical Society." Insert appropriate information in place of the capitalized words.
- One-time permission is granted only for the use specified in your request. No additional uses are granted (such as derivative works or other editions). For any other uses, please submit a new request.
If credit is given to another source for the material you requested, permission must be obtained from that source.

BACK   CLOSE WINDOW

APPENDIX E:

PERMISSION TO REPRODUCE FIGURE 2.1

APPENDIX F:

PERMISSION TO REPRODUCE FIGURE 2.2

All Journals ∨

PHILOSOPHICAL TRANSACTIONS OF THE ROYAL SOCIETY B

BIOLOGICAL SCIENCES

🔓 Open Access   🅝 Check for updates

Evolution of the eukaryotic protein kinases as dynamic molecular switches

Susan S. Taylor, Malik M. Keshwani, Jon M. Steichen and Alexandr P. Kornev

Abstract

Protein kinases have evolved in eukaryotes to be highly dynamic molecular switches that regulate a plethora of biological processes. Two motifs, a dynamic activation segment and a GHI helical subdomain, distinguish the eukaryotic protein kinases (EPKs) from the more primitive eukaryotic-like kinases. The EPKs are themselves highly regulated, typically by phosphorylation, and this allows them to be rapidly turned on and off. The EPKs have a novel hydrophobic architecture that is typically regulated by the dynamic assembly of two hydrophobic spines that is usually mediated by the phosphorylation of an activation loop phosphate. Cyclic AMP-dependent protein kinase (protein kinase A (PKA)) is used as a prototype to exemplify these features of the PKA superfamily. Specificity in PKA signalling is achieved in large part by packaging the enzyme as inactive tetrameric holoenzymes with regulatory subunits that then are localized to macromolecular complexes in close proximity to dedicated substrates by targeting scaffold proteins. In this way, the cell creates discrete foci that most likely represent the physiological environment for cyclic AMP-mediated signalling.

1. Introduction

The concept of protein phosphorylation as a mechanism for regulation began with the pioneering studies of Krebs and Fischer in the middle of the last century [1,2]. These studies, which demonstrated that glycogen phosphorylase was activated by the reversible addition of a single phosphate, laid the foundation for the family of eukaryotic protein kinases (EPKs). We now recognize that this family, termed as the 'kinome', represents one of the largest gene

PDF

Help

Acknowledgements

Footnotes

One contribution of 13 to a Theme Issue 'The evolution of protein phosphorylation'.

‹   ›

PHILOSOPHICAL TRANSACTIONS B

ROYAL SOCIETY PUBLISHING

THE ROYAL SOCIETY

THE ROYAL SOCIETY

f 🐦 ▶ Blog

APPENDIX G:

PERMISSION TO REPRODUCE FIGURE 2.3

Search mail

Compose

Inbox
Starred
Snoozed
Important
Sent
Drafts
Categories
Personal

Meet
New meeting
Join a meeting

Request for permission to reuse figure in PhD thesis.   Inbox ×

Malikotsi Qhobosheane <qhobosheane.ma@gmail.com>   Fri, No
to yanthy.eswaran, jhiggins, tefan.knapp, PNASpermissions

Good day

I wish to ask for permission to reuse figure 1 published in your article titled "Structure and functional characterization of th
(2009) National Academy of Sciences"

I am Miss Malikotsi Qhobosheane, a PhD student at North-West University (Potchefstroom Campus), South Africa.

My mailing address and contact details are as follows:
National University of Lesotho
Roma 180
Lesotho

tel: +266 5671 2128
email: qhobosheane.ma@gmail.com

Eswaran, J., Patnaik, D., Filippakopoulos, P., Wang, F., Stein, R.L., Murray, J.W., Higgins, J.M. & Knapp, S. 2009. S
atypical human kinase haspin. *Proceedings of the National Academy of Sciences*, 106(48):20198-20203.

Best regards

Miss Malikotsi Qhobosheane
PhD Student

Search mail   Loading...

Compose

Inbox   1
Starred
Snoozed
Important
Sent
Drafts
Categories
Personal

Meet
New meeting
Join a meeting

Request for permission to reuse figure in PhD thesis.   Inbox ×

Malikotsi Qhobosheane
Good day I wish to ask for permission to reuse figure 1 published in your article titled "Structure and functional charac

PNAS Permissions   Fri, No
to me, yanthy.eswaran@sgc.ox.ac.uk, jhiggins@rics.bwh.harvard.edu, tefan.knapp@sgc.ox.ac.uk

Thank you for your message. Permission is granted for your use of the material as described in your request
the original PNAS article when reusing its material. Because this material published after 2008, a copyright r
this material, either. Let us know if you have any questions.

Sincerely,

Kay McLaughlin for
Diane Sullenberger
PNAS Executive Editor

From: Malikotsi Qhobosheane <qhobosheane.ma@gmail.com>

APPENDIX H:
PERMISSION TO REPRODUCE FIGURE 2.17

RightsLink®

Home   Help   Email Support   Malikotsi Qhobosheane ⌄

ACS Publications
Most Trusted. Most Cited. Most Read.

Discovery of a Novel Series of 7-Azaindole Scaffold Derivatives as PI3K Inhibitors with Potent Activity

Author: Chengbin Yang, Xi Zhang, Yi Wang, et al
Publication: ACS Medicinal Chemistry Letters
Publisher: American Chemical Society
Date: Aug 1, 2017

Copyright © 2017, American Chemical Society

PERMISSION/LICENSE IS GRANTED FOR YOUR ORDER AT NO CHARGE

This type of permission/license, instead of the standard Terms & Conditions, is sent to you because no fee is being charged for your order. Please note the following:

- Permission is granted for your request in both print and electronic formats, and translations.
- If figures and/or tables were requested, they may be adapted or used in part.
- Please print this page for your records and send a copy of it to your publisher/graduate school.
- Appropriate credit for the requested material should be given as follows: "Reprinted (adapted) with permission from (COMPLETE REFERENCE CITATION). Copyright (YEAR) American Chemical Society." Insert appropriate information in place of the capitalized words.
- One-time permission is granted only for the use specified in your request. No additional uses are granted (such as derivative works or other editions). For any other uses, please submit a new request.
If credit is given to another source for the material you requested, permission must be obtained from that source.

   BACK   **CLOSE WINDOW**

APPENDIX I:

PERMISSION TO REPRODUCE FIGURE 2.18

APPENDIX J:

PERMISSION TO REPRODUCE FIGURE 2.20

Design, Synthesis and Cytotoxic Evaluation of Novel Chalcone Derivatives Bearing Triazolo[4,3-a]-quinoxaline Moieties as Potent Anticancer Agents with Dual EGFR Kinase and Tubulin Polymerization Inhibitory Effects
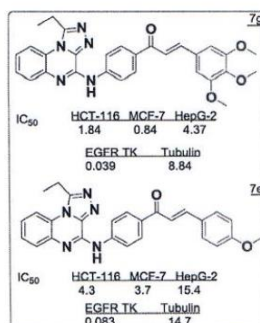
by Mohamed Alswah (https://sciprofiles.com/profile/359889) [1],
 Ashraf H. Bayoumi (https://sciprofiles.com/profile/37801) [1],
 Kamal Elgamal (https://sciprofiles.com/profile/183736) [1,2],
 Ahmed Elmorsy (https://sciprofiles.com/profile/author/VU5RcCs4S292T0tjTjNTNFArZEdFaHl0ajR1TDIRY1NZU3NISEY [1],
 Saleh Ihmaid (https://sciprofiles.com/profile/368447) [3] and

Molecules | Free Full-Text | Design, Synthesis and Cytotoxic Ev...   https://www.mdpi.com/1420-3049/23/1/48

MDPI

 (/toggle_desktop_layout_cookie)

Graphical abstract

APPENDIX K:

PERMISSION TO REPRODUCE FIGURE 2.21

Copyright Clearance Center

RightsLink®

Home | Help | Email Support | Malikotsi Qhobosheane ⌄

ACS Publications
Most Trusted. Most Cited. Most Read.

Chalcone: A Privileged Structure in Medicinal Chemistry

Author: Chunlin Zhuang, Wen Zhang, Chunquan Sheng, et al
Publication: Chemical Reviews
Publisher: American Chemical Society
Date: Jun 1, 2017

Copyright © 2017, American Chemical Society

PERMISSION/LICENSE IS GRANTED FOR YOUR ORDER AT NO CHARGE

This type of permission/license, instead of the standard Terms & Conditions, is sent to you because no fee is being charged for your order. Please note the following:

- Permission is granted for your request in both print and electronic formats, and translations.
- If figures and/or tables were requested, they may be adapted or used in part.
- Please print this page for your records and send a copy of it to your publisher/graduate school.
- Appropriate credit for the requested material should be given as follows: "Reprinted (adapted) with permission from (COMPLETE REFERENCE CITATION). Copyright (YEAR) American Chemical Society." Insert appropriate information in place of the capitalized words.
- One-time permission is granted only for the use specified in your request. No additional uses are granted (such as derivative works or other editions). For any other uses, please submit a new request.
If credit is given to another source for the material you requested, permission must be obtained from that source.

BACK   CLOSE WINDOW

APPENDIX L:

PERMISSION TO REPRODUCE PUBLISHED ARTICLE 1

Copyright Clearance Center

RightsLink®

🏠 Home   ❓ Help   ✉ Email Support   👤 Malikotsi Qhobosheane ∨
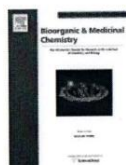
Synthesis and evaluation of 7-azaindole derivatives bearing benzocycloalkanone motifs as protein kinase inhibitors

Author: Malikotsi A. Qhobosheane,Lesetja J. Legoabe,Béatrice Josselin,Stéphane Bach,Sandrine Ruchaud,Jacobus P. Petzer,Richard M. Beteck

Publication: Bioorganic & Medicinal Chemistry

Publisher: Elsevier

Date: 1 June 2020

BACK   **CLOSE WINDOW**

APPENDIX M:
PERMISSION TO REPRODUCE PUBLISHED ARTICLE 2

JOHN WILEY AND SONS LICENSE
TERMS AND CONDITIONS

Sep 25, 2020

This Agreement between Malikotsi Qhobosheane ("You") and John Wiley and Sons ("John Wiley and Sons") consists of your license details and the terms and conditions provided by John Wiley and Sons and Copyright Clearance Center.

License Number	4915910680561
License date	Sep 25, 2020
Licensed Content Publisher	John Wiley and Sons
Licensed Content Publication	Chemical Biology & Drug Design
Licensed Content Title	Synthesis and evaluation of C3 substituted chalcone-based derivatives of 7-azaindole as protein kinase inhibitors
Licensed Content Author	Richard M. Beteck, Sandrine Ruchaud, Stéphane Bach, et al
Licensed Content Date	Aug 18, 2020
Licensed Content Volume	0
Licensed Content Issue	0
Licensed Content Pages	13
Type of use	Dissertation/Thesis

214

APPENDIX N:

AUTHOR GUIDELINES

BIOORGANIC CHEMISTRY

AUTHOR INFORMATION PACK

TABLE OF CONTENTS

DESCRIPTION

Bioorganic Chemistry publishes research that addresses biological questions at the molecular level, using organic chemistry and principles of physical organic chemistry. The scope of the journal covers a range of topics at the organic chemistry-biology interface, including: enzyme catalysis, biotransformation and enzyme inhibition; nucleic acids chemistry; medicinal chemistry; natural product chemistry, natural product synthesis and natural product biosynthesis; antimicrobial agents; lipid and peptide chemistry; biophysical chemistry; biological probes; bio-orthogonal chemistry and biomimetic chemistry.

For manuscripts dealing with synthetic bioactive compounds, the Journal requires that the molecular target of the compounds described must be known, and must be demonstrated experimentally in the manuscript. For studies involving natural products, if the molecular target is unknown, some data beyond simple cell-based toxicity studies to provide insight into the mechanism of action is required. Studies supported by molecular docking are welcome, but must be supported by experimental data. The Journal does not consider manuscripts that are purely theoretical or computational in nature.

The Journal publishes regular articles, short communications and reviews. Reviews are normally invited by Editors or Editorial Board members. Authors of unsolicited reviews should first contact an Editor or Editorial Board member to determine whether the proposed article is within the scope of the Journal.**Benefits to authors**
We also provide many author benefits, such as free PDFs, a liberal copyright policy, special discounts on Elsevier publications and much more. Please click here for more information on our author services.

Please see our Guide for Authors for information on article submission. If you require any further information or help, please visit our Support Center

IMPACT FACTOR

2019: 4.831 © Clarivate Analytics Journal Citation Reports 2020

ABSTRACTING AND INDEXING

Scopus
Current Contents - Life Sciences and Clinical Medicine
Current Contents - Physical, Chemical & Earth Sciences
BIOSIS Previews
Science Citation Index
Science Citation Index Expanded

EDITORIAL BOARD

216

GUIDE FOR AUTHORS

Your Paper Your Way

We now differentiate between the requirements for new and revised submissions. You may choose to submit your manuscript as a single Word or PDF file to be used in the refereeing process. Only when your paper is at the revision stage, will you be requested to put your paper in to a 'correct format' for acceptance and provide the items required for the publication of your article.
To find out more, please visit the Preparation section below.

Submission checklist

You can use this list to carry out a final check of your submission before you send it to the journal for review. Please check the relevant section in this Guide for Authors for more details.

Ensure that the following items are present:

One author has been designated as the corresponding author with contact details:
• E-mail address
• Full postal address

All necessary files have been uploaded:
Manuscript:
• Include keywords
• All figures (include relevant captions)
• All tables (including titles, description, footnotes)
• Ensure all figure and table citations in the text match the files provided
• Indicate clearly if color should be used for any figures in print
Graphical Abstracts / Highlights files (where applicable)
Supplemental files (where applicable)

Further considerations
• Manuscript has been 'spell checked' and 'grammar checked'
• All references mentioned in the Reference List are cited in the text, and vice versa
• Permission has been obtained for use of copyrighted material from other sources (including the Internet)
• A competing interests statement is provided, even if the authors have no competing interests to declare
• Journal policies detailed in this guide have been reviewed
• Referee suggestions, justifications and contact details provided, based on the Referees section below

For further information, visit our Support Center.

BEFORE YOU BEGIN

Ethics in publishing

Please see our information pages on Ethics in publishing and Ethical guidelines for journal publication.

Declaration of competing interest

All authors must disclose any financial and personal relationships with other people or organizations that could inappropriately influence (bias) their work. Examples of potential conflicts of interest include employment, consultancies, stock ownership, honoraria, paid expert testimony, patent applications/registrations, and grants or other funding. Authors should complete the declaration of competing interest statement using this template and upload to the submission system at the Attach/Upload Files step. **Note: Please do not convert the .docx template to another file type. Author signatures are not required.** If there are no interests to declare, please choose the first option in the template. This statement will be published within the article if accepted. More information.

Submission declaration and verification

Submission of an article implies that the work described has not been published previously (except in the form of an abstract, a published lecture or academic thesis, see 'Multiple, redundant or concurrent publication' for more information), that it is not under consideration for publication elsewhere, that its publication is approved by all authors and tacitly or explicitly by the responsible authorities where the work was carried out, and that, if accepted, it will not be published elsewhere in the same form, in

English or in any other language, including electronically without the written consent of the copyright-holder. To verify originality, your article may be checked by the originality detection service Crossref Similarity Check.

Preprints
Please note that preprints can be shared anywhere at any time, in line with Elsevier's sharing policy. Sharing your preprints e.g. on a preprint server will not count as prior publication (see 'Multiple, redundant or concurrent publication' for more information).

Use of inclusive language
Inclusive language acknowledges diversity, conveys respect to all people, is sensitive to differences, and promotes equal opportunities. Content should make no assumptions about the beliefs or commitments of any reader; contain nothing which might imply that one individual is superior to another on the grounds of age, gender, race, ethnicity, culture, sexual orientation, disability or health condition; and use inclusive language throughout. Authors should ensure that writing is free from bias, stereotypes, slang, reference to dominant culture and/or cultural assumptions. We advise to seek gender neutrality by using plural nouns ("clinicians, patients/clients") as default/wherever possible to avoid using "he, she," or "he/she." We recommend avoiding the use of descriptors that refer to personal attributes such as age, gender, race, ethnicity, culture, sexual orientation, disability or health condition unless they are relevant and valid. These guidelines are meant as a point of reference to help identify appropriate language but are by no means exhaustive or definitive.

Changes to authorship
Authors are expected to consider carefully the list and order of authors **before** submitting their manuscript and provide the definitive list of authors at the time of the original submission. Any addition, deletion or rearrangement of author names in the authorship list should be made only **before** the manuscript has been accepted and only if approved by the journal Editor. To request such a change, the Editor must receive the following from the **corresponding author**: (a) the reason for the change in author list and (b) written confirmation (e-mail, letter) from all authors that they agree with the addition, removal or rearrangement. In the case of addition or removal of authors, this includes confirmation from the author being added or removed.
Only in exceptional circumstances will the Editor consider the addition, deletion or rearrangement of authors **after** the manuscript has been accepted. While the Editor considers the request, publication of the manuscript will be suspended. If the manuscript has already been published in an online issue, any requests approved by the Editor will result in a corrigendum.

Article transfer service
This journal is part of our Article Transfer Service. This means that if the Editor feels your article is more suitable in one of our other participating journals, then you may be asked to consider transferring the article to one of those. If you agree, your article will be transferred automatically on your behalf with no need to reformat. Please note that your article will be reviewed again by the new journal. More information.

Copyright
Upon acceptance of an article, authors will be asked to complete a 'Journal Publishing Agreement' (see more information on this). An e-mail will be sent to the corresponding author confirming receipt of the manuscript together with a 'Journal Publishing Agreement' form or a link to the online version of this agreement.

Subscribers may reproduce tables of contents or prepare lists of articles including abstracts for internal circulation within their institutions. Permission of the Publisher is required for resale or distribution outside the institution and for all other derivative works, including compilations and translations. If excerpts from other copyrighted works are included, the author(s) must obtain written permission from the copyright owners and credit the source(s) in the article. Elsevier has preprinted forms for use by authors in these cases.

For gold open access articles: Upon acceptance of an article, authors will be asked to complete an 'Exclusive License Agreement' (more information). Permitted third party reuse of gold open access articles is determined by the author's choice of user license.

Author rights
As an author you (or your employer or institution) have certain rights to reuse your work. More information.

Elsevier supports responsible sharing
Find out how you can share your research published in Elsevier journals.

Role of the funding source

You are requested to identify who provided financial support for the conduct of the research and/or preparation of the article and to briefly describe the role of the sponsor(s), if any, in study design; in the collection, analysis and interpretation of data; in the writing of the report; and in the decision to submit the article for publication. If the funding source(s) had no such involvement then this should be stated.

Open access

Please visit our Open Access page for more information.

Elsevier Researcher Academy
Researcher Academy is a free e-learning platform designed to support early and mid-career researchers throughout their research journey. The "Learn" environment at Researcher Academy offers several interactive modules, webinars, downloadable guides and resources to guide you through the process of writing for research and going through peer review. Feel free to use these free resources to improve your submission and navigate the publication process with ease.

Language (usage and editing services)
Please write your text in good English (American or British usage is accepted, but not a mixture of these). Authors who feel their English language manuscript may require editing to eliminate possible grammatical or spelling errors and to conform to correct scientific English may wish to use the English Language Editing service available from Elsevier's Author Services.

Submission

Our online submission system guides you stepwise through the process of entering your article details and uploading your files. The system converts your article files to a single PDF file used in the peer-review process. Editable files (e.g., Word, LaTeX) are required to typeset your article for final publication. All correspondence, including notification of the Editor's decision and requests for revision, is sent by e-mail.

Referees
With their submitted manuscript, authors must submit the names of at least FIVE potential reviewers. Please submit the names and institutional e-mail addresses of each potential referees.
Along with the names, authors should provide an email address, institution and a justification for why the reviewer has been suggested. Justifications such as "expert in the field" or "expert in medicinal chemistry" are not useful. Instead, justifications that are more specific such as "expert with this enzyme", "expert with this receptor" or "expert with this class of compounds" should be used. Failure to provide this information will result in the manuscript being returned to the authors with a request for more information that will prolong the review process. For more details, visit our Support site. Note that the editor retains the sole right to decide whether or not the suggested reviewers are used

PREPARATION

NEW SUBMISSIONS

Submission to this journal proceeds totally online and you will be guided stepwise through the creation and uploading of your files. The system automatically converts your files to a single PDF file, which is used in the peer-review process.
As part of the Your Paper Your Way service, you may choose to submit your manuscript as a single file to be used in the refereeing process. This can be a PDF file or a Word document, in any format or lay-out that can be used by referees to evaluate your manuscript. It should contain high enough quality figures for refereeing. If you prefer to do so, you may still provide all or some of the source files at the initial submission. Please note that individual figure files larger than 10 MB must be uploaded separately.

References
There are no strict requirements on reference formatting at submission. References can be in any style or format as long as the style is consistent. Where applicable, author(s) name(s), journal title/book title, chapter title/article title, year of publication, volume number/book chapter and the article number or pagination must be present. Use of DOI is highly encouraged. The reference style used by the journal will be applied to the accepted article by Elsevier at the proof stage. Note that missing data will be highlighted at proof stage for the author to correct.

Formatting requirements
There are no strict formatting requirements but all manuscripts must contain the essential elements needed to convey your manuscript, for example Abstract, Keywords, Introduction, Materials and Methods, Results, Conclusions, Artwork and Tables with Captions.
If your article includes any Videos and/or other Supplementary material, this should be included in your initial submission for peer review purposes.
Divide the article into clearly defined sections.

Figures and tables embedded in text
Please ensure the figures and the tables included in the single file are placed next to the relevant text in the manuscript, rather than at the bottom or the top of the file. The corresponding caption should be placed directly below the figure or table.

Peer review
This journal operates a single anonymized review process. All contributions will be initially assessed by the editor for suitability for the journal. Papers deemed suitable are then typically sent to a minimum of two independent expert reviewers to assess the scientific quality of the paper. The Editor is responsible for the final decision regarding acceptance or rejection of articles. The Editor's decision is final. Editors are not involved in decisions about papers which they have written themselves or have been written by family members or colleagues or which relate to products or services in which the editor has an interest. Any such submission is subject to all of the journal's usual procedures, with peer review handled independently of the relevant editor and their research groups. More information on types of peer review.

REVISED SUBMISSIONS
Use of word processing software
Regardless of the file format of the original submission, at revision you must provide us with an editable file of the entire article. Keep the layout of the text as simple as possible. Most formatting codes will be removed and replaced on processing the article. The electronic text should be prepared in a way very similar to that of conventional manuscripts (see also the Guide to Publishing with Elsevier). See also the section on Electronic artwork.
To avoid unnecessary errors you are strongly advised to use the 'spell-check' and 'grammar-check' functions of your word processor.

LaTeX
You are recommended to use the Elsevier article class elsarticle.cls to prepare your manuscript and BibTeX to generate your bibliography.
Our LaTeX site has detailed submission instructions, templates and other information.

Article structure
Subdivision - numbered sections
Divide your article into clearly defined and numbered sections. Subsections should be numbered 1.1 (then 1.1.1, 1.1.2, ...), 1.2, etc. (the abstract is not included in section numbering). Use this numbering also for internal cross-referencing: do not just refer to 'the text'. Any subsection may be given a brief heading. Each heading should appear on its own separate line.

Introduction
State the objectives of the work and provide an adequate background, avoiding a detailed literature survey or a summary of the results.

Material and methods
Provide sufficient details to allow the work to be reproduced by an independent researcher. Methods that are already published should be summarized, and indicated by a reference. If quoting directly from a previously published method, use quotation marks and also cite the source. If a previously reported method was used such as an enzyme assay, the authors should still include the concentrations of all substrates since those parameters can affect the IC_{50} value. It is also essential that authors explain how inhibition constants or kinetic parameters were obtained by noting the mathematical equation employed. Note that all plots used to determine inhibition or kinetic parameters must be provided in the Supplementary material section. Any modifications to existing methods should also be described. For synthetic compounds, sufficient information to establish the structure of each compound is required. Typically, this means ^{1}H-NMR, ^{13}C NMR and either HR-MS or elemental analysis. For final compounds used in biological experiments, the authors should state the purity of the material and how that was determined.

Results

Results and Discussion may be combined if appropriate and may be organized into subheadings. The Conclusion may be presented in a short section that may stand alone or form a subsection of a Discussion or Results and Discussion section.

Discussion

This should explore the significance of the results of the work, not repeat them. A combined Results and Discussion section is often appropriate. Avoid extensive citations and discussion of published literature.

Conclusions

The main conclusions of the study may be presented in a short Conclusions section, which may stand alone or form a subsection of a Discussion or Results and Discussion section.

Glossary

Please supply, as a separate list, the definitions of field-specific terms used in your article.

Appendices

If there is more than one appendix, they should be identified as A, B, etc. Formulae and equations in appendices should be given separate numbering: Eq. (A.1), Eq. (A.2), etc.; in a subsequent appendix, Eq. (B.1) and so on. Similarly for tables and figures: Table A.1; Fig. A.1, etc.

Essential title page information

• **Title.** Concise and informative. Titles are often used in information-retrieval systems. Avoid abbreviations and formulae where possible.

• **Author names and affiliations.** Please clearly indicate the given name(s) and family name(s) of each author and check that all names are accurately spelled. You can add your name between parentheses in your own script behind the English transliteration. Present the authors' affiliation addresses (where the actual work was done) below the names. Indicate all affiliations with a lower-case superscript letter immediately after the author's name and in front of the appropriate address. Provide the full postal address of each affiliation, including the country name and, if available, the e-mail address of each author.

• **Corresponding author.** Clearly indicate who will handle correspondence at all stages of refereeing and publication, also post-publication. This responsibility includes answering any future queries about Methodology and Materials. **Ensure that the e-mail address is given and that contact details are kept up to date by the corresponding author.**

• **Present/permanent address.** If an author has moved since the work described in the article was done, or was visiting at the time, a 'Present address' (or 'Permanent address') may be indicated as a footnote to that author's name. The address at which the author actually did the work must be retained as the main, affiliation address. Superscript Arabic numerals are used for such footnotes.

Highlights

Highlights are mandatory for this journal as they help increase the discoverability of your article via search engines. They consist of a short collection of bullet points that capture the novel results of your research as well as new methods that were used during the study (if any). Please have a look at the examples here: example Highlights.

Highlights should be submitted in a separate editable file in the online submission system. Please use 'Highlights' in the file name and include 3 to 5 bullet points (maximum 85 characters, including spaces, per bullet point).

Abstract

A concise and factual abstract is required. The abstract should state briefly the purpose of the research, the principal results and major conclusions. An abstract is often presented separately from the article, so it must be able to stand alone. For this reason, References should be avoided, but if essential, then cite the author(s) and year(s). Also, non-standard or uncommon abbreviations should be avoided, but if essential they must be defined at their first mention in the abstract itself.

Graphical abstract

A graphical abstract is mandatory for this journal. It should summarize the contents of the article in a concise, pictorial form designed to capture the attention of a wide readership online. Authors must provide images that clearly represent the work described in the article. Graphical abstracts should be submitted as a separate file in the online submission system. Image size: please provide an image

with a minimum of 531 × 1328 pixels (h × w) or proportionally more. The image should be readable at a size of 5 × 13 cm using a regular screen resolution of 96 dpi. Preferred file types: TIFF, EPS, PDF or MS Office files. You can view Example Graphical Abstracts on our information site.
Authors can make use of Elsevier's Illustration Services to ensure the best presentation of their images also in accordance with all technical requirements.

Keywords
Immediately after the abstract, provide a maximum of 10 keywords, using American spelling and avoiding general and plural terms and multiple concepts (avoid, for example, "and", "of"). Be sparing with abbreviations: only abbreviations firmly established in the field may be eligible. These keywords will be used for indexing purposes.

Abbreviations
Define abbreviations that are not standard in this field in a footnote to be placed on the first page of the article. Such abbreviations that are unavoidable in the abstract must be defined at their first mention there, as well as in the footnote. Ensure consistency of abbreviations throughout the article.

Acknowledgements
Collate acknowledgements in a separate section at the end of the article before the references and do not, therefore, include them on the title page, as a footnote to the title or otherwise. List here those individuals who provided help during the research (e.g., providing language help, writing assistance or proof reading the article, etc.).

Formatting of funding sources
List funding sources in this standard way to facilitate compliance to funder's requirements:

Funding: This work was supported by the National Institutes of Health [grant numbers xxxx, yyyy]; the Bill & Melinda Gates Foundation, Seattle, WA [grant number zzzz]; and the United States Institutes of Peace [grant number aaaa].

It is not necessary to include detailed descriptions on the program or type of grants and awards. When funding is from a block grant or other resources available to a university, college, or other research institution, submit the name of the institute or organization that provided the funding.

If no funding has been provided for the research, please include the following sentence:

This research did not receive any specific grant from funding agencies in the public, commercial, or not-for-profit sectors.

Nomenclature and units
Follow internationally accepted rules and conventions: use the international system of units (SI). If other quantities are mentioned, give their equivalent in SI. You are urged to consult IUPAC: Nomenclature of Organic Chemistry for further information.

Math formulae
Please submit math equations as editable text and not as images. Present simple formulae in line with normal text where possible and use the solidus (/) instead of a horizontal line for small fractional terms, e.g., X/Y. In principle, variables are to be presented in italics. Powers of e are often more conveniently denoted by exp. Number consecutively any equations that have to be displayed separately from the text (if referred to explicitly in the text).

Footnotes
Footnotes should be used sparingly. Number them consecutively throughout the article. Many word processors build footnotes into the text, and this feature may be used. Should this not be the case, indicate the position of footnotes in the text and present the footnotes themselves separately at the end of the article.

Artwork
Electronic artwork
General points
• Make sure you use uniform lettering and sizing of your original artwork.
• Preferred fonts: Arial (or Helvetica), Times New Roman (or Times), Symbol, Courier.
• Number the illustrations according to their sequence in the text.
• Use a logical naming convention for your artwork files.

- Indicate per figure if it is a single, 1.5 or 2-column fitting image.
- For Word submissions only, you may still provide figures and their captions, and tables within a single file at the revision stage.
- Please note that individual figure files larger than 10 MB must be provided in separate source files.

A detailed guide on electronic artwork is available.
You are urged to visit this site; some excerpts from the detailed information are given here.
Formats
Regardless of the application used, when your electronic artwork is finalized, please 'save as' or convert the images to one of the following formats (note the resolution requirements for line drawings, halftones, and line/halftone combinations given below):
EPS (or PDF): Vector drawings. Embed the font or save the text as 'graphics'.
TIFF (or JPG): Color or grayscale photographs (halftones): always use a minimum of 300 dpi.
TIFF (or JPG): Bitmapped line drawings: use a minimum of 1000 dpi.
TIFF (or JPG): Combinations bitmapped line/half-tone (color or grayscale): a minimum of 500 dpi is required.
Please do not:
- Supply files that are optimized for screen use (e.g., GIF, BMP, PICT, WPG); the resolution is too low.
- Supply files that are too low in resolution.
- Submit graphics that are disproportionately large for the content.

Color artwork
Please make sure that artwork files are in an acceptable format (TIFF (or JPEG), EPS (or PDF), or MS Office files) and with the correct resolution. If, together with your accepted article, you submit usable color figures then Elsevier will ensure, at no additional charge, that these figures will appear in color online (e.g., ScienceDirect and other sites) regardless of whether or not these illustrations are reproduced in color in the printed version. **For color reproduction in print, you will receive information regarding the costs from Elsevier after receipt of your accepted article**. Please indicate your preference for color: in print or online only. Further information on the preparation of electronic artwork.

Figure captions
Ensure that each illustration has a caption. A caption should comprise a brief title (**not** on the figure itself) and a description of the illustration. Keep text in the illustrations themselves to a minimum but explain all symbols and abbreviations used.

Text graphics
Text graphics may be embedded in the text at the appropriate position. If you are working with LaTeX and have such features embedded in the text, these can be left. See further under Electronic artwork.

Tables
Please submit tables as editable text and not as images. Tables can be placed either next to the relevant text in the article, or on separate page(s) at the end. Number tables consecutively in accordance with their appearance in the text and place any table notes below the table body. Be sparing in the use of tables and ensure that the data presented in them do not duplicate results described elsewhere in the article. Please avoid using vertical rules and shading in table cells.

References
Citation in text
Please ensure that every reference cited in the text is also present in the reference list (and vice versa). Any references cited in the abstract must be given in full. Unpublished results and personal communications are not recommended in the reference list, but may be mentioned in the text. If these references are included in the reference list they should follow the standard reference style of the journal and should include a substitution of the publication date with either 'Unpublished results' or 'Personal communication'. Citation of a reference as 'in press' implies that the item has been accepted for publication.

Reference links
Increased discoverability of research and high quality peer review are ensured by online links to the sources cited. In order to allow us to create links to abstracting and indexing services, such as Scopus, CrossRef and PubMed, please ensure that data provided in the references are correct. Please

223

note that incorrect surnames, journal/book titles, publication year and pagination may prevent link creation. When copying references, please be careful as they may already contain errors. Use of the DOI is highly encouraged.

A DOI is guaranteed never to change, so you can use it as a permanent link to any electronic article. An example of a citation using DOI for an article not yet in an issue is: VanDecar J.C., Russo R.M., James D.E., Ambeh W.B., Franke M. (2003). Aseismic continuation of the Lesser Antilles slab beneath northeastern Venezuela. Journal of Geophysical Research, https://doi.org/10.1029/2001JB000884. Please note the format of such citations should be in the same style as all other references in the paper.

Web references
As a minimum, the full URL should be given and the date when the reference was last accessed. Any further information, if known (DOI, author names, dates, reference to a source publication, etc.), should also be given. Web references can be listed separately (e.g., after the reference list) under a different heading if desired, or can be included in the reference list.

Data references
This journal encourages you to cite underlying or relevant datasets in your manuscript by citing them in your text and including a data reference in your Reference List. Data references should include the following elements: author name(s), dataset title, data repository, version (where available), year, and global persistent identifier. Add [dataset] immediately before the reference so we can properly identify it as a data reference. The [dataset] identifier will not appear in your published article.

References in a special issue
Please ensure that the words 'this issue' are added to any references in the list (and any citations in the text) to other articles in the same Special Issue.

Reference management software
Most Elsevier journals have their reference template available in many of the most popular reference management software products. These include all products that support Citation Style Language styles, such as Mendeley. Using citation plug-ins from these products, authors only need to select the appropriate journal template when preparing their article, after which citations and bibliographies will be automatically formatted in the journal's style. If no template is yet available for this journal, please follow the format of the sample references and citations as shown in this Guide. If you use reference management software, please ensure that you remove all field codes before submitting the electronic manuscript. More information on how to remove field codes from different reference management software.

Users of Mendeley Desktop can easily install the reference style for this journal by clicking the following link:
http://open.mendeley.com/use-citation-style/bioorganic-chemistry
When preparing your manuscript, you will then be able to select this style using the Mendeley plug-ins for Microsoft Word or LibreOffice.

Reference formatting
There are no strict requirements on reference formatting at submission. References can be in any style or format as long as the style is consistent. Where applicable, author(s) name(s), journal title/ book title, chapter title/article title, year of publication, volume number/book chapter and the article number or pagination must be present. Use of DOI is highly encouraged. The reference style used by the journal will be applied to the accepted article by Elsevier at the proof stage. Note that missing data will be highlighted at proof stage for the author to correct. If you do wish to format the references yourself they should be arranged according to the following examples:

Reference style
Text: Indicate references by number(s) in square brackets in line with the text. The actual authors can be referred to, but the reference number(s) must always be given.
Example: '..... as demonstrated [3,6]. Barnaby and Jones [8] obtained a different result ....'
List: Number the references (numbers in square brackets) in the list in the order in which they appear in the text.
Examples:
Reference to a journal publication:
[1] J. van der Geer, J.A.J. Hanraads, R.A. Lupton, The art of writing a scientific article, J. Sci. Commun. 163 (2010) 51–59. https://doi.org/10.1016/j.Sc.2010.00372.
Reference to a journal publication with an article number:

[2] J. van der Geer, J.A.J. Hanraads, R.A. Lupton, 2018. The art of writing a scientific article. Heliyon. 19, e00205. https://doi.org/10.1016/j.heliyon.2018.e00205.
Reference to a book:
[3] W. Strunk Jr., E.B. White, The Elements of Style, fourth ed., Longman, New York, 2000.
Reference to a chapter in an edited book:
[4] G.R. Mettam, L.B. Adams, How to prepare an electronic version of your article, in: B.S. Jones, R.Z. Smith (Eds.), Introduction to the Electronic Age, E-Publishing Inc., New York, 2009, pp. 281–304.
Reference to a website:
[5] Cancer Research UK, Cancer statistics reports for the UK. http://www.cancerresearchuk.org/aboutcancer/statistics/cancerstatsreport/, 2003 (accessed 13 March 2003).
Reference to a dataset:
[dataset] [6] M. Oguro, S. Imahiro, S. Saito, T. Nakashizuka, Mortality data for Japanese oak wilt disease and surrounding forest compositions, Mendeley Data, v1, 2015. https://doi.org/10.17632/xwj98nb39r.1.

Journal abbreviations source
Journal names should be abbreviated according to the List of Title Word Abbreviations.

Video

Elsevier accepts video material and animation sequences to support and enhance your scientific research. Authors who have video or animation files that they wish to submit with their article are strongly encouraged to include links to these within the body of the article. This can be done in the same way as a figure or table by referring to the video or animation content and noting in the body text where it should be placed. All submitted files should be properly labeled so that they directly relate to the video file's content. In order to ensure that your video or animation material is directly usable, please provide the file in one of our recommended file formats with a preferred maximum size of 150 MB per file, 1 GB in total. Video and animation files supplied will be published online in the electronic version of your article in Elsevier Web products, including ScienceDirect. Please supply 'stills' with your files: you can choose any frame from the video or animation or make a separate image. These will be used instead of standard icons and will personalize the link to your video data. For more detailed instructions please visit our video instruction pages. Note: since video and animation cannot be embedded in the print version of the journal, please provide text for both the electronic and the print version for the portions of the article that refer to this content.

Data visualization

Include interactive data visualizations in your publication and let your readers interact and engage more closely with your research. Follow the instructions here to find out about available data visualization options and how to include them with your article.

Supplementary Material

Authors must provide copies of spectra (at least ^{1}H-NMR) for all final compounds in the Supplementary material section. For papers involving natural products, or more complex molecules, additional 2D NMR spectra should also be provided. For manuscripts involving enzyme inhibition or receptor binding assays, authors should provide a graph that shows the data that was used to calculate the IC_{50}, (or K_M, K_D etc) value for each compound. Provide a separate graph for each compound.

Supplementary material such as applications, images and sound clips, can be published with your article to enhance it. Submitted supplementary items are published exactly as they are received (Excel or PowerPoint files will appear as such online). Please submit your material together with the article and supply a concise, descriptive caption for each supplementary file. If you wish to make changes to supplementary material during any stage of the process, please make sure to provide an updated file. Do not annotate any corrections on a previous version. Please switch off the 'Track Changes' option in Microsoft Office files as these will appear in the published version.

Research data

This journal encourages and enables you to share data that supports your research publication where appropriate, and enables you to interlink the data with your published articles. Research data refers to the results of observations or experimentation that validate research findings. To facilitate reproducibility and data reuse, this journal also encourages you to share your software, code, models, algorithms, protocols, methods and other useful materials related to the project.

Below are a number of ways in which you can associate data with your article or make a statement about the availability of your data when submitting your manuscript. If you are sharing data in one of these ways, you are encouraged to cite the data in your manuscript and reference list. Please refer to the "References" section for more information about data citation. For more information on depositing, sharing and using research data and other relevant research materials, visit the research data page.

Data linking
If you have made your research data available in a data repository, you can link your article directly to the dataset. Elsevier collaborates with a number of repositories to link articles on ScienceDirect with relevant repositories, giving readers access to underlying data that gives them a better understanding of the research described.

There are different ways to link your datasets to your article. When available, you can directly link your dataset to your article by providing the relevant information in the submission system. For more information, visit the database linking page.

For supported data repositories a repository banner will automatically appear next to your published article on ScienceDirect.

In addition, you can link to relevant data or entities through identifiers within the text of your manuscript, using the following format: Database: xxxx (e.g., TAIR: AT1G01020; CCDC: 734053; PDB: 1XFN).

Mendeley Data
This journal supports Mendeley Data, enabling you to deposit any research data (including raw and processed data, video, code, software, algorithms, protocols, and methods) associated with your manuscript in a free-to-use, open access repository. During the submission process, after uploading your manuscript, you will have the opportunity to upload your relevant datasets directly to *Mendeley Data*. The datasets will be listed and directly accessible to readers next to your published article online.

For more information, visit the Mendeley Data for journals page.

Data in Brief
You have the option of converting any or all parts of your supplementary or additional raw data into a data article published in *Data in Brief*. A data article is a new kind of article that ensures that your data are actively reviewed, curated, formatted, indexed, given a DOI and made publicly available to all upon publication (watch this video describing the benefits of publishing your data in *Data in Brief*). You are encouraged to submit your data article for *Data in Brief* as an additional item directly alongside the revised version of your manuscript. If your research article is accepted, your data article will automatically be transferred over to *Data in Brief* where it will be editorially reviewed, published open access and linked to your research article on ScienceDirect. Please note an open access fee is payable for publication in *Data in Brief*. Full details can be found on the Data in Brief website. Please use this template to write your *Data in Brief* data article.

MethodsX
You have the option of converting relevant protocols and methods into one or multiple MethodsX articles, a new kind of article that describes the details of customized research methods. Many researchers spend a significant amount of time on developing methods to fit their specific needs or setting, but often without getting credit for this part of their work. MethodsX, an open access journal, now publishes this information in order to make it searchable, peer reviewed, citable and reproducible. Authors are encouraged to submit their MethodsX article as an additional item directly alongside the revised version of their manuscript. If your research article is accepted, your methods article will automatically be transferred over to MethodsX where it will be editorially reviewed. Please note an open access fee is payable for publication in MethodsX. Full details can be found on the MethodsX website. Please use this template to prepare your MethodsX article.

Data statement
To foster transparency, we encourage you to state the availability of your data in your submission. This may be a requirement of your funding body or institution. If your data is unavailable to access or unsuitable to post, you will have the opportunity to indicate why during the submission process, for example by stating that the research data is confidential. The statement will appear with your published article on ScienceDirect. For more information, visit the Data Statement page.

226

AFTER ACCEPTANCE

Online proof correction

To ensure a fast publication process of the article, we kindly ask authors to provide us with their proof corrections within two days. Corresponding authors will receive an e-mail with a link to our online proofing system, allowing annotation and correction of proofs online. The environment is similar to MS Word: in addition to editing text, you can also comment on figures/tables and answer questions from the Copy Editor. Web-based proofing provides a faster and less error-prone process by allowing you to directly type your corrections, eliminating the potential introduction of errors.

If preferred, you can still choose to annotate and upload your edits on the PDF version. All instructions for proofing will be given in the e-mail we send to authors, including alternative methods to the online version and PDF.

We will do everything possible to get your article published quickly and accurately. Please use this proof only for checking the typesetting, editing, completeness and correctness of the text, tables and figures. Significant changes to the article as accepted for publication will only be considered at this stage with permission from the Editor. It is important to ensure that all corrections are sent back to us in one communication. Please check carefully before replying, as inclusion of any subsequent corrections cannot be guaranteed. Proofreading is solely your responsibility.

Offprints

The corresponding author will, at no cost, receive a customized Share Link providing 50 days free access to the final published version of the article on ScienceDirect. The Share Link can be used for sharing the article via any communication channel, including email and social media. For an extra charge, paper offprints can be ordered via the offprint order form which is sent once the article is accepted for publication. Both corresponding and co-authors may order offprints at any time via Elsevier's Author Services. Corresponding authors who have published their article gold open access do not receive a Share Link as their final published version of the article is available open access on ScienceDirect and can be shared through the article DOI link.

AUTHOR INQUIRIES

Visit the Elsevier Support Center to find the answers you need. Here you will find everything from Frequently Asked Questions to ways to get in touch.

You can also check the status of your submitted article or find out when your accepted article will be published.

APPENDIX O:

CONFIRMATION OF MANUSCRIPT SUBMISSION

APPENDIX P:

PLAGIARISM REPORT

27836576:Synthesis_and_biological_evaluation_of_7-azaindole-based_chalcones_and_related_compounds_as_protein_kinase_i.

229